**Springer Series in Synergetics** 



Oleg G. Bakunin

# Chaotic Flows

Correlation Effects, Transport, and Structures



# **Springer Complexity**

Springer Complexity is an interdisciplinary program publishing the best research and academic-level teaching on both fundamental and applied aspects of complex systems — cutting across all traditional disciplines of the natural and life sciences, engineering, economics, medicine, neuroscience, social and computer science.

Complex Systems are systems that comprise many interacting parts with the ability to generate a new quality of macroscopic collective behavior the manifestations of which are the spontaneous formation of distinctive temporal, spatial or functional structures. Models of such systems can be successfully mapped onto quite diverse "real-life" situations like the climate, the coherent emission of light from lasers, chemical reaction-diffusion systems, biological cellular networks, the dynamics of stock markets and of the internet, earthquake statistics and prediction, freeway traffic, the human brain, or the formation of opinions in social systems, to name just some of the popular applications.

Although their scope and methodologies overlap somewhat, one can distinguish the following main concepts and tools: self-organization, nonlinear dynamics, synergetics, turbulence, dynamical systems, catastrophes, instabilities, stochastic processes, chaos, graphs and networks, cellular automata, adaptive systems, genetic algorithms and computational intelligence.

The two major book publication platforms of the Springer Complexity program are the monograph series "Understanding Complex Systems" focusing on the various applications of complexity, and the "Springer Series in Synergetics", which is devoted to the quantitative theoretical and methodological foundations. In addition to the books in these two core series, the program also incorporates individual titles ranging from textbooks to major reference works.

#### **Editorial and Programme Advisory Board**

Henry Abarbanel, Institute for Nonlinear Science, University of California, San Diego, USA

Dan Braha, New England Complex Systems Institute and University of Massachusetts Dartmouth, USA

Péter Érdi, Center for Complex Systems Studies, Kalamazoo College, USA, and Hungarian Academy of Sciences, Budapest, Hungary

Karl Friston, National Hospital, Institute Neurology, Wellcome Dept. Cogn. Neurology, London, UK

Hermann Haken, Center of Synergetics, University of Stuttgart, Stuttgart, Germany

Viktor Jirsa, Centre National de la Recherche Scientifique (CNRS), Université de la Méditerranée, Marseille, France

Janusz Kacprzyk, System Research, Polish Academy of Sciences, Warsaw, Poland

Kunihiko Kaneko, Research Center for Complex Systems Biology, The University of Tokyo, Tokyo, Japan

Scott Kelso, Center for Complex Systems and Brain Sciences, Florida Atlantic University, Boca Raton, USA

Markus Kirkilionis, Mathematics Institute and Centre for Complex Systems, University of Warwick, Coventry, UK

Peter Schuster, Theoretical Chemistry and Structural Biology, University of Vienna, Vienna, Austria

Jürgen Kurths, Nonlinear Dynamics Group, University of Potsdam, Potsdam, Germany

Linda Reichl, Department of Physics, Prigogine Center for Statistical Mechanics, University of Texas, Austin, USA

Frank Schweitzer, System Design, ETH Zurich, Zurich, Switzerland

Didier Sornette, Entrepreneurial Risk, ETH Zurich, Zurich, Switzerland

# Springer Series in Synergetics

Founding Editor: H. Haken

The Springer Series in Synergetics was founded by Herman Haken in 1977. Since then, the series has evolved into a substantial reference library for the quantitative, theoretical and methodological foundations of the science of complex systems.

Through many enduring classic texts, such as Haken's *Synergetics and Information and Self-Organization*, Gardiner's *Handbook of Stochastic Methods*, Risken's *The Fokker Planck-Equation* or *Haake's Quantum Signatures of Chaos*, the series has made, and continues to make, important contributions to shaping the foundations of the field.

The series publishes monographs and graduate-level textbooks of broad and general interest, with a pronounced emphasis on the physico-mathematical approach.

For further volumes: http://www.springer.com/series/712

Oleg G. Bakunin

# Chaotic Flows

Correlation Effects, Transport, and Structures





Oleg G. Bakunin
"Kurchatov Institute"
Plasma Physics Department
Kurchatova Square 1
123182 Moscow
Russia
oleg\_bakunin@yahoo.com

ISSN 0172-7389 ISBN 978-3-642-20349-7 e-ISBN 978-3-642-20350-3 DOI 10.1007/978-3-642-20350-3 Springer Heidelberg Dordrecht London New York

Library of Congress Control Number: 2011937176

#### © Springer-Verlag Berlin Heidelberg 2011

This work is subject to copyright. All rights are reserved, whether the whole or part of the material is concerned, specifically the rights of translation, reprinting, reuse of illustrations, recitation, broadcasting, reproduction on microfilm or in any other way, and storage in data banks. Duplication of this publication or parts thereof is permitted only under the provisions of the German Copyright Law of September 9, 1965, in its current version, and permission for use must always be obtained from Springer. Violations are liable to prosecution under the German Copyright Law.

The use of general descriptive names, registered names, trademarks, etc. in this publication does not imply, even in the absence of a specific statement, that such names are exempt from the relevant protective laws and regulations and therefore free for general use.

Printed on acid-free paper

Springer is part of Springer Science+Business Media (www.springer.com)



# **Preface**

The aim of this book is to summarize the current ideas and theories about the basic mechanisms for transport in chaotic flows. The dispersion of matter and heat in chaotic or turbulent flows is generally analyzed in different ways. The establishment of a paradigm for turbulent transport can substantially affect the development of various branches of physical sciences and technology. Thus, chaotic transport and mixing are intimately connected with turbulence, plasma physics, Earth and natural sciences, and various branches of engineering.

Since this book is on theory, it uses mathematics freely. This is a book on physical science, not on mathematics. The level of mathematics used should not be beyond that of a graduate student in physics since turbulent transport is a subject of which at least a basic understanding is essential in engineering and in many of the natural sciences. It was not written as a course that might be followed and used to introduce students to turbulence. Rather, it is a text useful for those beginning or already involved in research. It might form the basis of a number of advanced courses about plasma physics or ocean physics. In addition, this book contains material expanded from recent extended review articles.

My previous book "Turbulence and diffusion. Scaling versus equations" published by Springer in 2008 was devoted to the scaling concept, which plays a central role in the analysis of very complex systems. The goal was to present how scaling and renormalization technique might be applied to turbulent transport in plasma and to cover as many examples as possible. On the contrary, this new work is focused on the detailed description of the most often used theoretical models. This allows one to apply with confidence the phenomenological arguments and correlation methods to treat complex phenomena in many branches of the physical science. I thoroughly consider random shear flows, Richardson's relative dispersion, and convective turbulence, but the plasma physics problems are not the focus of our interest in this book. I have tried to include a number of examples apart from the standard ones, including in particular chaotic mixing in microchannels, scaling for strong convective turbulence, percolation models of turbulent transport, etc.

viii Preface

Part I of the book consists of three chapters, which contain a reasonably standard introduction to diffusion phenomena. In Part II, we give a brief but self-contained introduction to the Lagrangian description of chaotic flows. Part III contains discussions of phenomenological models of turbulent transport on the basis of the conventional diffusive equation. We briefly review the fractal concept and consider different models of random shear flows in Part IV. The percolation approach and fractional equations to analyze anomalous transport are presented in Part V. In Part VI, we study the cascade phenomenology and relative dispersion problem. The focus of Part VII is to provide an overview of the convective turbulence. In the last Part, we treat correlation effects and transport scaling in the presence of coherent structures and flow topology reconstruction.

The illustrations are an important supplement to the text. It is through figures that information is carried most readily, and often in the most pleasurable form, to the mind and memory of a reader.

Lists of suggested further reading are provided at the end of each chapter. These are of literature that students might be expected to peruse, if not read in detail, in the course of their study of the contents of the chapter, e.g., to appreciate better the historical derivation of knowledge. Also listed are reference works that will provide information about basic fluid dynamics or ocean physics, should it be required. In conclusion, we note that the table of contents is essentially self-explanatory.

The author thanks Profs. B.Cushman-Roisin, N.Erokhin, C.Gibson, G.Golitsyn, V.Kogan, E.Kuzntsov, F.Parchelly, T.Schep, V.Shafranov, A.Timofeev, E.Yurchenko, and G.Zaslavsky for the useful discussions and support.

Lawrence, KS, USA

O.G. Bakunin

# **Contents**

## Part I Diffusion and Correlations

1	Introduction	3
	1.1 Diffusion Phenomenon	. 3
	1.2 Self-Similar Solutions	. 7
	1.3 Inhomogeneous Media and Nonlinear Effects	11
	1.4 Periodic Media and Diffusion at Large Scales	
	Further Reading	
2	Advection and Transport	21
	2.1 Advection–Diffusion Equation	
	2.2 Transport and One-Dimensional Hydrodynamics	
	2.3 Advection in Two-Dimensional Shear Flow	
	2.4 Effective Diffusivity and Advection	
	2.5 Fluctuation Effects in Scalar Transport	
	2.6 The Zeldovich Scaling for Effective Diffusivity	
	Further Reading	
3	The Langevin Equation and Transport	27
3		
	3.1 Brownian Motion and Diffusion	
	3.2 Mean Square Velocity and Equipartition	
	3.3 Autocorrelation Function	
	3.4 Velocity Distribution Function	
	3.5 Kinetics and Diffusion Equation	46
	Further Reading	49

x Contents

Part II	Lagrangian	Description
		2 coer peron

4	Lagrangian Description of Chaotic Flows	53
	4.1 The Taylor Diffusion and Correlation Concept	53
	4.2 The Boltzmann Law Renormalization	56
	4.3 Turbulent Transport and Scaling	58
	4.4 Anomalous Diffusion in Turbulent Shear Flows	59
	4.5 Seed Diffusivity and Turbulent Transport	62
	Further Reading	67
5	Lagrangian Chaos	69
	5.1 The Arnold–Beltrami–Childress Chaotic Flow	69
	5.2 Hamiltonian Systems and Separatrix Splitting	73
	5.3 Stochastic Instability and Single-Scale Approximation	76
	5.4 Chaotic Mixing in Microchannels	80
	5.5 Multiscale Approximation	83
	Further Reading	85
	rt III Phenomenological Models	00
6	Correlation Effects and Transport Equations	89
	6.1 Averaging and Linear-Response	89
	6.2 Correlations and Phenomenological Transport Equation	93
	6.3 Heavy Particles in Chaotic Flow	95
	6.4 The Quasilinear Approach and Phase-space	
	6.5 The Dupree Approximation	100
	6.6 Renormalization Theory Revisited	102
	Further Reading	105
7	The Taylor Shear Dispersion	107
	7.1 Dispersion in Laminar Flow	107
	7.2 Scalar Distribution Function	111
	7.3 Transport in Coastal Basins	114
	7.4 The Taylor Approach to Chaotic Flows	116
	* **	
	7.5 The Lagrangian Mixing in Turbulent Flow in a Pipe	119
	<ul><li>7.5 The Lagrangian Mixing in Turbulent Flow in a Pipe</li><li>7.6 The Taylor Dispersion and Memory Effects</li></ul>	121
	7.5 The Lagrangian Mixing in Turbulent Flow in a Pipe	

Contents xi

Par	t IV Fractals and Anomalous Transport	
8	Fractal Objects and Scaling	129
Ü	8.1 Fractal Dimensionality	129
	8.2 Seacoast Length and the Mandelbrot Scaling	131
	8.3 Fractal Topology and Intersections	134
	8.4 Self-avoiding Random Walks	137
	8.5 Two-Dimensional Random Flows and Topography	139
	Further Reading	143
9	Random Shear Flows and Correlations	145
	9.1 Autocorrelation Function for Fluids	145
	9.2 Superdiffusion and Return Effects	147
	9.3 Longitudinal Diffusion and Quasilinear Equations	150
	9.4 Random Shear Flows and Generalized Scaling	151
	9.5 Isotropization and Manhattan flow	153
	9.6 Diffusion in Power-Law Shear Flows	157
	9.7 The Fisher Relation	160
	Further Reading	161
Par	t V Structures and Nonlocal Effects	
10	Transport and Complex Structures	165
	10.1 Bond Percolation Problem	165
	10.2 Fractal Dimensionality and Percolation	167
	10.3 Finite Size Scaling	169
	10.4 Comb Structures and Percolation Transport	170
	10.5 Hilly Landscape and Percolation	171
	10.6 Phenomenological Arguments for Percolation Parameter	174
	10.7 Subdiffusion and Percolation	176
	Further Reading	178
11	Fractional Models of Anomalous Transport	181
	11.1 Random Walks Generalization	181
	11.2 Functional Equation for Return Probability	184

11.3 Ensemble of Point Vortices and the Holtsmark Distribution .....

11.4 Fractal Time and Scaling .....

11.5 Fractional Derivatives and Anomalous Diffusion ......

11.6 Comb Structures and the Fractional Fick Law .....

11.7 Diffusive Approximation and Random Shear Flows ......

186

189

192

194

199

xii Contents

Par	t VI	Isotropic Turbulence and Scaling	
12	Isotı	opic Turbulence and Spectra	205
		The Reynolds Similarity Law	205
		Cascade Phenomenology	207
		The Taylor Microscale	211
		Dissipation and Kolmogorov's Scaling	213
		Acceleration and Similarity Approach	215
		ner Reading	216
13	Turl	bulence and Scalar	219
10		Scalar in Inertial Subrange	219
		The Batchelor Scalar Spectrum	222
		The Small Prandtl Number and Scalar Spectrum	225
		Seed Diffusivity and Turbulent Transport	227
		Fluctuation–Dissipative Relation and Cascade Arguments	228
		ner Reading	229
		· · · · · · · · · · · · · · · · · · ·	
14	Rela	tive Diffusion and Scaling	231
		The Richardson Law and Anomalous Transport	231
		The Batchelor Intermediate Regime	234
		Dissipation Subrange and Exponential Regime	237
		Gaussian Approximations and Relative Dispersion	239
		Fractional Equation Approach	242
		Turbulence Scaling and Fractality	244
		ner Reading	246
15	Two	-Dimensional Turbulence and Transport	249
	15.1	Two-Dimensional Navier–Stokes Equation	249
	15.2	Inverse Cascade	252
	15.3	Freely Evolving Two-Dimensional Turbulence	255
	15.4	Scalar Spectra in Two-Dimensional Turbulence	256
	15.5	Atmospheric Turbulence and Relative Dispersion	258
	15.6	Rough Ocean and Richardson's Scaling	260
	Furtl	ner Reading	263
Par	t VII	Convection and Scaling	
16	Con	vection and Rayleigh Number	267
		Buoyancy Forces	267
		The Oberbeck–Boussinesq Equations	269
		The Rayleigh–Benard Instability	270
		The Lorenz Model and Strange Attractor	274
		ner Reading	278

Contents xiii

17	Convection and Turbulence	279
	17.1 The Obukhov–Golitsyn Scaling for Turbulent Convection	279
	17.2 Quasilinear Regimes of Turbulent Convection	281
	17.3 Strong Convective Turbulence	283
	17.4 Diffusive Growth of Boundary Layer	285
	17.5 Chicago Scaling	287
	17.6 Turbulent Thermal Convection and Spectra	291
	Further Reading	293
Par	t VIII Structures and Complex Flow Topology	
18	Coherent Structures and Transport	297
	18.1 Regular Structures	297
	18.2 Scaling for Diffusive Boundary Layer	300
	18.3 Anomalous Transport in a Roll System	303
	18.4 Convection Towers and Thermal Flux	306
	18.5 Random Flow Landscape and Transport	308
	18.6 Transient Percolation Regime	314
	Further Reading	316
19	Flow Topology Reconstruction and Transport	319
	19.1 High-Frequency Regimes	319
	19.2 Time Dependence and the Taylor Shear Flow	321
	19.3 Oscillatory Rolls and Lobe Transport	324
	19.4 Flow Topology Reconstruction and Scaling	329
	Further Reading	333
Ref	erences	335
Ind	ex	345

# Part I Diffusion and Correlations

# Chapter 1 Introduction

#### 1.1 Diffusion Phenomenon

In this book, our attention is concentrated mainly on the underlying phenomenon of the diffusive action of chaotic flows (turbulence). Indeed, we shall be concerned with the subject of passive scalar transport, where by "scalar" we mean something like small particle or chemical species concentration and by "passive" we mean that the added substance does not change the nature of fluid to the point where turbulence is appreciably affected.

By designating the number of particles per unit of volume by  $n(\vec{r},t)$  and the flow of atoms or molecules by  $\vec{q}$ , that is, the number of particles crossing a unit of surface area per unit of time in concentration gradient  $\nabla n$ , we then have the following equation, which is Fick's first law for diffusion

$$\vec{q} = -D\nabla n,\tag{1.1.1}$$

where D is the diffusion coefficient. The diffusion coefficient D characterizes the migration of particles of a given kind in a given medium at a given temperature. It depends on the size of the particle, the structure of the medium, and the absolute temperature (for a small molecule in water at room temperature  $D \approx 10^{-5} \, \mathrm{cm}^2/\mathrm{s}$ ).

The "-" sign accounts for the fact that the flow and concentration gradient are of opposite sings. If the phase is pure, D is the self-diffusion coefficient. By taking into account the continuity equation:

$$\frac{\partial n}{\partial t} + \nabla \cdot \vec{q} = 0, \tag{1.1.2}$$

we have the general equation for three-dimensional diffusion:

$$\frac{\partial n}{\partial t} = D\nabla^2 n. \tag{1.1.3}$$

This equation states that the time rate of change in concentration is proportional to the curvature of the concentration function with the diffusion coefficient D (see Fig. 1.1.1). This equation is Fick's second law for diffusion. It does not have a simple solution particularly for a three-dimensional system.

The form of the problem generally solved with respect to the above applications of diffusion theory is the initial value problem, i.e., to determine the concentration distribution  $n(\vec{r},t)$  at time t when the initial distribution  $n(\vec{r},0)$  is known. Since much of our subsequent discussion is concerned with unbounded domains in the dependent variable, we present the solution of the initial value problem on an infinite one-dimensional domain. Let the Fourier transform of the concentration distribution be denoted by

$$\tilde{n}_k(t) = \int_{-\infty}^{\infty} n(x, t) e^{ikx} dx.$$
 (1.1.4)

Then if we multiply the one-dimensional form of the diffusion equation by  $e^{ikx}$  and integrate over all space, we find

$$\frac{\partial \tilde{n}_k(t)}{\partial t} = D \int_{-\infty}^{\infty} e^{ikx} \frac{\partial^2}{\partial x^2} n(x, t) dx.$$
 (1.1.5)

Now suppose that

$$n(\pm \infty, t) = 0$$
 and  $\frac{\partial}{\partial x} n(x, t) \Big|_{x=+\infty} = 0.$  (1.1.6)

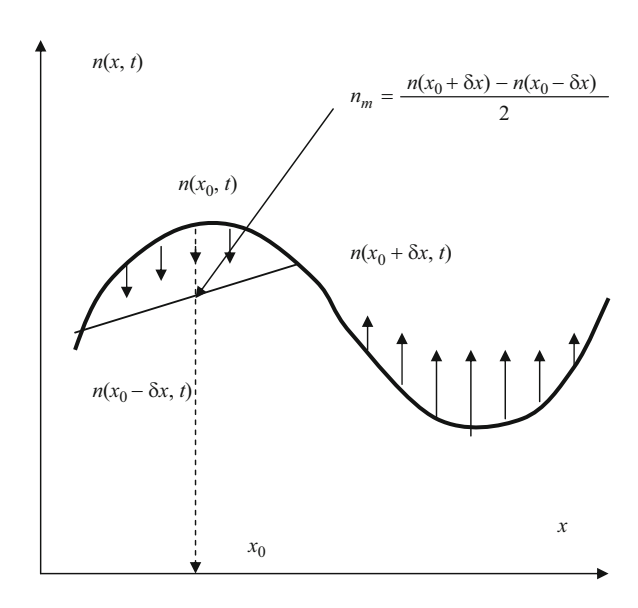


Fig. 1.1.1 Schematic illustration of the concentration profile evolution

Then upon integrating (1.1.5) by parts twice, we obtain

$$\frac{\partial}{\partial t}\tilde{n}_k(t) = -Dk^2\tilde{n}_k(t),\tag{1.1.7}$$

so that if  $\tilde{n}_k(0)$  is the Fourier transform of the initial concentration distribution, we have as the solution to

$$\tilde{n}_k(t) = e^{-Dk^2t}\tilde{n}_k(0).$$
 (1.1.8)

Hence, upon Fourier inversion we see that

$$n(x,t) = \frac{1}{2\pi} \int_{-\infty}^{\infty} dk \exp(-Dk^2t) \int_{-\infty}^{\infty} e^{ik(x-x')} n(x',0) dx'.$$
 (1.1.9)

If we interchange the order of the k and x integrations in this expression, we obtain

$$P(x - x'; t) = \frac{1}{2\pi} \int_{-\infty}^{\infty} e^{ik(x - x')} \exp(-Dtk^2) dk = \frac{1}{\sqrt{4\pi Dt}} \exp\left(-\frac{(x - x')^2}{4Dt}\right)$$
(1.1.10)

which is a special case of the traditional Gauss distribution

$$P(x) = \frac{1}{\sqrt{2\pi R^2}} \exp\left(-\frac{x^2}{2R^2}\right)$$
 (1.1.11)

with a time-dependent dispersion  $R(t) = \sqrt{2Dt}$ . The function P(x - x'; t) is the probability that a particle initially at x' diffuses to the point x in time t, so that the Fourier representation of the particle distribution function can be also rewritten as

$$n(x,t) = \int_{-\infty}^{\infty} P(x - x') n(x', 0) dx'.$$
 (1.1.12)

Here, it is clear that diffusion smoothly fills the available space  $\langle x^2 \rangle = 2Dt$ , where  $\langle x^2 \rangle$  is the mean square distance being covered. In terms of the transport scaling, one obtains

$$R(t) = \langle x^2 \rangle^{1/2} = (2Dt)^{1/2} \propto t^{1/2}.$$
 (1.1.13)

Displacement is not proportional to time but rather to the square root of the time; therefore, there is no such a notion as a diffusion velocity. This is an important result. Thus, the shorter period of observation t corresponds to the larger apparent velocity. This is an absurd estimate and we discuss this problem bellow. The definition of the diffusion coefficient,

$$D = \frac{\Delta_{\text{COR}}^2}{2\tau_{\text{COR}}},\tag{1.1.14}$$

is based on using the notions of the correlation length  $\Delta_{COR}$  and the correlation time  $\tau_{COR}$ . If the values of time and length are smaller than the correlation values, then the motion of particles has a ballistic character; whereas if these values are larger than the correlation scales, we deal with the diffusion mechanism  $R(t) \propto t^{1/2}$ .

The key problem in investigating diffusion in chaotic medium (turbulent flows) is the choice of the correlation scales responsible for the effective transport. This is not surprising, because models of transport in chaotic flows differ significantly from one-dimensional transport models [1, 2]. Indeed, chaotic velocity field generates fluctuations of various scalar quantities in the flow: concentration, temperature, humidity, and so on (see Fig. 1.1.2). Often, several different types of transports are present simultaneously in turbulent diffusion. In chaotic flows, among eddies could appear complex vortex structures, and the competition between the strain and rotation determines whether the material line will align (see Fig. 1.1.3). Therefore, by taking into account the initial diffusivity (seed diffusion), anisotropy, stochastic instability, and reconnection of streamlines, the presence of coherent structures, etc., appears to be important.

For three-dimensional case, the diffusion equation takes the form

$$\frac{\partial n}{\partial t} = D\nabla^2 n(x, y, z, t) = D \left[ \frac{\partial^2 n}{\partial x^2} + \frac{\partial^2 n}{\partial y^2} + \frac{\partial^2 n}{\partial z^2} \right], \tag{1.1.15}$$

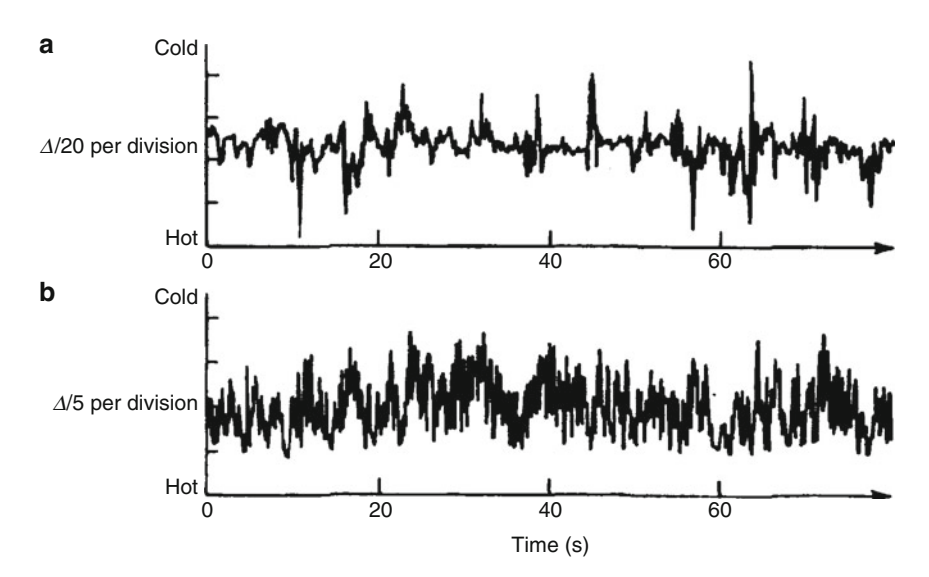


Fig. 1.1.2 Time recording of the temperatures in the hard convective turbulence regime,  $Ra = 2.1 \times 10^9$ . (After Castaing et al. [3] with permission)

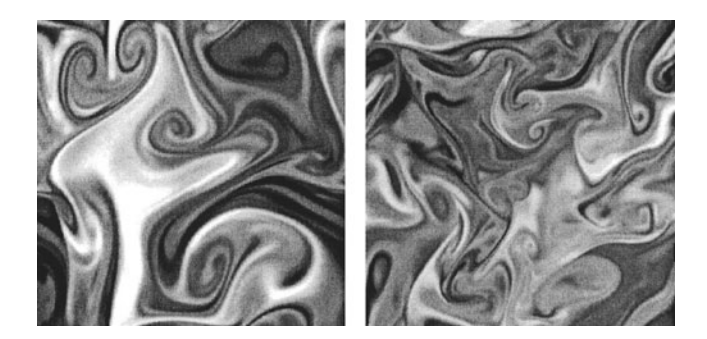


Fig. 1.1.3 The scalar distribution on a two-dimensional plane (After Brethouwer et al. [2] with permission)

where, for instance, the particle flux in the x direction is given by

$$q_x = -D\frac{\partial n(x, y, z)}{\partial x}. (1.1.16)$$

Here,  $\nabla^2$  is the Laplace operator.

In the case of spherical symmetry, one obtains

$$\frac{\partial n}{\partial t} = D \frac{1}{r^2} \frac{\partial}{\partial r} \left[ r^2 \frac{\partial n}{\partial r} \right]. \tag{1.1.17}$$

Then, we find the point source solution in the well-known form

$$n(r,t) = \frac{N_{\rm p}}{(4\pi Dt)^{3/2}} e^{-r^2/4Dt},$$
(1.1.18)

where  $N_p$  is the number of particles. This is a three-dimensional Gaussian distribution. The concentration remains highest at the source, but it decreases there as the three halves power of the time. An observer at radius r sees a wave that peaks at  $t = r^2/6D$ . Diffusion phenomena are at the heart of irreversible statistical mechanics, since the form of the diffusion equation shows that the solution must depend on the sign of t. Here, we are dealing with a phenomenon in which it matters whether t decreases or increases.

#### 1.2 Self-Similar Solutions

The Fourier procedure is effective to solve linear equations only. However, there is no escape from consideration of nonlinear problems because they are of acute interest in relation to investigation of transport and mixing in chaotic flows. There is

no unique recipe to solve nonlinear equations; therefore, we consider here a nonuniversal but widely applied self-similar approach. Near the end of the nineteenth century, Boltzmann noted in the study of the linear diffusion equation that the two independent variables space x and time t could be combined into a new variable  $\xi$ , where  $\xi = \xi(x, y)$ . With this new variable, the diffusion equation (partial differential equation) could be transformed into an ordinary differential equation. The Boltzmann "ansatz" was given as follows:

$$\xi(x,t) = \frac{x}{t^{1/2}}. (1.2.1)$$

Thus, he suggested to construct self-similar variables and to examine the self-similar behavior of partial differential equations [4–7]. In order to find the similarity variables, we use the Lie theory of groups where it has been shown that the similarity variables are identical to the invariants of a particular one (or more) parameter group of transformations. We briefly consider the procedure, details, and references that can be found in [7–9]. We shall examine the one-dimensional linear diffusion equation:

$$\frac{\partial n(x,t)}{\partial t} = \frac{\partial^2 n(x,t)}{\partial x^2}.$$
 (1.2.2)

We define one parameter group G as follows:

$$G = \begin{cases} n = a_{L}^{\alpha_{G}} \bar{n} \\ x = a_{L}^{\beta_{G}} \bar{x} \\ t = a_{L}^{\gamma_{G}} \bar{t} \end{cases}$$
 (1.2.3)

Here,  $a_{\rm L}$  is positive and real. This is called the "linear group." The exponents  $\alpha_G$ ,  $\beta_G$ , and  $\gamma_G$  are constants, which are defined such that the equation under consideration equation is "(absolutely) constant conformally invariant" under the group G. A function F(y) is said to be "constant conformally invariant" under G if

$$F(y) = f(a_L)F(\bar{y}),$$
 (1.2.4)

where  $f(a_L)$  is some function of the parameter  $a_L$ . If  $f(a_L) \equiv 1$ , the constant conformal invariance is called "absolute."

Thus, substitution of the new variables leads to

$$a_{\rm L}^{\alpha_G - 2\beta_G} \frac{\partial^2 \bar{n}}{\partial \bar{x}^2} - a_{\rm L}^{\alpha_G - \gamma_G} \frac{\partial \bar{n}}{\partial \bar{t}} = 0. \tag{1.2.5}$$

For this equation to be conformally invariant under the transformation group G, one requires

$$\alpha_G - 2\beta_G = \alpha_G - \gamma_G$$
 or  $\gamma_G = 2\beta_G$ . (1.2.6)

We will define these constants later. Let us now consider the "invariants" of the transformation group G. The invariants are obtained from the condition  $\hat{Q}I \equiv 0$ . Here, I is an invariant and  $\hat{Q}$  is the operator

$$\hat{Q} = \frac{\partial \bar{n}}{\partial a_{L}} \bigg|_{a_{L}=1} \frac{\partial}{\partial n} + \frac{\partial \bar{x}}{\partial a_{L}} \bigg|_{a_{L}=1} \frac{\partial}{\partial x} + \frac{\partial \bar{t}}{\partial a_{L}} \bigg|_{a_{L}=1}$$

$$\frac{\partial}{\partial t} = -\alpha_{G} n \frac{\partial}{\partial n} - \beta_{G} x \frac{\partial}{\partial x} - \gamma_{G} t \frac{\partial}{\partial t}$$
(1.2.7)

The solutions of the equation under consideration,  $\hat{Q}I \equiv 0$ , can be obtained by solving the Lagrange subsidiary equations

$$\frac{\mathrm{d}n}{-\alpha_G n} = \frac{\mathrm{d}x}{-\beta_G x} = \frac{\mathrm{d}t}{-\gamma_G t}.$$
 (1.2.8)

These "invariants" are the self-similar variables. Solutions of this equation are given by

$$\phi(\xi) = \frac{n(x,t)}{t^{\alpha_G/\gamma_G}},\tag{1.2.9}$$

$$\xi(x,t) = \frac{x}{t^{\beta_G/\gamma_G}},\tag{1.2.10}$$

where  $\gamma_G=2\beta_G$  .One can see that the Boltzmann transformation is recovered.

Having found the self-similar variables, let us transform the diffusion equation, using the new variables  $\phi$  and  $\xi$  into an ordinary differential equation

$$\frac{\partial^2 \phi}{\partial \xi^2} + \frac{\xi}{2} \frac{\partial \phi}{\partial \xi} - \frac{\alpha_G}{\gamma_G} \phi = 0. \tag{1.2.11}$$

The solution can be written in terms of complementary error function as follows:

$$\phi = Ai^{2\frac{2G}{\gamma_G}}\operatorname{erfc}\left(\frac{\xi}{2}\right) + Bi^{2\frac{2G}{\gamma_G}}\operatorname{erfc}\left(-\frac{\xi}{2}\right),\tag{1.2.12}$$

where  $i^{2\alpha_G/\gamma_G}$  is an ordering parameter and

$$i^{-1} \operatorname{erfc} \frac{\xi}{2} = \frac{2}{\sqrt{\pi}} e^{-\xi^{2/4}}, i^0 \operatorname{erfc} \frac{\xi}{2} = \operatorname{erfc} \frac{\xi}{2},$$
 (1.2.13)

$$i^k \operatorname{erfc} \frac{\xi}{2} = \int_{\frac{\xi}{2}}^{\infty} i^{k-1} \operatorname{erfc} t \, dt; \quad k = 0, 1, 2, \dots$$
 (1.2.14)

At this stage, the parameter  $\alpha_G/\gamma_G$  is still arbitrary.

Now we specify boundary conditions or a conservation law. Boundary conditions on particle density,  $n(x \to \infty, t) = 0$ , n(x, t = 0) = 0, have necessarily "consolidated" into one for  $\phi$ . Thus, one obtains the boundary condition for the self-similar variable  $\xi$  in the form  $\phi(\xi \to \infty) = 0$ . The third boundary condition could have one of two forms, which would yield self-similar solutions. They are  $n \times (x = 0, t) = \text{const}$  or in terms of the normalization condition (the conservation law)

$$\int_{0}^{\infty} n(x,t) dx = \text{const.}$$
 (1.2.15)

Since n(x=0,t) transforms to  $\phi(\xi=0)$ , we can see that n(x=0,t)= const requires that  $\alpha_G/\gamma_G=0$ . The self-similar solution of the diffusion equation for this boundary condition is

$$n(x,t) = \phi(\xi) = A \operatorname{erfc}\left(\frac{\xi}{2}\right) = A \operatorname{erfc}\left(\frac{x}{2\sqrt{t}}\right).$$
 (1.2.16)

The conservation law should be also invariant under the group transformation in order to have similarity solutions

$$\int_0^\infty n(x,t)\mathrm{d}x = a_\mathrm{L}^{\alpha_G + \beta_G} \int_0^\infty \bar{n}\mathrm{d}\bar{x}.$$
 (1.2.17)

For this to be conformally invariant, we have the relationship in the form

$$\frac{\alpha_G}{\gamma_G} = -\frac{\beta_G}{\gamma_G} = -\frac{1}{2}.\tag{1.2.18}$$

The self-similar solution that satisfies this conservation law and the boundary conditions are given by

$$n(x,t) = \frac{\phi}{\sqrt{t}} = \frac{2A'}{\sqrt{\pi}\sqrt{t}} e^{-\frac{x^2}{4t}},$$
 (1.2.19)

where the constant A' can be determined from the normalization condition.

This similarity solution was also found by direct physical and dimensional arguments. The intensive search for self-similar solution is motivated by the desire for a deeper understanding of the physical phenomena described by transport equations. Simple scaling arguments to built similarity solutions (self-similar solution of the first kind) were lucidly given in [8–11]. On the other hand, it is now clear the role of self-similar solution as intermediate asymptotic, which describes the behavior of solutions of wider class models in the ranges where they no longer depend on certain details. Thus, self-similar solutions provide important clues to a

wider class of solution of the original partial differential equations [12–16]. In the next section, we apply the procedure described here to several interesting examples.

### 1.3 Inhomogeneous Media and Nonlinear Effects

In studies of the evolution of the distribution function of particles in complex systems, it has been found that the mixing problem in inhomogeneous media could be modeled with a diffusion equation in the form

$$\frac{\partial n}{\partial t} = \frac{\partial}{\partial x} \left( x^{m_{\rm D}} \frac{\partial n}{\partial x} \right). \tag{1.3.1}$$

Here, we continue our treatment of self-similar solutions by the discussion of a fairly special class of self-similar solutions, which are named "self-similar solution of the second kind." In contrast to self-similar solutions of the first kind for which the similarity exponent is determined by dimensional arguments alone in this new case, the similarity exponent could be found in the process of solving the eigenvalues problem. Here, the dimensional consideration is not sufficient [7, 8].

Thus, using the linear group G defined above, we find the self-similar variables to be

$$\xi(x,t) = \frac{x}{\frac{1}{t^{2-m_{\rm D}}}} \tag{1.3.2}$$

and

$$\phi(\xi) = \frac{n(x,t)}{\frac{x_G}{t^2G}}.$$
(1.3.3)

Then the equation under analysis transforms to the expression

$$\frac{\alpha_G}{\gamma_G}\phi + \frac{\xi}{m_D - 2}\frac{\partial\phi}{\partial\xi} = \frac{\partial}{\partial\xi}\left(\xi^{m_D}\frac{\partial\phi}{\partial\xi}\right). \tag{1.3.4}$$

The requirement of "consolidation" specifies that

$$\frac{\beta_G}{\gamma_G} = \frac{1}{2 - m_D} > 0 \quad \text{or} \quad m_D < 2.$$
 (1.3.5)

The constant  $\alpha_G/\gamma_G$  can be specified by boundary conditions. The solutions for the two cases

$$n(0,t) = \text{const}$$
 and  $\int_0^\infty n(x,t) dx = \text{const}$  (1.3.6)

are given by the formulas

$$n(x,t) = K\left(\int \frac{1}{\xi^{m_{\rm D}}} \exp\left[-\frac{\xi^{2-m_{\rm D}}}{(2-m_{\rm D})^2}\right] d\xi - 1\right)$$
(1.3.7)

and

$$n(x,t) = \frac{K}{t^{\frac{1}{2-m_{\rm D}}}} \exp\left[-\frac{x^{2-m_{\rm D}}}{t(2-m_{\rm D})^2}\right],\tag{1.3.8}$$

respectively, where K is a constant.

On the other hand, many complex transport phenomena can be modeled with the nonlinear diffusion equation

$$\frac{\partial n}{\partial t} = \frac{\partial}{\partial x} \left( n^{m_{\rm N}} \frac{\partial n}{\partial x} \right). \tag{1.3.9}$$

For example, in studying of mixing it has been shown that the governing equation often has the nonlinear form because the diffusion coefficient for particles depends on the density of particles [6–9]. For such problems, the self-similar variables are of the form

$$\xi(x,t) = \frac{x}{t^{\beta_G/\gamma_G}} \tag{1.3.10}$$

and

$$\phi(\xi) = \frac{n}{\frac{1}{\ell^{m_N}} \left( 2 \frac{\beta_G}{\gamma_G} - 1 \right)},$$
(1.3.11)

where the parameter  $\beta_G/\gamma_G$  is chosen to satisfy the boundary conditions or conservation laws and  $\phi$  satisfies

$$\frac{\partial}{\partial \xi} \left( \phi^{m_{\rm N}} \frac{\partial \phi}{\partial \xi} \right) + \frac{\beta_G}{\gamma_G} \xi \frac{\partial \phi}{\partial \xi} - \frac{1}{m_{\rm N}} \left( 2 \frac{\beta_G}{\gamma_G} - 1 \right) \phi = 0. \tag{1.3.12}$$

We can again apply the boundary conditions considered above and then find that

$$\frac{\beta_G}{\gamma_G} = -\frac{1}{m_N} \left( 2 \frac{\beta_G}{\gamma_G} - 1 \right). \tag{1.3.13}$$

The equation for  $\phi$  can be directly integrated to yield

$$\phi(\xi) = \begin{cases} = \left(1 - \left(\frac{m_{N}}{m_{N}+2}\right)^{\frac{\xi^{2}}{2}}\right)^{\frac{1}{m_{N}}} & \xi < \xi_{0}, \\ = 0 & \xi > \xi_{0} \end{cases}$$
(1.3.14)

where

$$\xi_0 = \left(\frac{2(m_{\rm N}+2)}{m_{\rm N}}\right)^{\frac{1}{2}}, \quad m_{\rm N} > 0.$$
 (1.3.15)

This could be considered a "sharpfront" solution in that

$$\phi^{m_{\rm N}+1}(\xi=\xi_0)=0\tag{1.3.16}$$

and

$$\frac{\mathrm{d}\phi^{m_{\mathrm{N}}+1}}{\mathrm{d}\xi}\bigg|_{\xi=\xi_{0}} = 0. \tag{1.3.17}$$

The motion of a front is given by scaling

$$x_{\text{front}}(t) \propto Q^{\frac{m_{\text{N}}}{m_{\text{N}}+2}} t^{\frac{1}{m_{\text{N}}+2}},$$
 (1.3.18)

where

$$n(x,0) = Q\delta(x). \tag{1.3.19}$$

and hence

$$\int_{-\infty}^{+\infty} n(x,t) dx = Q = \text{const}, \quad t \ge 0.$$
 (1.3.20)

Figure 1.3.1 demonstrates the distribution of heat wave front. The velocity of the front is

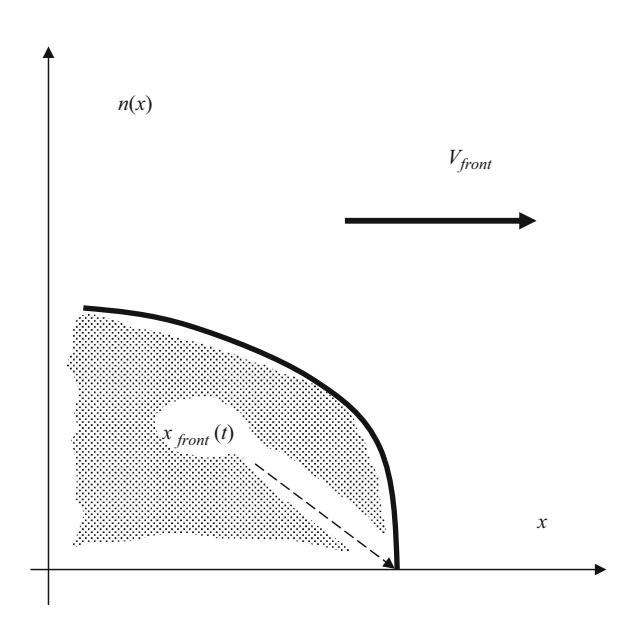
$$V_{\text{front}}(t) = \frac{dx_{\text{front}}}{dt} \propto Q^{\frac{m_{\text{N}}}{m_{\text{N}}+2}} t^{-\frac{m_{\text{N}n}+1}{m_{\text{N}}+2}}.$$
 (1.3.21)

The velocity  $V_{\text{front}}(t)$  decreases in time, but the front infinitely penetrates since  $x_{\text{front}}(t) \to \infty$  when  $t \to \infty$ .

If  $m_N > 1$ , the density gradient infinitely grows,

$$\left| \frac{\partial n}{\partial x} \right| \to \infty \text{ as } x \to \pm x_{\text{front}} \mp 0.$$
 (1.3.22)

Fig. 1.3.1 Schematic illustration of the concentration front propagation. Here  $V_{\text{front}}$  is the velocity of the heat front and  $x_{\text{front}}$  is the position of the heat front



Despite an infinite growth of the density gradient, the particle flux

$$q = -k_0 n^{m_N} \frac{\partial n}{\partial x} \tag{1.3.23}$$

tends to zero when  $x \to x_{\text{front}}(t) - 0$ .

When  $\sigma_n \to 0$ , we see

$$n(x,t) = \frac{Q}{2\sqrt{\pi t}} \frac{1}{e^{\frac{x^2}{4t}}}.$$
 (1.3.24)

This expression describes the conventional particle flux distribution for the case of classical linear diffusion equation.

Self-similarity is not the panacea to solve all problems. Some difficulties related to the ordinary differential equations may not be amenable to solution, neither analytical nor numerical. Moreover, even by solving mathematically, the solution may not describe a physically interesting phenomenon. Indeed, the technique considered above is limited to problems where neither scale length nor time scales such as fixed boundaries exist in the problem.

# 1.4 Periodic Media and Diffusion at Large Scales

In this section, we treat a fruitful multiscale technique for the construction of "macroscopic" equations from "microscopic" dynamics in terms of passive scalar transport. Let us begin with a presentation of the basic ingredients of the method,

which allows us to derive the effective diffusion coefficient  $D_{\text{eff}}$  from the transport equation in one spatial dimension:

$$\frac{\partial}{\partial t}n = \frac{\partial}{\partial x}\left(D(x)\frac{\partial}{\partial x}n\right),\tag{1.4.1}$$

where D(x) is a periodic function with the period  $L_0$  (see Fig. 1.4.1). We will find  $D_{\rm eff}$  in terms of D(x). Our aim is to write an effective diffusion equation valid at long time and large scales, which are much larger than the period  $L_0$ .

First we calculate the value  $n_b - n_a$ , where points a and b are the boundary points. One can represent this value in the discrete form as

$$n_b - n_a = \sum_i \Delta n_i, \tag{1.4.2}$$

where

$$D(x_i)\frac{\Delta n_i}{\Delta x_i} = q(x_i). \tag{1.4.3}$$

In the steady case and in the absence of internal sources, the flux does not depend on the spatial variable,  $q = q_{\text{eff}} = inv$ . This allows one to compute

$$n_b - n_a = \sum_i q \frac{\Delta x_i}{D(x_i)}. (1.4.4)$$

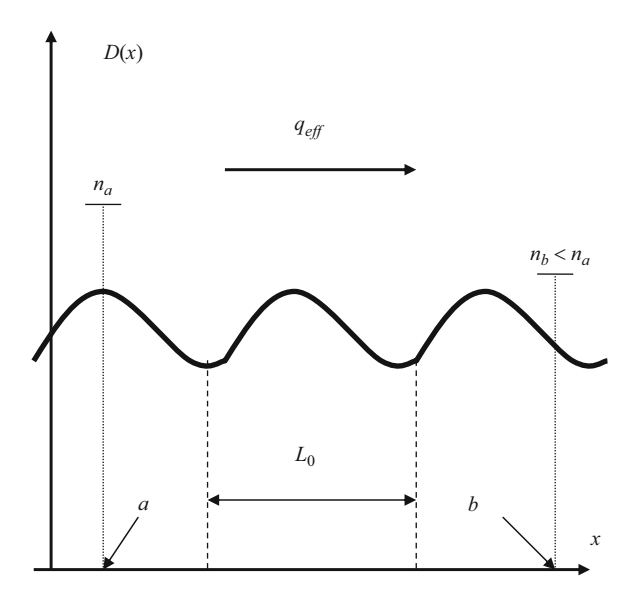


Fig. 1.4.1 Schematic illustration of the periodic media

Here, we are dealing with the segments of the length  $\Delta x$  centered in x. It is possible to rewrite this expression in the integral form

$$n_b - n_a = q \int \frac{\mathrm{d}x_i}{D(x)} = \frac{q}{\frac{\Delta x}{x_b - x_a}} \int_{x_a}^{x_b} \frac{\mathrm{d}x}{D(x)}.$$
 (1.4.5)

Here, the denominator is related to the mean value of the inverse diffusion coefficient

$$\frac{1}{x_b - x_a} \int_{x_a}^{x_b} \frac{\Delta x_i}{D(x_i)} = \left\langle \frac{1}{D(x)} \right\rangle. \tag{1.4.6}$$

Thus, one obtains the relation for the effective particle flux in the conventional form with the effective diffusion coefficient

$$q = q_{\text{eff}} = \left\langle \frac{1}{D(x)} \right\rangle \frac{\Delta n}{\Delta x}.$$
 (1.4.7)

Indeed, this elementary consideration gives the diffusion scaling

$$\left\langle (x(t) - x(0))^2 \right\rangle \cong 2D_{\text{eff}}t,$$
 (1.4.8)

where the effective diffusion coefficient is given by the formula

$$D_{\text{eff}} = \left\langle \frac{1}{D(x)} \right\rangle^{-1} = \left( \frac{1}{L_0} \int_0^{L_0} \frac{\mathrm{d}x}{D(x)} \right)^{-1}.$$
 (1.4.9)

The previous results use qualitative arguments. However, there is a way to rationalize these heuristic considerations by more precise calculations using the multiscale method [17, 18]. Let us introduce the hierarchy of interrelated spatial and temporal scales. We suppose that spatial and temporal scales are related diffusively as follows:

$$D \approx \frac{L^2}{T} \approx \frac{l^2}{t}.$$
 (1.4.10)

If we introduce a small spatial scale as  $X = \varepsilon x$ , the slow time T is given by the relation  $T = \varepsilon^2 t$ . Here,  $\varepsilon$  is the small parameter of the problem.

Now it is convenient to expand n in powers of  $\varepsilon$ :

$$n(x, X, t, T) = n_0(x, X, t, T) + \varepsilon n_1(x, X, t, T) + \varepsilon^2 n_2(x, X, t, T) + \cdots$$
 (1.4.11)

The space and time derivatives must be decomposed as follows:

$$\frac{\partial}{\partial x} \to \frac{\partial}{\partial x} + \varepsilon \frac{\partial}{\partial X}, \quad \frac{\partial}{\partial t} \to \frac{\partial}{\partial t} + \varepsilon^2 \frac{\partial}{\partial T}.$$
 (1.4.12)

Using the diffusive equation, we obtain the relations:

$$\hat{L}n_0 = 0, (1.4.13)$$

$$\hat{L}n_1 = \frac{\partial}{\partial x} \left( D(x) \frac{\partial}{\partial X} n_0 \right) + \frac{\partial}{\partial X} \left( D(x) \frac{\partial}{\partial x} n_0 \right), \tag{1.4.14}$$

$$\hat{L}n_2 = -\frac{\partial}{\partial T}n_0 + \frac{\partial}{\partial x}\left(D(x)\frac{\partial}{\partial X}(n_1 + n_2)\right) + \frac{\partial}{\partial X}\left(D(x)\left(\frac{\partial}{\partial x}n_1 + \frac{\partial}{\partial X}n_0\right)\right),\tag{1.4.15}$$

where the operator  $\hat{L}$  is given by the formula

$$\hat{L} = \frac{\partial}{\partial t} - \frac{\partial}{\partial x} \left( D(x) \frac{\partial}{\partial x} \right). \tag{1.4.16}$$

Because of the periodicity,  $n_0$  will relax to a constant, independent of x and t

$$\frac{\partial}{\partial x}n_0 = 0, (1.4.17)$$

and hence

$$\frac{\partial}{\partial t}n_1 = 0. ag{1.4.18}$$

The equation for  $\hat{L}n_1$  can be represented as

$$D(x)\left(\frac{\partial}{\partial x}n_1 + \frac{\partial}{\partial X}n_0\right) = \text{const.}$$
 (1.4.19)

Using the result  $\left\langle \frac{\partial}{\partial x} n_1 \right\rangle = 0$  and dividing by D(x), we obtain

$$\operatorname{const}\left\langle \frac{1}{D(x)} \right\rangle = \frac{\partial}{\partial X} n_0, \tag{1.4.20}$$

where the average is now over the fast variables. The equation for  $n_2$  can be solved only if solvability condition, on

$$n_0(X,T) = \langle n_0(x,X,t,T) \rangle, \tag{1.4.21}$$

is imposed. Taking the average of equation for  $\hat{L}n_2$ , one arrives at the expression

$$\frac{\partial}{\partial T}n_0 = \frac{\partial}{\partial X} \left( \langle D(x) \rangle \frac{\partial}{\partial X}(n_0) \right) + \frac{\partial}{\partial X} \left\langle D(x) \frac{\partial}{\partial x} n_1 \right\rangle. \tag{1.4.22}$$

By taking into account the results obtained above, we have the diffusion equation,

$$\frac{\partial}{\partial T}n_0 = D_{\text{eff}} \frac{\partial^2}{\partial X^2} n_0, \qquad (1.4.23)$$

with the effective diffusivity

$$D_{\text{eff}} = \left\langle \frac{1}{D(x)} \right\rangle^{-1}.\tag{1.4.24}$$

Such a multiscale technique can be applied to more general problems. For instance, it is applicable to models with two or three dimensions and problems of scalar transport with a fairly generic incompressible velocity field [19].

# **Further Reading**

# **Diffusion Concept**

- S.G. Brush, The Kind of Motion We Call Heat (North Holland, Amsterdam, 1976)
- C. Cercignani, *Ludwig Boltzmann*. The Man Who Trusted Atoms (Oxford University Press, Oxford, 1998)
- H.U. Fuchs, *The Dynamics of Heat* (Springer, Berlin, 2010)
- C.W. Gardiner, Handbook of Stochastic Methods (Springer, Berlin, 1985)
- D. Kondepudi, Introduction to Modern Thermodynamics (Wiley, Chichester, 2008)
- G.M. Kremer, An Introduction to the Boltzmann Equation and Transport Processes in Gases (Springer, Berlin, 2010)
- J.C. Maxwell, *The Scientific Papers* (Cambridge University press, Cambridge, 1890)
- R.M. Mazo, *Brownian Motion*, *Fluctuations*, *Dynamics and Applications* (Clarendon Press, Oxford, 2002)
- F. Schweitzer, Brownian Agents and Active Particles (Springer, Berlin, 2003)
- N.G. Van Kampen, *Stochastic Processes in Physics and Chemistry* (Elsevier, Amsterdam, 2007)

Further Reading 19

B. Zeldovich Ya, A.A. Ruzmaikin, D.D. Sokoloff, *The Almighty Chance* (World Scientific, Singapore, 1990)

### Diffusion Equation

- G.I. Barenblatt, *Scaling Phenomena in Fluid Mechanics* (Cambridge University Press, Cambridge, 1994)
- H.C. Berg, *Random Walks in Biology* (Princeton University Press, Princeton, NJ, 1969)
- R.B. Bird, W.E. Stewart, E.N. Lightfoot, *Transport Phenomena* (Wiley, New York, 2002)
- J.M. Burgers, *The Nonlinear Diffusion Equation* (D. Reidel, Dordrecht, 1974)
- H. Carslaw, *Mathematical Theory of Conduction of Heat in Solids* (Macmillan, London, 1921)
- L. Dresner, Similarity Solutions of Nonlinear Partial Differential Equations (Longman, London, 1983)
- B. Perthame, *Transport Equations in Biology* (Birkhauser, Boston, MA, 2007)
- A.P.S. Selvadurai, *Partial Differential Equations in Mechanics* (Springer, Berlin, 2000)
- G.H. Weiss, Aspects and Applications of the Random Walk (Elsevier, Amsterdam, 1994)
- D.V. Widder, *The Heat Equation* (Academic, New York, 1975)

# Anomalous Diffusion

- R. Balescu, Statistical Dynamics (Imperial College Press, London, 1977)
- D. Ben-Avraham, S. Havlin, *Diffusion and Reactions in Fractals and Disordered Systems* (Cambridge University Press, Cambridge, 1996)
- E.W. Montroll, M.F. Shlesinger, On the wonderful world of random walks, in *Studies in Statistical Mechanics*, ed. by J. Lebowitz, E.W. Montroll, vol. 11 (Elsevier Science Publishers, Amsterdam, 1984), p. 1
- E.W. Montroll, B.J. West, On an enriches collection of stochastic processes, in *Fluctuation Phenomena*, ed. by E.W. Montroll, J.L. Lebowitz (Elsevier, Amsterdam, 1979)
- A. Pekalski, K. Sznajd-Weron (eds.), *Anomalous Diffusion. From Basics to Applications* (Springer, Berlin, 1999)
- M.F. Shiesinger, G.M. Zaslavsky, Levy Flights and Related Topics in Physics (Springer, Berlin, 1995)
- D. Sornette, Critical Phenomena in Natural Sciences (Springer, Berlin, 2006)

# Chapter 2

# **Advection and Transport**

# 2.1 Advection-Diffusion Equation

The further extension to flowing fluids is easily accomplished if we merely replace the partial derivative with respect to time  $\partial/\partial t$  in the diffusion equation

$$\frac{\partial n}{\partial t} = D\nabla^2 n \tag{2.1.1}$$

by the total derivative [5, 10, 11]

$$\frac{\mathrm{d}}{\mathrm{d}t} = \frac{\partial}{\partial t} + V_i \frac{\partial}{\partial x_i},\tag{2.1.2}$$

which takes into account the effects of convection upon the time dependence. It follows that the diffusion equation becomes

$$\frac{\partial n}{\partial t} + \frac{\partial (nV_i)}{\partial x_i} = D\nabla^2 n. \tag{2.1.3}$$

Here,  $\vec{V} = (V_x, V_y, V_z)$  is the Eulerian velocity. In the case of incompressible flow

$$\operatorname{div}(\vec{V}) = \frac{\partial V_x}{\partial x} + \frac{\partial V_y}{\partial y} + \frac{\partial V_z}{\partial z} = 0, \tag{2.1.4}$$

one obtains the equation

$$\frac{\partial n}{\partial t} + \vec{V} \cdot \nabla n = D\nabla^2 n, \qquad (2.1.5)$$

which is so-called convection-diffusion equation.

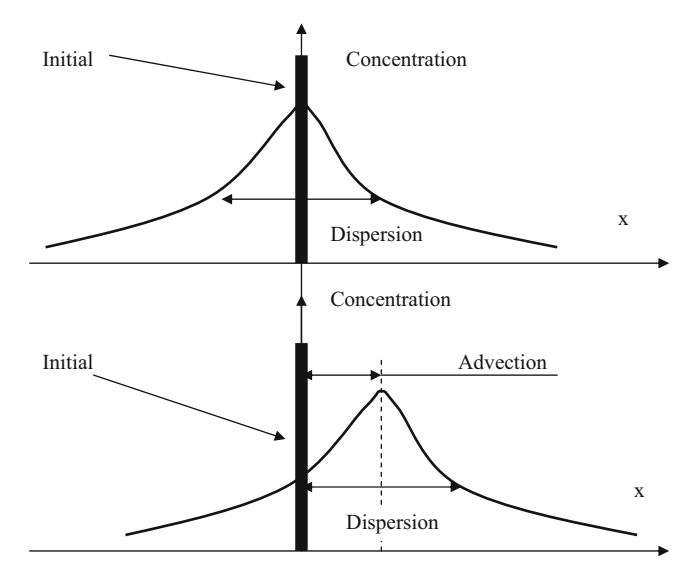


Fig. 2.1.1 Schematic diagram of the scalar diffusion and distortion of this purely diffusive behavior by advection

This equation can be interpreted in slightly different manner. The total flux  $\vec{q}$  of solute molecules through a motionless surface is equal to the sum of the diffusion flux and the convective flux (see Fig. 2.1.1):

$$\vec{q} = \vec{V}n - D\nabla n. \tag{2.1.6}$$

The relative importance of convection and diffusion in a given physical situation is usually appreciated with the Peclet number Pe. Suppose that the characteristic size of the fluid domain is  $L_0$  and that the characteristic velocity is  $V_0$ . At this stage, it is useless to define a dimension concentration. One easily obtains the following one-dimensional representation:

$$\frac{\partial n}{\partial \tilde{t}} + \tilde{V} \frac{\partial n}{\partial \tilde{x}} = \frac{1}{P_e} \frac{\partial^2 n}{\partial \tilde{x}^2},\tag{2.1.7}$$

where Pe represents the ration of convection to diffusion and

$$\tilde{t} = t \frac{V_0}{L_0}, \ \tilde{x} = \frac{x}{L_0};$$
 (2.1.8)

that is

$$Pe = \frac{V_0 L_0}{D}. (2.1.9)$$

The equation of convection-diffusion also must be completed by boundary conditions. For example, take an impermeable and motionless solid; the normal particle flux is obviously zero in this case.

It is important to note that in spite of the oversimplified character of the convection–diffusion equation, the use of the model functions for  $V(\vec{r},t)$  allows one to describe transport in chaotic flows as well as nontrivial correlation mechanisms responsible for the scalar transport in the presence of complex structures such as system of zonal flows, convective cells, braded magnetic fields, etc. [22–28].

Moreover, turbulent transport could have nondiffusive character where the scaling  $R^2 \propto t$  is not correct. To describe the anomalous diffusion, it is convenient to use the scaling with an arbitrary exponent H [29–31]

$$R^2 \propto t^{2H},\tag{2.1.10}$$

where H is the Hurst exponent. The case H=1/2 corresponds to the classical diffusion  $R^2(t) \propto t$ . The values 1 > H > 1/2 describe superdiffusion, whereas the values 1/2 > H > 0 correspond to the subdiffusive transport. The case H=1 corresponds to the ballistic motion of particles  $R^2(t) \propto t^2$ . Calculating the Hurst exponent H and determining the relationship between transport and correlation characteristics underlie the anomalous diffusion theory.

## 2.2 Transport and One-Dimensional Hydrodynamics

The advection–diffusion equation is linear, but it does not mean that this partial differential equation is simple. The advective term is responsible for fairly complicated behavior in the scalar distribution function. The concentration field and the velocity field are coupled in this case.

Indeed, advection creates gradients of concentration, whereas the molecular diffusion tends to wipe out gradients. That is why to solve the scalar transport problem we have to fulfill the transport equation by the equation describing the velocity field. The Navier–Stokes equation of motion for a Newtonian fluid

$$\frac{\partial V_i}{\partial t} + V_j \frac{\partial V_i}{\partial x_i} = -\frac{1}{\rho_m} \frac{\partial P}{\partial x_i} + v_F \frac{\partial^2 V_i}{\partial x_i \partial x_i}, \tag{2.2.1}$$

is often used. Here,  $V_i$  is the velocity in the  $x_i$  direction,  $\rho_m$  is the density, P is the pressure, and  $v_F$  is the kinematic viscosity. The situation becomes even more difficult because of the Navier–Stokes equation is nonlinear. The analytical solution of such a system of the partial differential equations is very difficult task.

However, there is an exception. The one-dimensional case is the most simple as usual. Suppose that the advection-diffusion equation through a velocity field is coupled with the equation of motion, which in one-dimensional hydrodynamics without pressure is Burgers' equation.

$$\frac{\partial V}{\partial t} + V \frac{\partial V}{\partial x} = v_{\rm F} \frac{\partial^2 V}{\partial x^2}.$$
 (2.2.2)

The Burgers model has long attracted a great deal of attention for describing deterministic and stochastic flows in aerodynamics and plasma physics [9, 22, 32]. This equation retains the inertial nonlinearity and high dissipation, which play a leading role in the formation of turbulent flow. The Burgers differential equation is especially attractive because it can be reduced to a linear diffusion equation by means of a nonlinear Cole–Hopf change of variables [33, 34]. This fact allows us to simplify our problem by reducing the nonlinear equation of motion to the linear one.

By following the above arguments and for the sake of simplicity, we consider the system of the coupled differential equations in the form

$$\frac{\partial V}{\partial t} + V \frac{\partial V}{\partial x} = D \frac{\partial^2 V}{\partial x^2},\tag{2.2.3}$$

$$\frac{\partial n}{\partial t} + V \frac{\partial n}{\partial x} = D \frac{\partial^2 n}{\partial x^2},$$
(2.2.4)

where the initial conditions for the velocity and density fields of the passive impurity are given by

$$V(x,t)|_{t=0} = \frac{\partial \Psi_0(x)}{\partial x}, \quad n(x,t)|_{t=0} = n(x).$$
 (2.2.5)

This system of equations with identical kinetic coefficients (unit Prandtl number  $Pr \equiv v_F/D = 1$ ) is just as simple as a separate Burgers equation. Indeed, using the generalized Cole–Hopf change of variables,

$$V(x,t) = -2v_{\rm F} \frac{\partial}{\partial x} \ln \chi(x,t)$$
 (2.2.6)

$$n(x,t) = \frac{\varsigma(x,t)}{\chi(x,t)},\tag{2.2.7}$$

it reduces to two ordinary linear heat conduction equations

$$\frac{\partial \chi}{\partial t} = D \frac{\partial^2 \chi}{\partial x},\tag{2.2.8}$$

$$\frac{\partial \varsigma}{\partial t} = D \frac{\partial^2 \varsigma}{\partial x},\tag{2.2.9}$$

where the initial conditions are given by

$$\chi(x,t)|_{t=0} = \exp\left(-\frac{\Psi_0(x)}{2D}\right),$$
 (2.2.10)

$$\varsigma(x,t)|_{t=0} = n_0(x) \exp\left(-\frac{\Psi_0(x)}{2D}\right).$$
(2.2.11)

Recall that the simplicity of the derivation of these analytic results depends on the ratio of the kinetic coefficients of the liquid (the Prandtl numbers). The situation becomes somewhat more complicated when the kinetic coefficients are different, and a reasonably complete analytic investigation is possible only for particular types of flows. Nevertheless, the analytical solutions of these equations can provide the basis for understanding complex problems such as scalar clustering and localization [9–12]. Indeed, scalar particles play the role of a marker for determining the localized dynamical structures of the velocity field of a fluid flow.

#### 2.3 Advection in Two-Dimensional Shear Flow

In this section, we consider the advection problem in relation to the general twodimensional linear shear velocity field. A tracer is released at the origin of a fluid that undergoes a linear shear characterized by the constant velocity gradient  $\hat{G}$ ; that is, the velocity field is given by

$$\vec{V} = \hat{G} \cdot \vec{r}. \tag{2.3.1}$$

The shear field can be expressed in the component form as

$$V_x(y) = G \cdot y, \tag{2.3.2}$$

$$V_{y}(x) = \alpha \cdot G \cdot x, \tag{2.3.3}$$

where G is the shear rate (a constant) and the parameter  $\alpha$  may range from -1 (pure rotation), through zero (simple shear), to +1 (pure elongation). Figure 2.3.1 illustrates this general field in some of its possible forms. For two-dimensional incompressible flow

$$\frac{\partial V_x}{\partial x} + \frac{\partial V_y}{\partial y} = 0 \tag{2.3.4}$$

this linearization correctly describes the qualitative behavior of streamlines in a small domain.

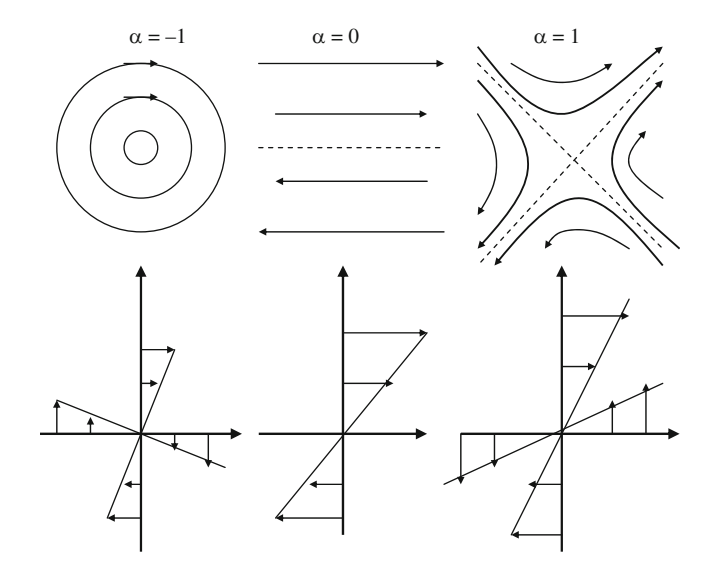


Fig. 2.3.1 Different types of two-dimensional linear flows. The characteristic parameter  $\alpha$  ranges from -1 to +1. The case  $\alpha=-1$  corresponds to the pure rotation. The case  $\alpha=+1$  corresponds to the pure shear

The general form of the solution of the convection-diffusion equation, which is

$$\frac{\partial n}{\partial t} + \vec{V} \cdot \nabla n - D\nabla^2 n = \delta(\vec{r}, t), \qquad (2.3.2)$$

with the velocity field under consideration is given by the relation [35]

$$n = B(t)\exp\left(-\frac{1}{2}\vec{r}^t \cdot \hat{\beta}(t) \cdot \vec{r}\right), \tag{2.3.5}$$

where  $\hat{\beta}(t)$  is a symmetric second-order tensor. The time function B(t) and  $\hat{\beta}(t)$  verify a coupled set of differential equations that can be readily deduced from the convection–diffusion equation.

For comparison purposes, the complete solution is presented for a simple shear flow in two-dimensional space. The velocity gradient  $\hat{G}$  can be expressed as

$$\hat{G} = \begin{bmatrix} 0 & G \\ 0 & 0 \end{bmatrix}. \tag{2.3.6}$$

The solution can be written as

$$n(\vec{r},t) = \frac{1}{4\pi Dt} \left( \frac{3}{12 + (Gt)^2} \right)^{1/2} \exp\left( -\frac{3\left(x - \frac{y}{2}Gt\right)^2}{Dt\left(12 + (Gt)^2\right)} - \frac{y^2}{4Dt} \right).$$
 (2.3.7)

This form can be compared to the purely diffusive solution

$$n(\vec{r},t) = \left(\frac{1}{4\pi dDt}\right)^{d/2} \exp\left(-\frac{\vec{r}^2}{4Dt}\right). \tag{2.3.8}$$

Here, d is the space dimensionality. For the two-dimensional case d=2 and  $\hat{G}=0$  one obtains the correct solution

$$n(\vec{r},t) = \frac{1}{4\pi Dt} \left(\frac{3}{12}\right)^{1/2} \exp\left(-\frac{x^2}{4Dt} - \frac{y^2}{4Dt}\right). \tag{2.3.9}$$

The opposite case when diffusivity is negligible, D = 0, leads to singularities. The solution in this situation is obvious: the particle stays at the origin forever.

#### 2.4 Effective Diffusivity and Advection

Fluctuation—dissipation relations are an intrinsic part of the statistical description of dynamical systems. On the macroscopic scale, the particle density fluctuations of the subcomponents of the system occur due to the interaction with the random velocity field, which, in our case of the scalar transport description, enter the convection—diffusion equation. Moreover, on the basis of the convection—diffusion equation,

$$\frac{\partial n}{\partial t} = D_0 \Delta n - \vec{V}(\vec{r}, t) \nabla n, \qquad (2.4.1)$$

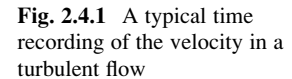
it is appropriate to raise a question about the estimation of effective transport in a turbulent (or chaotic) flow (see Fig. 2.4.1). Here, the vector  $\vec{V}(\vec{r},t)$  describes an arbitrary velocity field, and  $D_0$  is the seed diffusion coefficient. Here, we consider an incompressible fluid.

Let us multiply this equation by n and apply the Gauss theorem,

$$\int_{W} \operatorname{div} \vec{A} \, dW = \int_{S} A_{n} dS. \tag{2.4.2}$$

Here,  $\vec{A}$  is an arbitrary vector field and  $A_n$  is the normal component of this field on the boundary S. Then one finds the equation [36, 37]

$$\frac{1}{2}\frac{\partial}{\partial t}\int_{W} n^{2} dW = \int_{S} nD_{0}(\nabla n)_{N} dS - \int_{W} D_{0}(\nabla n)^{2} dW. \tag{2.4.3}$$



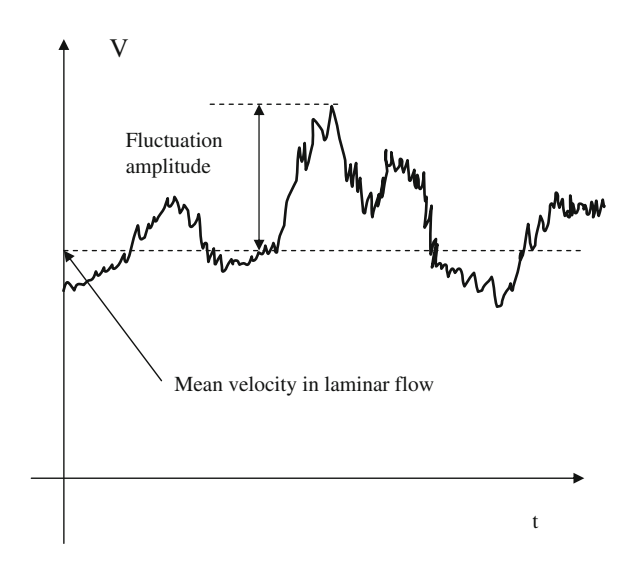
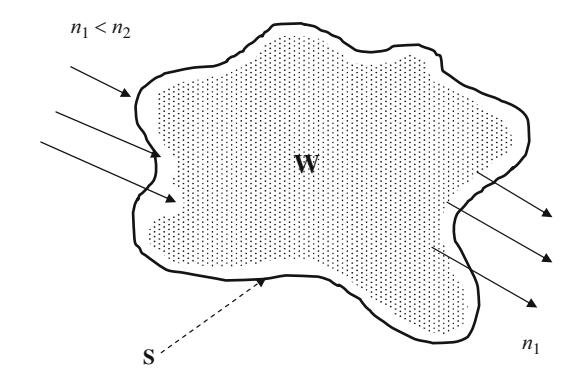


Fig. 2.4.2 A typical plot of a control volume of fluid



The flux  $D_0(\nabla n)_N$  characterizes the contribution of external sources inside the volume W, which is bounded by the surface S, whereas the term  $D_0(\nabla n)^2$  is related to the scalar redistribution inside the considered volume W(see Fig. 2.4.2).

For a single closed volume W in the absence of external flows, we arrive at

$$\frac{1}{2}\frac{\partial}{\partial t}\int_{W}n^{2}dW = -2D_{0}\int_{W}(\nabla n)^{2}dW. \tag{2.4.4}$$

This equation is correct even when the liquid within the inner vessel is kept in motion. Indeed, fluid mixing only indirectly affects the rate of evolution toward equilibrium in the presence of molecular diffusion. Advection enhances scalar density gradients and then diffusion is intensified.

The concept of turbulent diffusion is concerned with the evolution of a mean value (first moment) of the scalar distribution function. Naturally, the mean value cannot fully describe the behavior of a passive scalar. Of importance are

fluctuations of the scalar, which are particularly large in the case of small molecular diffusion  $D_0$ , which corresponds to the large Peclet numbers. To characterize fluctuations, one can study the evolution of the functional

$$\int_{W} (\delta n)^2 dW. \tag{2.4.5}$$

Here, the fluctuation of scalar density is

$$\delta n = n - \langle n \rangle, \tag{2.4.6}$$

and  $\langle n \rangle = 0$ , whereas  $\delta n = \delta n(t)$ . Then we obtain the Zeldovich fluctuation—dissipation relation,

$$\frac{1}{2}\frac{\partial}{\partial t}\int_{W}(\delta n)^{2}dW = -\int_{W}D_{0}(\nabla n)^{2}dW.$$
 (2.4.7)

Here, again the velocity field has dropped out of this averaged equation, but the effect of diffusion remains. The term on the right-hand side of fluctuation–dissipation relation is negative-definite (or zero). This means that the fluctuation of scalar density decreases (or is constant). This is true in the limit of  $t \to \infty$ .

In the case of quasi-steady random flow, we can omit the term describing density evolution,

$$\frac{\partial}{\partial t} \int_{W} n^2 \mathrm{d}W = 0, \tag{2.4.8}$$

and we arrive at the relation

$$\int_{S} nD_0(\nabla n)_N dS = \int_{W} D_0(\nabla n)^2 dW.$$
 (2.4.9)

Since the term  $D_0(\nabla n)^2$  is related to the scalar redistribution and that is why it is convenient to introduce here the effective diffusive coefficient in the form

$$D_{\text{eff}} = \frac{1}{n^2 L_0} \int_W D_0(\nabla n)^2 dW, \qquad (2.4.10)$$

where  $L_0$  is the system characteristic size. The minimum condition for the effective diffusivity  $D_{\rm eff}$  is given by the minimizing of the above functional. This gives a purely diffusive equation

$$D_0 \Delta n(\vec{r}) = 0. \tag{2.4.11}$$

The minimum value of the effective diffusivity  $D_{\text{eff}}$  in the case under consideration coincides with the molecular (seed) diffusivity  $D_0$ .

## 2.5 Fluctuation Effects in Scalar Transport

At the initial stage of relaxation, we are faced with a quite different scenario. To show this, we now consider the important differences between the diffusion from a continuous source, in which particles are released in sequence at a fixed position (see Fig. 2.5.1), and that of a single puff of particles. When a substance (scalar) is released into a turbulent flow from a source, it is transported by the motion of the fluid elements and by diffusion of molecules. It is essential to distinguish carefully between how scalar is transported by fluid elements and how it is transported by molecular motion (see Fig. 2.5.2). As was shown above in most environmental chaotic flows, the Peclet numbers based on the characteristic velocity scale  $V_0$  and

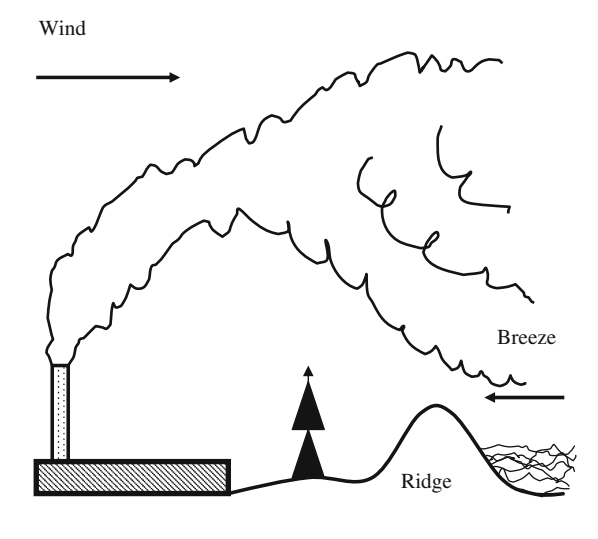


**Fig. 2.5.1** Schematic diagram of a chimney plume

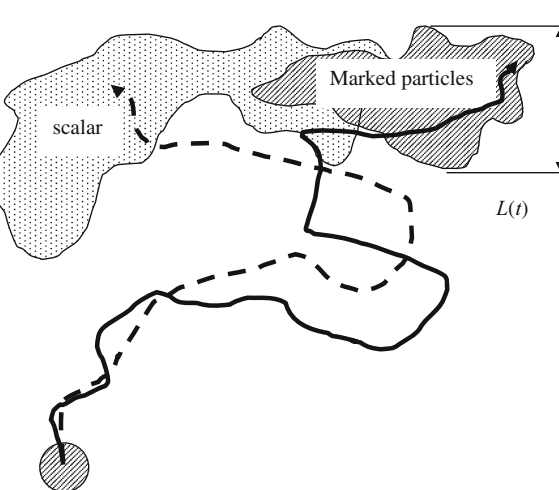


Fig. 2.5.2 Schematic illustration of the difference between displacements of the marked particle and tracer

the characteristic spatial scale  $L_0$  are large ( $\geq 10^2$ ). That is why it is natural to consider cases when the molecular diffusion effect could be neglected.

It is natural to analyze the initial stage of evolution of a single puff of particles by considering cloud of marked particles on the basis of mass conservation law [38],

$$\int_{W} n(\vec{r}, t) dW = N_{\rm p}. \tag{2.5.1}$$

Here,  $N_p$  is the number of particles in a single puff. By taking the ensemble mean, we find the integral relations

$$\int_{W} \delta n \mathrm{d}W = 0, \tag{2.5.2}$$

$$\int_{W} \langle n \rangle dW = N_{\rm p}. \tag{2.5.3}$$

By introducing the initial spatial scale of cloud of uniformly distributed particles as  $L_0 \propto W_0^{1/3}$ , we arrive at the formula

$$\int_{W} n^{2}(\vec{r}, 0) dW = \int_{W} \langle n(\vec{r}, 0) \rangle^{2} dW \propto \frac{N_{p}^{2}}{L_{0}^{6}} W_{0} \propto \frac{N_{p}^{3}}{L_{0}^{3}}, \qquad (2.5.4)$$

where  $\delta n(\vec{r},0) = 0$ . In the absence of molecular diffusivity, the number of contaminant within each fluid particle remains constant during a cloud spreading. By taking the ensemble mean, one obtains the relation

$$\int_{W} n^{2} dW = \int_{W} \langle n \rangle^{2} dW + \int_{W} (\delta n)^{2} dW = \frac{N_{p}^{2}}{L_{0}^{3}}.$$
 (2.5.5)

As time is growing, we have

$$\int_{W} \langle n(\vec{r}, t) \rangle^{2} dW \to 0, \qquad (2.5.6)$$

$$\int_{W} \delta n(\vec{r}, t)^{2} dW \to \frac{N_{p}^{2}}{L_{0}^{3}}.$$
 (2.5.7)

In the case when the fluctuation amplitude during the evolution has the same order over the whole cloud of size L(t) one finds

$$\delta n^2 W(t) \approx \delta n^2 L^3(t) \propto \frac{N_{\rm p}^2}{L_0^3},\tag{2.5.8}$$

whereas the mean concentration of scalar particles is given by the scaling

$$\langle n(\vec{r},t)\rangle^2 \approx \propto \left(\frac{N_{\rm p}}{L^3(t)}\right)^2.$$
 (2.5.9)

Thus, we arrive at the conclusion that the relative fluctuation magnitude is growing with time as

$$\frac{\delta n^2}{\langle n \rangle^2} \propto \frac{L^3(t)}{L_0^3}.$$
 (2.5.10)

However, there is considerable difference between a real cloud and a cloud of marked particles. Indeed, as a result of molecular diffusion, scalar particles cross the boundaries of fluid particles. From the fluctuation–dissipation relation considered above, we have

$$\frac{1}{2}\frac{\mathrm{d}}{\mathrm{d}t}\int_{W}n^{2}\mathrm{d}W = \frac{1}{2}\frac{\mathrm{d}}{\mathrm{d}t}\int_{W}\langle n\rangle^{2}\mathrm{d}W + \frac{1}{2}\frac{\mathrm{d}}{\mathrm{d}t}\int_{W}(\delta n)^{2}\mathrm{d}W = -\int_{W}D_{0}(\nabla n)^{2}\mathrm{d}W.$$
(2.5.11)

Here, the term on the right-hand side is always negative, and in the limit of  $t \to \infty$ , one obtains

$$\int_{W} n^2 \mathrm{d}W \to 0, \tag{2.5.12}$$

$$\int_{W} \langle n \rangle^2 dW \to 0. \tag{2.5.13}$$

Thus, in contrast to a cloud of marked fluid particles we find

$$\int_{W} (\delta n)^{2} dW \to 0, \quad \text{as} \quad t \to \infty.$$
 (2.5.14)

In fact, in a real cloud there exist two competing processes. Due to the chaotic advection, the minimum thickness of all parts of a scalar particle cloud tends to zero, resulting in a continual increase in the gradients of scalar density across the thinnest part of the cloud. Thus, turbulence intensifies the gradient, without increasing the maximum density. On the other hand, the molecular diffusion tends to extend the distance over which the tracer is spread. Batchelor [23, 24] was the first who recognized the importance of balance between those effects and pointed out that on the final stage the minimum thickness of the cloud remains constant, but particle density decays to zero due to the molecular diffusivity. We will develop these Batchelor phenomenological arguments below in relation to both the exponential instability effects and the Kolmogorov approach to well-developed turbulence.

#### 2.6 The Zeldovich Scaling for Effective Diffusivity

Above we defined the minimum value of the effective diffusivity  $D_{\rm eff}$  on the basis of the fluctuation–dissipation relation. However, the upper estimate of the effective diffusion coefficient is case of great interest. In the case of a quasi-steady turbulent flow, one can consider the steady scalar density equation

$$D_0 \Delta n(\vec{r}) - \vec{V} \nabla n(\vec{r}) = 0. \tag{2.6.1}$$

By following the simplified perturbation technique, we suppose that for the onedimensional problem the scalar density and the velocity fields are given by

$$n = \langle n \rangle + n_1 = n_0 + n_1,$$
 (2.6.2)

$$V = \langle V \rangle + v_1 = v_1, \tag{2.6.3}$$

where  $\langle V \rangle = 0$ ,  $n_1 \ll n_0$ , and  $D_0 \Delta n_0 = 0$ . Simple calculations lead to the equation for density perturbation  $n_1$  for a turbulent velocity field:

$$D_0 \frac{\partial^2 n_1(x)}{\partial x^2} = v_1 \frac{\partial n_0(x)}{\partial x}.$$
 (2.6.4)

For the sake of simplicity, this equation is presented in the one-dimensional form. In the framework of the dimensional estimate, we obtain

$$n_1 \approx v_1 \frac{L_0 n_0}{D_0} \approx n_0 Pe \propto V_0,$$
 (2.6.5)

where the Peclet number is small,  $Pe = V_0 L_0/D_0 \ll 1$ , which corresponds to weak turbulence case. By deriving this relation, we use the condition of smallness of the term  $v_1 \nabla n_1$  in comparison with  $v_1 \nabla n_0$ . The expression for the effective diffusion coefficient is given by

$$D_{\text{eff}} \approx \frac{1}{n_0^2 L_0} \int_W D_0 (\nabla n_0)^2 (1 + \text{const} \cdot Pe^2) dW.$$
 (2.6.6)

Note that the term  $\nabla n_0 \nabla n_1$  is illuminated because of the extreme properties of the distribution  $n_0$ . Thus, we obtain the scaling

$$D_{\rm eff} \propto D_0 (1 + {\rm const} \cdot Pe^2).$$
 (2.6.7)

For instance, in the case of atmospheric turbulence we have the following estimates:  $D_0 \approx 0.1\,\mathrm{cm^2/s}$ ;  $V_0 \approx 10\,\mathrm{cm/s}$ ;  $L_0 \approx 10^{-2}\,\mathrm{cm}$ ; and  $D_\mathrm{eff} \approx 10^3\,\mathrm{cm^2/s} \gg D_0$ . This upper estimate of transport  $D_\mathrm{eff}$  in the steady turbulent flow is given by the

scaling  $D_{\rm eff} \approx V_0^2 \tau \propto V_0^2$ , where Pe < 1 and the correlation time  $\tau$  has a diffusive nature  $\tau \approx \tau_{\rm D} \approx L_0^2/D_0$ . This result shows the important dependence of the effective diffusivity  $D_{\rm eff}$  on the turbulent fluctuation amplitude  $V_0$  in the limit of the small Peclet numbers.

#### **Further Reading**

#### Advection

- R.B. Bird, W.E. Stewart, E.N. Lightfoot, *Transport Phenomena* (Wiley, New York, 2002)
- W.C. Conner, J. Fraisserd, *Fluid Transport in Nanoporous Materials* (Springer, Berlin, 2006)
- L.A. Glasgow, Transport Phenomena. An Introduction to Advanced Topics (Wiley, New York, 2010)
- D.P. Kessler, R.A. Greenkorn, *Momentum, Heat, and Mass Transfer Fundamentals* (CRC, Boca Raton, FL, 1999)
- J.G. Knudsen, D.L. Katz, Fluid Dynamics and Heat Transfer (MGH, New York, 1958)
- A. Majda, P. Kramer, Phys. Rep. 314, 237–574 (1999)
- J.B. Weiss, A. Provenzale (eds.), *Transport and Mixing in Geophysical Flows* (Springer, Berlin, 2008)
- L.C. Van Rijn, Principles of Sediment Transport in Rivers, Estuaries and Coastal Seas (Aqua, Amsterdam, 1993)
- M. Van-Dyke, An Album of Fluid Motion (Parabolic Press, Stanford, CA, 1982)
- A. Zhao et al., Convective and Advective Heat Transfer in Geological Science (Springer, Berlin, 2008)

# Chaotic Flows and Transport

- O.G. Bakunin, Turbulent and Diffusion, Scaling Versus Equations (Springer, Berlin, 2008)
- R. Balescu, Statistical Dynamics (Imperial College, London, 1997)
- J. Cardy et al., *Non-Equilibrium Mechanics and Turbulence* (Cambridge University Press, Cambridge, 2008)
- P. Castiglione et al., *Chaos and Coarse Graining in Statistical Mechanics* (Cambridge University Press, Cambridge, 2008)
- R. Klages, G. Radons, I. Sokolov (eds.), *Anomalous Transport. Foundations and Applications* (Wiley, Weinheim, 2008)

Further Reading 35

A.J. Majda, A.L. Bertozzi, *Vorticity and Incompressible Flow* (Cambridge University Press, Cambridge, 2002)

- J.M. Ottino, *The Kinematics of Mixing. Stretchings Chaos, and Transport* (Cambridge University Press, Cambridge, 1989)
- T. Tel, Phys. Rep. 413, 91 (2005)
- G.M. Zaslavsky, *The Physics of Chaos in Hamiltonian Systems* (Imperial College Press, London, 2007)
- Ya B. Zeldovich, *Selected Works*. Chemical Physics and Hydrodynamics, vol. 1 (Princeton University Press, Princeton, NJ, 1992)
- Ya B. Zeldovich, A.A. Ruzmaikin, D.D. Sokoloff, *The Almighty Chance* (World Scientific, Singapore, 1990)

# Chapter 3

# The Langevin Equation and Transport

#### 3.1 Brownian Motion and Diffusion

To interpret the diffusion coefficient in terms of medium characteristic, we consider the Langevin equations of motion of particle suspended in a liquid (see Fig. 3.1.1). The irregular movements of small particles immersed in a liquid, caused by the impacts of the molecules of the liquid, were described by Brown in 1828. Since 1905, the Brownian movement has been treated statistically, on the basis of the fundamental works of Einstein and Langevin. Langevin's approach to Brownian motion was the first example of a stochastic differential equation and inspired the development of the mathematical theory of continuous time stochastic processes:

$$m\dot{V} = K_{\rm F}(t). \tag{3.1.1}$$

Here,  $K_F(t)$  is the fluctuating force caused by bombardment of the particle by the molecules of the liquid and m is the particle mass. We now make the important assumption that  $K_F(t)$  may be divided into two parts [25–30]:

$$K_{\rm F}(t) = -\beta_t mV + mA(t), \qquad (3.1.2)$$

where the term  $-\beta_t mV$  represents the usual viscous drag on a particle moving with velocity V, and mA(t) is a stochastic force of average value zero representing the effects of molecular impacts on a particle at rest. The viscous drag also arises, of course, from molecular impacts. When the particle is in motion the molecular momentum change on impact is greater on the advancing forward face of the particle than on the rear face – there is a net average force tending to slow up the particle (see Fig. 3.1.2). Thus, we have for the equation of motion

$$\dot{V} = -\beta_t V + A(t). \tag{3.1.3}$$

**Fig. 3.1.1** Pass of a two-dimensional Brownian motion

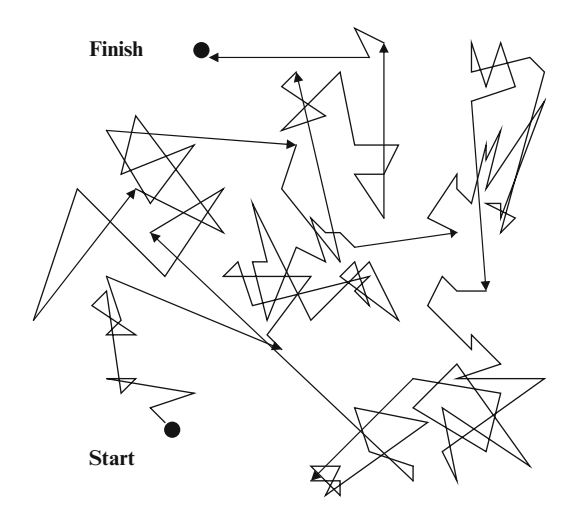
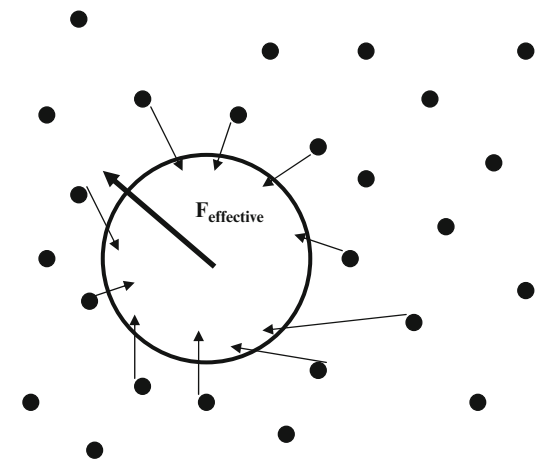


Fig. 3.1.2 Brownian particle



For a sphere of radius  $R_0$ , Stokes' law gives the relation in the form

$$\beta_t m = 6\pi R_0 \eta_F = \frac{1}{B_E},\tag{3.1.4}$$

where  $\eta_F$  is the coefficient of viscosity and  $B_E$  is the mobility coefficient. This law works quite well even down to molecular dimensions [45–47]. In order to obtain a solution, we multiply the equation of motion through by x

$$x\dot{V} = x\ddot{x} = -\beta_t x\dot{x} + xA(t). \tag{3.1.5}$$

Now one can use the formal relation

$$\frac{\mathrm{d}}{\mathrm{d}t}x^2 = 2x\dot{x}.\tag{3.1.6}$$

Using this we derive the new form of the Langevin equation of Brownian particle motion as follows:

$$\frac{1}{2}\frac{d^2}{dt^2}x^2 - (\dot{x})^2 = -\frac{\beta_t}{2}\frac{d}{dt}x^2 + xA(t),$$
(3.1.7)

Now we apply the averaging method. The time average of xA(t) is zero, because x and A are uncorrelated (see Fig. 3.1.3). We also take into account the equipartition theorem

$$\langle V^2 \rangle = \langle \dot{x}^2 \rangle = \frac{k_{\rm B}T}{m}.$$
 (3.1.8)

Here, T is the temperature of medium and  $k_{\rm B}$  the Boltzmann constant. In order to find the solution, let  $Z_{\rm L}$  be the time average of  $\frac{{\rm d}(x^2)}{{\rm d}t}$ ; then the time average of the Langevin equation is

$$\frac{1}{2}\frac{dZ_{L}}{dt} - \frac{k_{B}T}{m} = -\frac{\beta_{t}}{2}Z_{L}.$$
(3.1.9)

By integrating, we find the expression for value  $Z_L$  in the form

$$Z_{\rm L} = \frac{2k_{\rm B}T}{m\beta_t} + C_0 e^{-\beta_t t}, \tag{3.1.10}$$

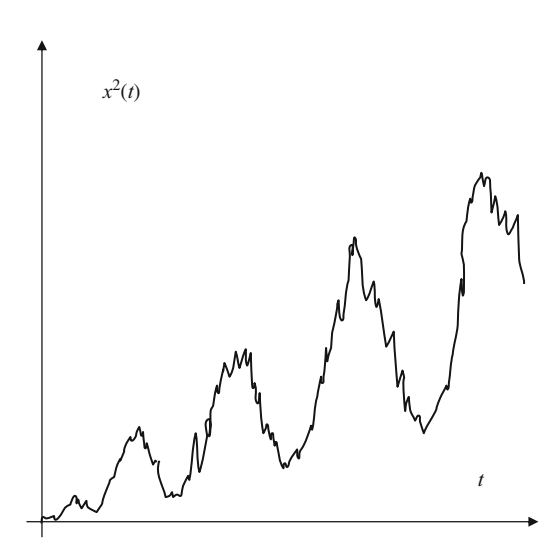


**Fig. 3.1.3** A typical plot of squared displacement of a Brownian particle

where  $C_0$  is a constant. We are not interested in the transient term, which merely would allow us to fit the initial conditions. Then, using angular parenthesis to denote time average,

$$\left\langle \frac{\mathrm{d}}{\mathrm{d}t}(x^2) \right\rangle = \frac{\mathrm{d}}{\mathrm{d}t} \left\langle x^2 \right\rangle = \frac{2k_{\mathrm{B}}T}{m\beta_t} = 2D_{\mathrm{B}}t,$$
 (3.1.11)

Note that  $\langle x^2 \rangle^{1/2} \propto t^{1/2}$ , as expected for diffusion process (see Fig. 3.1.4). Our derivation is due to Langevin.

We saw that the diffusion coefficient of the Brownian particle was given in terms of the damping time associated with the friction force by which we can now reexpress as

$$D_{\rm B} = \frac{k_{\rm B}T}{m\beta_t}, \quad D_{\rm B} = \frac{k_{\rm B}T}{B_E}.$$
 (3.1.12)

Here,  $B_E$  is the mobility. This connection between the diffusion coefficient and the mobility is known as the Einstein relation. For the special case of Stokes' law, this gives us

$$R^2 = \langle x^2 \rangle = \frac{k_{\rm B}T}{3\pi R_0 v_{\rm F}} t = 2D_{\rm B}t,$$
 (3.1.13)

as given originally by Einstein. Numerous experimental studies of the Brownian movement have confirmed with a great accuracy [45–47].

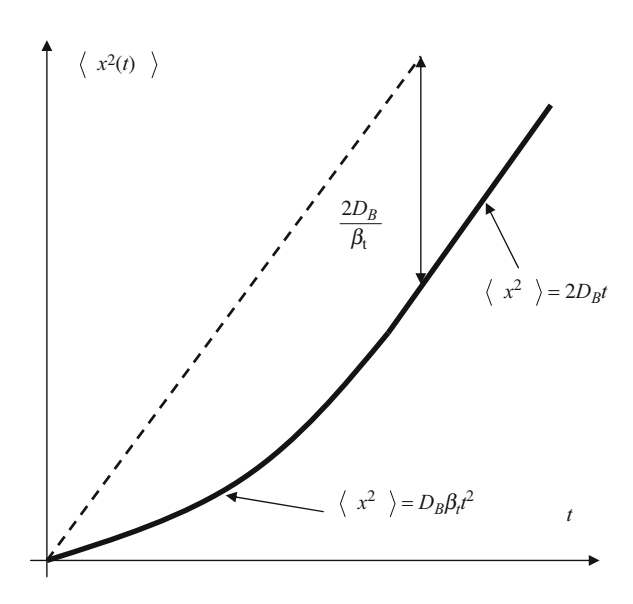


**Fig. 3.1.4** A typical plot of the mean-squared displacement of a Brownian particle

#### 3.2 Mean Square Velocity and Equipartition

The Langevin equation considered above has a linear form and therefore one can find its formal solution in the form

$$V(t) = V(0)e^{-\beta_t t} + \int_0^t e^{\beta_t (u-t)} A(z) dz.$$
 (3.2.1)

The first term represents the transient part of the solution: that which depends on the initial conditions and which arises from the solution to the corresponding homogeneous equation. This is the complementary function. The second term represents the steady-state response to the "source force" A(t). This is the particular integral and this part persists when all memory of the initial condition has gone. It is conventional to enunciate properties of the random force A(t). These are listed as  $\langle A(t) \rangle = 0$ . This follows from the considerations of the center of mass frame of the fluid. We also suppose that  $\langle A(t_1)A(t_2) \rangle = 0$ , unless  $t_1$  is "almost identical with"  $t_2$ , which means that the correlation time of the random force is short. The value  $\langle A^2(t) \rangle$  has some definite value, which leads to the formulas

$$\langle A(t_1)A(t_2)\rangle = A^2\delta(t_1 - t_2). \tag{3.2.2}$$

$$A^{2} = \int_{-\infty}^{\infty} \langle A(0)A(t)\rangle dt$$
 (3.2.3)

As a simple application of these results, we can consider the mean value of V(t). We find a given initial conditions (see Fig. 3.2.1)

$$\langle V(t)\rangle = V(0)e^{-\beta_t t} \tag{3.2.4}$$

Here,  $\langle A(t) \rangle = 0$ .

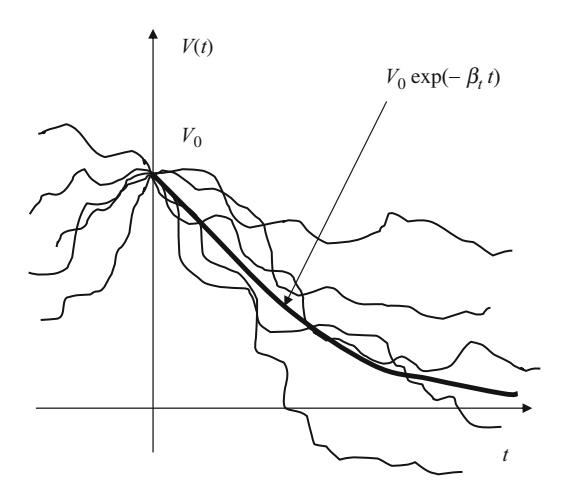


Fig. 3.2.1 Schematic diagram of velocity fluctuations of a Brownian particle

By similar arguments, we can now examine the mean square velocity. A key result then follows when we exploit the equipartition theorem to relate the equilibrium mean square velocity of the Brownian particle to the temperature of its surrounding medium. The expression for the mean square velocity is given by the relation

$$\langle V^{2}(t)\rangle = V^{2}(0)e^{-2\beta_{t}t} + 2e^{-2\beta_{t}t} \int_{0}^{t} e^{\beta_{t}z} \langle V(0)A(z)\rangle dz$$
$$+ e^{-2\beta_{t}t} \int_{0}^{t} dz \int_{0}^{t} dy \, e^{\beta_{t}(z+y)} \langle A(z)A(y)\rangle. \tag{3.2.5}$$

The first term is the transient response, which dies away at long times; it is of no interest. The second term vanishes since there is no correlation between V(0) and A(t). The third term is of interest since it describes the equilibrium state of the particle, independent of the initial conditions. In this term, we make use of the smallness of the correlation time and approximate the force autocorrelation function by the delta function expression:

$$\langle A(t_1)A(t_2)\rangle = A^2\delta(t_1 - t_2).$$
 (3.2.6)

Thus, we obtain at long times the relation in the following form:

$$\left\langle V^{2}(t)\right\rangle = A^{2} e^{-2\beta_{t}t} \int_{0}^{t} dz \, e^{2\beta_{t}z} = \frac{A^{2} e^{-2\beta_{t}t}}{2\beta_{t}} (e^{2\beta_{t}t} - 1) = \frac{A^{2}}{2\beta_{t}} (1 - e^{-2\beta_{t}t}). \quad (3.2.7)$$

In the long time limit, this gives the relation

$$V_0^2 = \langle V^2 \rangle = \frac{A^2}{2\beta_t} = \frac{k_{\rm B}T}{m}$$
 (3.2.8)

Using the equipartition theorem yields the important relationship

$$\beta_t = \frac{m}{2k_{\rm B}T}V_0^2,\tag{3.2.9}$$

On the other hand, one can express the mobility in the form

$$B_E = \frac{m^2}{2kT} \int_{-\infty}^{\infty} \langle A(0)A(t)\rangle dt.$$
 (3.2.10)

Thus, we relate the two forces in the Langevin equation: the mobility or friction force and the random force. Here, the dissipative force is expressed in terms of the autocorrelation function of the fluctuation force. This result is called the fluctuation dissipation theorem. The Boltzmann factor that appears in the fluctuation dissipation theorem between the macroscopic and the microscopic force is a consequence of equipartition.

#### 3.3 Autocorrelation Function

In the previous analysis of Brownian motion, we saw that the motion of particles was conveniently expressed in terms of the velocity autocorrelation function. The calculation of this is only slightly more complicated than that of the mean square velocity. We have

$$\langle V(t_0)V(t_0+t)\rangle = V^2(0)e^{-\beta_t(2t_0+t)} + e^{-\beta_t(2t_0+t)} \int_0^{t_0} dz \int_0^{t_0+t} dy \, e^{\beta_t(z+y)} \langle A(z)A(y)\rangle, \tag{3.3.1}$$

where the cross term vanishes, as above. The first term is of no interest since at long times t the memory of the initial state is lost. The steady-state behavior is contained in the remaining term. We also use the smallness of the correlation time of the force autocorrelation function and the delta function approximation. This forces y = z when the integral over z is performed. The calculation is identical to that for the mean square velocity, except for the additional  $e^{-\beta_t t}$  prefactor

$$\langle V(t_0)V(t_0+t)\rangle = \frac{A^2}{2\beta_t}e^{-\beta_t t},$$
 (3.3.2)

or

$$C_V(t) = \langle V^2(0) \rangle e^{-\beta_t t}. \tag{3.3.3}$$

Thus, we consider that the correlation time for the velocity autocorrelation function is simply the damping time associated with the friction force (see Fig. 3.3.1)

$$\tau = \frac{1}{\beta_t}.\tag{3.3.4}$$

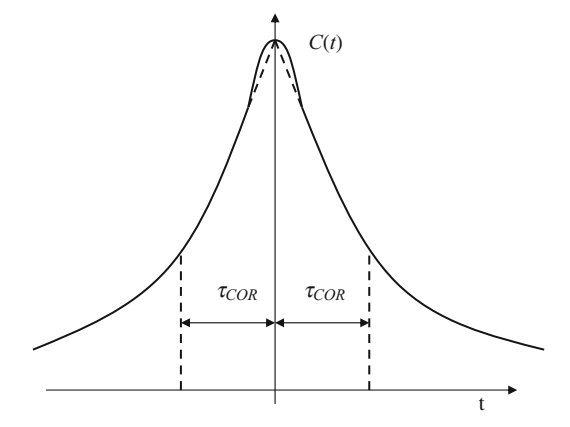
We saw that the diffusion coefficient of the Brownian particle was given in terms of correlation time  $\tau$  by

$$D_{\rm B} = \frac{k_{\rm B}T}{m}\tau = \frac{1}{2}A^2\tau^2. \tag{3.3.5}$$

Here, the correlation length  $\Delta_{COR}$  is given by the formula

$$\Delta_{\rm COR} \approx \frac{V_0}{\beta_t} = \frac{1}{\beta_t} \sqrt{\frac{k_{\rm B}T}{m}}.$$
 (3.3.6)

**Fig. 3.3.1** A typical plot of the velocity correlation function



One can estimate transport of the small sphere, which is floating in water, whose radius is  $R_0 \approx 5 \times 10^{-5}$  cm,  $\tau \approx m/3\pi\eta_{\rm F}R_0 \approx 8 \times 10^{-8}$  s,  $\eta_{\rm F} \approx 0.0135$  g/(cm s),  $m \approx 5 \times 10^{-13}$  g,  $T \approx 300$  K. This gives the diffusion coefficient  $D \approx 3.8 \times 10^{-6}$  cm²/s. However, when considering tracer transport in chaotic or turbulent flows, one has to take into account the specific nature of fluctuating velocity field (cascade mechanisms, coherent structures, etc.) to define the adequate characteristic spatial and temporal correlation scales.

## 3.4 Velocity Distribution Function

To obtain the velocity distribution function, we may first calculate all the moments  $\langle V^{2n} \rangle$ , from which we get the characteristic function [42–45]. In the stationary state, i.e., for large times,

$$V(t) = \int_0^\infty e^{-\beta_t \tau} A(t - \tau) d\tau.$$
 (3.4.1)

To derive this equation,  $t - t' = \tau$  was substituted, and then the range of integration was extended to infinity because of the factor  $\exp(-\beta_t t)$ . Then, we obtain the relations

$$\left\langle V(t)^{2k+1} \right\rangle = 0 \tag{3.4.2}$$

$$\left\langle V(t)^{2k} \right\rangle = \int_0^\infty \cdots \int_0^\infty e^{-\beta_t(\tau_1 + \dots + \tau_{2k})} \left\langle A(t - \tau_1) \cdots A(t - \tau_{2k}) \right\rangle d\tau_1 \cdots d\tau_{2k}$$

$$= \frac{(2k)!}{2^k k!} \left[ \int_0^\infty \int_0^\infty e^{-\beta_t(\tau_1 + \tau_2)} A^2 \delta(\tau_1 - \tau_2) d\tau_1 d\tau_2 \right]^k. \tag{3.4.3}$$

The double integral is equal to the value

$$\left\langle V^2 \right\rangle = \frac{A^2}{2\beta_t} \tag{3.4.4}$$

giving the expression of interest in the following form:

$$\left\langle V(t)^{2k} \right\rangle = \frac{(2k)!}{2^k k!} \left(\frac{A^2}{2\beta_t}\right)^k. \tag{3.4.5}$$

The characteristic function is given by the relation in the form

$$F_{p}(u) = 1 + \sum_{k=1}^{\infty} \frac{(iu)^{k} \left\langle V(t)^{k} \right\rangle}{k!} = \sum_{k=0}^{\infty} \frac{(iu)^{2k} \left\langle V(t)^{2k} \right\rangle}{(2k)!} = \sum_{k=0}^{\infty} \frac{(iu)^{2n}}{2^{k}k!} \left(\frac{A^{2}}{2\beta_{t}}\right)^{k}$$
$$= \sum_{k=0}^{\infty} \frac{1}{k!} \left(-\frac{u^{2}A^{2}}{4\beta_{t}}\right)^{k} = \exp\left(-\frac{u^{2}A^{2}}{4\beta_{t}}\right). \tag{3.4.6}$$

Now, the velocity distribution function is given by the formula

$$f(V) = \langle \delta(V(t) - V) \rangle = \frac{1}{2\pi} \int_{-\infty}^{\infty} F_p(u) e^{-iuV} du$$

$$= \frac{1}{2\pi} \int_{-\infty}^{\infty} \exp\left(-iuV - \frac{u^2 A^2}{4\beta_t}\right) du =$$

$$= \sqrt{\frac{\beta_t}{\pi A^2}} \exp\left(-\frac{\beta_t V^2}{A^2}\right) = \sqrt{\frac{m}{2\pi k T}} \exp\left(-\frac{mV^2}{2kT}\right).$$
(3.4.7)

This is the Maxwell stationary distribution [42–45]. The probability density times the length of the interval dV is then the probability of finding the particle in the interval (V, V + dV). This distribution function depends on time t and the initial distribution. Once we have found f(V, t), any averaged value of the velocity can be calculated by integration X(V)

$$\langle X(V(t))\rangle = \int_{-\infty}^{\infty} X(V)f(V,t)dV. \tag{3.4.8}$$

The distribution function can be also calculated in a much simpler way with the help of the Fokker–Plank equation. For the Langevin model, the equation of motion for the distribution function f(V, t) is given by

$$\frac{\partial f(V,t)}{\partial t} = \beta_t \frac{\partial (Vf)}{\partial V} + \beta_t \frac{k_B T}{m} \frac{\partial^2 f}{\partial V^2}.$$
 (3.4.9)

This equation is one of the simplest Fokker–Plank equations. By solving it starting with f(V,0) for t=0 and subject to the appropriate boundary conditions, one obtains the distribution function f(V,t) for all later times.

#### 3.5 Kinetics and Diffusion Equation

As soon as the theory for the free particle was established, a natural question arose as to how it should be modified in order to take into account outside forces as, for example, gravity. In this section, we briefly consider the Klein–Kramers or Kramers equation, which is an equation of evolution for the distribution functions f(V, x, t) in position and velocity space describing the Brownian motion of particles in an external field.

Let us assume that the outside force acts in the direction of the *x*-axis and Langevin equations should in this case be replaced by

$$\dot{x} = V, \tag{3.5.1}$$

$$\dot{V} = -\beta_t V + K_F(x) + A(t),$$
 (3.5.2)

where

$$\langle A(t')A(t)\rangle = 2\beta_t \left(\frac{k_{\rm B}T}{m}\right)\delta(t-t').$$
 (3.5.3)

Without any external force this system of equations reduces to the classical Langevin model. Two cases of special interest and importance are  $F_K(x) = -a_K$ , field of constant force (for example, gravity) and  $F_K(x) = -b_K x$ , elastically bound particle (for example, pendulum). The corresponding equation to describe probability density in the presence of nonuniform force  $mK_F(x)$  is given by

$$\frac{\partial f}{\partial t} + V \frac{\partial f}{\partial x} - K_{\rm F}(x) \frac{\partial f}{\partial V} = \frac{1}{\tau_0} \frac{\partial}{\partial V} \left( V f + \frac{k_{\rm B} T_p}{m} \frac{\partial f}{\partial V} \right). \tag{3.5.4}$$

Here, f(t,V,x) is the particle distribution function,  $K_F(x)$  is the acceleration, V is the velocity,  $T_p$  is the temperature,  $\tau_0$  is the characteristic time, and m is the mass of the particle. At this point it must be strongly emphasized that theories based on the Kramers equation are only approximate. They are valid only for relatively large t and, in the case of elastically bound particle ( $F_K(x) = -b_K x$ ), only in the overdamped case, that is, when the friction coefficient  $b_K$  is sufficiently large.

It is worth noting that a formal integration of this kinetic equation over velocity with accounting for the following conditions:

$$f(|V| \to \infty) \to 0$$
 and  $\frac{\partial}{\partial V} f(M \to \infty)$  (3.5.5)

leads only to the continuity equation for the particle density in physical space

$$\frac{\partial n}{\partial t} + \frac{\partial}{\partial x} U_* n = 0, \tag{3.5.6}$$

where the mean values are given by

$$n(x,t) = \int_{-\infty}^{\infty} f(x,V,t) dV,$$
 (3.5.7)

$$U_* = \frac{1}{n} \int_{-\infty}^{\infty} V f(x, V, t) dV.$$
 (3.5.8)

Indeed, as early as 1940, Kramers [48] pointed out the difficulties encountered in an attempt to obtain the diffusion equation in ordinary coordinate space

$$\frac{\partial n}{\partial t} = D \frac{\partial^2 n}{\partial x^2} - \frac{\partial}{\partial x} (V_0 n) \tag{3.5.9}$$

from the simplest kinetic equation which includes spatial nonuniformity,

$$\frac{\partial f}{\partial t} + V \frac{\partial f}{\partial x} - \frac{\partial}{\partial V} \left[ \left( \frac{V}{\tau_0} - K_F(x) \right) f \right] = \frac{1}{\tau_0} \frac{\partial}{\partial V} \left( \frac{k_B T_p}{m} \frac{\partial f}{\partial V} \right). \tag{3.5.10}$$

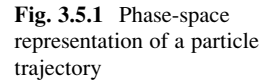
Even here a demand arose for a nontrivial approach with integration over a simplified trajectory  $r=r_0+V\tau_0$  in lieu of "conventional averaging" with the fixed value  $r_0$ . Here,  $r_0$  is an arbitrary initial point. This corresponds to the system of characteristic lines

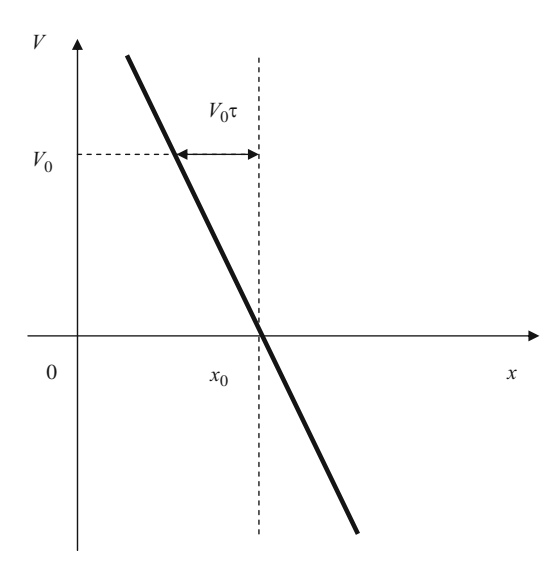
$$\frac{\mathrm{d}V}{\mathrm{d}t} = -\frac{V}{\tau_0} \tag{3.5.11}$$

and

$$\frac{\mathrm{d}r}{\mathrm{d}t} = V. \tag{3.5.12}$$

From this point of view, the spatial nonuniformity of the distribution function f at scales  $\lambda \leq V_0 \tau_0$  can be ignored:  $f(t, V, x) \approx f(t, V, x + \lambda)$ . This means that only local effects are described by this kinetic equation (see Fig. 3.5.1). However, this argument was not effective enough for the introduction of corrections to the kinetic





equation at that time. Kramers in fact pointed out the conventional character of the diffusion equation and its close relation to the correlation function behavior.

There is an interesting interrelation between the diffusion coefficient in a phase space  $D_V$  and the diffusion coefficient D in an ordinary space. Indeed, they have completely different kind of dependence on the characteristic frequency  $\beta_t$ 

$$D_V = \frac{k_{\rm B}T}{m}\beta_t,\tag{3.5.13}$$

$$D_B = \frac{k_{\rm B}T}{m} \frac{1}{\beta_t}.$$
 (3.5.14)

This allows us to eliminate the value  $\beta_t$  and to obtain the formula

$$D_V \cdot D_B = \left(\frac{k_{\rm B}T}{m}\right)^2. \tag{3.5.15}$$

One can see that diffusion in ordinary space depends inversely in the spacephase diffusivity. To visualize this relation let us consider an ensemble of collisionless particles (for instance, suprathermal electrons in turbulent plasma), which is beyond our simplified Brownian model. Thus, the ballistic particle motion can be interpreted as trapping in phase space. Indeed, if collisions (interactions) are absent, then the particle has constant velocity and, hence, does not change its position in the velocity space, whereas they passed a significant distance in the coordinate space [48–58]. Further Reading 49

There are certainly deep connections between the conventional approach to the transport equation in the configuration space and the phase-space representation. The Hamiltonian theory gives the advantage of using additional degrees of freedom to treat nonlocality and memory effects in the framework of phase-space. The kinetic model provides the possibility of describing ballistic modes and establishing the relationship between different exponents and distributions.

#### **Further Reading**

#### **Brownian Motion**

- H.C. Berg, Random Walks in Biology (Princeton University Press, Princeton, NJ, 1969)
- J. Bricmont et al., *Probabilities in Physics* (Springer, Berlin, 2001)
- J.L. Doob, Stochastic Processes (Wiley, New York, 1990)
- B. Duplantier, Brownian Motion. Poincare Seminar (2005)
- H. Fischer, A History of the Central Limit Theorem. From Classical to Modern Probability Theory (Springer, Berlin, 2011)
- J.A. Freund, T. Poeschel (eds.), Stochastic Processes in Physics, Chemistry, and Biology (Springer, Berlin, 2000)
- C.W. Gardiner, *Handbook of Stochastic Methods* (Springer, Berlin, 1985)
- D.S. Lemons, An Introduction to Stochastic Processes in Physics (JHUP, Baltimore, 2002)
- R. Mahnke, J. Kaupuzs, I. Lubashevsky, *Physics of Stochastic Processes. How Randomness Acts in Time* (Wiley, New York, 2009)
- R.M. Mazo, *Brownian Motion*, *Fluctuations*, *Dynamics and Applications* (Clarendon Press, Oxford, 2002)
- E.W. Montroll, M.F. Shlesinger, *On the Wonderful World of Random Walks*. Studies in Statistical mechanics, vol. 11 (Elsevier, Amsterdam, 1984), p. 1
- N.G. Van Kampen, *Stochastic Processes in Physics and Chemistry* (Elsevier, Amsterdam, 2007)
- D. Wax (ed.), Selected Papers on Noise and Stochastic Processes (Dover, London, 1954)

# The Langevin Equation

- S. Abe, Y. Okamoto (eds.), *Nonextensive Statistical Mechanics and Its Applications* (Springer, Berlin, 2001)
- D.J. Amit, Y. Verbin, *Statistical Physics. An Introductory Course* (Word Scientific, Singapore, 1999)

- R. Botet, M. Poszajczak, M. Ploszajczak, *Universal Fluctuations* (Word Scientific, Singapore, 2002)
- S. Chandrasekhar, Rev. Mod. Phys. 15, 1 (1943)
- W.T. Coffey, YuP Kalmykov, J.T. Waldron, *The Langevin Equation* (World Scientific, Singapore, 2005)
- B. Cowan, *Topics in Statistical Mechanics-Fluctuations* (Imperial College Press, London, 2005)
- H. Haken, Synergetics (Springer, Berlin, 1978)
- K. Jacobs, Stochastic Processes for Physicists. Understanding Noisy Systems (Cambridge University Press, Cambridge, 2010)
- K. Sekimoto, Stochastic Energetics (Springer, Berlin, 2010)

#### The Fokker-Planck Equation and Kinetic Theory

- P. Hanggi, P. Talkner (eds.), *New Trends in Kramers Reaction Rate Theory* (Kluwer, Boston, MA, 1995)
- H. Malchow, L. Schimansky-Geier, *Noise and Diffusion in Bistable Nonequilib*rium Systems (Teuber, Leipzig, 1985)
- L.E. Reichl, A Modern Course in Statistical Physics (Wiley, New York, 1998)
- P. Resibois, M.De Leener, Classical Kinetic Theory (Wiley, New York, 1977)
- H. Risken, *The Fokker–Planck Equation* (Springer, Berlin, 1989)
- N.G. Van Kampen, *Stochastic Processes in Physics and Chemistry* (North-Holland, Amsterdam, 1984)

# Part II Lagrangian Description

# Chapter 4

# **Lagrangian Description of Chaotic Flows**

### 4.1 The Taylor Diffusion and Correlation Concept

In the previous consideration, the scalar diffusion was discussed in terms of Eulerian (laboratory) coordinate frame. In modern studies in fluid dynamics, it is quite common to describe the velocity and pressure fields in the Eulerian way, with these quantities being measured and defined at a given point in space. Having found this Eulerian velocity field,  $u_i(x_j, t)$ , where i and j range over 1, 2, and 3 and  $u_i$  is associated with the coordinate  $x_j$ , we can then consider the equations

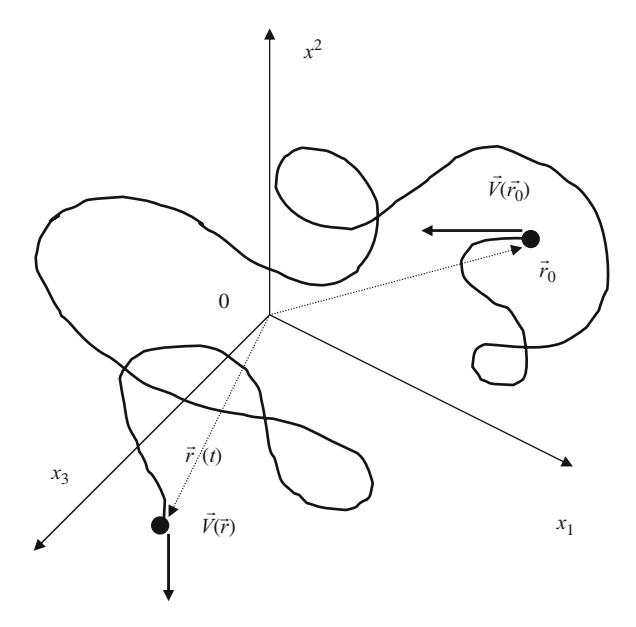
$$\frac{\mathrm{d}x_1}{u_1} = \frac{\mathrm{d}x_2}{u_2} = \frac{\mathrm{d}x_3}{u_3} = \mathrm{d}t,\tag{4.1.1}$$

in order to obtain the particle paths and properties associated with them. Such knowledge can be important for the understanding of flows visualized experimentally by dye or smoke.

An alternative approach is that of the Lagrangian description, in which the individual particles are marked and followed in a time-dependent way. A time derivative on a given marked particle gives its velocity, and this gives a connection with the Eulerian description mentioned above.

The partial differential equations for the Eulerian and Lagrangian schemes look superficially different, but are connected by the ordinary differential equations quoted above. However, there are some phenomena of relevance and importance in connection with turbulence and with transition to turbulence, in which an approach from the Lagrangian point of view gives rise to simpler and less intuitive nonlinear mathematics and leads to illuminating insights. The Lagrangian approach to such problems is described in this chapter.

Fig. 4.1.1 Schematic illustration of the Lagrangian coordinate system and motion of a wandering particle



Here, we discuss the Taylor definition of scalar dispersion from a continuous source [59, 60]. Figure 4.1.1 represents the motion of wandering particle. This is the Lagrangian position coordinate of the marked particle. The Lagrangian velocity V(t) is given by the formula

$$V(t) = \lim_{\Delta t \to 0} \frac{\Delta x}{\Delta t}.$$
 (4.1.2)

By following the Taylor statistical approach [59–63], we consider the displacement x(t) of a marked fluid particle in one dimension

$$x(t) = \int_0^t V(x_0, t') dt'. \tag{4.1.3}$$

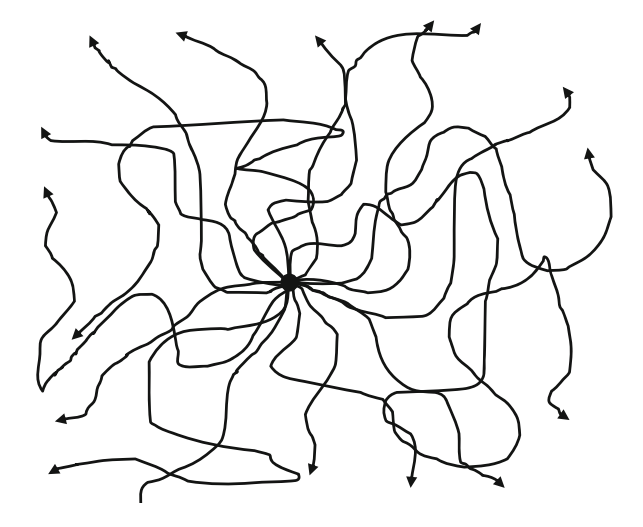
The displacement will be positive as often as it is negative; therefore, its mean value will be zero. That is why we will treat the mean squared particle displacement. The mean square of a large number of x is expressed as

$$\frac{1}{2}\frac{\mathrm{d}}{\mathrm{d}t}\langle x^2(t)\rangle = \left\langle x\frac{\mathrm{d}x}{\mathrm{d}t}\right\rangle = \langle x(t)V_x(t)\rangle. \tag{4.1.4}$$

If the turbulence field is spatially homogeneous, this formula can be represented as follows:

$$\frac{\mathrm{d}}{\mathrm{d}t}\langle x^2(t)\rangle = 2\int_0^t \mathrm{d}t' \langle V(t)V(t+t')\rangle. \tag{4.1.5}$$

**Fig. 4.1.2** Schematic diagram of the Lagrangian particle trajectories



The averaging procedure is based on the supposition that one considers simultaneously released a large number of particles at t = 0 (see Fig. 4.1.2), at different points in the fluids, and averaged over all the particle tracks.

Taylor introduced the Lagrangian correlation function C(t) in the form

$$C(t) = \langle V(x_0, z)V(x_0, z+t)\rangle = V_0^2 R_{\mathbf{L}}(t),$$
 (4.1.6)

where  $V_0$  is the characteristic scale of velocity fluctuations. Then the famous Taylor expression is given by

$$\frac{1}{2}\frac{\mathrm{d}}{\mathrm{d}t}\langle x^2(t)\rangle = \int_0^t C(t')\mathrm{d}t' = D_{\mathrm{T}}.$$
(4.1.7)

On the other hand, one obtains an important relationship, which is used in the subsequent discussions,

$$\frac{\mathrm{d}^2}{\mathrm{d}t^2} \langle x^2(t) \rangle \Big|_{t=\tau} = 2C(t). \tag{4.1.8}$$

The exponential form of the correlation function to describe turbulent transport is commonly attributed (see Fig. 4.1.3)

The turbulent diffusion coefficient is estimated by the scaling  $D_{\rm T} \approx V_0^2 \tau$ . Here,  $\tau$  is the Lagrangian correlation time, which is given by

$$\tau = \frac{1}{V_0^2} \int_0^\infty C(t) dt.$$
 (4.1.9)

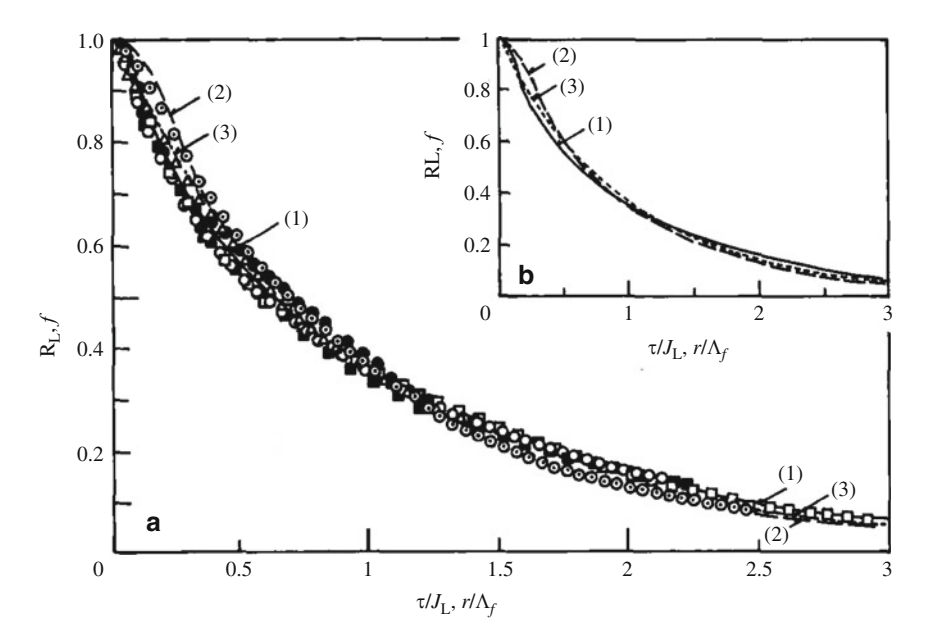


**Fig. 4.1.3** Distribution of the Lagrangian autocorrelation coefficient normalized with integral scale. (a) Measurements. (b) Calculations. (1) Re = 70; (2) Re = 25; (3) The exponential form of correlation function. (After Sato and Yamamoto [64] with permission)

Such definitions are especially relevant for the description of turbulent transport where velocity fluctuates in a fairly unpredictable way, whereas in a steady laminar flow the velocity does not change with time.

#### 4.2 The Boltzmann Law Renormalization

The Lagrangian representation of the diffusion coefficient can be used to study the distribution of particles suspended in a turbulent flow. Consider a suspension of particles in a fluid with a spatially constant external field (gravity) imposed upon it. We denote the external force by mg and choose the z-axis of the coordinate system in the direction of the external force. The motion will build up a concentration gradient in the z direction, and this concentration gradient will induce a diffusion current  $D_{\rm eff} \frac{\partial n}{\partial z}$  in the opposite direction to that induced by external force. Here,  $D_{\rm eff}$  is the effective diffusion coefficient. In the steady case, these two currents will cancel each other

$$nV_z = D_{\text{eff}} \frac{\partial n}{\partial z}.$$
 (4.2.1)

Here, the characteristic velocity is given by the formula

$$V_z \propto B_E mg = \tau_E g, \tag{4.2.2}$$

where  $B_E$  is the mobility coefficient and  $\tau_E$  is the characteristic time. By solving the differential equation, one obtains the conventional distribution of particles suspended in a fluid

$$n = n_0 \exp\left\{-V_z \int_0^z \frac{\mathrm{d}z}{D_{\text{eff}}(z)}\right\}. \tag{4.2.3}$$

The main question is the choice of the effective diffusion coefficient. In the framework of the Brownian motion description, it was applied the expression

$$D_{\rm eff} \approx (k_{\rm B}T)B_E \tag{4.2.4}$$

and hence the distribution of particles is given by the Boltzmann law

$$n = n_0 \exp\left\{-\left(\frac{mg}{k_{\rm B}T}\right)z\right\} = n_0 \exp\left\{-\left(\frac{3g}{V_{\rm T}^2}\right)z\right\}. \tag{4.2.5}$$

Here, T is the field temperature and  $V_{\rm T}$  is the thermal velocity.

However, to the case of particles suspended in a chaotic flow, the Lagrangian representation of the effective diffusivity

$$D_{\rm eff} \approx D_{\rm T} \approx \frac{1}{3} V_0^2 \tau_{\rm COR} z \tag{4.2.6}$$

is more relevant. The particle distribution obtained

$$n = n_0 \exp\left\{-\left(\frac{3g}{V_0^2}\right) \cdot \frac{\tau_E}{\tau_{\text{COR}}}z\right\}$$
 (4.2.7)

differs significantly from the Brownian case. Here,  $\tau_E = B_E m$ .

This form of the distribution of particles suspended in a turbulent flow takes into account the amplitude of velocity fluctuation  $V_0$  as well as correlation effects by the Lagrangian correlation time  $\tau_{\rm COR}$ . On the other hand, such a representation agrees well with experiments [65].

## 4.3 Turbulent Transport and Scaling

It is clear even intuitively that the result of action over a long period of a random flow is similar to the result of a large number of molecular actions. As we have seen above, transport in a chaotic flow depends on the behavior of the correlation function C(t). Let us employ the Taylor representation of the diffusion coefficient in the form

$$\frac{1}{2}\langle x^2(t)\rangle = \int_0^t dt' \int_0^{t'} c(t'')dt'' = \int_0^t (t - t')C(t')dt'$$
 (4.3.1)

to obtain transport scalings. In the framework of the Laplace transformation, one finds

$$C(z) \times \left(1 - \frac{z}{t}\right) = t \int_{0}^{\infty} \tilde{C}(\omega)\tilde{F}(\omega)d\omega,$$
 (4.3.2)

where the triangular filter is given by formula

$$F(z) = 1 - \frac{z}{t}. (4.3.3)$$

The ordinary calculations yield the relation

$$C(z) \times \left(1 - \frac{z}{t}\right) = \frac{t^2}{2} \int_0^\infty \tilde{C}(\omega) \left[\frac{\sin\frac{\omega t}{2}}{\frac{\omega t}{2}}\right]^2 d\omega. \tag{4.3.4}$$

Now we can derive two important asymptotic results. For times much greater than the correlation time,  $t \gg \tau$ ,  $\omega \approx 0$ , we are dealing with the narrow filter function. The mean squared displacement is given by the relation

$$\frac{1}{2}\langle x^2(t)\rangle \approx V_0^2 \tau t \approx D_{\rm T} t, \tag{4.3.5}$$

which coincides with the Taylor definition  $D_T = V_0^2 \tau$ . On the other hand, for times less than the correlation time,  $t \ll \tau$ , we find

$$\frac{1}{2}\langle x^2(t)\rangle \approx \frac{t^2}{2} \int_0^\infty \tilde{C}(\omega) d\omega \propto \frac{1}{2} V_0^2 t^2$$
 (4.3.6)

This leads to the ballistic scaling,  $\langle x^2(t) \rangle = \langle V^2 \rangle t^2$  (see Fig. 4.3.1).

Even from the general considerations, it is clear that the Taylor relationship between the diffusion coefficient and the Lagrangian correlation function of velocity is an effective tool of investigation. In the next sections, we show that the

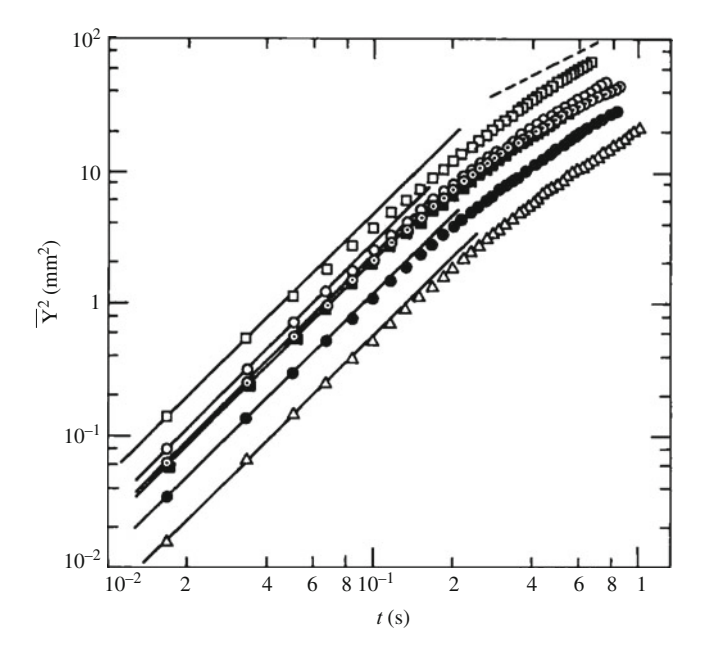


**Fig. 4.3.1** Lateral particle diffusion from a fixed point in a grid turbulence. *Continuous line*  $\bar{Y}^2 = V_0' 2t^2$ ; *Dotted line*  $\bar{Y}^2 \propto t$ . (After Sato and Yamamoto [64] with permission)

development of correlation ideas had essential influence on the form of diffusion equations as well as on the choice of the effective correlation length and correlation time.

#### 4.4 Anomalous Diffusion in Turbulent Shear Flows

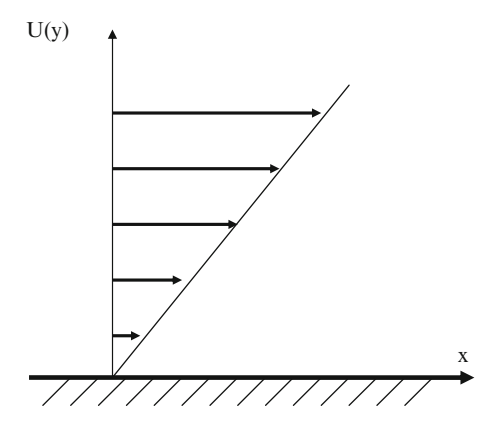
The model of isotropic steady random flow is an idealization; therefore, it would be interesting to consider anisotropy effects widely distributed in environmental and industrial flows. In this section, we discuss correlation mechanisms and transport in a turbulent flow in the presence of a uniform shear (see Fig. 4.4.1).

By following the statistical approach, we find the Lagrangian longitudinal and transverse displacements X(t) and Y(t) of a scalar particle on the basis of equations [66]

$$\frac{\mathrm{d}X}{\mathrm{d}t} = U(Y) + V_x(t),\tag{4.4.1}$$

$$\frac{\mathrm{d}Y}{\mathrm{d}t} = V_y(t). \tag{4.4.2}$$

**Fig. 4.4.1** A typical plot of shear velocity profile in the Corrsin (1953) model



Here, we suppose that the turbulence is homogeneous in planes normal to the mean velocity  $\bar{U}$ , where  $\bar{U}(x,0)=0$ . We are dealing with the uniform mean shear

$$\frac{\mathrm{d}}{\mathrm{d}y}\bar{U}(y) = \mathrm{const.} \tag{4.4.3}$$

These displacements can be expressed in terms of the shear velocity field as

$$X(t) = \int_0^t \left[ \frac{dU}{dy} Y(t') + V_x(t') \right] dt',$$
 (4.4.4)

$$Y(t) = \int_{0}^{t} V_{y}(t')dt'. \tag{4.4.5}$$

As before, we are not interested in the lowest order statistical moments. Squaring X(t) and Y(t) and averaging, we find in the limit of  $t \to \infty$ 

$$\langle Y^2(t) \rangle = 2D_{\rm T}t = 2(V_0^2 \tau_{\rm L})t,$$
 (4.4.6)

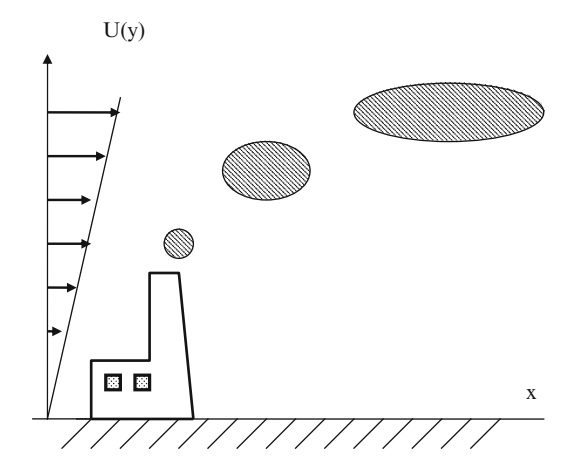
$$\left\langle X^{2}(t)\right\rangle = \frac{1}{3} \left(\frac{\mathrm{d}U}{\mathrm{d}y}\right)^{2} \left\langle Y^{2}\right\rangle t^{2} = \frac{2}{3} \left(\frac{\mathrm{d}U}{\mathrm{d}y}\right)^{2} V_{0}^{2} \tau_{\mathrm{L}} t^{3}. \tag{4.4.7}$$

Here,  $D_T = V_0^2 \tau_L$  is the Taylor turbulent diffusion coefficient,  $V_0$  is the characteristic amplitude of turbulent pulsations, and  $\tau_L$  is the Lagrangian correlation time. This formula describes the anomalous diffusion in the longitudinal direction at large times; the scalar blob becomes fairly elongated (see Fig. 4.4.2).

Such a nontrivial result could be interpreted in terms of characteristic spatial and temporal correlation scales  $\Delta_{\parallel},~\tau_{\perp},$ 

$$D_{\parallel} \propto \frac{{\Delta_{\parallel}}^2}{2\tau_{\perp}}.\tag{4.4.8}$$

**Fig. 4.4.2** A single puff evolution in a shear velocity field



In the model under consideration, the transverse temporal correlation scale is related to the statistical nature of turbulent pulsations,

$$\frac{1}{\tau_{\perp}} \propto \frac{2D_{\rm T}}{\delta_{\perp}^2},\tag{4.4.9}$$

and describes the diffusive character of "correlation cloud" transverse spreading, whereas the longitudinal spatial correlation scale is supposed to have a ballistic nature

$$\Delta_{\parallel}(t) = V_{\parallel}t. \tag{4.4.10}$$

Here,  $\delta_{\perp}$  is the spatial scale related to the velocity gradient, and  $V_{\parallel}$  is the characteristic velocity scale.

Now the scaling for the anomalous longitudinal transport in a turbulent shear flow is given by the formula with the time-dependent diffusion coefficient,

$$D_{\parallel}(t) \propto \left(\frac{V_{\parallel}}{\delta_{\perp}}\right)^2 D_{\mathrm{T}} t^2.$$
 (4.4.11)

On the other hand, in terms of longitudinal displacement one obtains the scaling

$$\langle X^2(t) \rangle \propto D_{\parallel} t \propto (\nabla_{\perp} V_{\parallel})^2 V_0^2 \tau_{\rm L} t^3.$$
 (4.4.12)

This corresponds to the anomalous diffusion with the Hurst exponent H=3/2. Solvable theoretical model considered here is rather simplified, but at the same time there are many advantages in its treatment. In our case, we are dealing with anisotropy related to shear effects, ballistic approximation of longitudinal

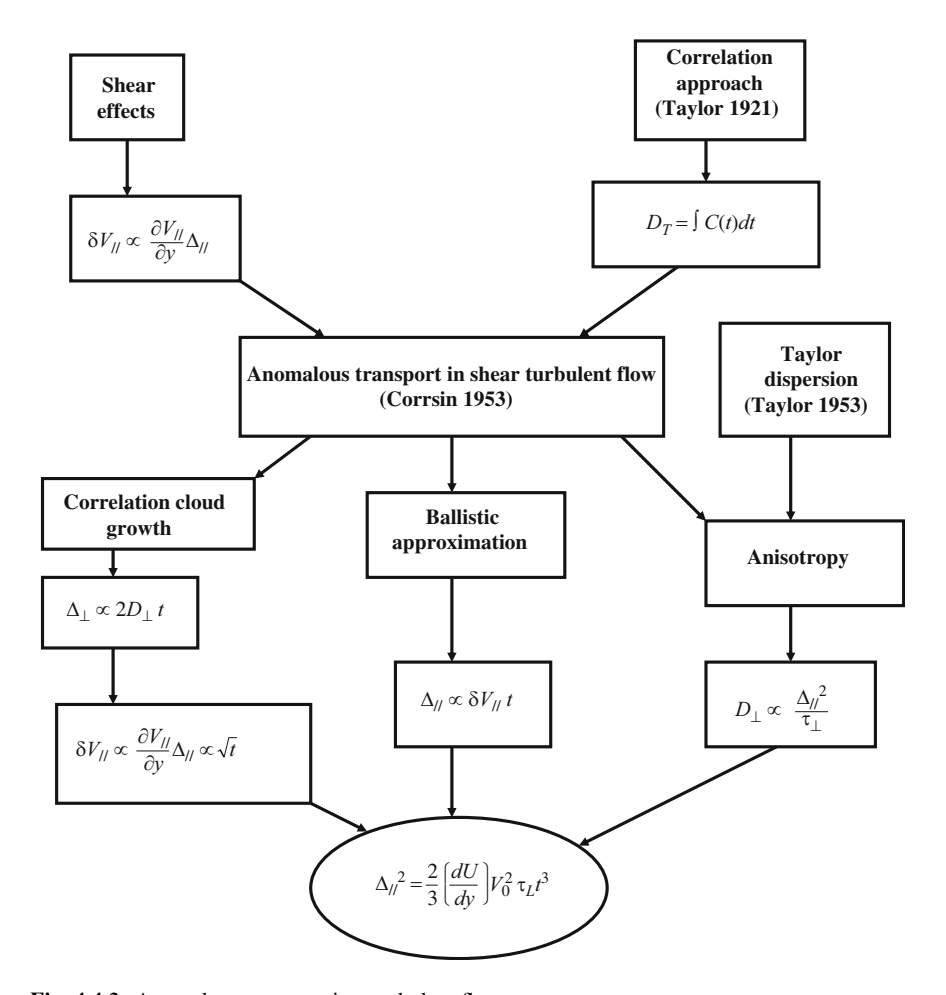


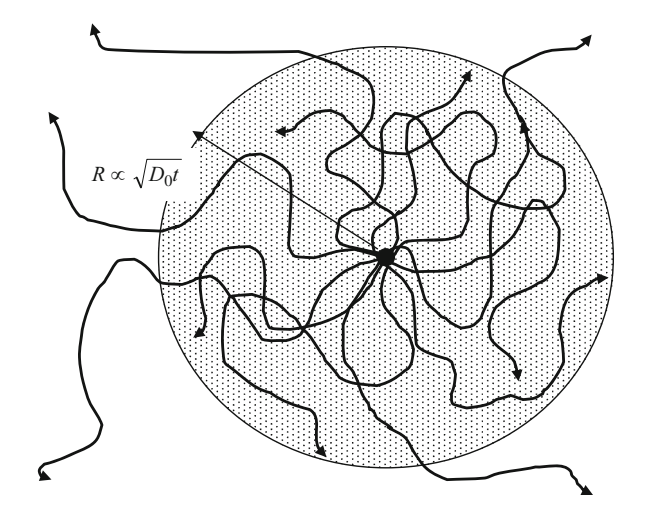
Fig. 4.4.3 Anomalous transport in a turbulent flow

displacements, and diffusive nature of transverse correlations in the presence of turbulence (see Fig. 4.4.3). Note that in the presence of the strong vertical stratification in environmental flows the ratio of longitudinal spatial scale of particle cloud to transverse scale continuously grows, confirming the above arguments [67–72].

## 4.5 Seed Diffusivity and Turbulent Transport

In the first section of this chapter, we have discussed the relation between singleparticle statistics (Lagrangian description) and transport effects in chaotic flows. The effects of molecular (seed) diffusion were ignored at that stage. However, the

Fig. 4.5.1 Schematic illustration of the domain of the main contribution to the Corrsin functional for the Lagrangian correlation function



"seed diffusivity" concept can be successfully applied to the consideration of correlation effects in turbulent flows. The conventional Taylor definition of the turbulent diffusion coefficient, which is based on the Lagrangian correlation function, does not contain any information on molecular diffusion (see Fig. 4.5.1). Serious problems obviously arise when we analyze the passive tracer transport. Thus, in the absence of streamline reconnections (steady flow cases), we certainly need the "seed diffusivity" mechanism responsible for the effective transport.

On the other hand, there are many observations, which provide extensive information on the Eulerian correlation function. In the framework of the Eulerian description, velocity correlations decay in both space and time and we have two characteristic correlation scales: the Eulerian characteristic time and the Eulerian characteristic spatial scale. Let us consider the Eulerian representation for the correlation function, which takes into account the velocity correlation at points separated by a distance  $\lambda$ 

$$C_{\mathcal{E}}(\lambda, t) = \langle u(x_0, T)u(x_0 + \lambda, T + t) \rangle. \tag{4.5.1}$$

Here,  $u(x_0,T)$  is the Eulerian velocity at point  $x_0$  and time T.

It would be important to establish the relationship between the Lagrangian and the Eulerian correlation functions as well as between the Lagrangian and the Eulerian characteristic time scales. Such relations are fairly useful for using Lagrangian measurement data in Eulerian simulation models. At present, there is no rigorous relation between the Lagrangian correlation function and the Eulerian one. Actually, there is no Lagrangian relation between the points  $x_0$  and  $x_0 + \lambda$  in the Eulerian correlation function definition, where  $\lambda$  is merely some arbitrary displacement.

To find a relation between the Lagrangian and the Eulerian correlation functions, one can represent the Lagrangian correlation function in the form

$$C(t) = \langle V(x(0))V(x(t))\rangle = \int_{-\infty}^{\infty} \langle V(0)V(y)\delta(y - x(t))\rangle dy.$$
 (4.5.2)

Corrsin [73] employed the factorization approach (the "independence hypothesis"):

$$\langle V(0)V(y)\delta(y-x(t))\rangle = \langle V(0)V(x)\rangle\langle\delta(y-x(t))\rangle, \tag{4.5.3}$$

where he applied the Gaussian distribution  $\rho(y,t)$  to describe trajectory correlations  $\langle \delta(y-x(t)) \rangle \approx \rho(y,t)$ , whereas the term  $\langle V(0)V(x) \rangle$  can now be interpreted as the Eulerian correlation function,  $C_{\rm E}(\lambda,t)$ . In this context, the approximation formula in terms of the randomization of the Lagrangian correlation function with the probability density  $\rho(\lambda,t)$  takes the form

$$C(t) = \int_{-\infty}^{\infty} \rho(\lambda, t) C_{E}(\lambda, t) d\lambda.$$
 (4.5.4)

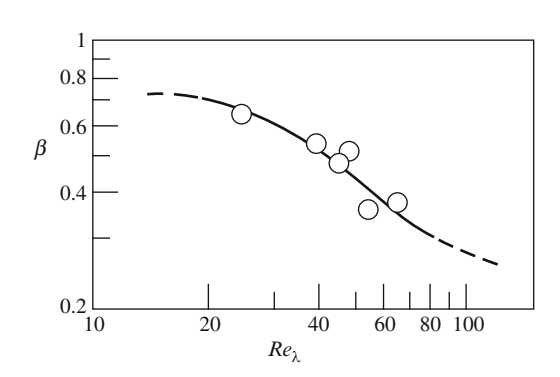
Thus, the Lagrangian correlation function can be expressed through the Eulerian one if we know the probability density function of particle displacements.

In a simplified case, for the probability density  $\rho(\lambda, t)$  it is natural to use the Gaussian distribution, which in three-dimensional space is given by the formula

$$\rho(\lambda, t) = \frac{1}{(4\pi D_0 t)^{3/2}} \exp\left(-\frac{\lambda^2}{4D_0 t}\right). \tag{4.5.5}$$

This formula includes the molecular diffusion coefficient  $D_0$ , which can be interpreted as the diffusive nature of the displacement  $\lambda$ . Note that such an elegant representation of  $\lambda$  plays the role of the Lagrangian distance and the diffusive displacement at the same time. It is possible to examine the Corrsin conjecture by assuming certain forms of the Eulerian correlation function basing on environmental data and to establish relations between the Lagrangian and the Eulerian

Fig. 4.5.2 Ratio of Lagrangian to Eulerian integral length scales against the turbulent Reynolds numbers. (After Sato and Yamamoto [64] with permission)



characteristic spatial and time scales (see Fig. 4.5.2). Such a phenomenological approach is not universal because the variety of turbulence types leads to a wide range of parameters, which describe the ration of the Lagrangian and the Eulerian characteristic scales [67–69, 81, 82].

The Corrsin approach allows one to employ phenomenological arguments to obtain simplified approximations of transport in turbulent flows where the molecular diffusion effects are significant [74–80]. In order to display effectiveness of the diffusive renormalization of correlation effects, we consider turbulent velocity field on small spatial scales, where viscous effects have considerable influence. In this small domain, the velocity profile could be represented as linear. This allows one to apply the Corrsin anomalous transport model,  $\langle X^2(t) \rangle = \frac{2}{3} \omega_V^2 D_{\rm T} t^3$ , to estimate scalar spot dispersion in a turbulent flow. Here, the shear flow parameter  $\omega_V$  is given by the relation  $\omega_V^2 = \left(\frac{{\rm d} U}{{\rm d} y}\right)^2$ . Then, the spot dispersion in a scalar center-of-mass system can be estimated as

$$L^2(t) \propto 2D_{\rm T}t + 2D_0t + \frac{2}{3}D_0\omega_V^2t^3,$$
 (4.5.6)

where the turbulent diffusion coefficient has the Taylor correlation representation

$$D_{\rm T} = \int_0^t C(t') dt'. \tag{4.5.7}$$

The correction found  $(2/3)D_0\omega_V^2t^3$  has to be small because the linear approximation of the velocity profile is valid only for small times. This estimate shows, as could be expected, that turbulence increases the effective tracer transport. However, a nontrivial effect arises in a new restatement of the problem, when one considers the dispersion of mean scalar density in a source reference system, as it was done by Saffman [249].

By following the Saffman approach, we describe the scalar evolution by the advection-diffusion equation

$$\frac{\partial n}{\partial t} + \vec{u} \, \nabla n = D_0 \nabla^2 n, \tag{4.5.8}$$

where the initial scalar distribution is given by

$$n(\vec{r}, t_0) = \delta(\vec{r} - \vec{r}_0). \tag{4.5.9}$$

It is convenient to apply the diffusive approximation of correlation effects in the form that is slightly different from the Corrsin conjecture

$$\langle V(t)\rangle = \int u_V(\vec{r}, t)n(\vec{r}, t|\vec{r}_0, t_0)d\vec{r}. \tag{4.5.10}$$

Here, V is the Lagrangian velocity and  $u_V$  is the turbulent velocity in the same direction as the Lagrangian velocity V. Then one obtains the Lagrangian correlation function

$$C(t) = \langle V(t)V(t_0)\rangle = \int \langle u_V(\vec{r},t)u_V(\vec{r}_0,t_0)n(\vec{r},t|\vec{r}_0,t_0)\rangle d\vec{r}$$
(4.5.11)

The solution of the diffusion equation can be obtained in the form

$$n = n_m(t) \exp\left\{-\frac{1}{2}s_{ij}x_i'x_j'\right\},\tag{4.5.12}$$

where  $\vec{r}' = (x'_1, x'_2, x'_3)$  is the position vector relative to the fluid particle with which element of substance originally coincided and the dimensional factor  $s_{ii}$  is given by

$$s_{ij} \approx \frac{\delta_{ij}}{D_0(t - t_0)}. (4.5.13)$$

By the same arguments, one expresses the velocity  $u_V(\vec{r},t)$  as follows:

$$u_V(\vec{r},t) \approx v(t) + x_j' \left(\frac{\partial u_V}{\partial x_i}\right).$$
 (4.5.14)

Here, v(t) is the velocity of the fluid particle, which was at  $\vec{r}_0$  at the moment  $t_0$ , and hence,  $V(t_0) = v(t_0)$ . Calculations lead to the relation

$$\langle V(t)\rangle \approx v(t) + D_0(t - t_0)\nabla^2 u_V. \tag{4.5.15}$$

To obtain the correlation function  $C(t) = \langle V(t)V(t_0) \rangle$  and the dispersion, we have to calculate the value

$$\langle v(t_0)(\nabla^2 u_V)\rangle = \langle u_V \nabla^2 u_V \rangle = \langle \nabla (u_V \nabla u_V)\rangle - \langle (\nabla u_V)^2 \rangle \approx (\nabla u_V)^2.$$
 (4.5.16)

Here, it is convenient to introduce the characteristic time  $\tau_u = \omega_V^{-1} = 1/\langle (\nabla u_V)^2 \rangle$ . Now the expression for the dispersion is given by the formula

$$L^{2}(t) = 2D_{T}(t - t_{0}) + 2D_{0}(t - t_{0}) - \frac{2}{3}D_{0}\omega_{V}^{2}(t - t_{0})^{3}.$$
 (4.5.17)

One can see that the effect of interaction between the chaotic velocity field and the molecular diffusion decreases the dispersion relative to the origin. As before the correction  $-(2/3)D_0\omega_V^2(t-t_0)^3$  has to be small because the approximation used is valid only for small times,  $t < \tau (LV_0/v_F)^{-1/2} \approx \tau Re^{-1/2}$ . For more detailed estimates, we refer the reader to [62, 249].

Further Reading 67

## **Further Reading**

#### Correlation and Diffusion

- J.-P. Bouchaund, A. Georges, Phys. Rep. 195, 127 (1990)
- H.L. Pecseli, *Fluctuations in Physical Systems* (Cambridge University Press, Cambridge, 2006)
- L.E. Reichl, *A Modern Course in Statistical Physics* (Wiley-Interscience, New York, 1998)
- D. Sornette, Critical Phenomena in Natural Sciences (Springer, Berlin, 2006)

#### Lagrangian Correlation Function and Turbulence

- G.K. Batchelor, *The Scientific Papers of Sir G.I. Taylor*. Meteorology, Oceanology, Turbulent Flow, vol. 2 (Cambridge University Press, Cambridge, 1960)
- G.K. Batchelor, H.K. Moffat, M.G. Worster, *Perspectives in Fluid Dynamics* (Cambridge University Press, Cambridge, 2000)
- P. Bernand, J.M. Wallace, *Turbulent Flow* (Wiley, New York, 2002)
- T. Cebeci, Analysis of Turbulent Flows (Elsevier, Amsterdam, 2004)
- O. Darrigol, Words of Flow: A History of Hydrodynamics from the Bernoullis to Prandtl (Oxford University press, New York, 2009)
- P.A. Davidson, *Turbulence, An Introduction for Scientists and Engineers* (Oxford University Press, Oxford, 2004)
- U. Frisch, *Turbulence: The Legacy of A.N. N. Kolmogorov* (Cambridge University Press, Cambridge, 1995)
- W. Frost, T.H. Moulden (eds.), *Handbook of Turbulence* (Plenum Press, New York, 1977)
- S. Heinz, Statistical Mechanics of Turbulent Flows (Springer, Berlin, 2003)
- M. Lesieur, *Turbulence in Fluids* (Kluwer, Dordrecht, 1997)
- W.D. McComb, *The Physics of Fluid Turbulence* (Clarendon Press, Oxford, 1994)
- A.S. Monin, A.M. Yaglom, Statistical Fluid Mechanics (MIT, Cambridge, 1975)
- H. Tennekes, J.L. Lumley, A First Course in Turbulence (MIT, New York, 1970)
- A. Tsinober, An informal Introduction to Turbulence (Kluwer, Dordrecht, 2004)

## Correlation Functions and Geophysical Turbulence

G.T. Csanady, Turbulent Diffusion in the Environment (D. Reidel, Dordrecht, 1972)
N.F. Frenkiel (ed.), Atmospheric Diffusion and Air Pollution (Academic, New York, 1959)

- F.T.M. Nieuwstadt, H. Van Dop (eds.), *Atmospheric Turbulence and Air Pollution Modeling* (D. Reidel, Dordrecht, 1981)
- H.A. Panofsky, I.A. Dutton, *Atmospheric Turbulence*, *Models and Methods for Engineering Applications* (Wiley Interscience, New York, 1970)
- F. Pasquill, F.B. Smith, *Atmospheric Diffusion* (Ellis Horwood Limited, New York, 1983)
- J.C. Wyngaard, *Turbulence in the Atmosphere* (Cambridge University Press, Cambridge, 2000)

#### Seed Diffusion Effects

- M.P. Brenner, Classical Physics Through the Work of GI Taylor (MIT, Cambridge, 2000)
- R.M. Mazo, *Brownian motion*, *Fluctuations*, *Dynamics and Applications* (Clarendon Press, Oxford, 2002)
- T. Squires, S. Quake, Rev. Mod. Phys. 77, 986 (2005)
- G.H. Weiss, Aspects and Applications of the Random Walk (Elsevier, Amsterdam, 1994)
- Ya B. Zeldovich, A.A. Ruzmaikin, D.D. Sokoloff, *The Almighty Chance* (World Scientific, Singapore, 1990)

## Chapter 5 Lagrangian Chaos

#### 5.1 The Arnold–Beltrami–Childress Chaotic Flow

Since a key ingredient of Lagrangian particle description is the relation between Eulerian and Lagrangian representations, we start by reiterating this well-known kinematic material: if  $\vec{V}(\vec{x},t)$  is the (Eulerian) velocity field, and if  $\vec{X}(t,\vec{a}_0)$  is the motion of a fluid particle that at t=0 was at position  $\vec{a}_0$ , then in terms of this (Lagrangian) data the connection between the two representations is given by the formula

$$\left(\frac{\partial \vec{X}}{\partial t}\right)_{\vec{a}_0} = \vec{V}(\vec{X}(t, \vec{a}_0), t). \tag{5.1.1}$$

Conversely, if we introduce the material derivative operator

$$\frac{\mathbf{D}}{\mathbf{D}t} = \frac{\partial}{\partial t} + \vec{V} \cdot \nabla, \tag{5.1.2}$$

then the above equation may be stated in the Eulerian representation by the formula

$$\frac{\mathbf{D}\vec{x}}{\mathbf{D}t} = \vec{V}(\vec{x}, t). \tag{5.1.3}$$

Either way we arrive at the following system of coupled ordinary differential equations for the motion of a point in the fluid continuum:

$$\dot{x} = V_x(x, y, z, t),$$
  
 $\dot{y} = V_y(x, y, z, t),$   
 $\dot{z} = V_z(x, y, z, t)$ 
(5.1.4)

where  $(V_x, V_y, V_z)$  are the Cartesian components of the velocity field  $\vec{V}$ . We call these the advection equations. Although they arise from purely kinematical

considerations in the fluid mechanical context, and thus must be considered "embedded" in the evolution of any flow, equations obtained have the format of a "dynamical system" in the usual sense of the mechanics of systems with a finite number of degree of freedom.

The behavior of streamlines in steady-state three-dimensional flows can be very complex. The following equations:

$$\frac{\mathrm{d}x}{V_x} = \frac{\mathrm{d}y}{V_y} = \frac{\mathrm{d}z}{V_z} \tag{5.1.5}$$

define streamlines of the field of velocities  $\vec{V}(x, y, z)$ . A more convenient notation of this system, for example, in the following form:

$$\frac{\mathrm{d}x}{\mathrm{d}z} = \frac{V_x}{V_z} \equiv f_1(x, y, z),\tag{5.1.6}$$

$$\frac{\mathrm{d}y}{\mathrm{d}z} = \frac{V_y}{V_z} \equiv f_2(x, y, z) \tag{5.1.7}$$

shows that we are dealing with the "non-steady-state" problem for a dynamics system with two-dimensional phase space (x, y). Variable z is playing the role of time. For fields with

$$\operatorname{div} \vec{V} = 0, \tag{5.1.8}$$

we can present the system under consideration in the Hamiltonian form in order to apply the already well-developed apparatus of the theory of dynamic system to the full.

Three-dimensional dynamics introduces us to a qualitatively new phenomenon – the existence of streamlines chaotically arranged in space – which is sometimes called the Lagrangian turbulence. Various forms of this phenomenon have interesting practical applications and have played an important role in our understanding of the onset of turbulence, as well. In 1965, V.I.Arnold [83] suggested that the following steady-state three-dimensional flow,

$$V_x = A \cdot \sin z + C \cdot \cos y, \tag{5.1.9}$$

$$V_{v} = B \cdot \sin x + A \cdot \cos z, \tag{5.1.10}$$

$$V_z = C \cdot \sin y + B \cdot \cos x, \tag{5.1.11}$$

has a nontrivial topology of streamlines, since it satisfies the Beltrami condition:

$$rot \vec{V} = const \vec{V}. \tag{5.1.12}$$

The numerical analysis carried out in [84] confirmed the peculiarity of this flow. This problem was also studied by Childress [85]. This flow was named the ABC-flow

(Arnold–Beltrami–Childress). For instance, it can be shown that by computing a Poincare section for the case  $A = \sqrt{3}$ ,  $B = \sqrt{2}$ ,  $C = \sqrt{1}$ , the phase space of ABC-flow is decomposed into regular and chaotic regions [84–88].

Another important characteristic of the ABC-flow is the fact that the set of equations

$$\frac{\mathrm{d}x}{A\sin z + C\cos y} = \frac{\mathrm{d}y}{B\sin x + A\cos z} = \frac{\mathrm{d}z}{C\sin y + B\cos x},$$
 (5.1.13)

defining streamlines of the velocity field can be presented in the explicit Hamiltonian form [86–88]. In order to do this, let us write the previous relation in the following form:

$$\frac{\mathrm{d}x}{\mathrm{d}z} = \frac{1}{\Psi} \frac{\partial}{\partial y} H_E, \tag{5.1.14}$$

$$\frac{\mathrm{d}y}{\mathrm{d}z} = -\frac{1}{\Psi} \frac{\partial}{\partial x} H_E \tag{5.1.15}$$

where

$$\Psi(x, y) = C \cdot \sin y + B \cdot \cos x, \qquad (5.1.16)$$

$$H_E(x, y, z) = \Psi(x, y) + A(y \sin z - x \cos z).$$
 (5.1.17)

This set of equations with the Hamiltonian  $H_E(x, y, z)$  is non-integrable, with the exception of an obvious case when it is reduced to the two-dimensional set (i.e., when one of the coefficients A, B, and C becomes zero). To be more definite, by assuming that A = 0, we find the first integral in this integrable case:

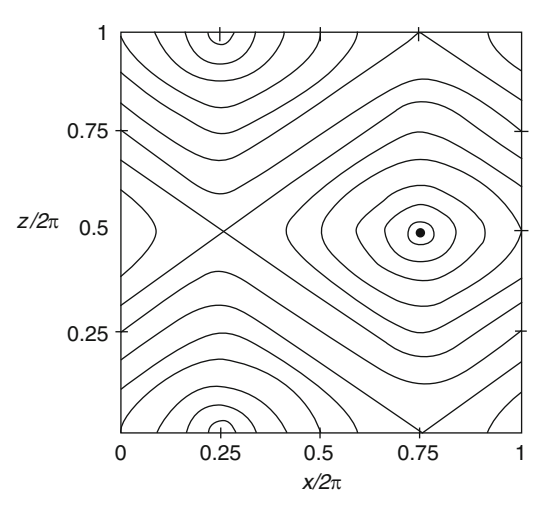
$$C \cdot \sin y + B \cdot \cos x = H_0 = \text{const.} \tag{5.1.18}$$

Streamlines on the plane (x, y) are shown in Fig. 5.1.1. There are three types of streamlines in it: closed streamlines, infinite streamlines, and singular streamlines, passing through saddle points of the surface  $H_0(x, y)$  and corresponding to separatrix.

Let us consider the Hamiltonian of streamlines  $H_E(x,y,z)$ . If A=0 (a two-dimensional case), it defines a family of cylindrical surfaces (stream tubes) corresponding to various values of the energy integral  $H_0=$  const (which is also the stream function). A perturbation of the Hamiltonian  $H_E(x,y,z)$  in the case of small A is equivalent to a small nonstationary perturbation of the dynamic system. A considerable proportion of stream tubes slightly change their shapes in accordance with the Kolmogorov–Arnold–Moser theory [89–91]. However, in the case of  $A \neq 0$ , there are such singular separatrix surfaces, which are heavily affected even by a small perturbation. The latter leads to formation of stochastic layers in the

72 5 Lagrangian Chaos

**Fig. 5.1.1** ABC-flow streamline topology for the integrable case C = 0



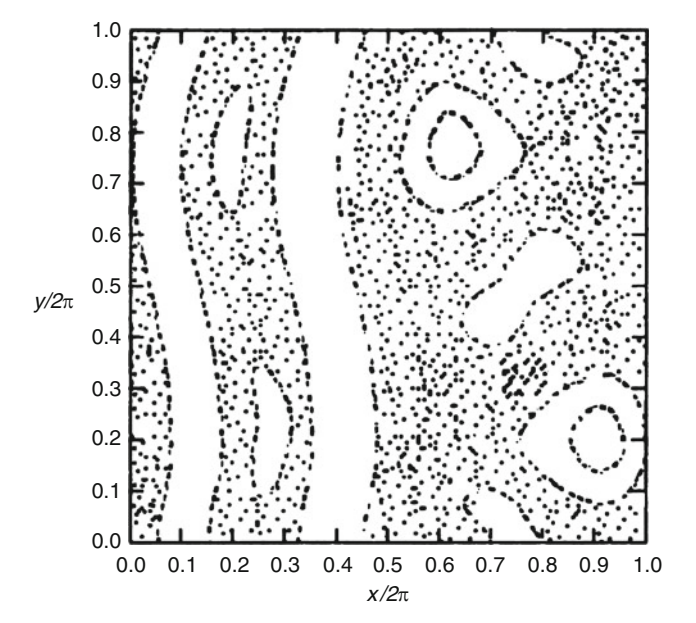


Fig. 5.1.2 ABC-flow streamline topology for the case  $A^2 = 1$ ,  $B^2 = 2/3$ , and  $C^2 = 1/3$ 

vicinity of destroyed separatrix and, consequently, to chaos of streamlines. In the case of large values of  $A \sim 1$ , stochastic layers expand (Fig. 5.1.2) and chaos of streamlines embraces a considerable portion of three-dimensional space. The appearance of large regions of chaos of streamlines in the *ABC*-flow is, in fact, the manifestation of a far more global phenomenon.

The existence of stochastic particle motion in flows that are laminar according to the conventional Eulerian measure (chaotic advection) is a key feature of the flow regime being discussed. The possibility of chaotic advection underscores why monitoring the motion of a single particle is not a reliable indicator of whether a flow is laminar or turbulent.

## 5.2 Hamiltonian Systems and Separatrix Splitting

If the flow is two-dimensional, there is no more z-dependency and, consequently, no chaos of streamlines. Indeed, three-dimensional dynamics differs drastically from two-dimensional dynamics where streamlines have a relatively simple structure and coincide with lines of the level of the stream function  $\Psi(x,y)$ . Hamiltonian systems with a low number of degrees of freedom  $(1\frac{1}{2}\text{or }2)$  can be considered as the simplest ones with chaotic dynamics. Conventionally,  $1\frac{1}{2}$  degree of freedom indicates a system with one degree of freedom driven by periodical perturbation  $\Psi(x,y,t)=\Psi_0(x,y)+\varepsilon_\omega\Psi_1(x,y,t)$ . Integrable dynamics of such a system in the phase space can be described more or less fairly completely because of its relatively simple topological structure. There are two kinds of singular points in the phase space: elliptic and hyperbolic. Motion near the elliptic points is stable and persists with a small perturbation in accordance with the KAM theory [92–95], and the motion near the hyperbolic (saddle) points is so dramatically unstable that a general perturbation leads to the chaotic dynamics near the separatrix. The separatrix represents an unperturbed singular trajectory that crosses the saddle points.

The motion in the neighborhood of a hyperbolic point is very complex. Without entering into technical details, we observe that a hyperbolic point in phase space has an analogy with a saddle point in physical space: two lines move toward the point (stable separatrix branch +) and two are moving away (unstable separatrix branch –) [92–95], as in Fig. 5.2.1. A point on the unstable line moves away from the hyperbolic point after each iteration. It will move toward another hyperbolic point but will never reach it. The unstable line intersects with the stable line of the

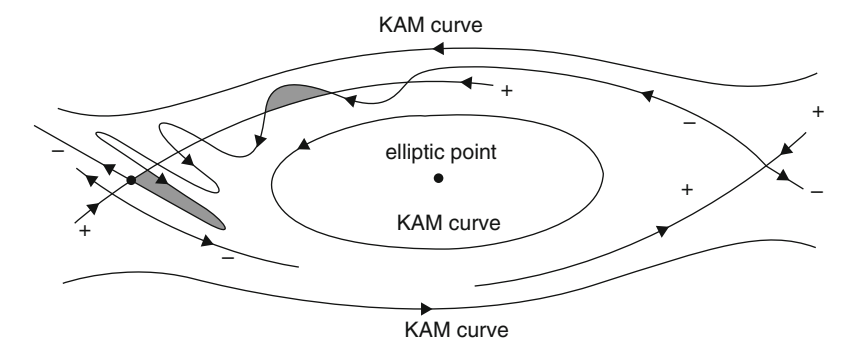


Fig. 5.2.1 Schematic illustration of the separatrix splitting and generation of the stochasticity near a separatrix

neighboring hyperbolic point at so-called homoclinic points. Because the homoclinic points are not stable points of the map and sit on the stable line of the neighboring hyperbolic point, they will move toward this point under the action of the map. However, because of the area-preserving property of the map (shaded in Fig. 5.2.2), the oscillations around the stable line become wilder and wilder producing an infinite sequence of homoclinic points on the stable line that prevents points on this line from reaching the hyperbolic point. The oscillations near the hyperbolic point result in a very complex behavior of the system between the stable KAM tori. A similar behavior accounts for an infinite number of iterations necessary for leaving a hyperbolic point along its unstable line. This wild behavior near hyperbolic points is also illustrated by a numerous numerical examples.

One can say that stochastic layer is a seed of chaos in Hamiltonian dynamics. A narrow domain near the separatrix is extremely sensitive to small perturbations. Perturbation destroys the unperturbed separatrix, and a finite width layer with chaotic motion inside it replaces the unperturbed separatrix. In fact, the stochastic layer has complicated topological structure. It consists of an infinite number of islands, subislands, island-around-islands, etc. An island is a domain with elliptic points inside and integrable KAM curves around the points (see Fig. 5.2.3). Smaller stochastic layers of higher order exist inside the islands, but invariant (integrable) curves isolate these layers from the main stochastic layer.

It became clear that the insight into the origin of chaotic dynamics can come from the understanding of the dynamics in the destroyed separatrix domain. Numerous publications were focused on the following specific problems: splitting of the separatrix, estimating the stochastic layer width, and applications [85–95]. The research on the separatrix splitting followed the original Melnikov's formula,

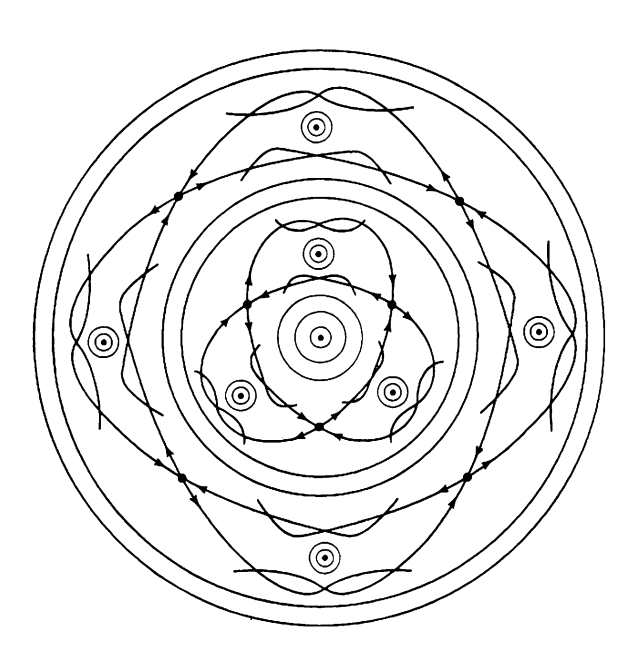
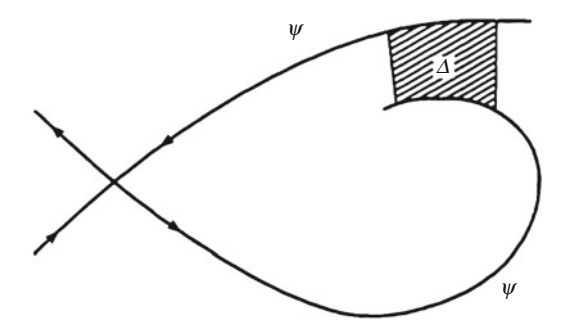


Fig. 5.2.2 Schematic illustration of stable and unstable of hyperbolic periodic orbits

74

Fig. 5.2.3 Schematic illustration of the separatrix splitting and generation of the stochastic layer of width  $\Delta$ 



the so-called Melnikov's integral, which gives the change in stream function amplitude  $\delta \Psi_0$  due to the separatrix splitting

$$\delta \Psi_0(t_0) = \int dt \frac{d\Psi_0(x(t, t_0), y(t, t_0))}{dt}.$$
 (5.2.1)

It gave an expression for the area of the lobe, which appeared due to the different asymptotics for stable and unstable perturbed separatrix. By taking into account the advection equation in terms of perturbated stream function

$$\Psi(x, y, t) = \Psi_0(x, y) + \varepsilon_{\omega} \Psi_1(x, y, t)$$
 (5.2.2)

one obtains the integral over Lagrangian trajectory of tracer in the following form:

$$\delta\Psi_0(t_0) = \int dt \,\varepsilon_\omega \,\vec{V} \,\nabla\Psi_0 = \varepsilon_\omega \int dt \left\{ \frac{\partial \Psi_1(t)}{\partial x} \,\frac{\partial \Psi_0}{\partial y} - \frac{\partial \Psi_1(t)}{\partial y} \,\frac{\partial \Psi}{\partial x} \right\}. \tag{5.2.3}$$

Here, the trajectory of scalar particle can be represented as the asymptotic expansions

$$x(t,t_0) \approx x(t_0) + \varepsilon_{\omega} x_1(t), \tag{5.2.4}$$

$$y(t,t_0) \approx y(t_0) + \varepsilon y_1(t), \tag{5.2.5}$$

where  $\varepsilon$  is the perturbation amplitude and  $(x(t_0))$  and  $y(t_0)$  are the initial points of the particle. At this stage of analysis of stochastic layer contribution to transport, we omit all these complicated calculations, which may be carried out exactly for different analytical representation of streamline functions, because the reader could find these results in many publications [85–95]. However, by concluding this section we note that because of an analogy between Hamiltonian models and two-dimensional incompressible flows, it is natural to consider stochastic layers in the vicinity of streamlines having the separatrix form (see Fig. 5.2.4). On the other hand, in the presence of stochastic layers we must obviously search for new correlation effects as well as characteristic spatial and temporal correlation scales necessary for phenomenological models of transport.

76 5 Lagrangian Chaos

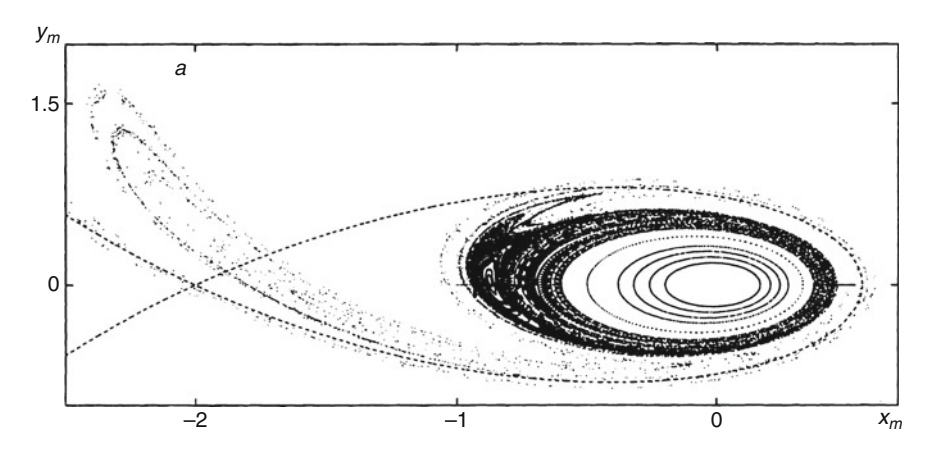


Fig. 5.2.4 A typical Poincare section (After Budyansky [96] with permission)

## 5.3 Stochastic Instability and Single-Scale Approximation

The stochastic instability of trajectories was first discovered [97–100] in billiard-like systems. Now let us turn our attention to the chaotic flow case. From the formal point of view, we can analyze this phenomena in the framework of the divergence of initially nearby trajectories

$$l(t) \approx l(0)\exp(h_{\rm K}t) \approx l(0)\exp\left(\frac{t}{\tau_{\rm S}}\right).$$
 (5.3.1)

Here, l(t) is the distance between trajectories at the moment t and  $h_{\rm K}$  is the Kolmogorov entropy expressed in terms of Lyapunov's exponent [101, 102]:

$$h_{\rm K} = \lim_{l(0)\to 0, t\to \infty} \left\{ \frac{1}{t} \ln \frac{|l(t)|}{|l(0)|} \right\}.$$
 (5.3.2)

Indeed, consider the case of a stationary velocity field

$$\frac{\mathrm{d}\vec{x}}{\mathrm{d}t} = \vec{V}(\vec{x}) \tag{5.3.3}$$

Let  $\vec{x}(t)$  be the trajectory corresponding to the initial condition  $\vec{x}(t=0) = \vec{x}_0$ . Let us find the equation of perturbation of this trajectory. With this aim in view, consider a close trajectory  $\vec{x}(t) + \vec{l}_0(t)$  with the initial condition

$$\vec{x}(t=0) = \vec{x}_0 + \vec{l}_0 \tag{5.3.4}$$

where  $\vec{l}_0$  is an infinitesimal vector. The perturbation of the trajectory  $\vec{l}(t)$  satisfies the following equation:

$$\frac{\mathrm{d}\vec{l}_0}{\mathrm{d}t} = (\vec{l}\nabla)\vec{V}(\vec{x}). \tag{5.3.5}$$

This can be rewritten on the following form:

$$\frac{d\vec{l}}{dt} + (\vec{V}\nabla)\vec{l} = (\vec{l}\nabla)\vec{V}.$$
 (5.3.6)

The stochasticity of streamlines and trajectories of particles of a liquid means that the Lyapunov exponent  $h_{\rm K}$  is positive. In this context, the chaotic properties of dynamic systems have been investigated in many textbooks [93–102]. An example of such exponential divergence of two orbits near the separatrix of Hamiltonian system with very close initial conditions is shown in Fig. 5.3.1.

We look here more closely at the scaling aspect of the problem, since both the Kolmogorov entropy  $h_K$  and the spatial scale l define decorrelation mechanisms and transport. Thus, by considering the evolution of fluid element of size  $L_*$  in hydrodynamical field with the characteristic velocity scale  $V_0$  and characteristic frequency  $\omega$ , it is easy to estimate stretching fluid element during the characteristic time  $\tau_0$ :

$$L_1 \approx L_* \frac{\delta L}{\lambda} \approx L_* \frac{V_0}{\omega \lambda}.$$
 (5.3.7)

Here,  $\lambda$  is the characteristic spatial scale. Then, the length of fluid element,

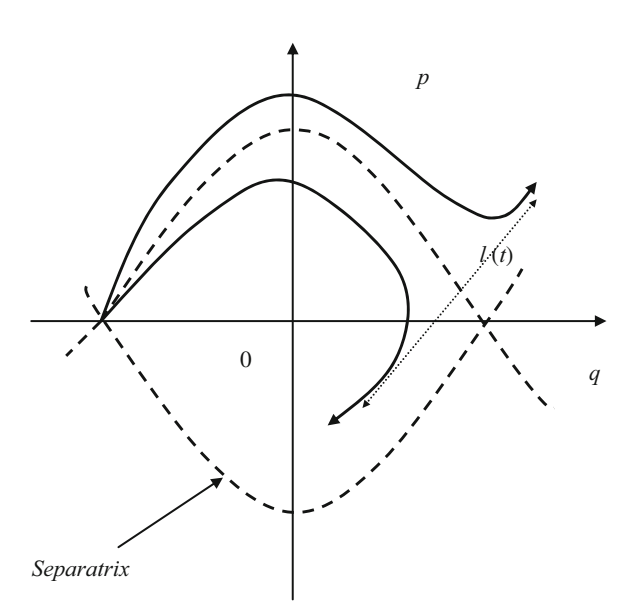


Fig. 5.3.1 Schematic diagram of exponential instability. Exponential divergence of orbits near the unperturbed separatrix with very small differences in the initial conditions

78 5 Lagrangian Chaos

$$L(t) \approx L_* \left(\frac{V_0}{\omega \lambda}\right)^{t/\tau_0} = L_* \exp\left[\frac{t}{\tau_0} \ln Ku\right] \approx L_* \exp\left(\frac{t}{\tau_S}\right), \tag{5.3.8}$$

corresponds to the time t (see Fig. 5.3.2). Here, the dimensionless parameter

$$Ku = \frac{V_0}{\omega \lambda} \tag{5.3.9}$$

is the Kubo number, which plays the role of the mapping parameter  $K_S$ . In the discrete form, it could be represented as the mapping procedure

$$\delta x_N \approx K_S^N \delta x_0 \approx \delta x_0 \exp(N \ln K_S).$$
 (5.3.10)

Here, N is the number of iterations,  $\delta x_0$  is the initial length of phase element, and  $\delta x_N$  is the length of the element under analysis after iterations. In the streamline chaos case

$$\tau_S(Ku) \approx \frac{\tau_0}{\ln Ku} \approx \frac{\tau_0}{\ln(\frac{V_0}{2\omega})}.$$
(5.3.11)

Note, the characteristic time  $\tau_0$  also must be interpreted in terms of flow parameters,  $\tau_0 = \tau_0(V_0, \lambda, \omega)$  [103, 104]. This allows us to treat stochastic instability effects, correlations, and transport properties from the common standpoint.

Here, we discuss a passive scalar transport in a random flow in the framework of single-scale approximation. We suppose that such a flow is characterized by the single velocity amplitude  $V_0$  and the length scale  $L_0$ . The characteristic magnitude of the velocity gradient is given by  $V_0/L_0$ . A scalar blob will be stretched and rolled up by the chaotic flow (see **Fig. 5.3.3**). In a steady random flow, the stretching and folding of volumes of the fluid proceed exponentially [106, 107]. The small scales of such a blob are given by the relation

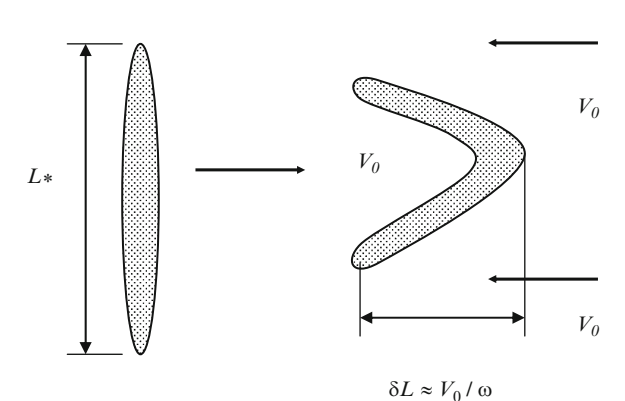
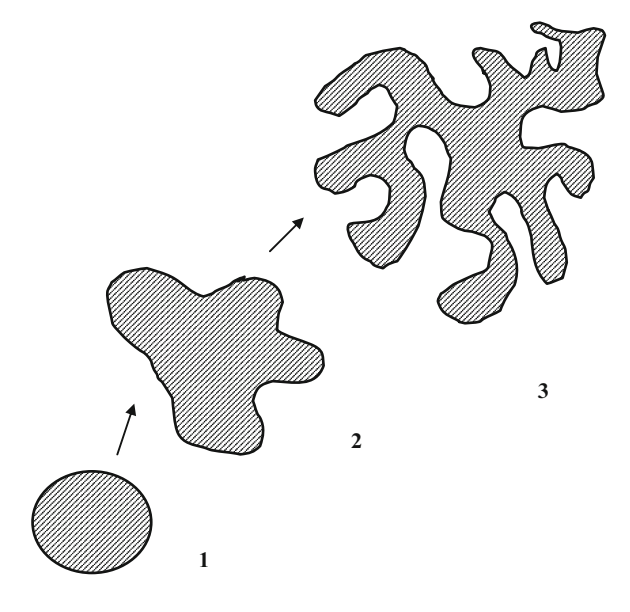


**Fig. 5.3.2** The figure shows hydrodynamic evolution of a small fluid element

**Fig. 5.3.3** Schematic diagram of evolution of a region of phase space



$$\Delta(t) = L_0 \exp(-\gamma_s t), \tag{5.3.12}$$

where  $\gamma_s$  is the stochastic instability increment. In the presence of molecular (seed) diffusivity gradients disappear. One can estimate the mixing spatial scale (the Batchelor scale)  $\Delta_{mix}$  by comparison of the diffusion rate

$$\gamma_D = \tau_D^{-1} \approx \frac{D_0}{\Delta_{\text{mix}}^2} \tag{5.3.13}$$

and the rate of stretching  $\gamma_s$ . In the case of the single-scale approximation, we find

$$\frac{D_0}{\Delta_{\min}^2(t_{\min})} \approx \frac{V_0}{L_0}.$$
 (5.3.14)

In terms of the Peclet number, one obtains the scaling for the dissipation scale in the framework of single-scale approximation

$$\Delta_{\text{mix}}(Pe) \propto \frac{L_0}{\sqrt{Pe}},$$
(5.3.15)

where  $Pe \gg 1$ . This allows us to derive the formula for the mixing time in the large Peclet number limit

$$\frac{L_0}{\sqrt{Pe}} = L_0 \exp(-\gamma_s t_{\text{mix}}),\tag{5.3.16}$$

and we arrive to the scaling,

$$t_{\rm mix}(Pe) \propto \frac{\ln Pe}{\gamma_{\rm s}}$$
 (5.3.17)

In the case of sufficiently random flow, the mixing time weakly depends on the seed diffusivity. We suppose the steady flow under consideration not to be concerned with the existence of separatrix or stagnation points. The case of chaotic advection where the flow topology reconstruction is related to the separatrix reconnection as well as the Batchelor dissipation scale cascade representation is considered later.

## 5.4 Chaotic Mixing in Microchannels

Mixing of the fluid flowing through microchannels is important in a variety of industrial applications such as the homogenization of solutions of reagents in chemical reactions, the control of dispersion of material along the direction of Poiseuille flows, and so on (see Fig. 5.4.1). At the low Reynolds numbers  $Re = \frac{V_0 L_0}{v_F}$  in channels with smooth walls, flows are usually laminar, so the mixing of material between streams in the flow is purely diffusive. Here,  $V_0$  is the characteristic velocity,  $L_0$  is the characteristic spatial scale, and  $v_F$  is the kinematic viscosity.

For instance, in the microchannel condition we are dealing with the following characteristic values:  $V_0 < 100 \text{ cm/s}$ ,  $L_0 \approx 0.01 \text{ cm}$ , and  $v_F \approx 0.01 \text{ g/(cm s)}$ , and this

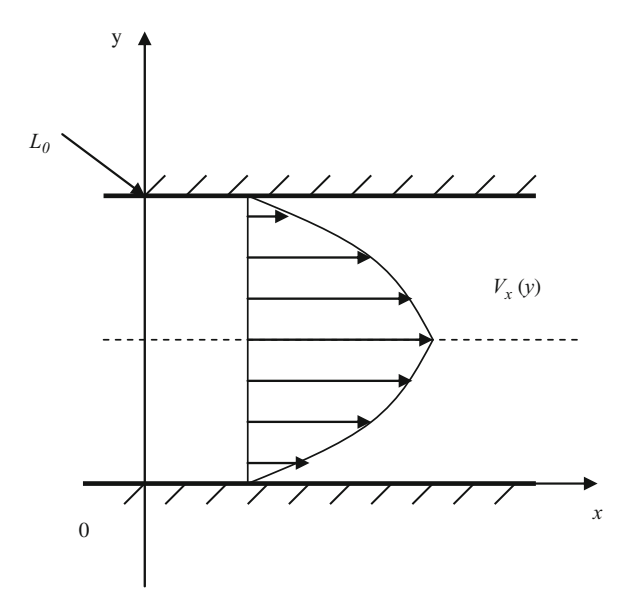


**Fig. 5.4.1** Characteristic geometry of the Poiseuille two-dimensional flow

leads to the estimate for the Reynolds number Re<100. On the scale of a microchannel, the diffusive mixing is slow in comparison with the convection along the channel. In this case, we are dealing with the large Peclet number,

$$Pe = \frac{V_0 L_0}{D_0} > 100, (5.4.1)$$

where  $D_0 < 10^{-5} \,\mathrm{cm^2/s}$  is the molecular diffusivity. For such laminar flows, the distance along the channel that is required for mixing to occur is

$$l_{\text{mix}} \propto V_0 \frac{L_0^2}{D_0} = Pe \cdot L_0.$$
 (5.4.2)

This mixing length can be prohibitively long ( $l_{\text{mix}} \gg 1 \text{ cm}$ ) and scales linearly with the Peclet number Pe.

To reduce the mixing length, there must be transverse components of flow that stretch and fold volumes of fluid over the cross section of the channel [108, 109]. These stirring flows will reduce the mixing length  $l_{\rm mix}$  by decreasing the average distance,  $\Delta$ , over which diffusion must act in the transverse direction to homogenize unmixed domains. In the case of a steady random flow, the stretching and folding of the volumes under consideration proceed exponentially as a function of the longitudinal distance traveled by the volume:

$$\Delta(l) = L_0 \exp\left(-\frac{l}{\lambda_s}\right),\tag{5.4.3}$$

where the initial transverse scale is taken to be  $L_0$ , and  $\lambda_s$  is a characteristic length determined by the geometry of trajectories in the chaotic flow. It is natural to estimate the mixing length by

$$l_{\text{mix}} \approx V_0 \tau_{\text{D}} \approx V_0 \frac{\Delta^2(l_{\text{mix}})}{D_0}, \tag{5.4.4}$$

where  $\tau_D$  is the diffusion characteristic time. After substitution, one obtains the equation for the mixing length in the form

$$\sqrt{\frac{l_{\text{mix}}}{L_0}} = \sqrt{\frac{V_0 L_0}{D_0}} \exp\left(-\frac{l_{\text{mix}}}{\lambda_s}\right),\tag{5.4.5}$$

For the large Pe, in a flow that is chaotic over most of its cross section, we expect an important reduction of the mixing length relative to that in an unstirred flow:

$$l_{\text{mix}}(Pe) \propto \lambda_s \ln(Pe).$$
 (5.4.6)

82 5 Lagrangian Chaos

The scaling for the transverse spatial scale takes the form

$$\Delta(l_{\rm mix}) \propto \frac{L_0}{\ln(Pe)}$$
 (5.4.7)

Indeed, asymmetric grooves in the channel walls induce an axially modulated secondary flow in the form of an asymmetric set of counter-rotating fluid rolls (see Fig. 5.4.2). The asymmetry of the rolls is periodically reversed, so that the distance between stripes halves with each cycle, leading to exponential stretching and folding of fluid volumes. Thus, after *N* cycles requiring the mixing time

$$\tau_{\text{mix}} \propto \frac{l_{\text{mix}}}{V_0} \approx N \frac{\lambda_s}{V_0},$$
(5.4.8)

where  $\lambda_s$  is the cycle length, stripes are separated by a distance

$$\Delta(N) \propto \frac{L_0}{2^N}.\tag{5.4.9}$$

It is now obvious that mixing occurs when the time to diffuse between stripes  $\tau_D$  is comparable to the cycle time  $\tau_{mix}$ ,

$$\frac{\Delta^2(N)}{D_0} \approx \tau_{\text{mix}} \propto \frac{N\lambda_s}{V_0},\tag{5.4.10}$$

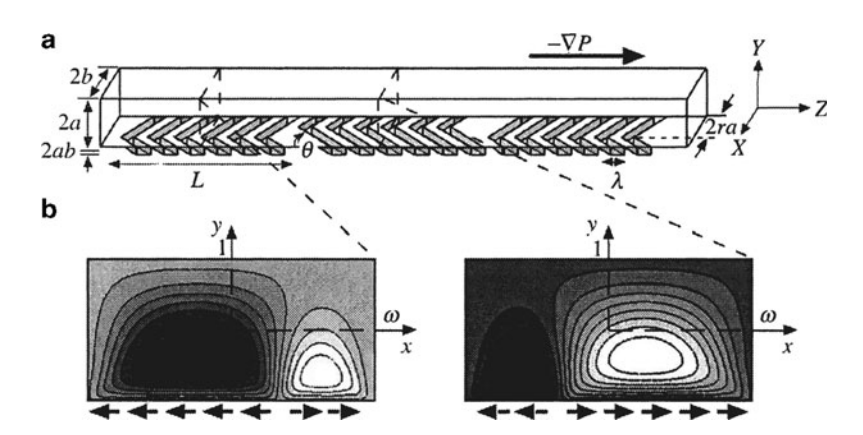


**Fig. 5.4.2** (a) Three-dimensional schematic of one-and-a-half cycles of the mixer device. Each cycle is composed of two sets of grooves (six per set in the case shown) in the floor of the channel. The grooves are in the form of herringbones that are asymmetric with respect to the center of the channel (along x); the direction of the asymmetry switches from one half-cycle to the next. The flow is driven by an axially applied pressure gradient,  $\nabla P$ . (b) Schematic of the lid-driven cavity model that is used to treat the flow in the cross section. The *arrows* beneath the cavity indicate the motion of the bottom wall. Contour plots of the approximate stream function of the flow in the cross sections are shown for each half-cycle. (After Stroock and McGraw [108] with permission)

which yields the scaling

$$N(Pe) \propto \ln Pe.$$
 (5.4.11)

After substitution, one obtains the expression for the mixing length in the form

$$l_{\text{mix}}(Pe) \approx \lambda_s N(Pe) \approx \lambda_s \ln Pe.$$
 (5.4.12)

Finally, we find the relation for the mixing time,

$$\tau_{\text{mix}}(Pe) \propto \frac{\lambda_s \Delta_0}{D_0} \frac{\ln Pe}{Pe}.$$
(5.4.13)

Indeed, the number of cycles (or mixing length) measured in the staggered herringbone mixer depends logarithmically on Pe,  $N(Pe) \propto \ln Pe$  over six decades.

One can see that the stochastic instability leads to the appearance of new decorrelation mechanisms. For example, it often "destroys" subdiffusion regimes, which are based on the repeated returns of particles. This problem has been studied in the context of both astrophysical and plasma physics applications where the exponential divergences of two neighboring streamlines of a chaotic flow play a significant role [110–114].

## 5.5 Multiscale Approximation

We already treated above the single-scale approximation of chaotic mixing in terms of the Peclet number. It would be natural to generalize this approach to a multiscale flow. The impressive description of chaotic mixing in the framework of the Kolmogorov theory of scalar cascade was done by Batchelor [39]. We discuss such an approach later in the context of the cascade phenomenology. Here, we represent simplified dimensional arguments to obtain transport scaling for a multiscale chaotic flow.

Let us suppose that for the spatial scales less than the mixing spatial scale  $\Delta_{mix}$ 

$$l \ll \Delta_{\text{mix}},$$
 (5.5.1)

a random flow stretches and folds volumes of the fluid exponentially,

$$l^{2}(t) = L_{0}^{2} \exp(-\gamma_{s}t), \tag{5.5.2}$$

where  $\gamma_s$  is the stochastic instability increment. In terms of transport scaling, this can be represented as

84 5 Lagrangian Chaos

$$\frac{\mathrm{d}}{\mathrm{d}t}l^2(t) \propto l^2(t). \tag{5.5.3}$$

On the other hand, in the presence of molecular (seed) diffusivity  $D_0$ , for the spatial scales greater than the mixing spatial scale

$$l \gg \Delta_{\text{mix}},$$
 (5.5.4)

we are dealing with the diffusive regime, which is described by the relation

$$\frac{\mathrm{d}}{\mathrm{d}t}l^2(t) \propto 2D_{\mathrm{T}}.\tag{5.5.5}$$

On the basis of these equations, it is possible to build the approximation formula describing both the exponential regime and the diffusive stage

$$\frac{\mathrm{d}}{\mathrm{d}t}l^2(t) \propto 2D_{\mathrm{eff}}(l). \tag{5.5.6}$$

In this context, we consider the dimensional approximation of the effective diffusion coefficient in the form

$$\frac{\mathrm{d}}{\mathrm{d}t}l^2(t) \propto 2D_0 + 2D_\mathrm{T} \left(\frac{l}{\Delta_{\mathrm{mix}}}\right)^2. \tag{5.5.7}$$

Basing on this expression, we are able to estimate the characteristic lifetime of a blob evolution in a multiscale chaotic flow as follows:

$$dt = \frac{2l dl}{2D_0 + 2D_T \left(\frac{l}{\Delta_{\text{mix}}}\right)^2}.$$
 (5.5.8)

After simple calculations, one obtains the scaling

$$\tau_{\text{mix}}(Pe) \approx \frac{\Delta_{\text{mix}}^2}{D_{\text{T}}} \ln \left( \frac{Pe}{1 + PeL_0/\Delta_{\text{mix}}} \right).$$
(5.5.9)

Here,  $L_0$  is the small initial distance. The estimate of the characteristic mixing time in the scaling form,

$$\tau_{\text{mix}}(Pe) \approx \frac{1}{\gamma_{\text{S}}} \ln Pe,$$
(5.5.10)

was repeatedly used in the explanation of anomalously long lifetimes of coherent structures in chaotic flows with the large Peclet numbers,  $Pe \gg 1$  [115, 116]. Thus,

Further Reading 85

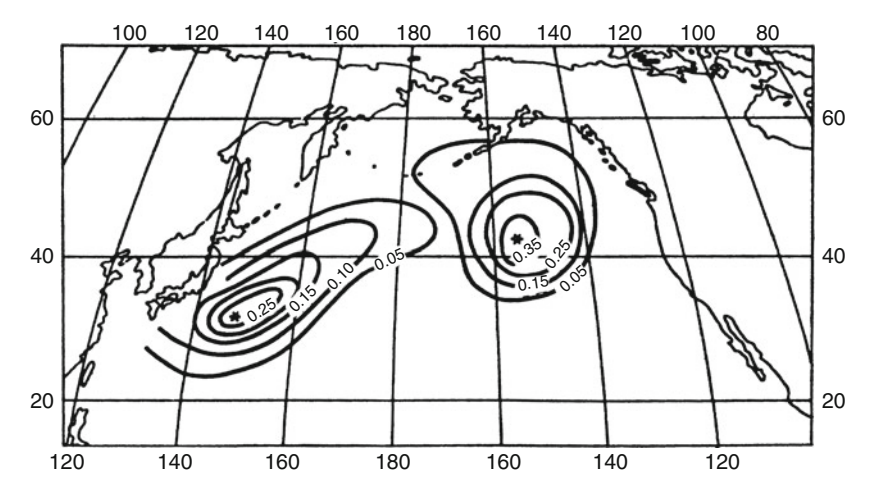


Fig. 5.5.1 A typical evolution of temperature spots (After Pitterbarg [117] with permission)

the very long lifetimes of temperature spots on the Ocean surface were interpreted in [117] on the basis of this logarithmical dependence (see Fig. 5.5.1). Besides, in the framework of the Lagrangian description of magnetic turbulence, it is possible to employ the approximation formula

$$\frac{\mathrm{d}}{\mathrm{d}z}l^2(z) \propto 2D_{\mathrm{eff}}(l) \tag{5.5.11}$$

to describe electron heat conductivity in galaxy clusters in terms of multiscale representation of force line walks [118].

Note that the estimate obtained here for  $\tau_{\rm mix}(Pe)$  insignificantly differs from the single-scale approximation. This encourages us to search for new physical arguments to treat stochastic instability effects in multiscale chaotic flows.

## **Further Reading**

## Chaos and Dynamical Systems

- V.I. Arnold, B.A. Khestin, *Topological Methods in Hydrodynamics* (Springer, Berlin, 2006)
- C. Beck, F. Schlogl, *Thermodynamics of Chaotic Systems* (Cambridge University Press, Cambridge, 1993)
- V. Berdichevski, *Thermodynamics of Chaos and Order* (Longman, White Plains, NY, 1998)

P. Castiglione et al., *Chaos and Coarse Graining in Statistical Mechanics* (Cambridge University Press, Cambridge, 2008)

- J.R. Dorfman, An Introduction to Chaos in Nonequilibrium Statistical Mechanics (Cambridge University Press, Cambridge, 1999)
- P. Gaspard, *Chaos, Scattering and Statistical Mechanics* (Cambridge University Press, Cambridge, 2003)
- A.J. Lichtenberg, M.A. Liberman, *Regular and Stochastic Motion* (Springer, Berlin, 1983)
- R.S. MacKay, J.D. Meiss, Hamiltonian Dynamical Systems (Hilger, Bristol, 1987)
- E. Ott, *Chaos in Dynamical Systems* (Cambridge University Press, Cambridge, 1993)
- G.M. Zaslavsky, *The Physics of Chaos in Hamiltonian Systems* (Imperial College, London, 2007)

#### Chaos and Mixing

- H. Aref, M.S. El Naschie, Chaos Applied to Fluid Mixing (Pergamon, London, 1994)
- T. Bohr, M.H. Jensen, P. Giovanni, A. Vulpiani, *Dynamical Systems Approach to Turbulence* (Cambridge University Press, Cambridge, 2003)
- J. Cardy, *et al* (Non-equilibrium Mechanics and Turbulence, Cambridge University Press, Cambridge, 2008)
- S. Childress, A.D. Gilbert, *Stretch, Twist, Fold: The Fast Dynamo* (Springer, Berlin, 1995)
- E. Guyon, J.-P. Nadal, Y. Pomeau (eds.), *Disorder and Mixing* (Kluwer, Dordrecht, 1988). 1988
- W. Horton, Y.-H. Ichikawa, *Chaos and Structures in Nonlinear Plasmas* (Word Scientific, Singapore, 1994)
- H.K. Moffatt, G.M. Zaslavsky, P. Comte, M. Tabor, *Topological Aspects of the Dynamics of Fluids and Plasmas* (Kluwer, Dordrecht, 1992)
- J. Ottino, *The Kinematics of Mixing* (Cambridge University Press, Cambridge, 1989)
- J.M. Ottino, Physics of Fluids 22, 021301 (2010)
- A. Ruzmaikin, A. Shukurov, D. Sokoloff, *Magnetic Fields of Galaxies* (Springer, Berlin, 1988)
- T. Tel, Physics Reports **413**, 91 (2005)
- M. Van-Dyke, An Album of Fluid Motion (Parabolic, Stanford, CA, 1982)
- S. Wiggins, *Introduction to Applied Nonlinear Dynamical Systems and Chaos* (Springer, New York, 1999)
- S. Wiggins, Chaotic Transport in Dynamical Systems (Springer, New York, 1990)

# Part III Phenomenological Models

## Chapter 6

# **Correlation Effects and Transport Equations**

#### 6.1 Averaging and Linear-Response

It is rather natural to wonder about the effective equation, which rules the asymptotic evolution in the case of diffusion in chaotic (turbulent) flow instead of the Fick one. Indeed, we would like to know what are equations replacing the conventional diffusion equation at large spatial scales and long times.

In the framework of Lagrangian approach, it is convenient to employ the scalar evolution equation in the form

$$\frac{dn}{dt} = \frac{\partial n}{\partial t} + V_i \frac{\partial n}{\partial x_i} = 0, \tag{6.1.1}$$

where the assumption of incompressibility is applied

$$\frac{\partial V_x}{\partial x} + \frac{\partial V_y}{\partial y} + \frac{\partial V_z}{\partial z} = 0. \tag{6.1.2}$$

In terms of Lagrangian representation, the solution of this equation is given by the formula  $n(\vec{r},t) = n_0(\vec{a})$ . Here,  $n_0$  is the initial scalar distribution function. Note, for a single scalar particle situated at the point a at the moment t, one obtains

$$n(t=0) = \delta(\vec{r} - \vec{a}),$$
 (6.1.3)

where symbol  $\delta$  denotes the Dirac function.

However, the continuity equation could be the grounds for more fruitful approach to build the effective diffusion equation on the basis of Lagrangian correlation function. For the sake of simplicity, we analyze the continuity equation for the density of a passive scalar in the one-dimensional case:

$$\frac{\partial n}{\partial t} + V(t)\frac{\partial n}{\partial x} = 0, (6.1.4)$$

where n(x, t) is the spatial density of the passive scalar. For an incompressible flow

$$\operatorname{div} \vec{V} = \frac{\partial V_x}{\partial x} = 0. \tag{6.1.5}$$

and V = V(t) is the random velocity field. The general solution of the continuity equation is given by the formula

$$n(x,t) = n_0(x) \left\{ x - \frac{1}{m} \int_0^t V(t') dt' \right\}.$$
 (6.1.6)

In principle, if we know the distribution function f(V) for the random velocity field V(t), then one obtains the mean scalar density

$$n(x,t) = \int_{-\infty}^{\infty} n_0(x) \left\{ x - \frac{1}{m} \int_{0}^{t} V(t') dt' \right\} f(V) dV.$$
 (6.1.7)

To incorporate the information on correlation effects, we average the continuity equation over the ensemble of realizations, assuming that the density field can be represented as a sum of the mean density  $n_0$  and the fluctuation component  $n_1 = n - \langle n \rangle$ ,

$$n(x,t) = n_0(x,t) + n_1(x,t). (6.1.8)$$

We also set  $\langle n_1 \rangle = 0$  and the velocity field is represented as a sum of the mean velocity  $v_0$  and the fluctuation amplitude  $v_1$ ,  $V = v_0 + v_1$ , where  $v_0 = \text{const}$  and  $\langle v_1 \rangle = 0$ .

After simple algebra, one obtains

$$\frac{\partial n_0}{\partial t} + \frac{\partial n_1}{\partial t} + (v_0 + v_1) \left( \frac{\partial n_0}{\partial x} + \frac{\partial n_1}{\partial x} \right) = 0. \tag{6.1.9}$$

Upon averaging this equation, we arrive at the equation for the mean density  $n_0$ 

$$\frac{\partial n_0}{\partial t} + v_0 \frac{\partial n_0}{\partial x} + \left\langle v_1 \frac{\partial n_1}{\partial x} \right\rangle = 0. \tag{6.1.10}$$

By subtracting this equation from the previous one, we find the equation for the density perturbation  $n_1$ 

$$\frac{\partial n_1}{\partial t} + v_0 \frac{\partial n_1}{\partial x} + v_1 \frac{\partial n_0}{\partial x} + v_1 \frac{\partial n_1}{\partial x} - \left\langle v_1 \frac{\partial n_1}{\partial x} \right\rangle = 0. \tag{6.1.11}$$

Here, it was assumed

$$\left\langle v_1 \frac{\partial n_0}{\partial x} \right\rangle = 0, \ \left\langle v_0 \frac{\partial n_1}{\partial x} \right\rangle = 0.$$
 (6.1.12)

As a result of these manipulations, we arrive at the following set of equations for both the mean density  $n_0$  and the density perturbation  $n_1$ :

$$\frac{\partial n_0}{\partial t} + v_0 \frac{\partial n_0}{\partial x} + \left\langle v_1 \frac{\partial n_1}{\partial x} \right\rangle = 0; \tag{6.1.13}$$

$$\frac{\partial n_1}{\partial t} + v_0 \frac{\partial n_1}{\partial x} + v_1 \frac{\partial n_0}{\partial x} + v_1 \frac{\partial n_1}{\partial x} - \left\langle v_1 \frac{\partial n_1}{\partial x} \right\rangle = 0. \tag{6.1.14}$$

Let us introduce a small parameter  $\varepsilon$ . We assume that the fluctuations  $n_1$  and  $v_1$  are as small as  $\varepsilon$  in comparison with the mean density  $n_0$ ,  $n_1 \sim \varepsilon n_0$ , and  $v_1 \sim \varepsilon v_0$ . The quasilinear character of the approximation indicates that, in the equation for  $n_0$ , we keep the nonlinear term of the order of  $\varepsilon^2$  but, in the equation for  $n_1$ , we keep only the terms that are of the first order of  $\varepsilon$ . As a result, the transformations put the equation for density fluctuations  $n_1$  into the form

$$\frac{\partial n_1}{\partial t} + v_0 \frac{\partial n_1}{\partial x} = -v_1 \frac{\partial n_0}{\partial x}.$$
 (6.1.15)

This equation could be solved by the Green function method. The solution for  $n_1(x,t)$  has the form

$$n_1(x,t) = -\int_0^t v_1(t_1) \frac{\partial n_0(z,t)}{\partial z} dt_1.$$
 (6.1.16)

Here, z is given by  $z = x - v_0(t - t_1)$ . Substituting this expression for  $n_1$  into the equation for the mean density  $n_0$  and performing simple manipulations yield

$$\frac{\partial n_0}{\partial t} + v_0 \frac{\partial n_0}{\partial x} = \int_0^t \langle v_1(t)v_1(t_1) \rangle \frac{\partial^2 n_0(z, t_1)}{\partial z \partial x} dt_1.$$
 (6.1.17)

The integral nature of this equation reflects the Lagrangian character of the relationships between the derivatives of  $n_0(x,t)$ . The particular form of the transport equation is governed by the choice of the correlation function  $C(t,t_1)=\langle v_1(t)v_1(t_1)\rangle$ . If we assume that the correlations are short-range, the quasilinear equation takes the conventional form with the diffusivity,  $D_T\approx v_1^2\tau$ ,

$$\frac{\partial n_0}{\partial t} + v_0 \frac{\partial n_0}{\partial x} = D_{\rm T} \frac{\partial^2 n_0(x, t)}{\partial x^2}.$$
 (6.1.18)

Thus, in this approximation, we arrive at the familiar Taylor representation for the turbulent diffusion coefficient. The method considered here is named as quasilinear because in the set of the equation we had to solve, the equation for the mean density had the nonlinear term  $\langle v_1 \frac{\partial v_1}{\partial x} \rangle$ , whereas the approximation equation for the density perturbation was linear. Below we will treat different methods of renormalization of this quasilinear approach based on the phenomenological modification of the equation for density perturbations.

Basing on the averaging procedure for the short-range correlation function, we obtain the Taylor expression for the turbulent diffusivity

$$D_{\rm T} = \int_0^\infty \langle V(0)V(\tau)\rangle d\tau, \qquad (6.1.19)$$

which is also the famous Kubo-Green formula for the transport coefficient

$$D = \int_{0}^{\infty} C(\tau) d\tau. \tag{6.1.20}$$

This correlation representation allows one to interpret the classical Einstein formula  $\frac{k_{\rm B}T}{m\beta_t}=D$  as the fluctuation-response relation, which connects the response coefficient (friction factor)  $\beta_t$  and the corresponding correlation function (velocity autocorrelation function) C(t). Such a formulation of the problem leads to linear-response concept, which provides the fairly general formalism for the transport coefficient description. Thus, in the presence of small temporal and spatial variations of the field  $\alpha(\vec{r},t)$ , the evolution of the system under consideration is described by the set of the Onsager equations

$$\frac{\partial \alpha(\vec{r},t)}{\partial t} = -\nabla J(\vec{r},t), \tag{6.1.21}$$

$$J(\vec{r},t) = L_J \chi(\vec{r},t), \qquad (6.1.22)$$

$$\chi(\vec{r},t) = -\nabla \alpha(\vec{r},t). \tag{6.1.23}$$

Here,  $J(\vec{r},t)$  is a flux,  $\chi(\vec{r},t)$  is a thermodynamic force, and  $L_J$  is the corresponding transport coefficient, which is represented by Kubo–Green formula

$$L_J = \text{const} \int_0^\infty \langle J(0)J(\tau)\rangle d\tau. \tag{6.1.24}$$

It is obvious that in the case of scalar particle transport in a chaotic flow we are dealing with the particle density, particle flux, and scalar diffusivity. However, the linear-response concept was originally developed in the framework of equilibrium statistical mechanics based on Hamiltonian description of systems. This leads to the methodological problem, which was clearly formulated by Van Kampen [58]. Thus,

when considering the perturbation of the dynamical system  $\delta x_i(t)$ , one can write a Taylor expansion for the difference between perturbed and unperturbed values in the form

$$\delta x_i(t) = \sum_j \frac{\partial x_i(t)}{\partial x_j(0)} \delta x_j(0) + O(\delta \vec{r}^2(0)), \qquad (6.1.25)$$

where  $\delta \vec{r} = \{\delta x_i\}$ . As we discussed in the previous chapter devoted to the stochastic instability, in the presence of chaos the term  $\partial x_i(t)/\partial x_j(0)$  grows exponentially with time. This means that the region of applicability of the linear approach under consideration could be very limited. Nevertheless, the linear-response theory successfully describes the transport coefficients on the basis of correlation function and the Kubo–Green relation, which is confirmed by numerous observations as well as simulations [43]. However, we have to take into account that the conventional description of transport has an average character because the measured quantities are always the result of averaging over the ensemble of trajectories. From this point of view, the stochastic instability works as a decorrelation mechanism and supports to the mixing. This is very important conclusion since the main task of the turbulent transport theory is the search for phenomenological arguments to describe complex correlation effects basing on the different approximations of particle trajectories, topology of coherent structures, etc.

## 6.2 Correlations and Phenomenological Transport Equation

When studying complex correlation effects, one can obtain different phenomenological equation to describe transport in the framework of the quasilinear approach. Thus, in the case of steady random processes, the function  $C(t, t_1) \approx C(t - t_1)$  in the equation under analysis,

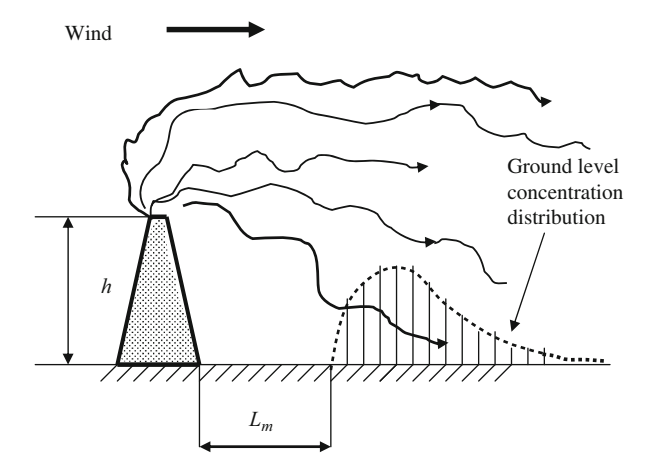
$$\frac{\partial n_0}{\partial t} + v_0 \frac{\partial n_0}{\partial x} = \int_0^t C(t - t_1) \frac{\partial^2 n_0(z, t_1)}{\partial z \partial x} dt_1, \tag{6.2.1}$$

plays the role of the memory function. By differentiating this equation with respect to x and then by differentiating the same equation with respect to t, after simple calculations, one obtains

$$\frac{\partial n_0}{\partial t} + v_0 \frac{\partial n_0}{\partial x} + \tau_0 \left( \frac{\partial^2 n_0}{\partial t^2} + 2v_0 \frac{\partial^2 n_0}{\partial x \partial t} + (v_0^2 - C_0) \frac{\partial^2 n_0}{\partial x^2} \right) = 0.$$
 (6.2.2)

Here, it is convenient to introduce the new set of variables  $\eta = x - v_0 t$ ,  $\xi = t$ . This leads to the telegraph equation:

**Fig. 6.2.1** Schematic illustration of a chimney plume



$$\frac{\partial n_0}{\partial \xi} + \tau_0 \frac{\partial^2 n}{\partial \xi^2} = C_0 \tau_0 \frac{\partial^2 n_0}{\partial \eta^2}, \tag{6.2.3}$$

where  $\sqrt{C_0}$  is the propagation velocity. This is the hyperbolic telegraph equation in frame of reference related to the coordinates  $\xi, \eta$ . The telegraph equation is known by this name because it was first derived by Kelvin in his analysis of signal propagation in the first transatlantic cable and then was often applied to describe turbulent diffusion [119–127]. The example of interest is the diffusion of the chimney plume. Particle mixing is important in a variety of industrial and natural settings (see Fig. 6.2.1). How can a paint manufacturer assure that pigments are mixed thoroughly into the paint medium? Usually the source is a buoyant plume emitted from a chimney of height  $h_A$ , which first mixed with the atmosphere under the action of its own thermal and mechanical energy, by the processes of 'entraining' the surrounding fluid. At some stage, this process is overtaken by the diffusing action of the external turbulence and then the pollutant is assumed to diffuse like a passive scalar from a source at greater height  $\Delta h$  above the original source. To treat the transition process, one can take into account the limited velocity of particle propagation, which is related to the limitation on wind velocity fluctuations creating turbulent mixing [119, 120].

To obtain the telegraph equation from the phenomenological point of view, one could consider the relation for the particle flux in the form

$$q = q_0 - \tau \frac{\partial q}{\partial t}. ag{6.2.4}$$

where

$$q_0(x,t) = -D_0 \frac{\partial n(x,t)}{\partial x}.$$
 (6.2.5)

The term  $\tau(\partial q/\partial t)$  describes the influence of the turbulent pulsations. The general solution has the form

$$q(x,t) = \int_0^t q_0(x,t') \exp\left[-\frac{t-t'}{\tau}\right] \frac{dt'}{\tau} + q_0 \exp\left[-\frac{t}{\tau}\right].$$
 (6.2.6)

In the case when  $t \gg \tau$ , one finds the asymptotic solution in the form

$$q(x,t) = -\int_0^t D_0 \frac{\partial n}{\partial x} \exp\left[-\frac{t-t'}{\tau}\right] \frac{\mathrm{d}t'}{\tau}.$$
 (6.2.7)

On the basis of the conventional Fick relation,

$$\frac{\partial n(x,t)}{\partial t} = -\frac{\partial q(x,t)}{\partial x},\tag{6.2.8}$$

we arrive at the telegraph equation in the form

$$\frac{\partial n}{\partial t} + \tau \frac{\partial^2 n}{\partial t^2} = D_0 \frac{\partial^2 n}{\partial x^2}.$$
 (6.2.9)

This equation can be regarded as an interpolation between the wave and diffusion equation. On the other hand, the expression for the particle flux describes memory effects. Therefore, it is possible to replace the exponential function by an arbitrary memory function  $M_{\rm m}(t-t')$ 

$$q(x,t) = \int_0^t q_0(x,t') M_{\rm m}(t-t') \frac{\mathrm{d}t'}{\tau}.$$
 (6.2.10)

In this general case, one obtains the renormalized diffusion equation in the form

$$\frac{\partial n(x,t)}{\partial t} = \int_0^t D \frac{\partial^2 n(x,t')}{\partial x^2} M_{\rm m}(t-t') \frac{\mathrm{d}t'}{\tau}. \tag{6.2.11}$$

From the modern point of view, such an approach to the turbulent transport looks fairly naive. However, in essence, the idea of using the additional derivative in the equations describing the anomalous character of diffusion was clearly formulated as early as 1934 [119].

## **6.3** Heavy Particles in Chaotic Flow

Phenomenological arguments based on the memory function formalism are rather effective tool to build simplified models of transport in chaotic flows. Here, we study the influence of particle inertia on the turbulent diffusion using the memory function approach [45–47].

Let us consider an equation for inertial particles of finite size  $R_0$  suspended in a turbulent flow. In the framework of the passive scalar approach, one obtains the simplified relation

$$\frac{\mathrm{d}\vec{V}}{\mathrm{d}t} = -\frac{\vec{V} - \vec{U}}{\tau_0} + \vec{g}.\tag{6.3.1}$$

Here,  $\vec{V}$  is the inertial particle velocity,  $\vec{U}$  is the fluid velocity, and  $\vec{g}$  is the gravitational acceleration. The characteristic time is given by the conventional Stokes formula

$$\tau_0 = \frac{2R_0^2 \rho_0}{9\rho v_E},\tag{6.3.2}$$

where  $\rho_0$  is the particle density,  $\rho$  is the fluid density, and  $v_F$  is the fluid viscosity.

As experimentally discovered, inertia effects in turbulent flow lead to decrease of the settling velocity  $\vec{V}$  because of chaotic nature of the fluid velocity  $\vec{U}$  [67–72]. The first attempts to estimate this effect were based on using the linear dependence of the fluid velocity on time (see Fig. 6.3.1). However, the memory function formalism is more relevant to this problem. In terms of the Langevin approach, such a description was successfully used to investigate complex correlation effects [45–47]. Thus, for the classical Langevin model we have the equation of motion in the form

$$\frac{\mathrm{d}V}{\mathrm{d}t} = -\frac{V}{\tau_0} + A(t),\tag{6.3.3}$$

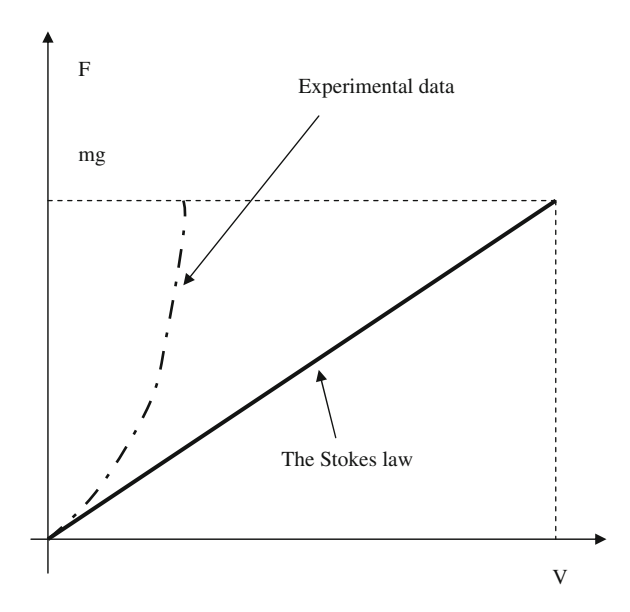


**Fig. 6.3.1** A typical plot of gravitational settling of aerosol particles

where A(t) is a stochastic acceleration of average value zero representing the effects of molecular impacts on a particle at rest. This leads to the relation for the correlation function

$$\frac{\mathrm{d}}{\mathrm{d}t}\langle V(t)V(0)\rangle = \frac{\mathrm{d}C(t)}{\mathrm{d}t} = -\frac{C(t)}{\tau_0}.$$
(6.3.4)

Using the memory function formalism, we find the renormalized equation of motion,

$$\frac{dV}{dt} = -\frac{1}{\tau_0} \int_0^t M(t - t')V(t')dt' + A(t), \tag{6.3.5}$$

and hence, we obtain the integral equation for the autocorrelation function as follows:

$$\frac{dC(t)}{dt} = -\int_0^t M(t - t')C(t')dt'.$$
 (6.3.6)

Here, M(t) is the memory function. This allows one to investigate the correlation functions, which differ significantly from the exponential representation.

In our case, such a renormalized equation takes the form

$$\frac{d\vec{V}}{dt} = -\int_{0}^{t} M(t - t') \left[ \vec{V}(t') - \vec{U}(t') \right] dt' + \vec{g}, \tag{6.3.7}$$

where M(t) is the phenomenological memory function describing the inertia effects in the presence of "ensemble" of turbulent pulsations.

On the other hand, when the characteristic time  $\tau_0$  is less than the temporal scale of turbulent pulsations (small particle inertia), one can obtain an approximation relation for the velocity of the inertial particle [128]

$$\vec{V} \approx \vec{U} - \tau_0 \frac{d\vec{U}}{dt} + \tau_0 \vec{g}. \tag{6.3.8}$$

We must make special note here. The Lagrangian (total) acceleration of the small fluid element is given by the conventional relation

$$\frac{\mathrm{d}\vec{U}}{\mathrm{d}t} = \frac{\partial \vec{U}}{\partial t} + \vec{U}\nabla\vec{U},\tag{6.3.9}$$

and the velocity field of the surrounding fluid  $ec{U}$  is incompressible so that

$$\operatorname{div} \vec{U} = 0, \tag{6.3.10}$$

whereas the velocity field  $\vec{V}$  is compressible and by calculating the divergence of the inertial particle velocity, we find

$$\operatorname{div} \vec{V} = -\tau_0 \nabla (\vec{U} \nabla) \vec{U} = -\tau_0 \left( \frac{\partial U_i}{\partial x_j} \right) \left( \frac{\partial U_j}{\partial x_i} \right). \tag{6.3.11}$$

Here, the standard index notation is used and the gravitational acceleration does not contribute to this compressibility effect. The equation for the particle density takes the following form:

$$\frac{\mathrm{d}n}{\mathrm{d}t} = \frac{\partial n}{\partial t} + \vec{V}\nabla n = -n\operatorname{div}\vec{V}.$$
(6.3.12)

In the framework of the Lagrangian approach, this gives the integral formula for the coarse-grained particle density,  $n(\vec{r}, t)$ 

$$n(\vec{r},t) = n(0,0) \exp\left\{\tau_0 \int_0^t \left[\nabla \left(\vec{U}(t')\nabla\right)\vec{U}(t')\right] dt'\right\}. \tag{6.3.13}$$

This representation is valid for spatial scales, which exceed the particle size as well as the Brownian diffusion scale (see Fig. 6.3.2).

For instance, inertia effects are really important when describing particle-turbulence interactions in atmospheric clouds. Turbulence in atmospheric clouds is related to enormous Reynolds numbers on order of 10<sup>6</sup> to 10<sup>7</sup>. Thus, the ratio of

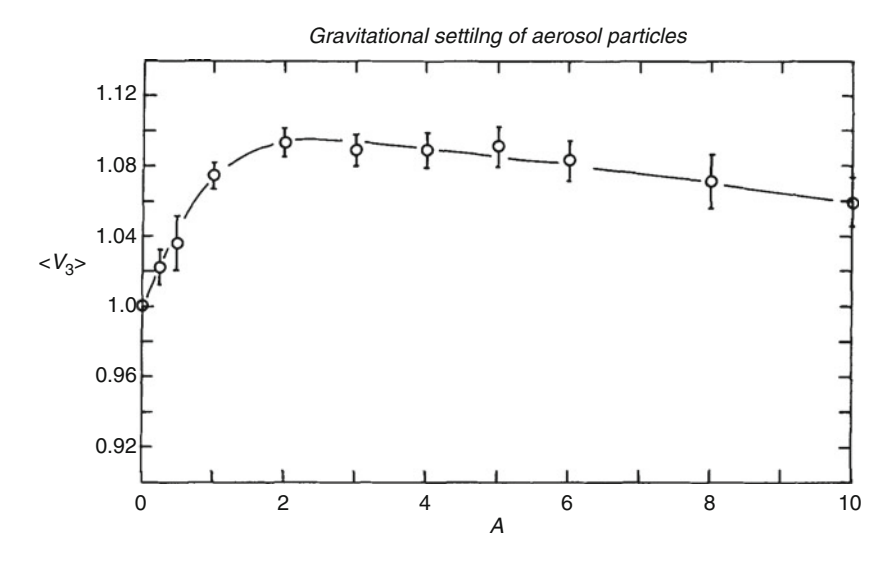


Fig. 6.3.2 Simulation results for average setting velocity  $\langle V_3 \rangle$  against inertia parameter. (After Maxey [128] with permission)

energy-containing and dissipative spatial scales is on order of  $10^5$  for typical convective cloud. For small cloud droplets, the renormalized Stokes drag force model is a reasonable approximation. The equation of motion for the droplets often includes the memory term (the Basset "history" force due to diffusion of vorticity from an accelerating particle). For more details, we refer the reader to [67-72].

#### 6.4 The Quasilinear Approach and Phase-space

In the previous sections, we considered the quasilinear approximation in the framework of the hydrodynamic approach. However, the quasilinear equations (which are based on keeping a nonlinear term in the equation for mean density and using a nonlinear equation for perturbations) were first obtained in kinetics considering the problem of waves and particles interaction on the basis of Vlasov's equation [129, 130]

$$\frac{\partial f(V, x, t)}{\partial t} + \vec{V} \frac{\partial f}{\partial x} + \vec{E} \frac{\partial f}{\partial V} = 0, \tag{6.4.1}$$

$$\operatorname{div} \vec{E} = 4\pi ne \int f(V, x, t) d\vec{V}. \tag{6.4.2}$$

Here, f(V, x, t) is the velocity distribution function,  $\vec{E}$  is the electric field, and n is the plasma density. The quasilinear formulation of this problem was repeatedly discussed in detail [131–134]. Therefore, we will consider only those aspects that play an important role for the subsequent consideration. A kinetic problem is naturally much more complex. Thus, in the one-dimensional case the equations for the mean part of the distribution function  $f_0(V,t)$  and perturbation  $f_1(V,x,t)$  have the form, which is analogous to the quasilinear approximation for the passive scalar equations

$$\frac{\partial f_0}{\partial t} + \frac{e}{m} \left\langle E \frac{\partial f_0}{\partial V} \right\rangle = 0, \tag{6.4.3}$$

$$\frac{\partial f_1}{\partial t} + V \frac{\partial f_1}{\partial x} + \frac{e}{m} \frac{\partial f_0}{\partial V} = 0. \tag{6.4.4}$$

However, the diffusive equation in the velocity space, which was obtained as the result of transformations

$$\frac{\partial f_0}{\partial t} = \frac{\partial}{\partial V} \left[ D_V \frac{\partial f_0}{\partial V} \right],\tag{6.4.5}$$

with the quasilinear diffusion coefficient

$$D_V = \left(\frac{e}{m}\right)^2 \int \frac{|E_k|^2}{\omega(k) - kV} dk$$
 (6.4.6)

is added by the equation describing the energy dissipation of electric field due to the Landau damping

$$\frac{\mathrm{d}}{\mathrm{d}t}|E_k|^2 = -2\gamma_k|E_k|^2,\tag{6.4.7}$$

where the characteristic frequency  $\gamma_k$  is defined by the equation

$$\gamma_k = 2\pi e^2 \omega \int \frac{\partial f_0}{\partial V} \delta(\omega - kV) dV. \tag{6.4.8}$$

Here,  $\omega(k)$  describes the frequency dependence on the wave number k, and  $|E_k|^2$  is the spectral function of electric field. It is natural that the expression for the quasilinear diffusion coefficient  $D_V$  in a velocity space can be interpreted in terms of the autocorrelation function of accelerations  $C_{\rm a}$ 

$$D_V \approx \int_0^\infty C_{\rm a}(t) dt \approx \left(\frac{e}{m}\right)^2 \int_0^\infty \langle E(0)E(t)\rangle dt.$$
 (6.4.9)

One can see the analogy with the Taylor representation for the coefficient of turbulent diffusion

$$D_{\rm T} \approx \int_0^\infty C(t) dt = \int_0^\infty \langle V(0)V(t)\rangle dt. \tag{6.4.10}$$

However, in the case of phase space we deal with the more complex problem. It is well known that the quasilinear description of weak-turbulent plasma is based on the notion about stochastic instability and randomness of phases [129–134].

## **6.5** The Dupree Approximation

Many theoretical and numerical investigations confirm the appearance of diffusion in a space of velocities in the stochastic limit. In spite of the effectiveness of the quasilinear approximation, some correlation effects were not considered. Thus, the mixing process of stochastically instable trajectories leads to the nonlinear irreversible decay of correlations with the characteristic time [134]

$$\tau_k \propto \frac{1}{(k^2 D_V)^{1/3}}.$$
(6.5.1)

Here,  $D_V$  is the diffusion coefficient in velocity space and k is the wave number. In the Dupree papers, it was suggested to consider the correlations decay by analogy with the Landau damping [135–137] using the frequency "renormalization" in the form

$$\omega(k) \to \omega(k) + \frac{i}{\tau_k}.$$
 (6.5.2)

Such an approach can be interpreted as the renormalization (modification) of the equation for the perturbation of the distribution function  $f_1$ 

$$\frac{\partial f_1}{\partial t} + \vec{V} \frac{\partial f_1}{\partial x} + \vec{E} \frac{\partial f_0}{\partial V} = \frac{f_1}{\tau_{\nu}}.$$
 (6.5.3)

Here, the term  $f_1/\tau_k$  approximates the terms omitted in the quasilinear approximation.

It is natural to consider the renormalization of the quasilinear diffusion coefficient in terms of the autocorrelation function of accelerations

$$C(t) = \left(\frac{e}{m}\right)^2 \langle E(x(t), t)E(x(0), 0)\rangle. \tag{6.5.4}$$

Then, the particle velocity in the framework of one-dimensional electrostatic turbulence is given by

$$V(t) = V_0 + \frac{e}{m} \int_0^t E[x(t'), t'] dt'.$$
 (6.5.5)

By representing the electric field as the totality of many independent Fourier components, one obtains

$$E(x,t) = \sum_{k} E_k \exp[i(kx - \omega_k t)]. \tag{6.5.6}$$

The formal substitution of this expression in the formula for the correlation function yields

$$C(t) = \left(\frac{e}{m}\right)^2 \sum_{kk'} \langle E_k \exp[\mathrm{i}(kx(t) - \omega_k t)] E_{k'} \exp[\mathrm{i}(k'x(0))] \rangle. \tag{6.5.7}$$

Then, by analogy with Corrsin, Dupree used the independence hypothesis

$$C(t) = \left(\frac{e}{m}\right)^2 \sum_{k} |E_k|^2 \langle \exp[i(kx(t) - \omega_k t) + i(k\Delta x(t))] \rangle. \tag{6.5.8}$$

For the Gaussian statistics, one obtains  $\langle \exp A \rangle = \exp \frac{\langle A^2 \rangle}{2}$  and hence the formula for the correlation function takes the form

$$C(t) = \left(\frac{e}{m}\right)^2 \sum_{k} |E_k|^2 \exp\left[i(kx - \omega_k t) - \frac{k^2 \langle \Delta x^2(t) \rangle}{2}\right]. \tag{6.5.9}$$

Using the dimensional estimate  $\frac{d}{dt}\langle \Delta V^2(t)\rangle \approx 4D_V$ , it is easy to find the scaling for  $\langle \Delta x^2(t)\rangle \approx \frac{2}{3}D_Vt^3$ . Then, the expression for the diffusion coefficient for one-dimensional electrostatic turbulence for  $t\to\infty$  takes the Dupree form [134–137]

$$D = \int_0^t C(\tau) d\tau = \left(\frac{e}{m}\right)^2 \sum_k \int_0^\infty |E_k|^2 \exp\left[i(kV - \omega_k \tau) - \frac{1}{3}k^2 D_V \tau^3\right] d\tau. \quad (6.5.10)$$

It is easy to note that this expression differs essentially from quasilinear one

$$D_{\rm QL} = \pi \left(\frac{e}{m}\right)^2 \sum_{k} |E_k|^2 \delta(\omega_k - kV), \tag{6.5.11}$$

where  $\delta$  is the symbol of the Dirac function. Thus, the Dupree diffusivity scales with  $E_k$  as  $D \propto |E_k|^{3/2}$ , whereas the quasilinear prediction is  $D_{\rm QL} \propto |E_k|^2$ .

# 6.6 Renormalization Theory Revisited

The Dupree renormalized scaling  $D_V \propto |E_k|^{3/2}$  was tested in numerical test particle simulations [138–142]. The results were mixed, and no definitive conclusions were drawn. The authors of [138] observed that the diffusivity numerically found is significantly smaller than that predicted by the Dupree theory. Ishihara and Hirose [138] confirmed their finding. Moreover, by adopting the method proposed by Salat [139], they recalculated the diffusivity without assuming Markovian process and concluded that  $D_V$  should be time-dependent [141]. An explicit analytical expression for the diffusivity has been represented by Salat [82] and Ishihara et al. [142]. It has been shown that in the asymptotic limit,  $D_V$  scales with the turbulent field and time as

$$D_V \propto |E_k|^{4/3}/t^{1/3}$$
. (6.6.1)

The predicted velocity variance  $\langle [\Delta V]^2 \rangle \propto t^{2/3}$  in one-dimensional electrostatic turbulence increases with time more slowly than the usual Brownian motion,  $\langle [\Delta V]^2 \rangle \propto t$ . This indicates a diffusion process, which is not free, but restricted, and dependent on the past history of particle trajectory.

The time integration is to be carried out along the perturbed particle trajectory x(t) given by

$$x(t) = x_0 + V_0 t + \Delta x(t), \tag{6.6.2}$$

where

$$\Delta x(t) = \frac{e}{m} \int_{0}^{t} dt' \int_{0}^{t'} E[x(t''), t''] dt''$$
 (6.6.3)

is the derivation from the free streaming trajectory  $x_0 + V_0 t$ .

Then, the velocity variance is formally given, with  $V = V_0$ , by

$$\left\langle \left[ \Delta V(t) \right]^2 \right\rangle = \left( \frac{e}{m} \right)^2 \sum_{k} |E_k|^2 \int_0^t dt' \int_{t'-t}^{t'} ds' \exp[i(kV - \omega_k)s'] \left\langle \exp[ik[\Delta x(t') - \Delta x(t' - s')]] \right\rangle$$
(6.6.4)

For a Gaussian statistics, the average in this expression can be approximated by the equation

$$\langle \exp[ik[\Delta x(t') - \Delta x(t'-s')]] \rangle \approx \exp\left[-\frac{k^2}{2} \langle [\Delta x(t') - \Delta x(t'-s')]^2 \rangle\right].$$
 (6.6.5)

In the quasilinear theory  $\Delta x = 0$ . This is equivalent to the assumption that the particles continue to experience the Eulerian field. In the original resonance broadening theory by Dupree, the variance of particle trajectories is assumed to be independent of the memory effects, which lead to the following approximation,

$$\left\langle \left[ \Delta x(t') - \Delta x(t' - s') \right]^2 \right\rangle \approx \left\langle \left[ \Delta x(s') \right]^2 \right\rangle.$$
 (6.6.6)

The correlation function  $\langle [\Delta x(t) - \Delta x(t-s)]^2 \rangle$  was calculated more rigorously as follows. Each term in the expansion

$$\left\langle \left[ \Delta x(t) - \Delta x(t-s) \right]^2 \right\rangle = \left\langle \left[ \Delta x(t) \right]^2 \right\rangle - 2 \left\langle \Delta x(t) \Delta x(t-s) \right\rangle + \left\langle \left[ \Delta x(t-s) \right]^2 \right\rangle, \quad (6.6.7)$$

is in the form of

$$\langle \Delta x(t_1)x(t_2)\rangle = \left(\frac{e}{m}\right)^2 \int_0^{t_1} dt'_1 \int_0^{t_2} dt''_1 \int_0^{t_2} dt'_2 \int_0^{t_2} dt''_2 \langle E[x(t''_1), t''_1]E[x(t''_2), t''_2]\rangle.$$
(6.6.8)

If the velocity variance is a result of diffusive process, we can make the following approximation:

$$\left(\frac{e}{m}\right)^2 \int_0^{t_1} dt''_1 \int_0^{t_2} dt''_2 \langle E[x(t_1'), t''_1] E[x(t_2'), t''_2] \rangle \approx 2D_V \min(t_1', t_1'), \qquad (6.6.9)$$

provided time-dependence of  $D_V$ , if any, is sufficiently weak. The substitution yields

$$\langle \Delta x(t_1)x(t_2)\rangle = 2D_V \int_0^{t_1} dt'_1 \int_0^{t_2} dt'_2 \min(t'_1, t'_2).$$
 (6.6.10)

For  $t_1>t_2$ , the double integral reduces to  $\frac{1}{6}(3t_1-t_2)t_2^2$ , and thus for t>s>0, the variance  $\left\langle \left[\Delta x(t)-\Delta x(t-s)\right]^2\right\rangle$  becomes

$$\left\langle \left[ \Delta x(t) - \Delta x(t-s) \right]^2 \right\rangle = \frac{2}{3} (3t - 2s)s^2 D_V,$$
 (6.6.11)

which does depend on t as well as the relative time s. This non-Markovian nature of the spatial variance will be responsible for the time-dependence of the velocity diffusivity. The substitution of this expression into the cumulant yields the following closed form for the diffusivity  $D_V$ :

$$D_V(t) = \left(\frac{e}{m}\right)^2 \sum_k \int_0^t |E_k|^2 \exp\left[i(kV - \omega_k)\tau - \frac{1}{3}k^2 D_V \tau^2 (3t - 2\tau)\right] d\tau. \quad (6.6.12)$$

For resonant particles with  $V \approx \omega_k/k$ , the upper limit of  $D_V$  is given by

$$D_V = \left(\frac{e}{m}\right)^2 \sum_{k} |E_k|^2 \int_0^t \exp\left[-\frac{1}{3}k^2 D_V t \tau^2\right] d\tau.$$
 (6.6.13)

In the asymptotic limit  $t \to \infty$ , the integral approaches  $\frac{\sqrt{3\pi}}{2} \frac{1}{k\sqrt{D_V t}}$ . Therefore, the upper limit of the diffusivity is

$$D_{V\max} = \left(\frac{\sqrt{3\pi}}{2}\right)^{2/3} \left(\frac{e^2}{m^2} \sum_{k} \frac{1}{k} |E_k|^2\right)^{2/3} \frac{1}{t^{1/3}}.$$
 (6.6.14)

Actually, in the approach suggested in [138–142], applying the substitution of a ballistic scaling  $\langle \Delta x^2(\tau) \rangle \propto \langle \Delta V^2(t) \rangle \tau^2 \propto (D_V t) \tau^2$ , where t is the parameter of the integrand, for a Dupree dimensional approximation  $\langle \Delta x^2(\tau) \rangle \propto D_V \tau^3$  yields the coordination of theoretical results and simulations. Naturally, the correlation effect approximation suggested by Dupree and based on the independence hypothesis and dimensional estimates is fairly rough. However, it allows one to visualize correlation effects omitted in the quasilinear approach and opens new possibilities to obtain transport estimates.

Further Reading 105

#### **Further Reading**

#### The Quasilinear Approach

- R. Balescu, Aspects of Anomalous Transport in Plasmas (IOP, Bristol, 2005)
- B.B. Kadomtsev, Collective Phenomena in Plasma (Nauka, Moscow, 1976)
- A.S. Kingsep, *Introduction to the Nonlinear Plasma Physics Mosk* (Fiz.-Tekh. Inst, Moscow, 1996)
- M.N. Rosenbluth, R.Z. Agdeev (eds.), *Handbook of Plasma Physics* (North-Holland, Amsterdam, 1984)
- V.N. Tsytovich, *Theory of Turbulent Plasma* (Plenum Press, New York, 1974)

#### Renormalization

- R. Badii et al. (eds.), *Complexity Hierarchical Structures and Scaling in Physics* (Cambridge University Press, Cambridge, 1997)
- J. Cardy (ed.), Finite-Size Scaling (Elsevier, Amsterdam, 1988)
- J. Cardy, *Scaling and Renormalization in Statistical Physics* (Cambridge University Press, Cambridge, 2000)
- P.H. Diamond, S.-I. Itoh, K. Itoh, *Modern Plasma Physics* (Cambridge University Press, Cambridge, 2010)
- L.P. Kadanoff, Statistical Physics: Dynamics and Renormalization (World Scientific, Singapore, 1999)
- J.A. Krommes, Physics Reports **360**, 1–352 (2002)
- V. Privman (ed.), Finite Size Scaling and Numerical Simulation of Statistical Systems (World Scientific, Singapore, 1990)
- Y. Zhou, Physics Reports 488, 1 (2010)

# The Telegraph Equation

- N.F. Frenkiel (ed.), Atmospheric Diffusion and Air Pollution (Academic, New York, 1959)
- D.D. Joseph, L. Prezioso, Reviews of Modern Physics **61**, 41 (1989)
- A.S. Monin, A.M. Yaglom, Statistical Fluid Mechanics (MIT, Cambridge, 1975)
- V. Uchaikin, Physics-Uspekhi **173**, 765 (2003)
- G.H. Weiss, Aspects and Applications of the Random Walk (Elsevier, Amsterdam, 1994)

# Chapter 7

# The Taylor Shear Dispersion

#### 7.1 Dispersion in Laminar Flow

As early as in 1953, Taylor found that the dispersion of solute along the tube axis for long times, i.e., for times longer than the diffusive time to explore the tube section, is simply described as a translation with the mean solvent velocity plus a diffusive dispersion characterized by an effective diffusion coefficient. It was shown analytically that the distribution of concentration is centered on a point, which moves with this mean velocity and is symmetrical about it in spite of the asymmetry of the flow along the tube. The effective diffusivity can be calculated from observed distributions of concentration. The analysis relates the longitudinal diffusivity to the coefficient of molecular diffusion and that is why observations of concentration along a tube provide a new method for measuring diffusion coefficients.

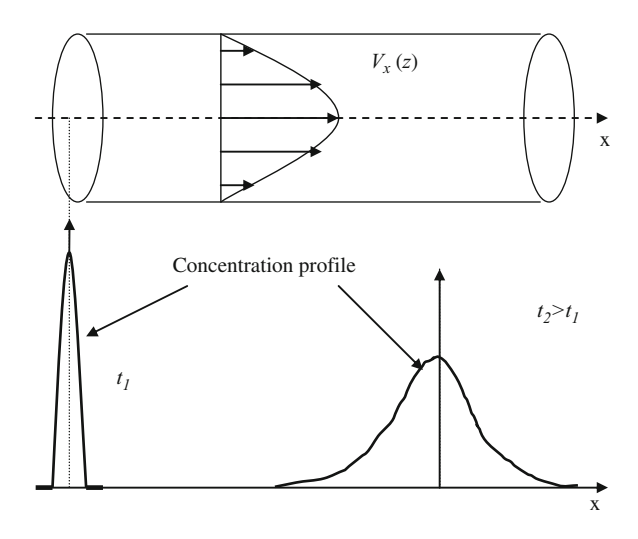
We discuss here the model of the effective transport of tracer in a laminar shear flow in the presence of seed diffusivity. Taylor pointed out that vertical mixing, in the presence of vertical shear, and a horizontal concentration gradient must lead to horizontal diffusion simply because particles mixed in the vertical will experience a range of horizontal advective velocities (see Fig 7.1.1). It was suggested [143] a fruitful method of obtaining the effective diffusion coefficient, which is based on averaging the transport equation to investigate dispersion in laminar tube flow

$$\frac{\partial n}{\partial t} + V_x \left[ 1 - \left( \frac{r}{R_0} \right)^2 \right] \frac{\partial n}{\partial x} = D_0 \left[ \frac{1}{r} \frac{\partial}{\partial r} \left( r \frac{\partial n}{\partial r} \right) + \frac{\partial^2 n}{\partial x^2} \right]. \tag{7.1.1}$$

Here, n is the scalar density,  $V_x$  is the characteristic longitudinal (along the x-axis) velocity, and  $D_0$  is the seed diffusivity. In this approach, the influence of molecular diffusion on longitudinal convective transport is analyzed. We consider the Poiseuille flow in a cylindrical tube.

To solve the equation under consideration, it is convenient to introduce the new axial coordinate

Fig. 7.1.1 Schematic diagram of the Taylor longitudinal dispersion



$$z(x,t) = x - V_0 t, (7.1.2)$$

where

$$V_0 = \langle V \rangle = \frac{V_x}{2} \tag{7.1.3}$$

is the mean velocity of the flow. After substitution, one obtains the diffusion equation in the following form:

$$\frac{\partial n}{\partial t} + V_x \left[ \frac{1 - 2y^2}{2} \right] \frac{\partial n}{\partial z} = \frac{D_0}{R_0^2} \left[ \frac{1}{y} \frac{\partial}{\partial y} \left( y \frac{\partial n}{\partial y} \right) \right], \tag{7.1.4}$$

where  $y = r/R_0$ 

Now we can learn the scalar transport problem in the framework of the decomposition method, where the density field n can be represented as a sum of the mean density  $\langle n \rangle$  and the fluctuation component  $n_1$ ,

$$n = \langle n \rangle + n_1(z, y, t) = n_0 + n_1(x, z, t),$$
 (7.1.5)

$$V_x = \langle V \rangle + V_1 \equiv V_0 + V_1.$$
 (7.1.6)

Here, use is made of the expression for mean values

$$\langle A \rangle \equiv \frac{\int_0^{2\pi} \int_0^{R_0} rA dr d\theta}{\int_0^{2\pi} \int_0^{R_0} rdr d\theta} = \frac{2}{R_0^2} \int_0^{R_0} rA dr.$$
 (7.1.7)

To simplify the calculations, we consider the steady case. Then, substitution yields

$$V_{x} \left[ \frac{1 - 2y^{2}}{2} \right] \frac{\partial \langle n \rangle}{\partial z} = \frac{D_{0}}{R_{0}^{2}} \left[ \frac{1}{y} \frac{\partial}{\partial y} \left( y \frac{\partial n}{\partial y} \right) \right]. \tag{7.1.8}$$

By accounting for the no flux condition

$$\frac{\partial n}{\partial r} = 0$$
, at  $r = 0$  and  $r = R_0$  (7.1.9)

we easily find the expression for n,

$$n(z,y) = \frac{\partial n_0}{\partial z} \frac{V_x R_0}{8D_0} \left[ \frac{2y^2 - y^4}{2} \right] + n(z,0).$$
 (7.1.10)

For the density perturbation, one obtains the formula

$$n_1(z,y) = \frac{\partial n_0}{\partial z} \frac{V_0 R_0}{2D_0} \left[ -\frac{y^4}{2} + y^2 - \frac{1}{3} \right]. \tag{7.1.11}$$

Note that the order of  $n_1$  is given by the Zeldovich scaling

$$n_1(Pe) \propto n_0 \frac{V_0 L_0}{D_0} \approx n_0 Pe,$$
 (7.1.12)

where *Pe* is the Peclet number.

Now, the term  $\langle V_1 \frac{\partial n_1}{\partial x} \rangle$ , which defines an additional contribution in longitudinal diffusive transport, can be rewritten in the form

$$\left\langle V_1 \frac{\partial n_1}{\partial x} \right\rangle = -\frac{\left(V_0 L_0\right)^2}{D_0} \frac{\partial^2 n_0}{\partial x^2} \int_0^1 \left[ -\frac{y^4}{2} + y^2 - \frac{1}{3} \right] \left( \frac{1}{2} y^2 \right) y dy. \tag{7.1.13}$$

After simple calculations, we find

$$\left\langle V_1 \frac{\partial n_1}{\partial x} \right\rangle = -\frac{\left(V_0 L_0\right)^2}{48 D_0} \frac{\partial^2 n_0}{\partial x^2} = -D_* \frac{\partial^2 n_0}{\partial x}.$$
 (7.1.14)

The equation for  $n_0$  takes the following form:

$$\frac{\partial}{\partial t}n_0 + V_0 \frac{\partial}{\partial x}n_0 = (D_0 + D_*) \frac{\partial^2 n_0}{\partial x^2}.$$
 (7.1.15)

This method is a good example of a general mathematical technique: the simplification of a complicated system by the elimination of "fast modes." The result obtained is not trivial,

$$D_{eff} = D_0 + \frac{V_0^2 L_0^2}{48D_0} = D_0 + D_0 \left(\frac{1}{48}\right) Pe^2$$
 (7.1.16)

because this additional diffusive contribution  $D_*$  depends inversely on seed diffusivity  $D_0$ . The physical interpretation of this result is the limitation of the influence of nonuniformity of the longitudinal velocity profile  $V_x(z)$  by transverse diffusion. Hence, nonuniform longitudinal convection in combination with transverse diffusion leads to longitudinal diffusion. Naturally, the new diffusive mechanism manifests itself at a large distance downstream only, since the equation obtained is correct only for

$$t >> \tau_D \approx \frac{L_0^2}{D_0}$$
. (7.1.17)

On the other hand, the condition of smallness of the transverse spatial scale in comparison with the longitudinal one l was used:  $L_0 << l$  (see Fig. 7.1.2).

In conclusion, we note that the Taylor formula could be also interpreted in terms of correlation scales phenomenology

$$D_* \propto \frac{\Delta_{//}^2}{\tau_D} \propto \frac{V_0^2 \tau_\perp^2}{\tau_D} \propto \frac{V_0^2 L_0^2}{D_0} \propto D_0 P e^2.$$
 (7.1.18)

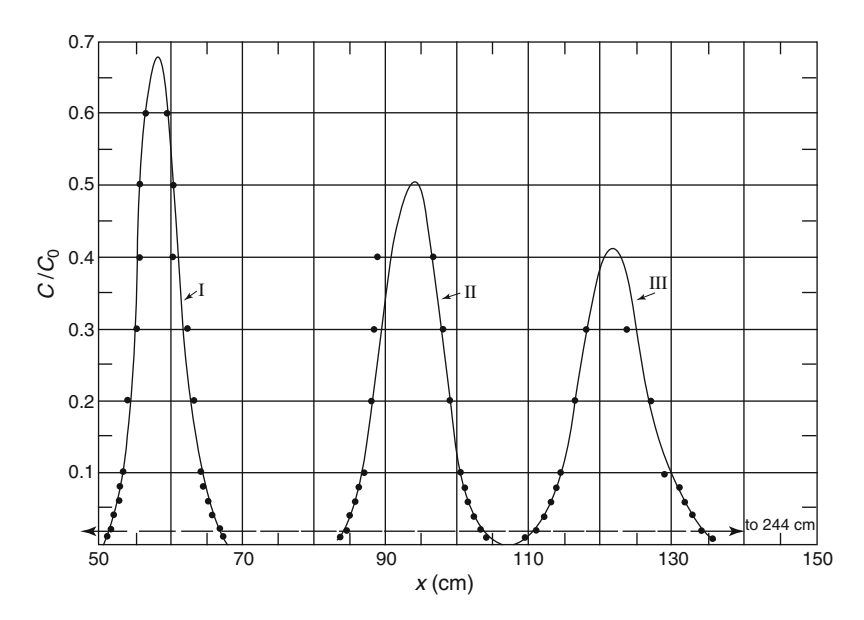


**Fig. 7.1.2** Distribution of concentration at three stages of dispersion. *Broken line* shows distribution in the absence of molecular diffusion for comparison with curve III. (After Taylor [143] with permission)

Here, it is supposed that the diffusive characteristic time is proportional to the transverse correlation time  $\tau_D \propto \tau_\perp \propto L_0^2/D_0$ . Below we will demonstrate an efficiency of such arguments to investigate anomalous transport mechanism in strongly anisotropic media.

#### 7.2 Scalar Distribution Function

Let us consider a different (more general) method to describe particle distribution in the framework of the Taylor model of scalar dispersion. The Poiseuille flow in cylindrical geometry is analyzed

$$\frac{\partial n}{\partial t} + 2V_m \left( 1 - \frac{r^2}{R_0^2} \right) \frac{\partial n}{\partial x} = D_0 \left( \frac{\partial^2 n}{\partial r^2} + \frac{1}{r} \frac{\partial n}{\partial r} + \frac{\partial^2 n}{\partial x^2} \right), \tag{7.2.1}$$

where x is the longitudinal coordinate and r is the radial coordinate. The boundary condition is given by

$$\frac{\partial n(x,r,t)}{\partial r}|_{r=R_0} = 0. (7.2.2)$$

It is necessary to introduce an initial condition, which in this case is

$$n(x, r, t = 0) = \varphi_n(x, r).$$
 (7.2.3)

Let us introduce values  $n_k(r,t)$ , which can be obtained by integrating the distribution function in the form

$$n_k(r,t) = \int_{-\infty}^{+\infty} n(x,r,t) x^k dx, \qquad (7.2.4)$$

Then, we derive the set of equations

$$\frac{\partial n_0}{\partial t} = D_0 \left( \frac{\partial^2 n_0}{\partial r^2} + \frac{1}{r} \frac{\partial n_0}{\partial r} \right), \tag{7.2.5}$$

$$\frac{\partial n_1}{\partial t} = D_0 \left( \frac{\partial^2 n_1}{\partial r^2} + \frac{1}{r} \frac{\partial n_1}{\partial r} \right) + 2V_m \left( 1 - \frac{r^2}{R_0^2} \right) n_0. \tag{7.2.6}$$

For  $k \ge 2$ , the distributions  $n_k$  can be calculated as follows:

$$\frac{\partial n_k}{\partial t} = D_0 \left( \frac{\partial^2 n_k}{\partial r^2} + \frac{1}{r} \frac{\partial n_k}{\partial r} \right) + 2kV_m \left( 1 - \frac{r^2}{R_0^2} \right) n_{k-1} + D_0 k(k-1) n_{k-2}, \quad (7.2.7)$$

with the boundary condition:

$$\frac{\partial n_k(r,t)}{\partial r}|_{r=R_0} = 0. ag{7.2.8}$$

The initial condition has the following form:

$$n_k(r, t = 0) = \int_{-\infty}^{+\infty} \varphi_n(x, r) x^k dx$$
 (7.2.9)

It is easy to resolve the set of above equations and obtain the expression for  $n_k(r,t)$ . Consider the central moments of the distribution function:

$$\mu_k(r,t) = \int_{-\infty}^{+\infty} n(x,r,t)(x-\langle x\rangle)^k dx.$$
 (7.2.10)

One can see that  $\mu_0 = \text{const.}$  We put  $\mu_0 = 1$ , since such a supposition corresponds to the particle balance relation. By definition  $\mu_1$  will be zero. The second and third moments are expressed as

$$\mu_2 = 2\left(D_0 + \frac{V_m^2 R_0^2}{48D_0}\right)t + \psi_2(r),\tag{7.2.11}$$

$$\mu_3 = \frac{1}{480} \frac{V_m^3 R^4}{D_0^2} t + \psi_3(r), \tag{7.2.12}$$

where functions  $\psi_2$  and  $\psi_3$  are given by

$$\psi_2(r) = \frac{V_m^2 R_0^4}{48 D_0^2} \left( -\frac{3}{8} \xi^8 + \frac{4}{3} \xi^6 - \frac{3}{2} \xi^4 + \frac{1}{2} \xi^2 + C_2 \right), \tag{7.2.13}$$

$$\psi_3(r) = \frac{1}{64} \frac{V_m^3 R_0^6}{D_0^3} \left( \frac{1}{12} \xi^{12} - \frac{11}{25} \xi^{10} + \frac{7}{8} \xi^8 - \frac{7}{9} \xi^6 + \frac{1}{4} \xi^4 + \frac{1}{30} \xi^2 + C_3 \right). \tag{7.2.14}$$

Here,  $\xi \equiv r/R_0$ . The constants  $C_2$  and  $C_3$  are related to the particle distribution as

$$n(x, r, t = 0) = \varphi_n(x, r).$$
 (7.2.15)

Note, the mean values

$$\langle \mu_k(t) \rangle = \frac{2}{R_0^2} \int_0^R \mu_k(r, t) r \mathrm{d}r$$
 (7.2.16)

are of central interest. One can see that  $\langle \mu_2(t) \rangle$  and  $\langle \mu_3(t) \rangle$  have the linear dependence on time.

Let us consider the case when the initial distribution is given by  $\varphi_n(x,r) = \delta(x)$ , where  $\delta(x)$  is the delta-function. As was mentioned above, the values  $\langle \mu_2(t) \rangle$  and  $\langle \mu_3(t) \rangle$  are proportional t, and hence, we have

$$\langle \mu_2(t) \rangle \equiv \sigma^2 = 2 \left( D_0 + \frac{V_m^2 R_0^2}{48D_0} \right) t,$$
 (7.2.17)

$$\langle \mu_3(t) \rangle = \frac{1}{480} \frac{V_m^3 R_0^4}{D_0^2} t.$$
 (7.2.18)

We supposed here that the mean values  $\langle \mu_2 \rangle$  and  $\langle \mu_3 \rangle$  are not zero, at the initial point.

In order to represent particle distribution function, it is convenient to introduce a dimensionless parameter  $\varepsilon_R = 12D_0 t/R_0^2$ . Let us consider the expression

$$\frac{\langle \mu_3 \rangle}{\sigma_n^3} = \frac{3\sqrt{2}}{5(1+\eta_R)^{3/2}} \frac{1}{\varepsilon_R^{1/2}} \equiv \frac{\lambda_3}{\varepsilon_R^{1/2}},$$
 (7.2.19)

where the parameter  $\eta_R = 48D_0^2/V_m^2R_0^2$  is introduced. Now the particle distribution function is given by the expression

$$n_{\theta}(\theta_n) = \varphi_n(\theta_n) - \frac{\lambda_3}{3!} \frac{\varphi_n^{(3)}(\theta_n)}{\varepsilon_R^{1/2}} + \dots$$
 (7.2.20)

Here,

$$\theta_n = \frac{x - \langle x \rangle}{\sigma_n} = \sqrt{2} \frac{n_\theta - \varepsilon_R}{(1 + \eta_R)^{1/2} \varepsilon_P^{1/2}}.$$
 (7.2.21)

We apply a parameter  $n_{\theta} = 12D_0x/V_mR_0^2$  as well as distributions

$$\varphi_n(\theta_n) = \frac{1}{\sqrt{2\pi}} e^{-\frac{\theta^2}{2}}, \quad \varphi_n^{(3)}(\theta_n) = \frac{d^3 \varphi_n(\theta_n)}{d\theta_n^3}. \tag{7.2.22}$$

The particle distribution obtained is valid when

$$t \gg T_D = \varepsilon_R \frac{R_0}{12D_0}. (7.2.23)$$

The approach considered in this section, although fairly general, does not exhibit correlation effects, which are the key to analyze the scalar transport in complex flows.

#### 7.3 Transport in Coastal Basins

On the basis of the Taylor model of the longitudinal dispersion, it is possible to analyze the process of salt and heat transport in partially mixed coastal basins. It is well known that vertical mixing through vertically sheared horizontal currents is caused by horizontal dispersion (see Fig. 7.3.1). The velocity shear is usually related to tidal and wind-driven flows. Under conditions of strong vertical mixing and horizontal advection, one can consider a steady-state balance between advection and vertical mixing of a tracer as an appropriative approximation

$$D_0 \frac{\partial^2 n_1}{\partial z^2} = V_x(z) \frac{\partial n_0}{\partial x}.$$
 (7.3.1)

Here,  $D_0$  is the coefficient of seed (vertical) diffusivity,  $n_0$  is the depth-averaged concentration of a tracer, and  $n_1$  is the perturbation of tracer concentration in the water column. This equation shows that the perturbation of tracer concentration in the vertical direction is the steady-state response to a source term that describes advection in coastal basins under consideration. The velocity profile  $V_x(z)$  is supposed to be known and  $n_1$  is an unknown quantity. Using the Taylor equation, we find the diffusive flux of tracer in the horizontal direction. Water column has the height  $H_0$ 

$$-\frac{H_0}{2} < z < \frac{H_0}{2}. (7.3.2)$$

For the sake of simplicity, the velocity profile  $V_x(z)$  is supposed to be linear,  $V_x(z) = V_0 \frac{z}{H_0}$ . As it was mentioned above, the velocity shear is due to either wind-

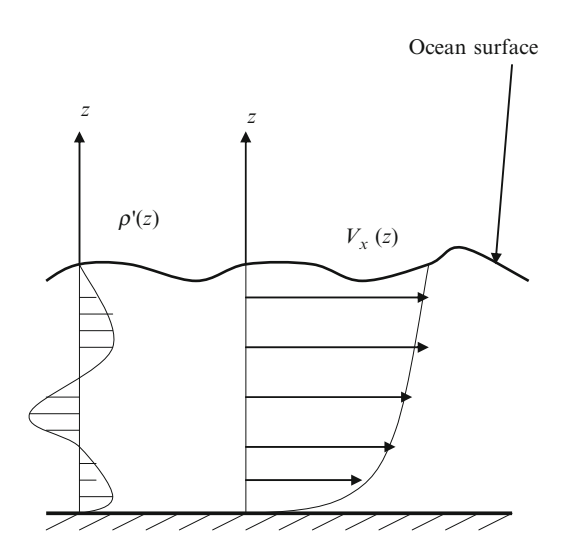


Fig. 7.3.1 Schematic illustration of velocity and density profile in a coastal basin

driven or tidal currents. The conventional normalization condition (the conservation law) is given by the relation:

$$\int_{-\frac{H'_0}{2}}^{\frac{H'_0}{2}} n' dz = 0, \tag{7.3.3}$$

An appropriative approximation for the Taylor dispersion could be the experimentally observed simple scaling:

$$D_x(D_0) \approx \frac{V_0^2 H_0^2}{100 D_0}$$
 (7.3.4)

Let us list the typical magnitudes corresponding to our model. Thus, for a coastal basin 10 m deep with tidal currents having a velocity difference between top and bottom  $V_0 \approx 0.1 \,\mathrm{m/s}$ , and seed diffusion of order  $D_0 = 10^{-3} \,\mathrm{m^2/s}$ , the above scaling leads to the estimate of  $D_x \approx 10 \,\mathrm{m^2/s}$ . It is interesting to estimate the characteristic time to reach a near uniform concentration of a tracer in a basin of the spatial scale  $L_0$ . The relevant approximation is the diffusive representation,  $2\sqrt{D_x t}$ . Taking  $L_0 = 20 \,\mathrm{km}$ , and  $D_0 = 10 \,\mathrm{m^2/s}$ , we easily obtain the characteristic time  $t = 120 \,\mathrm{days}$  [144–146].

The flow dynamics is a consequence of a horizontal pressure gradient responsible for the greater density of water at one end of the basin

$$\rho \frac{\partial V_x}{\partial t} = -\frac{\partial P}{\partial x} + \frac{\partial}{\partial z} \left[ \rho D_0 \frac{\partial V_x}{\partial z} \right]. \tag{7.3.5}$$

Here,  $D_0$  is the coefficient of seed (vertical) diffusivity. It is convenient to introduce a new nondimensional coordinate y as follows:

$$y(z) \equiv 1 + 2\frac{z}{H_0}. (7.3.6)$$

Let us suppose that the velocity shear stress is zero at the surface. By solving the dynamical equation under consideration for the steady case, one obtains the formula

$$V_x = -\frac{gy}{2\rho D_0} \left(\frac{H_0}{2}\right)^3 \frac{\partial \rho}{\partial x} \left(\frac{y^2}{3} - 1\right). \tag{7.3.7}$$

Note that this expression shows that, as predicted, the current  $V_x$  is inversely proportional to  $D_0$ . After substitution of the previous result into the diffusion equation, we find the expression for the density perturbation

$$n_1 = -\frac{gy}{6\rho D_0^2} \left(\frac{H_0}{2}\right)^5 \left(\frac{\partial \rho}{\partial x}\right) \frac{\partial n}{\partial x} \left(y^2 - \frac{y^4}{10} - \frac{5}{2}\right). \tag{7.3.8}$$

Now, the tracer flux is given by the relation

$$\langle n_1 V_x \rangle = -C_b \frac{g^2 H_0^8}{\rho^2 D_0^3} \left( \frac{\partial \rho}{\partial x} \right)^2 \frac{\partial n}{\partial x}, \tag{7.3.9}$$

where the constant  $C_b$  is estimated as  $C_b \approx 1.7 \times 10^{-4}$ . The tracer flux has the classical diffusive form of the Fick law. This allows one to represent the diffusion coefficient as follows:

$$D_x = C_b \frac{g^2 H_0^8}{\rho^2 D_0^3} \left(\frac{\partial \rho}{\partial x}\right)^2 \propto \frac{1}{D_0^3}.$$
 (7.3.10)

This expression corresponds to the Taylor shear dispersion under condition when vertical shear is produced by the longitudinal density gradient. Note that in this model the effective diffusivity is inversely proportional to the cube of the vertical (seed) diffusivity  $D_0$ . Now one can easily estimate the effective diffusivity taking into account the orders of magnitudes:  $H_0=10$  m,  $V_0\approx 0.5$  m/s,  $D_0=10^{-2}V_0H_0\approx 10^{-3}$  m²/s. If the characteristic spatial scale of the density gradient is of order  $l_\rho=-\rho/\left(\frac{\partial\rho}{\partial x}\right)\approx 1,000$  km, simple algebra gives  $D_x\approx 2$  m²/s. On the other hand, the effective diffusion coefficient is proportional to the square of the longitudinal density gradient. This can lead to nonlinear diffusion equation because when the tracer is replaced by salt the diffusivity becomes a function of function of the gradient since salt affects the density.

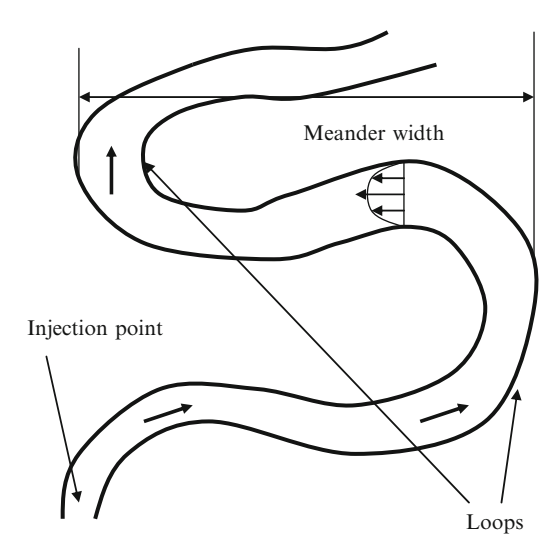
# 7.4 The Taylor Approach to Chaotic Flows

Many of the worst problems of water pollution are found in estuaries because the pollutant may travel up and down the estuary several times before reaching the sea; the process for its removal depends more on turbulent mixing than on simple advection. There has been a much greater revolution in the ideas about river and estuarine dispersion than about air pollution dispersion. Consider a river of depth  $H_0 \approx 3$  m and typical turbulent velocity of  $V_0 \approx 0.03$  m/s. Whereas estimates of the eddy diffusivity based simply on turbulent motion are of the order of  $D_T \approx 10^{-2}$  m<sup>2</sup>/s, Taylor's theory for the effect of shear on the longitudinal turbulent dispersion showed that the diffusivity  $D_{\rm eff}$  may be of the order of 1 m<sup>2</sup>/sin straight two-dimensional channels [148–150]. Later work shows that, in curved rivers (see Fig. 7.4.1) about  $L_0 \approx 200$  m wide,  $D_{\rm eff}$  is of the order of  $10^3$  m<sup>2</sup>/s [151].

For turbulent flows in straight tubes, Taylor [148] derived and experimentally verified the axial dispersion scaling,  $D_{\text{eff}}$ ,

$$D_{\rm eff}(V_*) \approx 10.1 \cdot R_0 V_*.$$
 (7.4.1)

**Fig. 7.4.1** Sketch of a meandering river



Here,  $R_0$  is the pipe radius,  $V_* = \sqrt{\frac{\tau_F}{\rho}}$  is the friction velocity,  $\tau_F$  is the Reynolds stress, and  $\rho$  is the fluid density (see Fig. 7.4.2).

It is interesting that similar scaling laws were obtained for an open channel of the depth  $H_0$  [149].

$$D_{\rm eff}(V_*) \approx 5.9 \cdot H_0 V_* \tag{7.4.2}$$

and for curved pipes (curved rivers) [150]

$$D_{\text{eff}}(V_*) \approx 20 \cdot R_0 V_*, \tag{7.4.3}$$

In these studies, note that the viscous sublayers were ignored as well as the variation of the turbulence properties across the width of the channel, although it is now known that this is unjustified in many natural channels, in which the value of  $D_{\text{eff}}$  may consequently be much higher than that given for an open channel.

Consider phenomenological arguments to explain a universality of these scaling laws. On the basis of the correlation concept, the value of  $D_{\rm eff}$  can be written as

$$D_{\text{eff}} = V_*^2 \int_0^\infty R_L(t) dt = V_*^2 \tau_\perp.$$
 (7.4.4)

Here,  $\tau_{\perp}$  is a measure of the time taken for a fluid particle to sample the whole cross section. The time taken to sample the part of the cross section outside the viscous sublayer is, on dimensional grounds, of order  $\tau_{\perp}(V_*) \propto R_0/V_*$  in a pipe and in an open channel is of order  $\tau_{\perp}(V_*) \propto H_0/V_*$ . These times give values of  $D_{\rm eff}$  consistent with the Taylor prediction. But these times are not normally accurate estimates of the times taken to sample the whole cross section since within the viscous sublayer the properties of the turbulence depend directly on the viscosity  $v_F$ , and the lateral mixing sufficiently near the wall is dominated by molecular

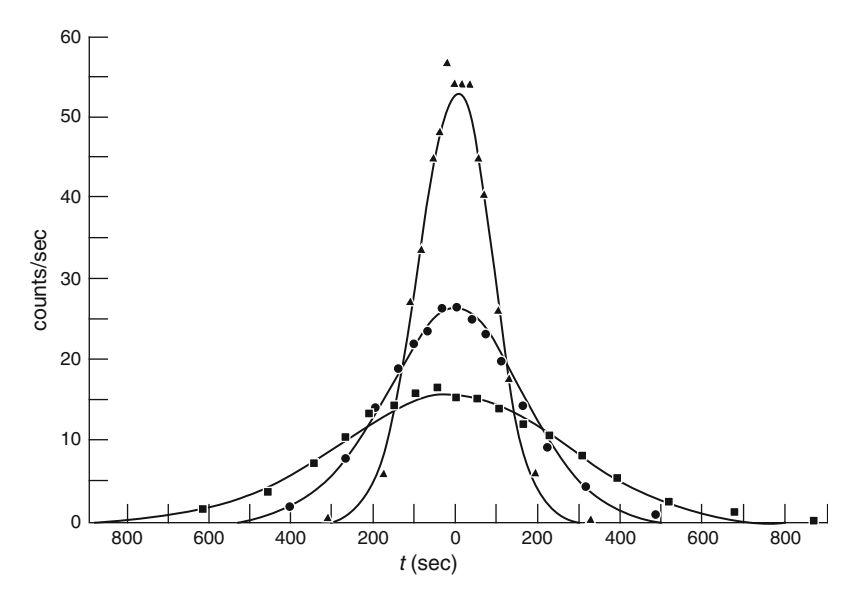


**Fig. 7.4.2** Distribution of concentration in Hull and Kent's experiment. Observation stations: *Filled triangle* Bonanza (13.8 miles); *Filled circle* Green River (43.1 miles); *Filled square* Hanna (108.5 miles). (After Taylor [148] with permission)

processes whose intensity is measured by the molecular diffusivity  $D_0$ . This suggests that the time taken to sample the whole cross section is greater than  $R_0/V$  or  $H_0/V_*$  by an amount that increases as  $D_0$  decreases and as the height of the viscous sublayer increases (that is as the Reynolds number decreases).

An estimate of the increase can be made if it is assumed that the lateral transfer of contaminant everywhere including the sublayer obeys the gradient law of diffusion with a diffusivity, which is the sum of the molecular diffusivity  $D_0$  and an eddy diffusivity  $D_T$  calculated by means of the Reynolds analogy. This assumption is not theoretically well founded; in particular, the lateral transfer of contaminant within the sublayer depends on  $D_0$ , whereas the lateral transfer of momentum does not and this makes the validity of Reynolds analogy very unlikely [151].

In terms of the dissipation rate  $\varepsilon_D$ , one can represent the friction velocity  $V_*$  in the form

$${V_*}^2 = \frac{\varepsilon_D R_0}{2V_0},\tag{7.4.5}$$

where  $V_0$  is the characteristic velocity scale. Then we can obtain a modified scaling relation

$$D_{\text{eff}} \approx 10.1 R_0 V_* \approx 10.1 \left(\frac{V_*}{V_0}\right)^{1/3} R_0^{4/3} \varepsilon_D^{1/3}.$$
 (7.4.6)

The effect of tidal oscillations and stratifications, which are often present in environmental flows, may increase effective diffusivity further. Nevertheless, the simple water pollution models, in which mixing is assumed to take place rapidly between "boxes" of water moving up and down the estuary, are often adequate approximations.

#### 7.5 The Lagrangian Mixing in Turbulent Flow in a Pipe

The phenomenological approach to the longitudinal dispersion has become widely popular due to its exceptional efficiency in describing transport in the presence of anisotropy. On the other hand, the Lagrangian description of turbulent diffusion on the basis of the Taylor statistical method is valid under conditions of steady and homogenous turbulence. Batchelor pointed out that such strong conditions are accomplished even for flows in straight pipes and channels if we restrict ourselves by consideration of the longitudinal direction only [152].

Let us consider the case of the large Reynolds numbers when fluid flows along a pipe under the action of a steady pressure gradient. The Lagrangian representation for the longitudinal velocity of the small fluid element is given by the formula

$$\frac{\mathrm{d}X(t)}{\mathrm{d}t} = V_x(\vec{r}_0, \ t_0 + t). \tag{7.5.1}$$

This longitudinal velocity  $V_x$  depends on the fluid element initial position  $\vec{r_0}$  in the pipe cross section at the time  $t = t_0$ . However, because of turbulent mixing (see Fig. 7.5.1) after a long time (correlation time  $\tau$ ), a random velocity function becomes steady and independent of the initial position  $\vec{r_0}$ .

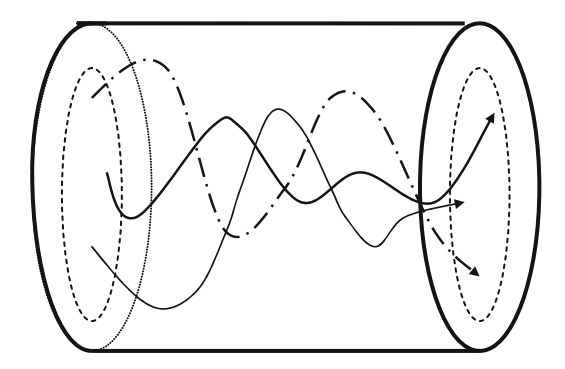
$$\langle V_x(\vec{r}_0, t_0 + t) \rangle = U_0. \tag{7.5.2}$$

This means that for flows in a pipe under the action of a steady pressure gradient, the conditions of steady and homogenous turbulence are accomplished in the longitudinal direction. That is why it is convenient to employ the Taylor formula for turbulent dispersion in the form

$$\langle [X(t) - \langle X(t) \rangle)]^2 \rangle \propto 2D_T t,$$
 (7.5.3)

where  $D_T$  is the longitudinal turbulent diffusion coefficient. Here, we consider the central region of the turbulent flow in a straight pipe. When the Reynolds number is large, the thickness of the viscous layer takes a negligible fraction of the pipe cross section. Then, if a scalar particle is near the viscous layer, where the fluctuation of the velocity is likely to be negative, there must be a tendency to move in the

**Fig. 7.5.1** Schematic diagram of the Batchelor mixing in a circular pipe



direction away from the boundary. In fact, if a fluid element is once inside the central region of turbulent motion, it remains within it [153].

The diffusion in the turbulent flow under consideration is related with the variation of mean velocity with position over cross section of the pipe. Recall that the distribution of velocity across the pipe is determined by the friction velocity

$$V_*(\rho) = \sqrt{\frac{\tau_F}{\rho}},\tag{7.5.4}$$

where  $\tau_F$  is the Reynolds stress and  $\rho$  is the fluid density. In such a case, it would be natural to expect that the longitudinal turbulent diffusion coefficient  $D_T \approx 2 V_0^2 \tau$  depends only on the friction velocity  $V_*$  and the pipe radius  $R_0$ 

$$D_T \approx 2V_0^2 \tau \propto R_0 V_*,\tag{7.5.5}$$

which corresponds exactly to the Taylor result considered above.

It is a result of ergodic theory [152, 153] that after a long time all the small fluid elements in the pipe must have the same mean velocity  $U_0$ 

$$\frac{\langle X(t) \rangle}{t} = U_0. \tag{7.5.6}$$

Indeed, fluid elements in the case under consideration move freely over the whole cross section of the pipe and it is impossible to distinguish them one from another. This mean velocity is equal to the discharge velocity  $U_0 = U_D$ . Now the expression

$$\left\langle [X(t) - U_0 t]^2 \right\rangle \propto \text{const } V_* L_0 t$$
 (7.5.7)

is represented by the longitudinal dispersion in flows in straight pipes and channels with the transverse spatial characteristic scale  $L_0$ .

#### 7.6 The Taylor Dispersion and Memory Effects

The universality of the Taylor convective dispersion impels us to use the heuristic methods of including nonlocal effects and memory effects into the initial local equation. Indeed, in environmental flows (rivers, estuaries, etc.) there are often stationary eddy structures next to the bed that could trap scalar particles [154, 155]. In a river, there are lagoons, recirculating eddies, beaver dams, etc., which are responsible for scalar trapping in "dead zones" (see Fig. 7.6.1). In the framework of the heuristic approach, it is easy to include such memory effects in the transport equation under analysis. This allows us to analyze trapping effects, which play an important role in tracer transport. Thus, one can represent the total concentration of tracer n(x,t) as two parts

$$n(x,t) = P_A(x,t) + q_{Tr}(t),$$
 (7.6.1)

where  $P_A(x,t)$  corresponds to actively transporting particles and  $q_{Tr}(x,t)$  describes trapping. In the simplest case, the relationship between  $P_A$  and  $q_{Tr}$  is given by

$$\frac{\partial q_{\rm Tr}}{\partial t} = \alpha_T (\beta_T P_{\rm A} - q_{\rm Tr}). \tag{7.6.2}$$

Here,  $\alpha_T$  and  $\beta_T$  are the parameters of the problem. If all the particles are released in the untrapped region at t = 0, one obtains

$$q_{\mathrm{Tr}}(x,t) = \alpha_T \beta_T \int_0^t P_{\mathrm{A}}(x,\tau) \mathrm{e}^{-\alpha_T(t-\tau)} \mathrm{d}\tau. \tag{7.6.3}$$

Here,

$$M(t - \tau) = \alpha_T \beta_T \exp[-\alpha_T (t - \tau)] \tag{7.6.4}$$

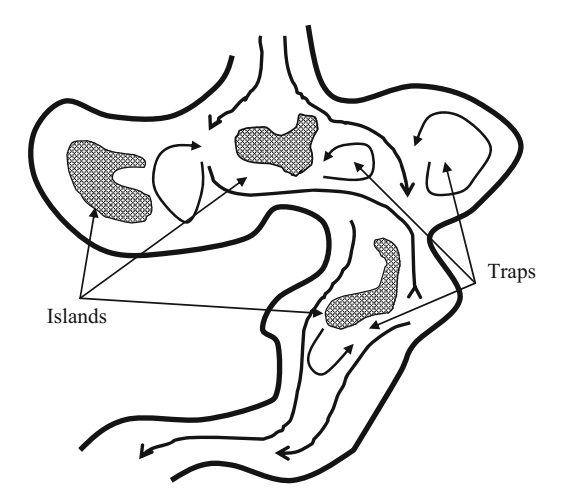


**Fig. 7.6.1** Schematic illustration of the vortex trapping in a river

is the memory function. In general, we can rewrite the expression in the form with an arbitrary memory function M

$$q_{\rm Tr}(x,t) = \int_0^t P_A(x,t) M(t-\tau) d\tau.$$
 (7.6.5)

Then, based on tracer conservation, it is possible to describe transport by the equation

$$\frac{\partial P_A}{\partial t} + \frac{\partial q_{Tr}}{\partial t} + V \frac{\partial P_A}{\partial x} = D \frac{\partial^2 P_A}{\partial x^2}.$$
 (7.6.6)

Using the Taylor method, the modified equation for the mean density can be rewritten in the form

$$\frac{\partial n_0}{\partial t} = \int_0^t M(t - \tau) \frac{\partial^2 n_0(x, \tau)}{\partial x^2} d\tau.$$
 (7.6.7)

The expression for the effective diffusion coefficient, which takes into account memory effects, is then given by

$$D_{\text{eff}} = \int_0^\infty M(\tau) d\tau. \tag{7.6.8}$$

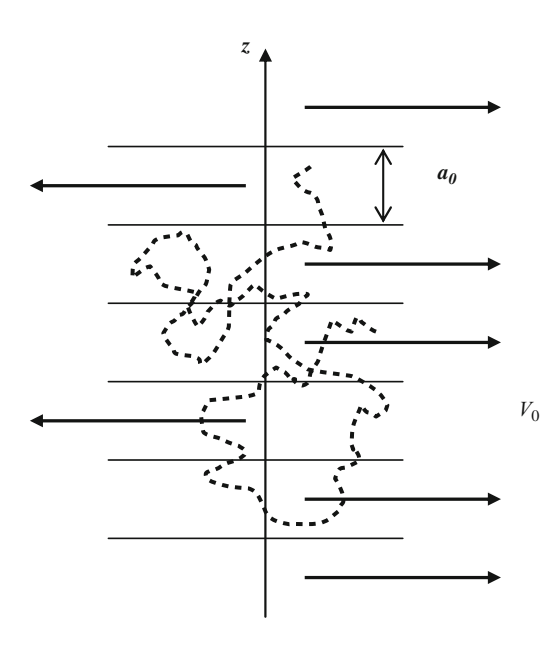
Here, we consider the behavior over a long time.

Note that tracer transport in the presence of vortex structures or complex profiles of shear flows could be even nondiffusive and we have to employ sophisticated phenomenological arguments to describe such an anomalous dispersion.

# 7.7 Dispersion in Random Shear Flows

Analysis of random shear flows is a natural generalization of the Taylor approach to the scalar dispersion. Such a model was proposed in a paper by Dreizin and Dykhne [156] where a physically clear model of strongly anisotropic transport in a random velocity field was investigated. First, we assume that "seed" diffusion with the coefficient  $D_0$  acts on the plane. In our model, the longitudinal direction coincides with the z-axis (Fig. 7.7.1). In the transverse direction, the diffusing particle experiences random pulsations, which produce narrow convective flow with a velocity  $V_0$  and a width  $a_0$ . Here, the velocity field has a "quenched" randomness. In the transverse direction, the diffusion can be neglected compared to the velocity drift carrying the molecule with the flow. In the framework of this consideration, there is no drift in the direction perpendicular to the layers.

**Fig. 7.7.1** The Dreizin–Dykhne random shear flow geometry



Let us consider a simple model for calculating the diffusion coefficient in the transverse direction  $D_{\perp}$  using characteristic correlation scales:

$$D_{\perp} \approx V_0^2 \tau_{\perp},\tag{7.7.1}$$

where the transverse correlation time  $\tau_{\perp}$  is given by  $\tau_{\perp}(x) \propto t/N(t)$ . Here, N(t) is the number of shear flows intersected by the particle during its longitudinal motion (the number of particle-jet interactions)

$$N(t) \approx \frac{\sqrt{2D_0 t}}{a_0}. (7.7.2)$$

Thus, we obtain the following formula for the transverse diffusion coefficient:

$$D_{\perp}(t) \propto V_0^2 a_0 \sqrt{\frac{t}{D_0}}.$$
 (7.7.3)

This leads to transport scaling in the form

$$\lambda_{\perp}(t) \propto V_0 \, a_0^{1/2} \left(\frac{t}{D_0}\right)^{3/4}.$$
 (7.7.4)

In the superdiffusive case under consideration, it was found that the Hurst exponent is H = 3/4 > 1/2. Such a representation is valid only if the perpendicular

spatial displacement is no larger than the perpendicular correlation length  $\lambda_{\perp}(t) < \Delta_{\rm COR} \approx a_0$ .

Note that there are different scaling approaches to treat anomalous transport in a system of random shear flows. One can employ the ballistic representation for the transverse displacement of scalar particles similar to the Corrsin shear wind model

$$\lambda_{\perp}(t) \approx V_0 t_{\text{eff}}(t) \approx V_0 t P_{\infty}(t).$$
 (7.7.5)

Here,  $P_{\infty}$  is the relative number of the small fraction of "noncompensated" fluctuations  $\delta N$ ,  $P_{\infty}(N) = \frac{\delta N}{N}$ . Using the Gauss representation for a number of "noncompensated" fluctuations  $\delta N$ , one obtains

$$\delta N(t) \approx \sqrt{N} \propto t^{1/4}, \quad \lambda_{\perp} \propto V_0 \, a_0^{1/2} \left(\frac{t}{D_0}\right)^{3/4}.$$
 (7.7.6)

The same result can be obtained by the insignificant modification of the phenomenological expression for  $\lambda_{\perp}(t)$ ,

$$\lambda_{\perp}(t) \approx V_{\rm eff}(t)t,$$
 (7.7.7)

where

$$V_{\rm eff}(t) \approx V_0 P_{\infty} \approx V_0 \frac{\delta N}{N(t)}$$
 (7.7.8)

The search for a more satisfactory method of nondiffusive transport description is the subject of the following chapters. Nevertheless, the Dreizin–Dykhne model of anomalous diffusion in a system of random shear flows is the very effective tool to investigate complex correlation effects in the framework of random walk phenomenology.

### **Further Reading**

#### The Taylor Dispersion

- P.M. Adler, *Porous Media* (Butterworth-Heinemenn, Stoneham, 1992)
- G.K. Batchelor, *The Scientific Papers of Sir G.I. Taylor*. Meteorology, Oceanology, Turbulent Flow, vol. 2 (Cambridge University Press, Cambridge, 1960)
- R.B. Bird, W.E. Stewart, E.N. Lightfoot, *Transport Phenomena* (Wiley, New York, 2002)
- M.P. Brenner, Classical Physics Through the Work of G.I. Taylor (MIT, Cambridge, 2000)

Further Reading 125

W.C. Conner, J. Fraisserd, *Fluid Transport in Nanoporous Materials* (Springer, Berlin, 2006)

- A. Crisanti, M. Falcioni, A. Vulpiani, Rivista Del Nuovo Cimento 14, 1–80 (1991)
- R.M. Mazo, *Brownian Motion*, *Fluctuations*, *Dynamics and Applications* (Clarendon Press, Oxford, 2002)
- H.K. Moffatt, J. Fluid Mech. **106**, 27 (1981)
- A.S. Monin, A.M. Yaglom, Statistical Fluid Mechanics (MIT, Cambridge, 1975)
- T. Squires, S. Quake, Rev. Mod. Phys. 77, 986 (2005)
- Ya.B. Zeldovich, *Selected Works*. Chemical Physics and Hydrodynamics, vol. 1 (Princeton University, Princeton, NJ, 1992)

#### Taylor Dispersion and Environmental Flows

- F.T.M. Nieuwstadt, H. Van Dop (eds.), *Atmospheric Turbulence and Air Pollution Modeling* (D. Reidel, Dordrecht, 1981)
- L.C. Van Rijn, *Principles of Sediment Transport in Rivers, Estuaries and Coastal Seas* (Aqua, Amsterdam, 1993)
- S.A. Thorpe, *Introduction to Ocean Turbulence* (Cambridge University Press, Cambridge, 2007)
- C.J. Hearn, *The Dynamics of Coastal Models* (Cambridge University Press, Cambridge, 2008)
- B. Cushman-Roisin, J.-M. Beckers, *Introduction to Geophysical Fluid Dynamics* (Academic, San Diego CA, 2010)

# Part IV Fractals and Anomalous Transport

# **Chapter 8 Fractal Objects and Scaling**

#### 8.1 Fractal Dimensionality

Many physical systems do exhibit self-similarity, although, of course, within some finite range of scales. The list includes Brownian motion, turbulent flows, porous media, polymers, clusters, etc. The geometry of these systems, often based on random processes, is complicated. The concept of fractal dimension helps to express, model, and comprehend both the geometrical complexity and its physical consequence [157–164]. Furthermore, fractal concepts and scaling laws establish similarities between correlation effects and growth phenomena in a variety of equilibrium (such as percolation) and far-from-equilibrium (such as diffusion-limited aggregation and viscous fingering) processes. This connection is of heuristic significance, because presently there is no first-principle theory to describe, for example, turbulence, turbulent transport, or diffusion-limited aggregation, which are markedly far-from-equilibrium and nonlocal processes.

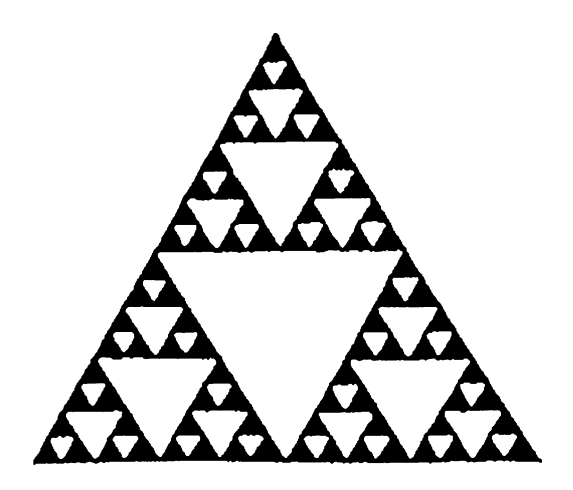
The fractal dimension  $d_F$  serves as an exponent in the power law of the type

$$M(\lambda r) = \lambda^{d_{\rm F}} M(r), \tag{8.1.1}$$

which shows how the "property" M of the fractal (for example, its mass) changes when the characteristic size in the embedding space is rescaled by a factor  $\lambda$ ,  $r \to \lambda$ . Note that  $\lambda$  is independent of r, which stresses the self-similarity at all scales. Regular homogeneous (called also compact) objects satisfy this definition with  $d_F$  being the "usual" integer dimension 1, 2, 3, and so on.

The most interesting feature of this definition is that there are indeed objects – fractals – fitting (8.1.1) with  $d_{\rm F}$  "fractional" (see Fig 8.1.1). For example,  $d_{\rm F} = \frac{\ln 3}{\ln 2} = 1.58496...$ , indicating that the fractal under consideration (the Sierpinski gasket) is not a line and not a surface. This shows that an object can be self-similar if it is formed by parts similar to the whole. Isotropic fractals are self-similar: they are invariant under isotropic scale transformations and such exactly self-similar objects are named deterministic fractals.

Fig. 8.1.1 Force stage of the construction of the Sierpinski gasket



In contrast to the idealized objects, which are invariant under isotropic scale transformations, there are many natural objects, which are random. Despite this randomness, such objects could be self-similar in a statistical sense (for example, the Brownian particle path, clusters, and the coastline of a continent). Nontrivial topology of both deterministic fractals and random fractal structures can be described qualitatively by the generalization of the Euclidean dimension concept. Thus, by embedding dimension,  $d_E$ , we understand the smallest Euclidean dimension of the space in which a given object can be embedded. To decide on the fractality of an object, we need to measure its Hausdorff dimension. The volume  $W(\delta)$  of an arbitrary object can be measured by covering it with balls of linear size  $\delta$ , and volume  $\delta^{d_E}$ . If  $N(\delta)$  balls will cover it, then

$$W(\delta) = N(\delta)\delta^{d_E}.$$
 (8.1.2)

We can expect that for any object, the number of balls is given by the scaling

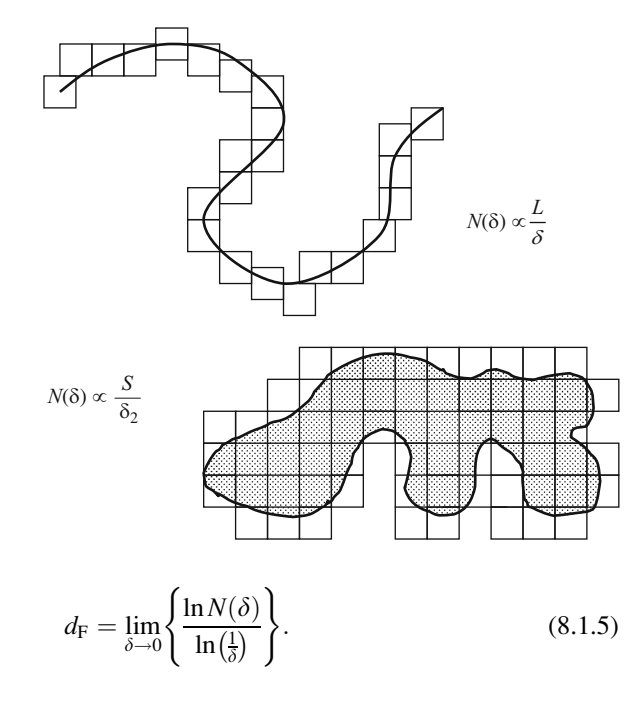
$$N(\delta) \propto \frac{1}{\delta^{d_E}}$$
 (8.1.3)

since the volume of an object does not change if we change the unit of measurement  $\delta$ . To generalize the previous definition for the case of fractal objects, we can write the new scaling for the number of balls in the form (see Fig. 8.1.2)

$$N(\delta) \propto \frac{1}{\delta^{d_{\rm F}}},$$
 (8.1.4)

where  $d_{\rm F}$  is the fractal dimension. Usually objects with nontrivial geometry where  $d_{\rm F} \neq d_E$  are called fractals [157–164]. From this definition, we obtain the formula to calculate the fractal dimensionality as follows:

**Fig. 8.1.2** Schematic illustration of the box dimension for a smooth curve of length *L* and for planar region of area *A* bounded by a smooth curve



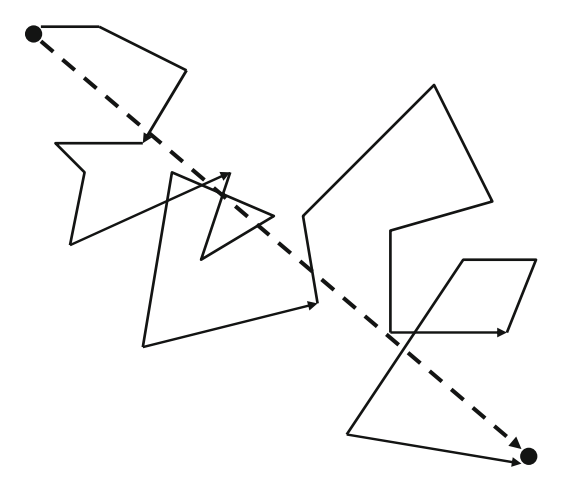
For the Sierpinski gasket, the natural unit to measure the length of the set at iteration k is the length of the smallest interval  $\delta_k = (1/2)^k$ . The number of intervals of length  $\delta_k$  at level k is given by  $N(\delta_k) = 3^k$ . In this case, the corresponding fractal dimensionality  $d_F = 1.584... < d_E = 1$ , and that is why the Sierpinski gasket is a fractal object.

The discussion of a new geometry of nature, one that embraces the irregular shapes of objects such as coastlines, lighting bolts, cloud surfaces, and molecular trajectories, began in the 1960s [157]. A common feature of these objects is that their boundaries are so irregular that such fundamental concepts as dimension and length measurement must be generalized. Therefore, we shall consider some of the metric peculiarities of a few usual mathematical objects, which we subsequently adopt to describe turbulent transport and anomalous diffusion.

# 8.2 Seacoast Length and the Mandelbrot Scaling

The Brownian motion of a small (micron-size) particle suspended in an isotropic solvent is one of the simplest examples of stochastic fractals. The Brownian particle is in uninterrupted and irregular motion with a zigzag trajectory (see Fig. 8.2.1) due to the fluctuative movement of the solvent molecules and their collisions with the particle.

**Fig. 8.2.1** Zigzag trajectory of Brownian particle in a two-dimensional plane



Let us consider the Gaussian distribution

$$\rho(x,t) = \frac{1}{(4\pi Dt)^{d/2}} \exp\left(-\frac{x^2}{4Dt}\right),$$
(8.2.1)

which satisfies the scaling law

$$P(\lambda^{1/2}x, \lambda t) = \frac{P(x, t)}{\lambda^{1/2}}$$
(8.2.2)

so that the distribution for the random variable  $\lambda^{1/2}X(\lambda t)$  is the same as that for X(t). This scaling relation establishes that the irregularities are generated at each scale in a statistically identical manner, i.e., if the fluctuations are known in a time interval  $\lambda t' \geq t \geq t'$  they can be determined in the expanded interval  $\lambda^2 t' \geq t \geq \lambda t'$  as well as in the contracted interval  $t' \geq t \geq \frac{t'}{\lambda}$ . Thus, as expressed by Feder (1988), the Brownian process is invariant in distribution under a transformation that changes the time interval by a factor  $\lambda$  and the space interval by a factor  $\lambda^{1/2}$ . Such a distribution that is invariant under a transformation that scales time and space by different factors is called self-affine. When the distribution is invariant under a transformation that scales space and time by the same it is called self-similar. The same considerations could be applied to curves; i.e., they can be either self-similar or self-affine depending on how they scale. Thus, the scaling properties of the concentration are determined by those of the Gaussian probability density.

From the formal standpoint, the length of the very "tortuous" curve (the fractal curve)  $L(\delta)$  can be rewritten in the form

$$L(\delta) \approx \delta N(\delta) \propto \frac{\delta}{\delta^{d_{\rm F}}} = \frac{1}{\delta^{d_{\rm F}-1}}.$$
 (8.2.3)

In this fractal approach, the full length  $L(\delta)$  is approximated by the small segments of size  $\delta$ ,  $N(\delta)$  is the number of these segments, which are necessary

for such an approximation, and  $d_{\rm F}$  is the fractal dimensionality of the curve. In the framework of the conventional representation of the geometry of curves, we have to use the value  $d_{\rm F}=d=1$ . However, in this case there are the drawbacks of the conventional method of length measurement by a "yardstick" (ruler). Mandelbrot considered the problem of measurement of a tortuous seacoast length in which the increase of measurement accuracy (the decrease of the value  $\delta$ ) leads to the growth of the value  $N(\delta)$  ( $d_{\rm F}>1$ ). From the formal standpoint, this approach yields:

$$L(\delta) \approx \delta N(\delta)|_{\delta \to 0} \to \infty.$$
 (8.2.4)

This means that such a fractal line embraces "almost" the full plane. The advantage of this definition is the possibility to describe the longest and more complex lines (fractal lines). It is natural to generalize the previous definition. We can obtain the expression for the fractal region in the form:

$$W_d \approx \delta^d N(\delta) \approx \delta^{d-d_F}$$
. (8.2.5)

Here, we are dealing with the fractal cases  $d_{\rm E} > d$ . Note that in practice, the power law holds only over an internal range of  $\delta$  (see Fig. 8.2.2).

The simplest model, which permits us to analyze the fractal properties of transport processes, is d-dimensional random walks. For the mean square displacement, one obtains

$$R^2(t) \approx 2 dDt \approx 2 d\frac{\Delta_{COR}^2}{2 d\tau} t \approx \Delta_{COR}^2 \frac{t}{\tau} \approx \Delta_{COR}^2 N(t).$$
 (8.2.6)

Here,  $\Delta_{COR}$  is the correlation length and  $\tau$  is the correlation time. For this case, it is easy to obtain an expression that includes the fractal dimensionality of the Brownian trajectory for the number of "steps" in the scaling form

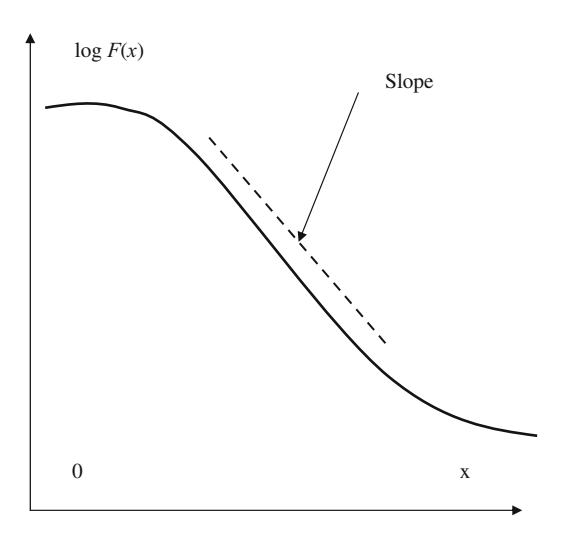


**Fig. 8.2.2** A typical plot of power law, which holds only over and intermediate range of parameter X

$$N(t, \Delta_{\rm COR}) \approx \frac{2 dDt}{\Delta_{\rm COR}^2} \propto \frac{1}{\Delta_{\rm COR}^2}$$
 (8.2.7)

This means that fractal dimensionality of random walks,  $d_{\rm F}=2$ . Note that the value  $d_{\rm F}$  is independent of the space dimensionality d. Here, we assume that  $\Delta_{\rm COR}$  is the small quantity,  $\Delta_{\rm COR}\approx\delta$ . This corresponds to the definition of the fractal curve,  $N(\delta)=1/\delta^{d_{\rm F}}$ .

From the "fractal" point of view, the scaling laws describing anomalous transport in terms of the Hurst exponent  $R(t) \propto t^H$  can be treated analogously

$$R(t) \approx \Delta_{\text{COR}} N(\Delta_{\text{COR}}) \approx \Delta_{\text{COR}} \frac{t}{\tau} \approx \Delta_{\text{COR}} \frac{t}{(\Delta_{\text{COR}})^{\frac{1}{H}}}.$$
 (8.2.8)

The fractal dimensionality in this case is given by the relationship

$$d_{\rm F}(H) = \frac{1}{H}.\tag{8.2.9}$$

When we are dealing with the Brownian motion, H = 1/2, we arrive at the familiar result  $d_F = 2$ .

Fractal ideas have wide applicability to anomalous transport in chaotic (turbulent) flows. Not only the walking particle trajectory, but also percolation streamlines, diffusive fronts, etc., appear to be fractal objects. More detailed information can be found in many textbooks and reviews on fractal geometry and fractal models [157–164].

# 8.3 Fractal Topology and Intersections

We can analyze the fractal topology from a more general point of view. Consider two objects of dimension  $d_1$  and  $d_2$  embedded in a space of dimension d. It is a well-known result that the intersection of the two objects has dimension  $d_1 + d_2 - d$  with probability 1 [157–160]. Indeed, let  $S_1$  and  $S_2$  be fractal sets with Hausdorff dimension  $d_{F_1}$  and  $d_{F_2}$ , respectively, embedded in a space of dimension d. We denote the potential dimension of their intersection by  $S_1 \cap S_2$ . A simple sum rule is known for their co-dimensions:

$$d - d_{F_{1\times 2}}^* = d - d_{F_1} + d - d_{F_2}. (8.3.1)$$

Thus, we get the following equation:

$$d_{F_{1\times 2}}^* = d_{F_1} + d_{F_2} - d. (8.3.2)$$

By knowing the potential dimension, we can immediately determine the true value of the Hausdorff dimension, which lies between 0 and d. In particular, in the case where  $S_2$  is an ordinary set with integer dimension  $d_2$  such as a line or a plane, we have

$$d_{F_{1\times 2}}^* = d_{F_1} - (d - d_2). (8.3.3)$$

For instance, two planes in space intersect generically along a line (see Fig. 8.3.1)

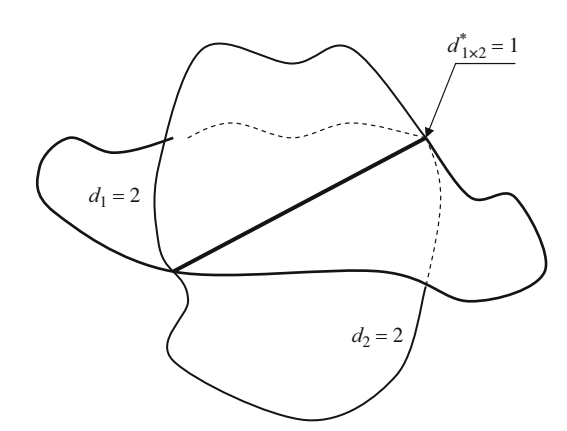
$$d_{1\times 2}^* = d_1 + d_2 - d = 2 + 2 - 3 = 1. (8.3.4)$$

A plane and a line in space intersect generically at a point

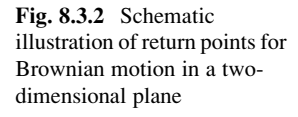
$$d_{1\times 2}^* = d_1 + d_2 - d = 2 + 1 - 3 = 0. (8.3.5)$$

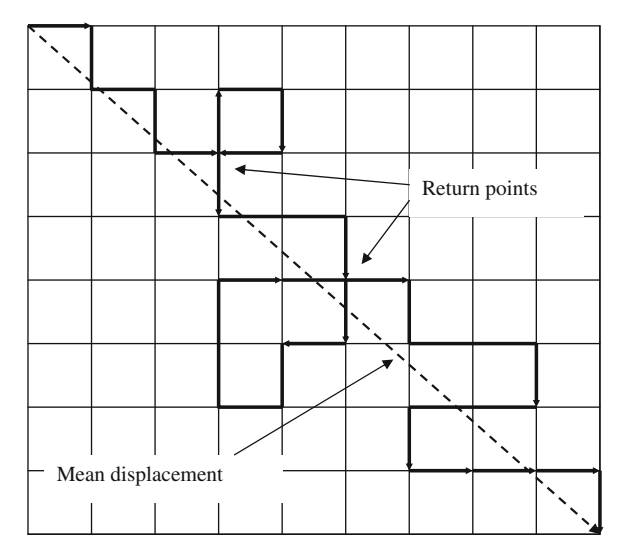
For a random walk in one dimension, this means that the random walk, which is intrinsically a two-dimensional fractal object, has been "folded" many times to fit within a one-dimensional space. In other words, the random walker comes back an infinite number of times on its previous steps. It does so marginally within a plane and only a finite number of times in three and higher dimensions. This shows us why dimensionality plays such a significant role in the correlation effect description.

Long-range correlation effects are responsible for anomalous transport in complex systems. In everyday language, "correlation" means some relation between events. The probability theory employs the rigorous mathematical notion of "return of a walking particle" to the initial point [13, 15, 16] to describe simple correlation effects (see Fig. 8.3.2). This is best illustrated by considering the problem of one-dimensional random walks at the very beginning of the process. In the problem as formulated, the particle will definitely return to its initial position, thereby



**Fig. 8.3.1** Schematic diagram of two manifolds intersection





providing a clear realistic interpretation of the abstract notion of correlations. Rigorous analysis of returns on complicated spatial grids is necessarily based on the chain functional equation for the return probability  $P_0(t)$ . Recall that most of the fundamental problems in the theory of random-walk processes can be formulated in terms of chain functional equations [15, 16]. However, we restrict ourselves here to the brief consideration of return effects.

Qualitative estimates for these effects can be obtained from the classical solution to the equation for the probability density function  $\rho(x,t)$  describing the random walks of a particle. For a space of dimensionality d, one obtains the distribution for a particle returning to the point x=0 at the time t

$$P_0 = \rho(x, t) (\delta x)^d |_{x \to 0} = \frac{(\delta x)^d}{(4\pi Dt)^{d/2}} \exp\left(-\frac{x^2}{4Dt}\right)_{x \to 0} \propto \frac{(\delta x)^d}{(4\pi Dt)^{d/2}}.$$
 (8.3.6)

Here,  $(\delta x)^d$  is the small area around the point x and D is the diffusion coefficient. In the one-dimensional case, we arrive at  $P_0(t) \propto t^{-1/2}$ . This simple formula serves merely to obtain estimates. However, for our purposes here, this solution is important because it provides the evidence that the dimensionality of the space, d, which was used above as a formal parameter, plays a significant role. The correct dependence for  $P_0$  when d=2 and d=3 is given by [13, 15]

$$P_0(N) \propto \frac{1}{N^2} \ll \frac{1}{N^{d/2}}.$$
 (8.3.7)

For grids of dimensionality  $d \le 2$ , the particle will inevitably return to its initial position. For grids with d > 2, the particle can execute random walks without returning.

Note that for a random walk with  $d_F = 2$ , we need to go to a space of dimension d = 4 for the number of intersections to constitute a set of zero dimension,

$$d_{F_{1,2}}^* = d_1 + d_2 - d = 2 + 2 - 4 = 0, (8.3.8)$$

i.e., for the set of crossing to become almost vanishing. In other words, in a space of four or more dimensions, a random walk has very little chance to cross itself and this explains why four dimensions play a special role in theories of interacting fields, such as spin models that we will study later on. At and above four dimensions, these theories are well described by so-called mean-field approaches, while below four dimensions, the large number of crossings of a random walk makes the role of fluctuations important and leads to complex behaviors.

#### 8.4 Self-avoiding Random Walks

The model of random walk can be used as a very idealized model of a linear polymer in good solvent. This model would consider each step in the random walk as the monomer of the polymer chain and would assume that any two neighboring links can point in arbitrary directions. Moreover, the polymer is allowed to intersect, as the Brownian trajectory does. A more realistic model of a polymer is that of a self-avoiding random walk that prohibits self-intersections. Obviously, if the self-avoiding random walk is fractal, then its fractal dimension should be smaller than  $d_{\rm F}=2$  calculated above. Using such probabilistic approximations, we derive an important scaling relation for particles executing random motion with no self-intersections. A self-avoiding random walk is a random walk that never intersects its own trajectory (see Fig. 8.4.1). Though this condition is rather simple, theoretical treatment becomes extremely difficult, since the whole past trajectory affects the

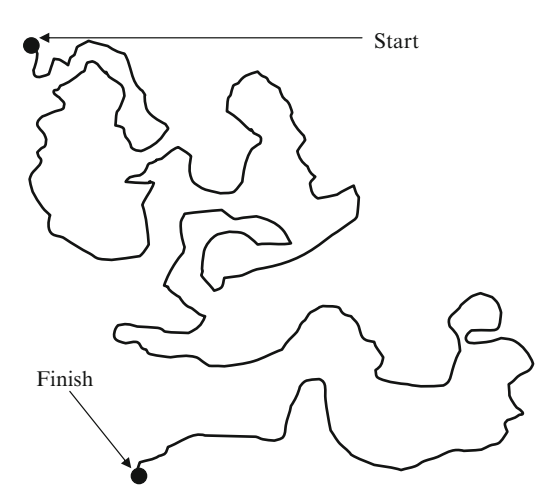


**Fig. 8.4.1** A typical example of self-avoiding random walk in a two-dimensional plane

present motion. We introduce the probability p(N) of self-intersection after N random walks [15, 16],

$$p(N) \approx \frac{N}{R^d(N)}, \tag{8.4.1}$$

where  $R^2(N)$  is the root-mean-square displacement, d is the space dimensionality, and  $N=t/\tau$  is the number of random walks. Here, t is the time and  $\tau$  is the correlation time. In fact, we are assuming that the probability of the particle trajectory intersecting itself is proportional to the number of visited grid points within the region of random particle motion. Then, the probability for a particle to execute N self-avoiding random walks can be estimated as

$$P_S(N) \approx (1-p)^N|_{N\to\infty} \approx \exp(-pN) \approx \exp\left(-\frac{N^2}{R^d}\right).$$
 (8.4.2)

By taking into account the fact that the relationship between the quantities R and N is of a diffusive nature, we can estimate the effective probability of self-avoiding random walks by averaging the probability  $P_S(N)$  with the Gauss distribution:

$$P_S(t) = \int_{-\infty}^{\infty} \exp\left(-\frac{1}{R^d} \left(\frac{t}{\tau}\right)^2\right) \frac{1}{(4\pi Dt)^{d/2}} \exp\left(-\frac{R^2}{4Dt}\right) (\mathrm{d}R)^d. \tag{8.4.3}$$

We assume that the main contribution to the integral comes from the extremum of the integrand, and simple manipulations lead to the scaling:

$$R(t) \propto t^{\frac{3}{2+d}} \gg t^{\frac{1}{2}},$$
 (8.4.4)

for  $d \le 3$ . Here, we must take into account the fact that, in a space of dimensionality d = 1, non-self-intersecting random walks can occur only for the particles moving in one direction, which indicates that  $R \propto t$ . We see that this scaling satisfies this condition automatically. The corresponding Hurst exponent is

$$H(d) = \frac{3}{2+d}. (8.4.5)$$

This scaling was first obtained in the theory of polymers by Flory [165–167] and it gives a correct value in the case d=1, d=2, and d=4. In the case d=3, we obtain the estimate  $d_{\rm F}=1/H=5/3$ , which is a little bit different from the renormalization group method, where  $d_{\rm F}(3)=1.701\pm0.003$ .

Note, the Flory scaling for self-avoiding random walks gives, in the case d=4, the fractal dimension

$$d_{\rm F}(d) = \frac{2+d}{3} = 2,\tag{8.4.6}$$

which coincides with the fractal dimensionality of the conventional Brownian motion. This confirms the previous estimate,  $d_{F_{1\times2}}^* = d_1 + d_2 - d = 2 + 2 - 4 = 0$ , where Brownian motion in four dimensions was represented as walk without self-intersections.

#### 8.5 Two-Dimensional Random Flows and Topography

The analysis of transport in three-dimensional chaotic flow in a general case is too complicated. However, in two dimensions for incompressible flows we are faced with a quite different scenario. Here, one should employ a stream function formalism. The streamlines  $\Psi = \Psi(x,y,t)$  of a random two-dimensional flow could be considered as the coastlines in a hilly landscape flooded by water. Recall that incompressibility implies that the velocity field is related to the stream function  $\Psi$ 

$$V_x = \frac{\mathrm{d}x}{\mathrm{d}t} = -\frac{\partial \Psi(x, y, t)}{\partial y},\tag{8.5.1}$$

$$V_{y} = \frac{\mathrm{d}y}{\mathrm{d}t} = \frac{\partial \Psi(x, y, t)}{\partial x}.$$
 (8.5.2)

Here,  $\Psi(x, y, t)$  is, at the same time, the Hamiltonian function.

In the framework of the Lagrangian description of scalar particles, the character of behavior of streamlines is of great interest. There are different types of streamlines topology. For instance, Fig. 8.5.1 demonstrates flighting-type of jets, which could contribute most to the effective scalar transport due to the convective character of scalar motion along streamlines. The correlation scales here are related to the ballistic motion of tracer (see Fig. 8.5.2). On the other hand, there exist trapping-type streamlines, which are related to loop (vortex) structures (see Fig. 8.5.3). In this case, the effective transport could be defined by the correlation time, which is given by the dimensional estimate

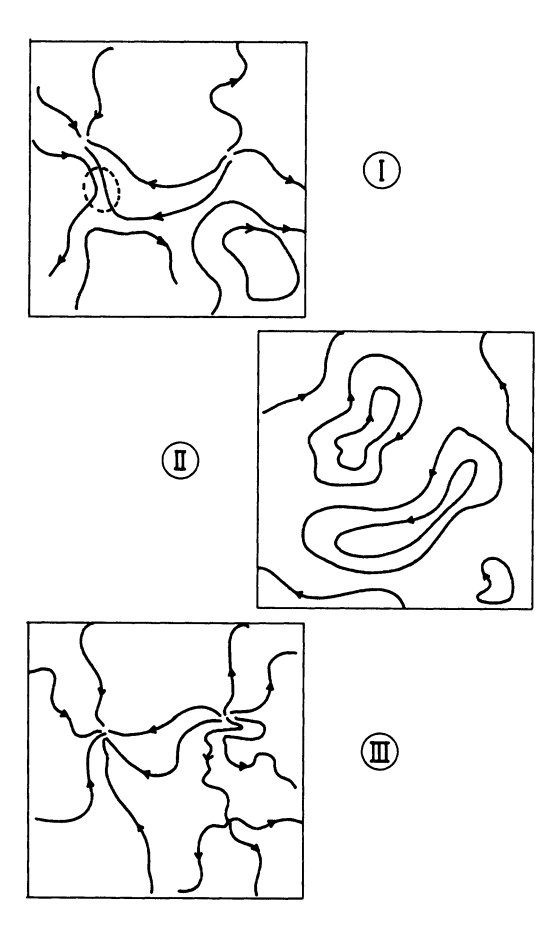
$$\tau(L_0, V_0) \approx \frac{L_0}{V_0},$$
(8.5.3)

where  $V_0$  is the characteristic velocity scale and  $L_0$  is the characteristic length of vortex loop. However, for steady two-dimensional flows the effective transport takes place only when the seed diffusivity  $D_0$  is superimposed. This allows one to introduce one more characteristic time

$$\tau(L_0, D_0) \approx \frac{L^2_0}{D_0}. (8.5.4)$$

The case of great interest arises when a closed fractal streamline embraces almost full the flow domain. It is obvious that the characteristic spatial scale

Fig. 8.5.1 A typical configurations of streamline geometry for two-dimensional chaotic flows. (After Kravtsov [168] with permission)



plays a key role in the description of the effective transport. The problem is to express the characteristic spatial scale through the flow parameters such as characteristic velocity scale  $V_0$ , characteristic frequency  $\omega$  in the case of frequency driven flow, seed diffusivity  $D_0$ , etc.

Let us consider streamlines topology via the scaling representation of closed fractal loops, which are a key to this complex problem. The interesting interpretation of such a model is based on the representation of a "rough" ID + ID landscape as a graph of one-dimensional random walks in the x-t axes, where the t-axis can be interpreted as a horizontal coordinate and the x-axis can be a vertical one. Then, different values of the Hurst exponent correspond to different types of landscape "roughness",  $\langle (\Delta x)^2 \rangle \propto t^{2H}$ . This implies that the "rough landscape" is a statistically self-affine fractal over a corresponding range of length scales with the characteristic Hurst exponent, which is equal to the roughness exponent H (see Fig. 8.5.4). For such landscapes, the mean height difference  $\sqrt{(\Delta h)^2}$  between the pairs of points separated by a "horizontal" distance  $\Delta r$  is given by

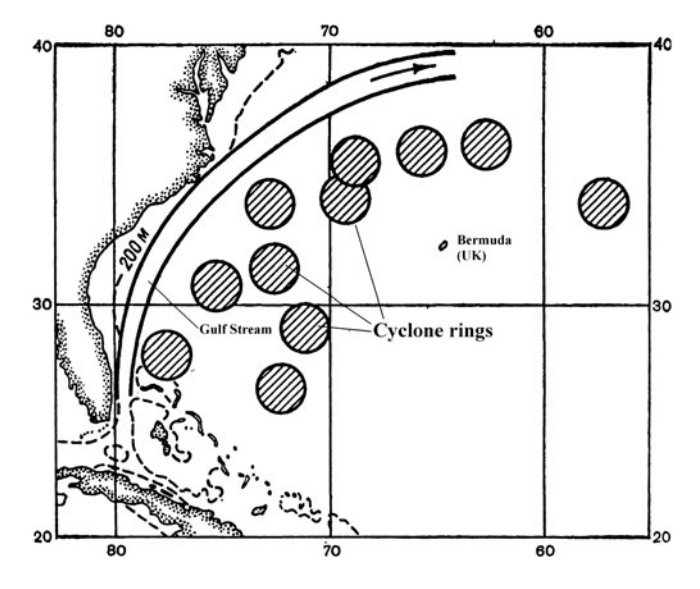


Fig. 8.5.2 Schematic diagram showing the Gulf Stream

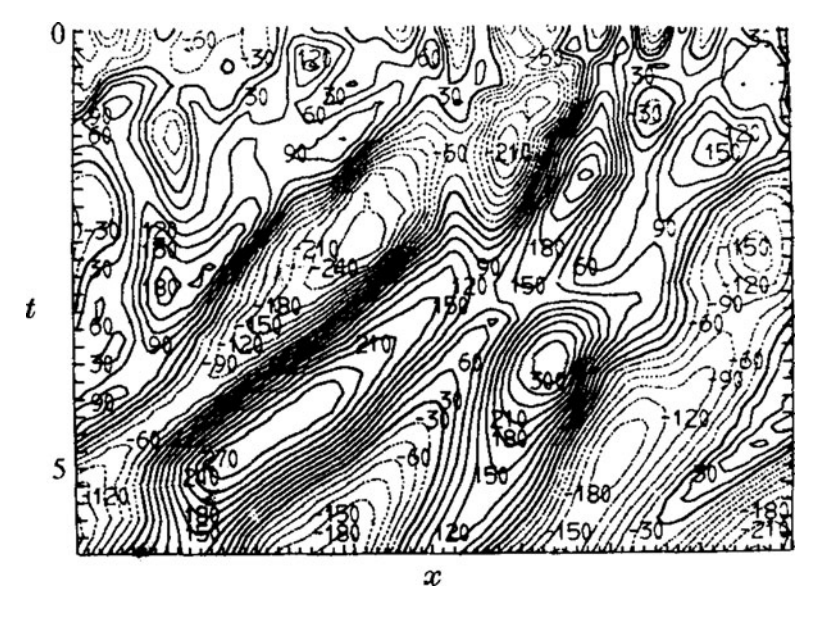
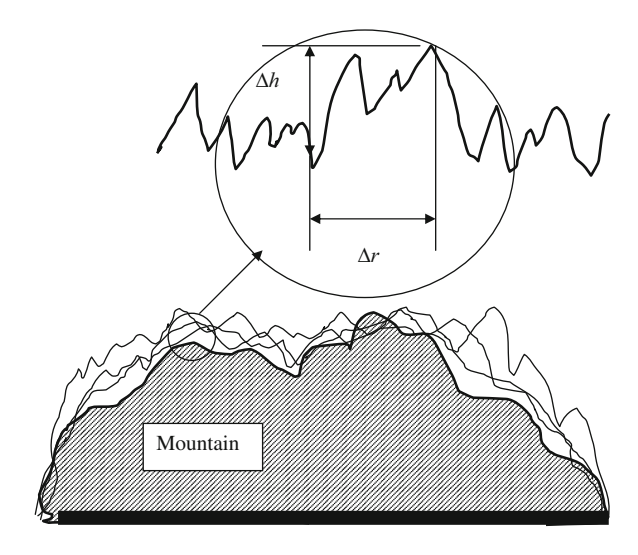


Fig. 8.5.3 The stream function of two-dimensional turbulent flow. (After Rhines [169] with permission)

**Fig. 8.5.4** Schematic illustration of the Brownian landscape



$$\Delta h(\Delta r) \propto (\Delta r)^H$$
. (8.5.5)

It is easy to generalize this representation for the case of a rough surface with another dimensionality. In the framework of turbulent transport description, a similar model was analyzed, where the streamline function  $\Psi_{\lambda}$  is used as the "height" characteristic of the two-dimensional random field:

$$\Psi_{\lambda}(\lambda) \approx \Psi_0 \left(\frac{\lambda}{\lambda_0}\right)^H$$
 (8.5.6)

In this connection, there is a problem in obtaining the relationship between the fractal dimensionality characterizing a single loop  $\tilde{D}_h$  and the Hurst exponent H (the stream function exponent) [170, 171].

The probabilistic approximation is, as usual, the simplest method. The authors of [172, 173] used the model of self-avoiding random walks to describe the single loop character. However, to describe cases with different Hurst's exponents it is necessary to use the probability density function with the arbitrary values  $H:R(N) \propto N^H$ , instead of the Brownian case, where H=1/2. Then, the expression for the probability of self-avoiding Brownian motion takes the form

$$P_S(t) = \int_{-\infty}^{\infty} \exp\left(-\frac{1}{R^d}(N)^2\right) \frac{1}{(N^H)^d} \exp\left(-\frac{R^2}{N^{2H}}\right) (dR)^d.$$
 (8.5.7)

By minimizing the integrand over R, we arrive at the scaling:

$$N(R) \propto R^{\frac{d+2}{2(1+H)}}$$
 (8.5.8)

Further Reading 143

For the two-dimensional case (d = 2), this fractal dimensionality can be considered as dimensionality of a single contour loop (coastline) of a self-affine surface

$$d_{\rm F}(d=2,H) \approx \tilde{D}_h(H) = \frac{2}{1+H}.$$
 (8.5.9)

The value of H=1 yields result, which corresponds to the linear type of behavior with  $\tilde{D}_h=1$ . The random walk with H=1/2 corresponds to  $\tilde{D}_h=4/3$ . However, this is not correct estimate in the region of small H. Indeed, the fractal dimensionality of the percolation hull  $D_h=7/4$  [174–176] has to be larger than the fractal dimensionality of the coastline of the self-affine surface  $\tilde{D}_h(H)$ .

This chapter provides only a quick overview of fractal structures analysis. A more detailed account can be found in [177–182]. The fractal concepts appear to be very fruitful to obtain the relationships between the parameters, which characterize transport, correlation, and geometric properties of the model under consideration. One of the reasons of such efficiency is the possibility to describe the geometric properties of different natural objects by using the scaling terminology.

#### **Further Reading**

#### Chaos and Fractals

- J.B. Bassingthwaighte, L.S. Liebovitch, B.J. West, *Fractal Physiology* (Oxford University Press, Oxford, 1994)
- H.V. Beijeren (ed.), Fundamental Problems in Statistical Mechanics (North Holland, Amsterdam, 1990)
- A. Bunde, S. Havlin (eds.), Fractals and Disordered Systems (Springer, Berlin, 1995)
- A. Bunde, S. Havlin (eds.), *Fractals in Science* (Springer, Berlin, 1996)
- J. Feder, Fractals (Plenum, New York, 1988). Department of Physics University of Oslo, Norway
- J.-F. Gouyet, *Physics and Fractal Structure* (Springer, Berlin, 1996)
- H.M. Hastings, G. Sugihara, *Fractals* (Oxford University Press, Oxford, 1993)
- L.S. Liebovitch, *Fractals and Chaos Simplified for the Life Sciences* (Oxford University Press, Oxford, 1998)
- B.B. Mandelbrot, *The Fractal Geometry of Nature* (Freemen, San Francisco, CA, 1982)
- R.A. Meyers, *Encyclopedia of Complexity and Systems Science* (Springer, Berlin, 2009)
- G. Nicolis, Foundations of Complex Systems (World Scientific, Singapore, 2007)
- M. Schroeder, Fractals, Chaos, Power Laws. Minutes from an Infinite Paradise (W.H Freeman, New York, 2001)
- S.H. Strogatz, Nonlinear Dynamics and Chaos (Perseus, Cambridge, 2000)

#### Diffusion and Fractals

- R. Badii et al. (eds.), *Complexity Hierarchical Structures and Scaling in Physics* (Cambridge University Press, Cambridge, 1997)
- D. Ben-Avraham, S. Havlin, *Diffusion and Reactions in Fractals and Disordered Systems* (Cambridge University Press, Cambridge, 1996)
- G.P. Bouchaud, A. Georges, Phys. Rep. 195, 132–292 (1990)
- A. Bovier, *Statistical Mechanics of Disordered Systems*. A Mathematical Perspective (Cambridge University Press, Cambridge, 2006)
- O. Coussy, *Mechanics and Physics of Porous Solids* (Wiley, New York, 2010)
- P.G. De Gennes, *Introduction to Polymer Dynamics* (Cambridge University Press, Cambridge, 1990)
- P.G. De Gennes, *Scaling Concepts in Polymer Physics* (Cornell University Press, Ithaca, NY, 1979)
- J.W. Haus, K.W. Kehr, Phys. Rep. **150**, 263 (1987)
- M. Kleman, O.D. Lavrentovich, Soft Matter Physics (Springer, Berlin, 2003)
- R. Metzler, J. Klafter, Phys. Rep. 339, 1 (2000)
- M.E. Raikh, I.M. Ruzin, in *Mesoscopic Phenomena in Solids*, ed. by B.L. Altshuler, P.A. Lee, R.A. Webb (North-Holland, Amsterdam, 1991)

## Chapter 9

## **Random Shear Flows and Correlations**

#### 9.1 Autocorrelation Function for Fluids

Lagrangian velocity correlations are certain quantities in turbulent diffusion because of Taylor's relation, which expresses the mean square displacements of fluid particles as a double integral over time of two-time Lagrangian velocity correlations. Taylor's relation also has important physical consequences for anomalous transport. Indeed, long-range correlations are responsible for anomalous transport. Thus, the representation of the autocorrelation function C(t) in the power form  $C(t) \propto t^{-\alpha_c}$  leads to the nondiffusive estimate for effective transport

$$D_{\rm eff}(t) \propto \int C(t) \, \mathrm{d}t \propto t^{1-\alpha_C}$$
 (9.1.1)

or in terms of the mean squared displacement

$$R^2(t, \alpha_C) \propto D_{\text{eff}}(t) \cdot t \propto t^{2-\alpha_C}$$
. (9.1.2)

This relation allows one to determine the Hurst exponent as follows:

$$R^2(t,H) \propto t^{2H} \propto t^{2-\alpha_C},$$
 (9.1.3)

$$H(\alpha_C) = 2 - \alpha_C. \tag{9.1.4}$$

We now go one step further in modeling the correlation effects. It is well known that interactions both create and destroy correlations. There is a useful example, which illustrates this in terms of the correlation function. Let us consider "the collective" (hydrodynamic) nature of the evolution of a correlation cloud by the formal calculation of the autocorrelation function. Suppose a tagged particle in a system in equilibrium is conditioned to be at the origin at t=0 with velocity  $\vec{V}$ 

$$\rho(\vec{r}, 0) = \delta(\vec{r}), \quad \vec{u}(\vec{r}, 0) = \vec{V}\delta(\vec{r}).$$
 (9.1.5)

For times much longer than the mean free time between collisions, the time development of  $\rho(\vec{r},t)$  and  $\vec{u}(\vec{r},t)$  is described to be a first approximation by the solution of linearized hydrodynamic equations. For the particle density,  $\rho(\vec{r},t)$ , this is the diffusion equation in the conventional form

$$\frac{\partial \rho}{\partial t} = D_0 \Delta \rho. \tag{9.1.6}$$

The hydrodynamic equations for the divergence free part  $\vec{u}_{tr}$  of the velocity density are

$$\frac{\partial \vec{u}_{tr}}{\partial t} = -v_F \nabla \times (\nabla \times \vec{u}_{tr}) \tag{9.1.7}$$

$$\operatorname{div} \vec{u}_{tr} = 0 \tag{9.1.8}$$

where  $v_F$  is the kinematic viscosity. The irrotational part  $\vec{u}_{long}$  of the velocity density does not contribute to the leading long-time tail in the velocity autocorrelation function. These equations are most easily solved for the Fourier transform  $\vec{u}_{tr}(\vec{k},t)$  of  $\vec{u}_{tr}(\vec{r},t)$  with

$$\vec{u}_{tr}(\vec{k},t) = (\vec{V} - (\vec{V} \cdot \hat{k})\hat{k}) e^{-\nu_F k^2 t}$$
(9.1.9)

for the initial condition under consideration. Here,  $\hat{k}$  is the unit vector along k, and the Gaussian solution of the diffusion equation (for its Fourier transformation) is given by

$$\tilde{\rho}_k(t) = e^{-D_0 k^2 t}. (9.1.10)$$

Now assume that, if after a not too short time t, the tagged particle is at a position  $\vec{r}$ , its average velocity is given by  $\vec{u}(\vec{r},t)$ . In other words, assume that at time t the tagged particle on the average has the same velocity as the other particles in its neighborhood, and that the average velocity  $\vec{u}(\vec{r},t)$  to first approximation is not influenced by the fact that the tagged particle is located at  $\vec{r}$  at time t. Then the average velocity of the tagged particle to leading order can be found as

$$\vec{V}_I(t) \approx \int d\vec{r} \, \rho(\vec{r}, t) \, \vec{u}(\vec{r}, t) \approx d\vec{r} \, \rho(\vec{r}, t) \vec{u}_{tr}(\vec{r}, t)$$
(9.1.11)

In terms of the Fourier transformation, we find

$$\vec{V}_I(t) \approx \frac{1}{(2\pi)^d} \int d\vec{k} \tilde{\rho}_k(t) \ \vec{u}_{tr} \left(-\vec{k}, t\right)$$
 (9.1.12)

After calculations, one obtains the formula

$$\vec{V}_I(t) \approx \frac{d-1}{d} \left[ 2\pi (v_F + D_0) \ t \right]^{-\frac{d}{2}} \vec{V}.$$
 (9.1.13)

The velocity autocorrelation function could be calculated by averaging  $\vec{V}\vec{V}_I(t)$  over the equilibrium velocity distribution,

$$C(t) = \frac{d-1}{d} \left[ 2\pi (v_F + D_0)t \right]^{-\frac{d}{2}} \frac{1}{d} \int d\vec{V} V \left( \frac{\beta_d m}{2\pi} \right)^{\frac{d}{2}} e^{-\frac{\beta_d m V^2}{2}}.$$
 (9.1.14)

Now we arrive at the scaling

$$C(t,d) \approx \frac{d-1}{\beta_d m d} [2\pi(\nu_F + D_0)t]^{-\frac{d}{2}} \propto \frac{1}{t^{d/2}}.$$
 (9.1.15)

This is in accord with the Corrsin assumptions on diffusive spreading of a "correlation cloud." From the dimensional point of view, the correlation function can be expressed in the form

$$C(t,d) = \langle V(0)V(t)\rangle \approx \frac{V_0^2}{n(D_0 t)^{d/2}},$$
 (9.1.16)

where it was assumed that the number of interactions  $N_I$  is proportional to the number of particles that are located in the correlation region  $W_D(t)$ ,  $N_I(t) \approx nW_D(t) \approx n(D_0t)^{d/2}$ . Here, n is the concentration of particles in this region. One may conclude that the velocity autocorrelation function has a long-time tail, due to the conservation of particle number and momentum. This result agrees with that of the more sophisticated theories as well as the results from computer simulations [182–184].

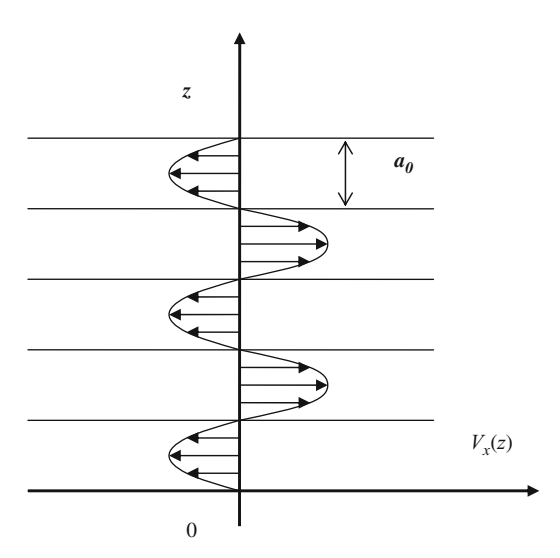
## 9.2 Superdiffusion and Return Effects

We briefly considered above a strongly anisotropic transport in the system of random shear flows basing on the scaling arguments. Note that the simplest example of the system of shear flows is given by the streamline function (see Fig. 9.2.1)

$$\Psi(x) = \Psi_0 \sin(z). \tag{9.2.1}$$

Here,  $\Psi_0$  is an arbitrary stream function amplitude. The velocity field for this streamline function is represented as

**Fig. 9.2.1** Schematic illustration of the periodic shear flow



$$\vec{u}(x) = \begin{pmatrix} \partial \Psi / \partial z \\ -\partial \Psi / \partial x \end{pmatrix} = \begin{pmatrix} \Psi_0 \cos(z) \\ 0 \end{pmatrix}. \tag{9.2.2}$$

Randomization of this sinusoidal velocity field leads to the Dreizin–Dykhne random shear flow (see Fig. 9.2.2). Here, we discuss this anomalous transport model on the basis of the Corrsin conjecture

$$C(t) = \int_{-\infty}^{\infty} \rho(\lambda, t) C_E(\lambda, t) \, d\lambda, \tag{9.2.3}$$

where the Lagrangian correlation function is expressed through the Eulerian one. For the probability density  $\rho(\lambda, t)$ , it is natural to use the Gaussian distribution. Indeed, we have seen that the molecular diffusivity in the presence of velocity shear generates random jumps of scalar particles. This permits employing Taylor's analysis when considering transport in a given velocity profile.

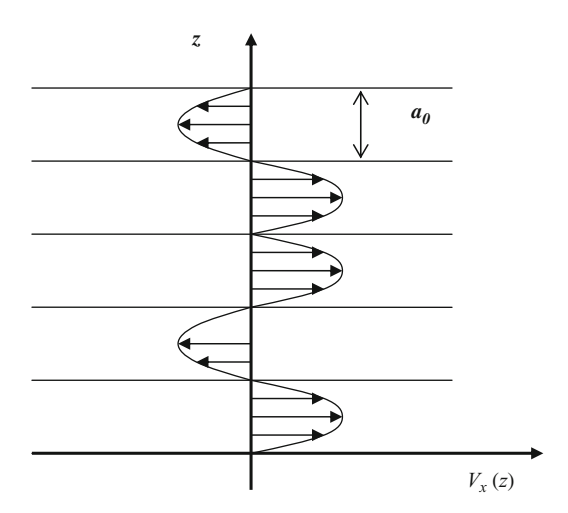
On the other hand, by taking into account the one-dimensional character of the correlation cloud spreading,  $N_I(t) \propto R_D(t) \propto (D_0 t)^{1/2}$ , one can employ the scaling for the correlation function obtained in the previous section:

$$C(t, d = 1) \approx \frac{V_0^2}{n(D_0 t)^{1/2}}.$$
 (9.2.4)

This yields the transport estimate in the form

$$\lambda_{\perp}^{2}(t) \approx \int_{0}^{t} \int_{0}^{t'} C(t'') \, dt' dt'' \propto t^{3/2}.$$
 (9.2.5)

Fig. 9.2.2 Schematic diagram of the Dreizin–Dykhne random shear-flow geometry



To explain the Dreizin and Dykhne result in the framework of the correlation approach, we consider the correlation function of shear flows in the following form:

$$C(t) = \int_{-\infty}^{\infty} \langle V_x(0)V_x(z)\rangle \frac{\exp\left(-\frac{z^2}{4D_0t}\right)}{\sqrt{4\pi D_0t}} dz.$$
 (9.2.6)

Here,  $V_x(z)$  is the velocity of the flow at the point z and the supposition was made that the probability density has the Gaussian form. Using the conjecture about the significant role of returns has become the main step in the description of anomalous diffusion, since the condition  $z \to 0$  for the probability density  $\rho(z,t)$  corresponds to the return to the initial point. After calculations, one finds the expression

$$C(t) \propto \frac{V_0^2 a_0}{\sqrt{4\pi D_0 t}} \propto \frac{1}{t^{1/2}}.$$
 (9.2.7)

Using the classical Taylor definition of the turbulent diffusivity, one defines the mean square displacement in the perpendicular direction,

$$\lambda_{\perp}^{2}(t) \approx \int_{0}^{t} \int_{0}^{t'} C(t'') \, \mathrm{d}t' dt'' \propto \frac{V_{0}^{2} a_{0}}{\sqrt{4\pi D_{0}}} t^{3/2}.$$
 (9.2.8)

Here, we are dealing with the superdiffusion regime,  $\lambda_{\perp} \propto t^{3/4}$ , and the Hurst exponent H = 3/4.

In concluding this chapter, we note that the Dreizin and Dykhne model of the anomalous transport in the system of shear flows [156] became well known after the paper [185] by Matheron and de Marsily. Their work has close relation to percolation transport in a porous media. Below we discuss the percolation concept and percolation transport in more detail.

### 9.3 Longitudinal Diffusion and Quasilinear Equations

In the random shear-flow model, the longitudinal and transverse correlation effects are separated. It would be interesting to apply here the renormalized quasilinear approach, which is fairly efficient in describing anomalous diffusion. The conventional quasilinear equations for passive scalar problem in the two-dimensional case under consideration are given by

$$\frac{\partial n_0}{\partial t} = -\langle V_X(z) \frac{\partial n_1}{\partial x} \rangle; \tag{9.3.1}$$

$$\frac{\partial n_1}{\partial t} + V_X(z) \frac{\partial n_0}{\partial x} = 0. {(9.3.2)}$$

The dependences  $n_0 = n_0(x,t)$  and  $n_1 = n_1(x,z,t)$  were used to describe the two-dimensional case. In fact, the equation for  $n_1$  is linear and hyperbolic and it keeps the Lagrangian character of correlations. This opens up the possibility of describing the omitted correlation effects by including the additional diffusive term, which is in agreement with the Corrsin diffusive renormalization.

Let us derive an equation for the passive tracer density under conditions when longitudinal correlation effects can be approximated by the longitudinal diffusive term  $D_0 \frac{\partial^2 n_1}{\partial z^2}$ . Thus, in the two-dimensional case the renormalized quasilinear equations for the system of random shear flows have the form

$$\frac{\partial n_0}{\partial t} = -\langle V_X(z) \frac{\partial n_1}{\partial x} \rangle, \tag{9.3.3}$$

$$\frac{\partial n_1}{\partial t} = D_0 \frac{\partial^2 n_1}{\partial z^2} - V_X(z) \frac{\partial n_0}{\partial x}.$$
 (9.3.4)

Here, the diffusion coefficient  $D_0$  characterizes the seed diffusion. Thus, we kept equation for the density perturbation  $n_I$  linear but passed from a hyperbolic equation of form to the parabolic equation.

Then, applying the method of Green's functions to the equation for the density perturbation  $n_1$  yields

$$n_1 = -\int dz' \int dt' \left\{ V_X(z') \frac{\partial n_0(x, t')}{\partial x} \int \frac{dk}{2\pi} e^{ik(z-z')} e^{-D_0 k^2(t-t')} \right\}.$$
 (9.3.5)

The substitution of this expression in the formula for a flux leads to the relation in terms of the memory function:

$$q_X \approx \left\langle -V_X(z) \frac{\partial n_1}{\partial x} \right\rangle = \int_0^t dt' \frac{\partial n(x, t')}{\partial x} M(t - t').$$
 (9.3.6)

Here, M(t - t') is the memory function represented as

$$M(t - t') = \int \frac{\mathrm{d}k}{2\pi} \left\{ e^{-D_0 k^2 (t - t')} \int \mathrm{d}(z - z') \langle V_X(z) V_X(z') \rangle e^{-ik(z' - z)} \right\}. \tag{9.3.7}$$

Consider the system of random flows with the Eulerian correlation function

$$C_E(z-z') = \langle V_X(z) V_X(z') \rangle. \tag{9.3.8}$$

Using the Fourier transform  $\tilde{C}_E(k)$  of the function  $C_E(z-z') = \langle V_X(z)V_X(z') \rangle$ , we can rewrite the expression for the flux  $q_x$  in the form

$$q_X \approx \int_0^t dt' \int \frac{\mathrm{d}k}{2\pi} \left\{ \tilde{C}_E(k) \mathrm{e}^{-D_0 k^2 (t-t')} \frac{\partial n_0(x,t')}{\partial x} \right\} \approx \int \frac{\mathrm{d}k}{2\pi} \left\{ \frac{\tilde{C}_E(k)}{D_0 k^2} \right\} \frac{\partial n_0(x,t)}{\partial x} \quad (9.3.9)$$

for the case of a smooth profile  $n_0(x, t)$ . The effective diffusion coefficient is given by the expression that coincides with the Howells form [186], but for an anisotropic model

$$D_{\text{eff}}(D_0) \approx \int_{-\infty}^{\infty} \frac{\tilde{C}_E(k)}{D_0 k^2} \frac{dk}{2\pi}.$$
 (9.3.10)

If this integral is finite, one has conventional diffusion with an effective diffusivity in accordance with Taylor's scaling,  $D_{\text{eff}} \propto \frac{V_0^2}{D_0}$ .

## 9.4 Random Shear Flows and Generalized Scaling

On the other hand, Matheron and de Marsily [185] showed that the anomalous transport in the longitudinal direction occurs if

$$D_{\rm eff} pprox \int\limits_{-\infty}^{\infty} \frac{\tilde{C}_E(k)}{D_0 k^2} \frac{\mathrm{d}k}{2\pi} \propto \int\limits_{-\infty}^{\infty} \mathrm{d}k \frac{\tilde{C}_E(k)}{k^2} \to \infty.$$
 (9.4.1)

This condition for the anomalous diffusion has the clear physical interpretation in terms of dimension of

$$\left[\frac{C_E}{k^2}\right] = \int_{-\infty}^{\infty} dk \ \tilde{C}_E(k) k^{-2} \propto V_0^2 a_0^2. \tag{9.4.2}$$

Here,  $V_0$  is the characteristic velocity scale and  $a_0$  is the typical distance between two sequent zeros of V(z). In the case of

$$V_0^2 < \infty$$
 and  $\int_{-\infty}^{\infty} dk \ \tilde{C}_E(k) k^{-2} < \infty$  (9.4.3)

the transport in random shear flows is similar to the transversal Taylor diffusion in channels of size  $a_0$ . The origin of anomalous diffusion is related to the fact that a scalar travels in a given direction for a very long time before changing direction.

The case of anomalous diffusion can also be interpreted in terms of scaling representation of Eulerian correlation function

$$C_E(z-z') \propto V_0^2 \left(\frac{\lambda}{z-z'}\right)^{\alpha_E}$$
 (9.4.4)

or in terms of the spectrum

$$\tilde{C}_E(k) \approx k^{\alpha_E - 1} \tag{9.4.5}$$

and the assumption about the diffusive character of the wave numbers, which make the main contribution to the transport

$$k(t) \propto \frac{1}{\lambda_{//}(t)} \propto \frac{1}{\sqrt{D_0 t}}.$$
(9.4.6)

Here,  $k \to 0$ . By taking into account the simplified version of the Corrsin conjecture, we arrive at

$$\lambda_{\perp}^{2}(t) \approx \int_{0}^{t} \int_{0}^{t'} C(t'') \, dt' \, dt'' \propto C_{E}(\lambda_{//}(t)) t^{2}.$$
 (9.4.7)

Then simple calculations yield a scaling:

$$\lambda_{\perp}^{2}(t) \approx D_{\text{eff}} t \approx V_{0}^{2} \left(\frac{\lambda}{\sqrt{D_{0}t}}\right)^{\alpha_{E}} t^{2} \propto \frac{t^{2}}{\lambda_{//}^{\alpha_{E}}(t)} \propto t^{2-\frac{\alpha_{E}}{2}}, \tag{9.4.8}$$

which relates the Hurst exponent

$$H(\alpha_E) = 1 - \frac{\alpha_E}{4} \tag{9.4.9}$$

describing anomalous transport in the transverse direction to the exponent  $\alpha_E$  characterizing the spatial correlation properties of a system of random shear flows [187, 188]. Note that for incompressible flows subdiffusive regimes are impossible, and hence,  $0 \le \alpha_E \le 2$ . The special case  $\alpha_E - 1 = 0$  corresponds to a white spectrum

$$\tilde{C}(k) \propto k^{\alpha_E - 1} = k^0 \tag{9.4.10}$$

and recovers the anomalous diffusion found previously by Dreizin–Dykhne with H = 3/4. For  $0 \le \alpha_E \le 2$ , one has superdiffusion, while for  $\alpha_E > 2$  we arrive to the conventional diffusive behavior.

#### 9.5 Isotropization and Manhattan flow

Besides the simplified model of random shear flow, more interesting is the understanding of the anomalous diffusion in incompressible velocity fields. Avellaneda and others [187] obtained a very important and general result about the asymptotic diffusion in an incompressible velocity field  $\vec{u}(\vec{r})$ . If the molecular diffusivity  $D_0$  is nonzero and the infrared contribution to the velocity field is weak enough,

$$\int d\vec{k} \frac{\left\langle \left| \tilde{u} \left( \vec{k} \right) \right|^2 \right\rangle}{k^2} < \infty. \tag{9.5.1}$$

Then one has the standard diffusion with the finite effective diffusion coefficient  $D_{\rm eff}$ .

On the other hand, there are several ways to generalize the model of anomalous transport in random shear flows [189, 190]. Here, we consider a superdiffusion regime for the "Manhattan grid" flow. Thus, from the formal standpoint, for the incompressible case the velocity field is given by

$$V_x(x,z) = -\frac{\partial \Psi(x,z)}{\partial z},$$
(9.5.2)

$$V_z(x,z) = -\frac{\partial \Psi(x,z)}{\partial x}.$$
 (9.5.3)

We construct a two-dimensional random steady flow (quenched disorder) by the superposition of two random stream functions  $\Psi^x(z)$ ,  $\Psi^z(x)$ 

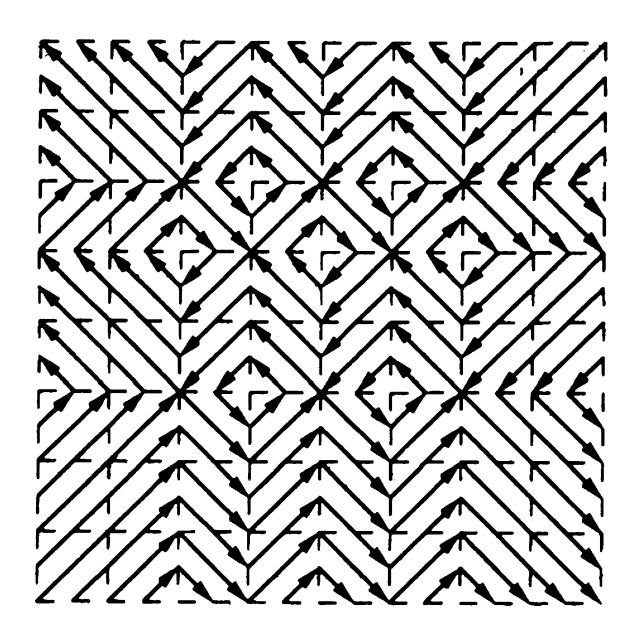
$$\Psi(x, z) = \Psi^{x}(z) + \Psi^{z}(x). \tag{9.5.4}$$

A flow with the stream function  $\Psi(x,z)$  is then a two-dimensional generalization of the random shear flows model (see Fig. 9.5.1). Note, in the case when  $\Psi^x(z)$  and  $\Psi^z(x)$  are regular sinusoidal functions such a superposition gives a periodical two-dimensional system of swirling eddies (cell system).

For the Dreizin-Dykhne flow, we have obtained the scaling for the effective diffusivity in the transverse direction in the form

$$D_{\rm eff}(t) \propto V_0^2 \left(\frac{a_0}{\sqrt{D_0}}\right) t^{1/2} \propto \sqrt{t}. \tag{9.5.5}$$

**Fig. 9.5.1** A typical plot of a random Manhattan grid flow



In this two-dimensional case, we are faced with a quite different scenario. It is believed that there exists a common effective diffusivity for both x-direction and z-direction  $D_{\rm eff}(t)=D_0$ ,

$$D_{\rm eff}(t) \propto V_0^2 \left(\frac{a_0}{\sqrt{D_{\rm eff}}}\right) t^{1/2}.$$
 (9.5.6)

After calculations, one obtains a new scaling for the effective diffusivity for the "Manhattan grid" flow,

$$D_{\text{eff}}(t) \propto V_0 a_0 \left(\frac{V_0}{a_0}t\right)^{1/3} \propto t^{1/3}.$$
 (9.5.7)

Using the classical Taylor definition of the turbulent diffusivity, one defines the mean square displacement,

$$R(t) \propto D_{eff}(t)t \propto a_0 \left(\frac{V_0}{a_0}t\right)^{2/3} \propto t^{2/3}.$$
 (9.5.8)

Here, the Hurst exponent is denoted as H = 2/3. New scaling for the correlation function takes the following form:

$$C(t) \propto \frac{D_{\text{eff}}(t)}{t} \propto V_0^2 \left(\frac{a_0}{V_0 t}\right)^{2/3} \propto \frac{1}{t^{2/3}}.$$
 (9.5.9)

This scaling could be interpreted in terms of the number of interactions  $N_I(t)$ 

$$C(t) = \langle V(0)V(t)\rangle \propto V_0 \frac{V_0}{N_I(t)}, \tag{9.5.10}$$

where

$$N_I(t) \propto \left(\frac{V_0 t}{a_0}\right)^H \propto t^H.$$
 (9.5.11)

The number of interactions  $N_I(t)$  could be represented as the number of visited sites. Here, it is natural to use the Alexander–Orbach conjecture [31]  $N_I(t) \propto t^{2/3}$ , for  $2 \le d \le 6$ . Indeed, the value  $N_I$  corresponds to the number of "layers" intersected by the test particle.

On the other hand, it is possible to generalize the renormalization applied above,  $D_0 \to D_{\rm eff}(t)$ , to a multiscale random flow. For this purpose, we consider the relation found in the previous section

$$\lambda_{\perp}^{2}(t) \approx D_{\text{eff}}t \approx V_{0}^{2} \left(\frac{\lambda}{\sqrt{D_{0}t}}\right)^{\alpha_{E}} t^{2},$$
 (9.5.12)

which have to be modified to

$$D_{\rm eff}t \approx V_0^2 \left(\frac{\lambda}{\sqrt{D_{\rm eff}}t}\right)^{\alpha_E} t^2. \tag{9.5.13}$$

Here,  $0 \le \alpha_E \le 2$ . After calculations, one obtains the relation for the Hurst exponent in the following form:

$$H(\alpha_E) = \frac{2}{2 + \alpha_E}.\tag{9.5.14}$$

When  $\alpha_E = 1$ , one obtains the Hurst exponent H = 2/3, which corresponds to the Manhattan grid flow.

This estimate looks fairly rough, but this scaling coincides with the rigorous result obtained by the sophisticated renorm-group technique [191, 192]. Now we can make one more step further. On the basis of scaling obtained, it is possible to relate the Eulerian and the Lagrangian correlation exponents. The Hurst exponent in terms of the Lagrangian correlation exponent is given by the formula

$$R^2 \propto D_{\text{eff}} t \propto t \int C(t) dt \propto t^{2-\alpha_C} \quad H(\alpha_C) = 1 - \alpha_C/2.$$
 (9.5.15)

Here,  $0 \le \alpha_C \le 2$ . By comparing the relations for  $H(\alpha_C)$  and  $H(\alpha_E)$ , one easily finds the relationship

$$\alpha_C(\alpha_E) = \frac{2\alpha_E}{2 + \alpha_E}.\tag{9.5.16}$$

In the region of applicability  $\alpha_C \leq \alpha_E$ . Obviously, this is an approximation only, but such relationship could be useful for the qualitative analysis of anomalous transport problem. Note that two statistical ensembles are involved in all these random flow models, namely the distribution of velocities and the different walks for a given random velocity distribution. The effective transport depends on both, and we must take into account this fact in discussing such nontrivial correlation effects (see Fig. 9.5.2).

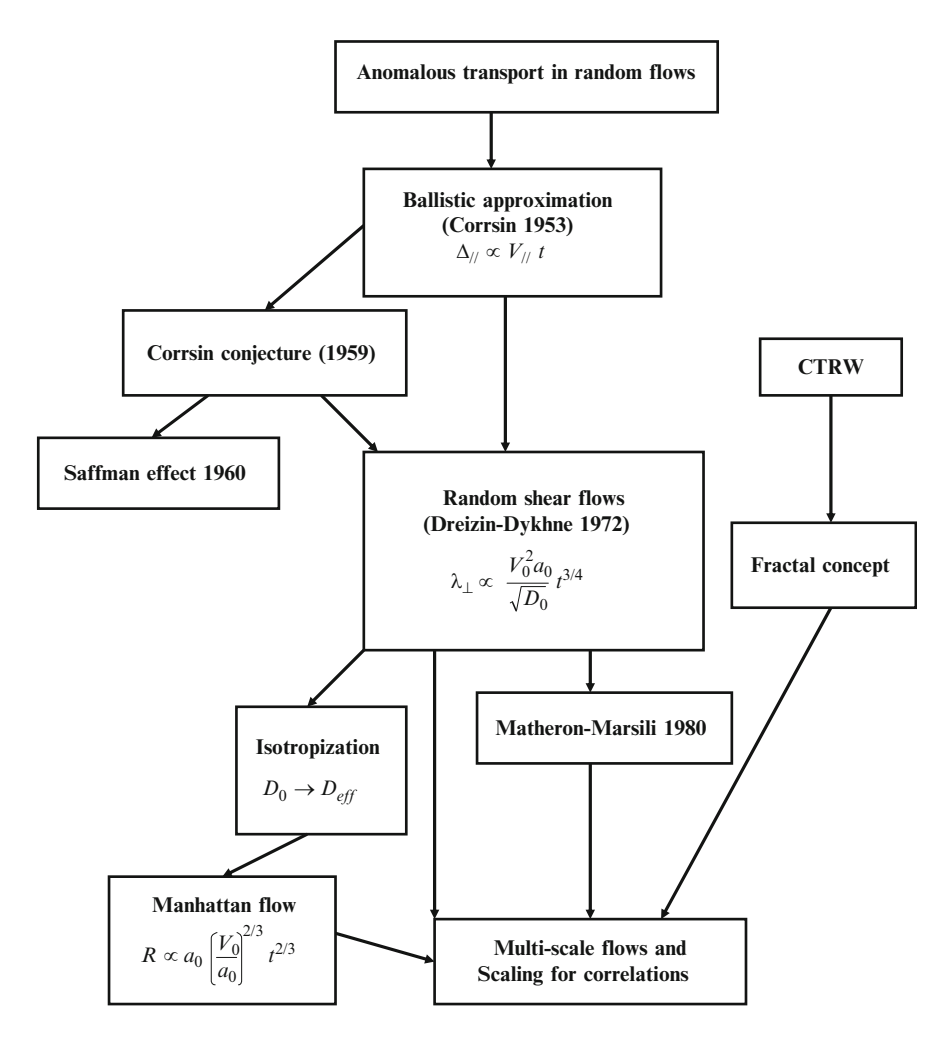


Fig. 9.5.2 Anomalous transport in random flows

#### 9.6 Diffusion in Power-Law Shear Flows

In this section, in contrast to the random shear-flow model, we investigate the motion of a tracer particle moving in a steady velocity field (see Fig. 9.6.1)

$$\vec{V}(x,z) = V_0|z|^{\beta_R} \text{sgn}(z)\hat{x}.$$
 (9.6.1)

This can be viewed as the average over many configurations of the random walk in shear-flow problem. For power-law shear flow, the most longitudinally stretched walk must have each transverse step in the same direction, in order that the walk has the largest possible velocity at each time step. In a typical realization of such a flow, the longitudinal velocity  $V_x(z)$  at transverse coordinate z increases as  $z^{1/2}$ , a feature that leads to faster-than-ballistic motion of a tracer particle. The transverse displacement has a diffusive character,

$$z(t) \propto \sqrt{D_0 t} \tag{9.6.2}$$

Here,  $D_0$  is the seed diffusion coefficient. On the other hand, the root mean square longitudinal displacement R may be roughly estimated through the longitudinal velocity at time t [193]

$$V_x(z(t)) \propto V_0(D_0 t)^{\frac{\beta_R}{2}}.$$
 (9.6.3)

Then one obtains the relation in the form

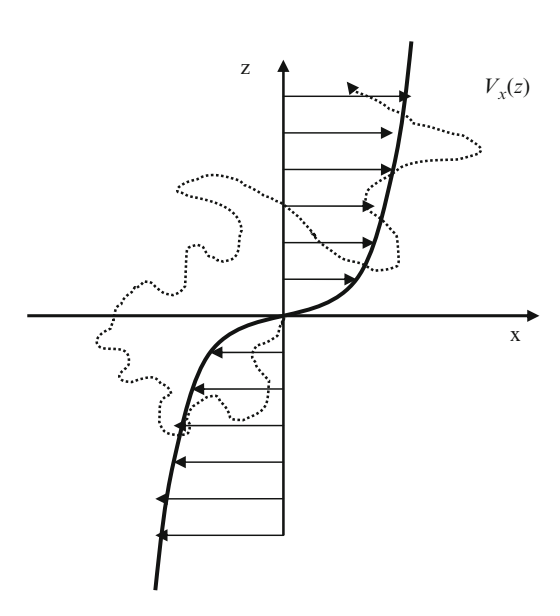


**Fig. 9.6.1** Schematic illustration of a power-law shear flow

$$R(t) \propto V_0 t(D_0 t)^{\frac{\beta_R}{2}},$$
 (9.6.4)

where the Hurst exponent is given by the formula

$$H(\beta_R) = 1 + \frac{\beta_R}{2}. (9.6.5)$$

The increase in longitudinal velocity with timescale is the underlying mechanism that leads to R(t) growing faster than linearly with time. It is interesting to notice that for  $\beta_R = 0$ , x is independent of the diffusion coefficient  $D_0$ . This is the case of "split flow" (see Fig. 9.6.2)

For the power-law shear flow  $\vec{V}(x,z) = V_0 |z|^{\beta_R} \mathrm{sgn}(z) \hat{x}$ , the probability distribution of a Brownian particle can be described by the advection–diffusion equation

$$\frac{\partial \rho(x,z,t)}{\partial t} + \operatorname{sgn}(z)|z|^{\beta_R} V_0 \frac{\partial \rho(x,z,t)}{\partial x} = D_0 \frac{\partial^2 \rho(x,z,t)}{\partial z^2}.$$
 (9.6.6)

Here, the contribution of diffusion in the longitudinal direction has been neglected. It would be interesting to determine the distribution of longitudinal displacements,

$$\rho_L(x,t) \equiv \int \rho(x,z,t) dz. \tag{9.6.7}$$

The initial condition is given by  $\rho(\vec{r}, t=0) = \delta(0)$ . For describing the probability distribution, it will be convenient to introduce the scaled longitudinal and transverse displacements,

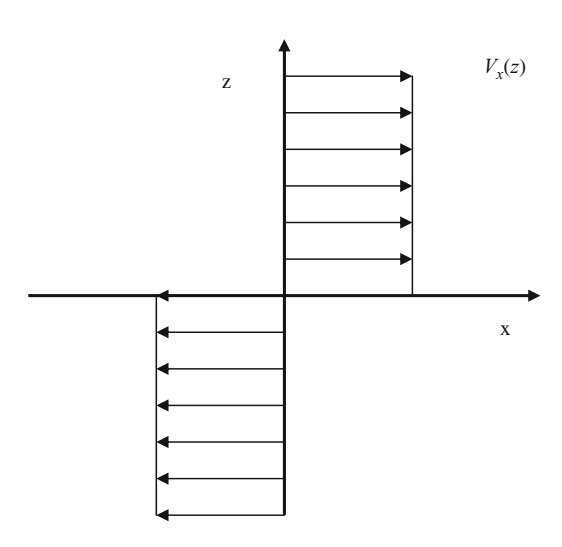


Fig. 9.6.2 A typical plot of velocity profile of a split flow

$$\xi(x,t) = \frac{x}{(V_0 t)(D_0 t)^{\beta_R/2}}, \quad \eta(z,t) = \frac{z}{\sqrt{D_0 t}}.$$
 (9.6.8)

In terms of these variables, we may write the probability distribution in the scaling form as follows:

$$f(\xi, \eta) \equiv V_0 t(D_0 t)^{\frac{1+\beta_R}{2}} \rho(x, z, t).$$
 (9.6.9)

The longitudinal probability distribution is give by the formula

$$f_L(\xi) \equiv \int f(\xi, \eta) d\eta.$$
 (9.6.10)

We expect that this function has the asymptotic behaviors  $f_L(\xi) \to {\rm const}$  as  $\xi \to 0$  and

$$f_L(\xi) \propto \frac{1}{e^{\xi^{\delta_R}}} \quad \text{as} \quad \xi \to 0.$$
 (9.6.11)

Now we are able to find the value of the shape exponent  $\delta_R$  by constructing an estimate for the probability of finding the extreme walks that contribute to the tail of the distribution [193]. This implies that the probability of finding a stretched walk decays as a pure exponential in t,  $e^{-\alpha t}$ . On the other hand, a stretched walk has a longitudinal displacement, which scales as

$$R(t) \propto \int_{0}^{t} z^{\beta_R} dz \propto t^{1+\beta_R}.$$
 (9.6.12)

This maximal value corresponds to a scaled displacement  $\xi(t) \propto t^{\beta_R/2}$ , and hence, the distribution function is given by

$$f_L(\xi) \propto \exp\left(-t^{\frac{\delta_R \beta_R}{2}}\right).$$
 (9.6.13)

Since we have supposed that this function decays exponentially in *t*, we find the shape exponent as

$$\delta_R(\beta_R) = \frac{2}{\beta_R}. (9.6.14)$$

Using the relation for the Hurst exponent

$$H(\beta_R) = 1 + \frac{\beta_R}{2},$$
 (9.6.15)

the expression for  $\delta_R$  can be written as

$$\delta_R(H) = \frac{1}{1 - H}. (9.6.16)$$

This is of the same form as the phenomenological Fisher relation [194] between the shape and size exponents for the usual situation where H < 1. We discuss the Fisher relation in next section.

#### 9.7 The Fisher Relation

Fractional exponents need not only appear in algebraic tails of distributions. An important case involves exponential functions. Thus, in the case when there exists a single special scale the configuration-averaged probability distribution of displacements decays at large distances as

$$P(x,t) \propto \exp\left(-\left(\frac{x}{t^H}\right)^{\delta_R}\right).$$
 (9.7.1)

Here,  $\delta_R$  is the large-distance shape exponent, and H is the transport Hurst exponent.

In the case of Gaussian distribution, one has the formula

$$P(x,t) \propto \exp\left(-\left(\frac{x}{t^{1/2}}\right)^2\right).$$
 (9.7.2)

Here, H = 1/2 and  $\delta_R = 2$ . For the self-avoiding random walks H = 3/5 and  $\delta_R = 5/2$ . Indeed, for many random-walk processes, the size and shape exponents, H and  $\delta_R$ , respectively, satisfy [194]

$$\delta_R = \frac{1}{1 - H} \tag{9.7.3}$$

Here, we consider the range 0 < H < 1. This relation can be deduced simply from the observation that walks, which are completely stretched, contribute to the tail of the probability distribution. Thus, the probability of finding a stretched walk, where x scales as t, is

$$P(x \propto t, t) \propto \exp\left(-t^{(1-H)\delta_R}\right).$$
 (9.7.4)

Further Reading 161

On the other hand, a completely stretched walk is constructed by choosing only one direction at each step of a walk, and clearly this leads to a probability at time t, which decays as

$$P(t) \propto \exp(-\text{const} \cdot t).$$
 (9.7.5)

Equating these two forms yields the famous Fisher relation,  $\delta_R = \frac{1}{1-H}$ .

The probability distribution of displacements in two-dimensional random flow (Manhattan grid flow) satisfies this Fisher hyperscaling with the exponents H=2/3 and  $\delta_R=3$ . However, the Fisher argument appears to work for isotropic random velocities but fails for layered random velocities. Indeed, this relation fails in the case of the Dreizin–Dykhne model, where the anisotropic nature of the problem plays a crucial role in determining the tail of the distribution function. In their case, the shape exponent is much smaller than the value that is expected on the basis of the Fisher scaling because the value of the Hurst exponent H=3/4 would imply  $\delta_R=4$ . In this model, hyperscaling leads to anomalously slow large-distance decay of the probability distribution, whereas the authors of Ref. [185] found  $\delta_R=4/3$ .

We can conclude that the investigation of complex random walks provides a foundation for understanding a very wide range of transport phenomena. In particular, they play an important role in turbulent transport, kinetics, polymer physics, biology, etc. Random walks can be generated on simple lattices or in continuous spaces. Thus, the well-known example is the nearest neighbor walk on a square lattice, where the random walk starts on a site that can be placed at the origin. Return of particles to the initial point is one of the important and nontrivial properties of random walk models. There are many cases where such correlation effects are dominated. For instance, this related to random walks on random substrates, including fractal substrates, as models for transport phenomena in disordered systems. Below, we extensively investigate random walks on fractal and percolation clusters in connection with turbulent transport in random two-dimensional flows, where an extract enumeration approach is valuable.

## **Further Reading**

## Random Shear Flows and Transport

- G.P. Bouchaud, A. Georges, Phys. Rep. **195**, 132–292 (1990)
- J. Cardy et al., *Non-Equilibrium Mechanics and Turbulence* (Cambridge University Press, Cambridge, 2008)
- P. Castiglione et al., *Chaos and Coarse Graining in Statistical Mechanics* (Cambridge University Press, Cambridge, 2008)

- W.C. Conner, J. Fraisserd, *Fluid Transport in Nanoporous Materials* (Springer, Berlin, 2006)
- A. Crisanti, M. Falcioni, A. Vulpiani, Rivista Del Nuovo Cimento 14, 1–80 (1991)
- J.W. Haus, K.W. Kehr, Phys. Rep. 150, 263 (1987)
- M.B. Isichenko, Rev. Mod. Phys. 64, 961 (1992)
- R. Klages, G. Radons, I. Sokolov (eds.), *Anomalous Transport, Foundations and Applications* (Wiley, New York, 2008)
- A. Majda, P. Kramer, Phys. Rep. **314**, 237–574 (1999)
- R.M. Mazo, *Brownian Motion*, *Fluctuations*, *Dynamics and Applications* (Clarendon Press, Oxford, 2002)
- A. Scott, *Nonlinear Science* (Oxford University Press, Oxford, 2003)
- D. Sornette, Critical Phenomena in Natural Sciences (Springer, Berlin, 2006)
- G.H. Weiss, Aspects and Applications of the Random Walk (Elsevier, Amsterdam, 1994)

# Part V Structures and Nonlocal Effects

## **Chapter 10 Transport and Complex Structures**

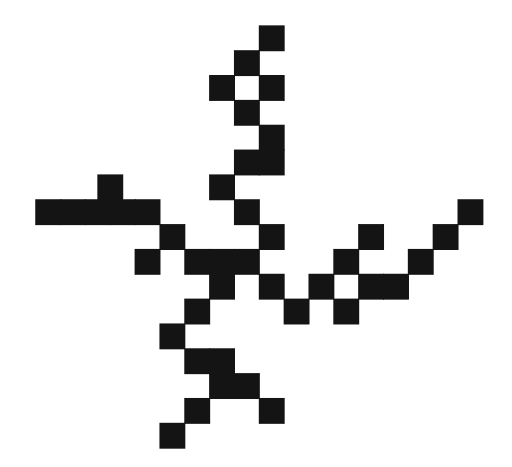
#### 10.1 Bond Percolation Problem

Percolation problems are a prime example where fractal geometries play an important role in determining the macroscopic properties of a system [195–199]. On the other hand, percolation is a powerful tool for the study of transport properties of complex systems, including such problems as electrical conductivity, the flow of liquids through porous materials, and anomalous diffusion in chaotic flows. In principle, the percolation approach describes statistically complex systems and does not relate to classical dynamical laws. That is why the percolation method has the similar status as the random walk approach.

To illustrate the basic definitions of the percolation theory, let us consider a square grid. The cells of the grid are occupied with a probability p and empty with the probability 1-p. Neighboring occupied sites (black in Fig. 10.1.1) with a common edge form a connected cluster. If  $p \ll 1$ , the clusters are small and isolated. When p increases from 0 to 1, so does the mass of the largest clusters. There is a value of  $0 , at which a unique cluster appears that connects opposite sides of the grid. When the size of the grid <math>L_0 \to \infty$ , this percolating cluster is infinite;  $p_c$ , at which the infinite cluster appears, is called the percolation threshold or critical probability. Numerical calculations performed on finite grids allow one to conclude that  $p_c \approx 0.59275$  for clusters formed by neighboring sites on a 2D square lattice; they also show that the clusters are fractal distributions of occupied cells.

As p approaches  $p_c$ , the finite clusters increase in size; a, being the radius of clusters that contribute most to this increase, diverges to infinity at  $p_c$ . When a diverges, there is no characteristic length to scale the length-dependent physical properties of the system. As fractal structures, the system looks the same at different magnifications. The properties of the system become nonsensitive to many local details, such as small changes in interactions of particles, lattice structure, and so on, which do not influence the large-scale behavior. This feature results in the universality of the critical exponents that describe diverging parameters near  $p_c$ .

**Fig. 10.1.1** Schematic picture of a percolation cluster



These universal exponents depend on the model under consideration and the dimensionality of the system but not on the details of the local structure.

Near the transition point  $p = p_c$ , geometrical percolation can be described in the same terms as thermal second-order phase transition, say, a transition from a parametric state at high temperatures and a ferromagnetic state at low temperatures. The analogue of temperature T is the occupation probability p of one site; the analogue of the order parameter, say, the magnetization  $M_c(T)$ , is the probability  $P_{\infty}(p)$  that a randomly chosen site belongs to an infinite cluster

$$p - p_c \leftrightarrow T_c - T, \tag{10.1.1}$$

$$P_{\infty}(p) \leftrightarrow M_c(T).$$
 (10.1.2)

In magnetic materials, the magnetization vanishes at the critical temperature  $T_c$  according to the power law [200]

$$M_c(T) \propto (T_c - T)^{\beta} \tag{10.1.3}$$

with the critical exponent  $\beta$ . Immediately above the percolation threshold,

$$0$$

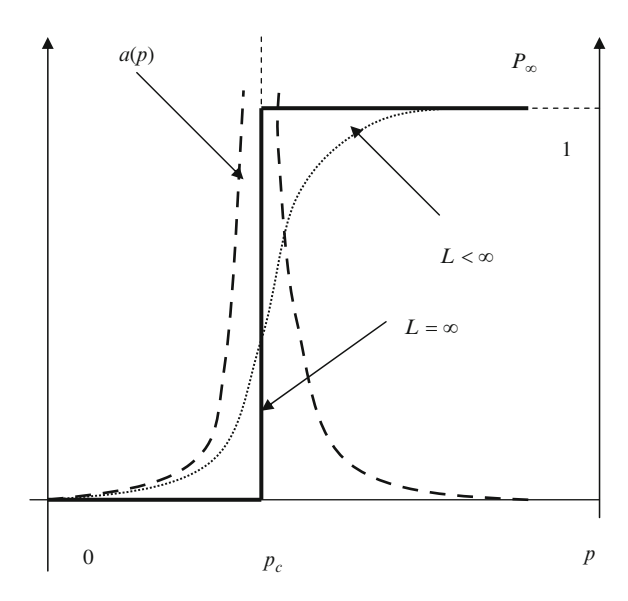
the order parameter  $P_{\infty}(p)$  behaves in a similar way (see Fig. 10.1.2):

$$P_{\infty}(\varepsilon) \propto (p - p_c)^{\beta} = |\varepsilon|^{\beta}.$$
 (10.1.5)

Of course,  $P_{\infty}(p < p_c) = 0$ , because only finite clusters exist at  $p < p_c$ .

The correlation length a also diverges when p approaches (both from below and from above) (see Fig. 10.1.2), with a new critical exponent v:

Fig. 10.1.2 A typical plot of characteristic correlation length and the probability of finding a site belonging to an infinite percolation cluster



$$a(\varepsilon) \propto \frac{1}{\left|p - p_c\right|^{\nu}} = \frac{1}{\left|\varepsilon\right|^{\nu}},$$
 (10.1.6)

where  $\varepsilon$  is the small percolation parameter characterizing nearness of the system to the percolation threshold. Such a behavior resembles the divergence of the correlation length near critical points for thermal phase transitions. Both critical exponents  $\beta$  and  $\nu$  are universal, because they depend on the dimensions of the system  $\beta = \beta(d)$  and  $\nu = \nu(d)$  but not on the local details. The aim of the percolation theory is to calculate these exponents from the first principles and to find relationships among them. Below we illustrate relationships between the critical exponents and the fractal characteristics of the percolation networks; the techniques of calculating the values of critical exponents are discussed in [196–202].

## 10.2 Fractal Dimensionality and Percolation

At percolation threshold  $p_c$ , the infinite percolating cluster contains holes of all possible sizes because the correlation length a diverges. Above  $p_c$ , the length a is finite and corresponds to the linear size of the largest "holes" left by the percolating cluster. It means that at  $p > p_c$ , the percolation cluster is self-similar only on length scales  $\lambda < a$  and homogeneous at larger scales  $\lambda > a$ . At  $\lambda < a$  and  $\lambda > a$ , the mass of the infinite cluster scales differently:

$$M_c(\lambda) \propto \lambda^{d_{\rm F}}, \quad \lambda < a,$$
 (10.2.1)

$$M_c(\lambda) \propto P_{\infty} \lambda^d, \quad \lambda > a.$$
 (10.2.2)

Here, the cluster density is given by the formula

$$\rho(\lambda) = \frac{M_c}{\lambda^d}.\tag{10.2.3}$$

At  $\lambda = a$ , the two last expressions should recover the same mass:

$$P_{\infty}\lambda^d \approx (p - p_c)^{\beta \xi d} = a^{d_{\rm F}}.$$
 (10.2.4)

But according to the definition,  $a \propto |p - p_c|^{-\nu}$ . Hence,

$$d_{\rm F} = d - \frac{\beta}{v},\tag{10.2.5}$$

which relates the fractal dimension of the percolation cluster to the exponents  $\beta$  and  $\nu$ . The expression for the density is given by

$$\rho(a) \propto a^{-\beta/\nu} = a^{d_{\rm F}-d}.$$
 (10.2.6)

The exponents  $\beta$  and  $\nu$  are the universal constants in the sense discussed above; therefore,  $d_F$  is universal as well. For two-dimensional grids with  $\beta=5/36$  and  $\nu=4/3$ , one gets  $d_F=91/48\approx 1.8958$ . In three-dimensional case, the key percolation exponents are  $\nu=0.875$ ,  $\beta=0.417$ . There has been considerable progress over the last decades in the determination of the geometrical properties of two-dimensional random percolation cluster for different lattice models [103, 196]. Thus, scaling exponent for the hull fractal dimensions  $D_h=1+1/\nu=7/4$  is known exactly, so is the exponent  $\nu=4/3$  characterizing the divergence of correlation length near the percolation threshold. The values of these scaling exponents are confirmed by numerous computer simulations [203, 204]. The scaling exponents  $\nu$  and  $\nu$ 0 characterize the geometrical properties of percolation clusters and allow one to determine other exponents, which arise in the theory of critical phenomena through the hyperscaling relations [204, 205]. In the subsequent consideration, we use these results to analyze two-dimensional random flows.

The percolation problem is very closely connected with the theory of phase transition in statistical physics. It was shown that the problem of the lattice bond percolation is equivalent to the one-state Potts model. Later it was realized that the one-state Potts model at the tricritical point (which is a diluted model with percolation vacancies) is geometrically equivalent to the critical Ising model [103]. At these points in the phase diagrams, the three coexisting phases become identical. At the tricritical points, the mean field theory based on the Landau representation for the free energy becomes valid.

#### 10.3 Finite Size Scaling

At the first stage of our analysis, we have restricted our attention to systems of infinite size. Estimates of percolation effects in finite systems can be obtained on the basis of phenomenological arguments, which were first suggested by Fisher as early as in 1971 [206]. Indeed, scaling laws for finite systems are important for practical application as well as for simulations.

Let us consider some property  $z(L_0, \varepsilon)$  of a system of finite size  $L_0$ . We assume that this quantity for infinite systems is proportional to  $\varepsilon^{\vartheta}$ ,

$$z(\varepsilon) \propto \varepsilon^{\vartheta}$$
. (10.3.1)

Here,  $\vartheta$  is an exponent. In the framework of the scaling concept, the quantity  $z(L_0, \varepsilon)$  should be scaled only by the correlation length and that is why we find

$$z(L_0, \varepsilon) \propto a^{-\sigma} Z\left(\frac{L_0}{a}\right),$$
 (10.3.2)

where  $\vartheta$  is an exponent. The basic idea is that for  $L_0 > a(\varepsilon)$  one can break the system into  $\left(\frac{L_0}{a}\right)^{d_F}$  blocks of linear size a. Within each of these, the behavior is self-similar [207–209]. For infinite system, where  $L_0 \to \infty$ , the value under consideration does not depend on  $L_0$  that leads to the condition

$$Z\left(\frac{L_0}{a}\right) = Z(y)|_{y\to\infty} = \text{const.}$$
 (10.3.3)

Thus, we obtain the relation for the quantity  $z(L_0, \varepsilon)$  in the following form:

$$z(L_0, \varepsilon)|_{L_0 \to \infty} \propto a(\varepsilon)^{\sigma} \propto \frac{1}{\varepsilon^{\nu \sigma}}.$$
 (10.3.4)

By comparing this result with the initial percolation representation, one finds the relationship among the percolation exponents

$$\sigma(\vartheta, v) = \frac{\vartheta}{v}.\tag{10.3.5}$$

The final result is the following:

$$z(L_0, \varepsilon) \propto a^{-\frac{\vartheta}{2}} Z\left(\frac{L_0}{a}\right).$$
 (10.3.6)

When the correlation length is much greater than the system size, the value  $z(L_0, \varepsilon)$  does not depend on a. This leads to the scaling

$$z(L_0, \varepsilon) \propto {L_0}^{-\vartheta/\nu}, \quad a \gg L_0.$$
 (10.3.7)

On the other hand, this relation is valid when  $\varepsilon \to 0$  for any finite large size of system under consideration. The exponent  $\vartheta$  can be found on the basis of simulations or experiments because the correlation exponent v is usually known.

#### 10.4 Comb Structures and Percolation Transport

Most percolation problems cannot be solved analytically, and numerical simulation is indispensable tool in this field. However, there exists simple and effective model of comb structure (see Fig. 10.4.1) to investigate transport on an infinite cluster at the threshold percolation. Diffusion processes on such structures have been studied intensively [210–212].

Comb structures comprise of a backbone and orthogonal close-ended teeth. In this setting, the backbone represents the connected pathways, which span the cluster, while the orthogonal close-ended teeth represent the dead-end pathways, which emanate from backbone. In the electrical analogy problem, the backbone represents the conducting pathway and the teeth represent the dangling bonds along which current does not flow. Here, transport properties of 'regular' comb structures having teeth of infinite length are identified in terms of scaling. In this model, there are no loops to form connections between different dangling bonds, and the dangling bonds are uniformly spaced along the backbone.

Elementary estimates lead to a simple scaling for transport along this comb structure

$$\langle \Delta x^2 \rangle \propto D_{xx} \langle T \rangle,$$
 (10.4.1)

where  $D_{xx}$  is diffusion coefficient along the axis x and  $\langle T \rangle$  is the mean effective time of longitudinal movement. Let  $\langle T \rangle$  be

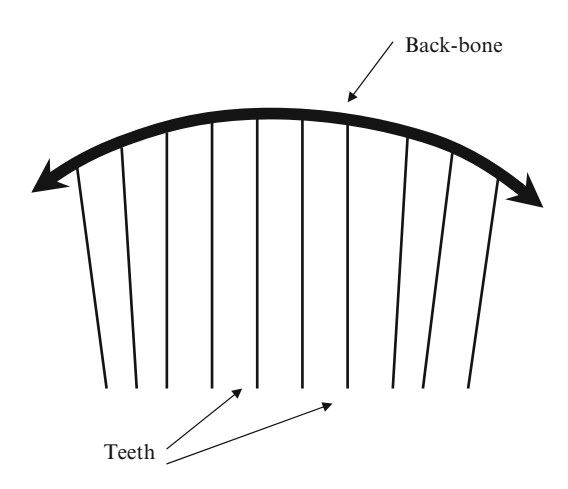
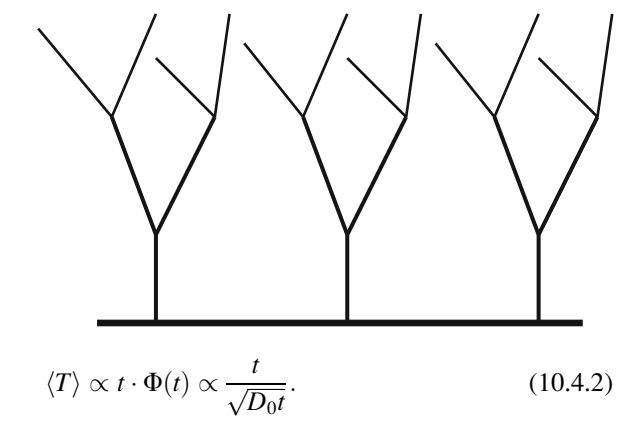


Fig. 10.4.1 Schematic picture of a comb structure

Fig. 10.4.2 Schematic diagram of complex comb structure



Here, we introduce the return probability  $\Phi_{\infty}(t)$ , which in the one-dimensional case is given by

$$\Phi_{\infty}(t) \approx \rho(0, t) \Delta \approx \frac{\Delta}{\sqrt{4\pi D_0 t}},$$
(10.4.3)

where  $\rho$  is the Gaussian distribution function,  $D_0$  is the seed diffusion coefficient, and  $\Delta$  is the distance between teeth.

Now we obtain an anomalous regime of diffusion (subdiffusion) with the Hurst exponent H=1/4

$$\left\langle \Delta x^2 \right\rangle \propto \frac{D_{xx}}{\sqrt{D_0}} \sqrt{t},$$
 (10.4.4)

or for  $D_{xx} = D_0$ , we can rewrite

$$\langle \Delta x^2 \rangle \propto \sqrt{D_0 t}.$$
 (10.4.5)

However, in this approach the percolation character of correlation effects was lost and we did not use the correlation length  $a(\varepsilon)$ , which is the main magnitude characterizing spatial scales of the system near the percolation threshold. Models of anomalous transport on comb structures are widely applied due to the fairly universal kind of topology. More complex comb structures (see Fig. 10.4.2) could be also investigated by an analytical way [210–212].

## 10.5 Hilly Landscape and Percolation

The mathematical analysis of continuum percolation is quite different from lattice analogue. In a discrete problem, the sites  $\vec{r_j}$  (or bonds) in a lattice are occupied with the probability p and nearest-neighbor sites are regarded as linked. There exists a

unique percolation threshold  $p_c$  above which,  $p > p_c$ , occupied sites belong to an infinite percolation cluster. In the work presented here, we consider percolation on a continuum. In a continuum problem,  $\vec{r}_j$  is replaced by the continuum variable  $\vec{r}$  and we study the isolines (in two dimensions) or isosurfaces (in three dimensions) of a smooth potential  $\vec{V}(\vec{r})$ .

The basic problem of continuum percolation theory can be formulated very simply. Given a continuous potential  $\vec{V}(\vec{r})$ , then for each h there may or may not exist an infinite connected set with  $\vec{V}(\vec{r}) < h$ . If such a set does not exist for a range of  $h < h_c$ , and does exist for a range of  $h > h_c$ , then  $h_c$  is known as the percolation threshold.

In 2D, there exists a better visualizable representation of this problem. One can consider a topographical analogy where areas with  $\vec{V}(x,y) < h$  are the valleys filled with water to a given level h in a mountain range  $\vec{V}(x,y) > h$  (see Fig. 10.5.1). An interconnected ocean of water of infinite extent exists if the level of water h is greater than critical percolation threshold  $h_c$ . The case of incompressibility implies that the velocity field is related to the stream function  $\Psi$ 

$$V_x(x, y, t) = -\frac{\partial \Psi(x, y, t)}{\partial y}, \quad V_y(x, y, t) = \frac{\partial \Psi(x, y, t)}{\partial x}$$
 (10.5.1)

Here,  $\Psi(x,y,t)$  is the Hamiltonian (streamline) function. If the potential  $\vec{V}(\vec{r})$  is a random function, in a sense that coordinate

$$C(\vec{r} - \vec{r}') = \langle \vec{V}(\vec{r})\vec{V}(\vec{r}')\rangle \tag{10.5.2}$$

is a sufficiently fast decay function, then both discrete and continuum problems are equivalent, and the contours of constant  $\vec{V}(\vec{r}) = h$  can be considered as the

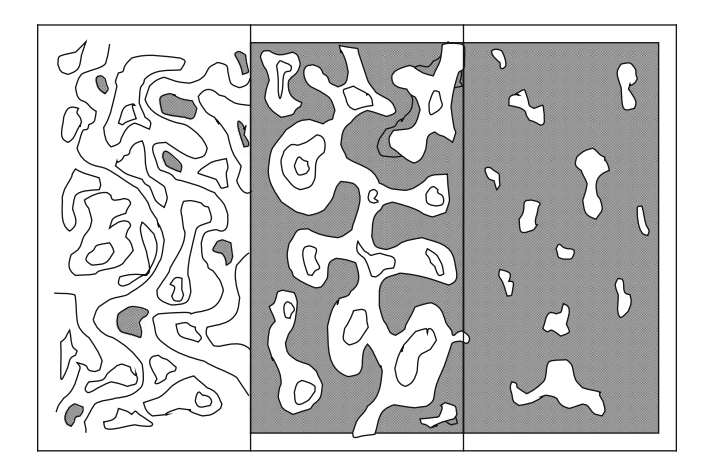


Fig. 10.5.1 Schematic picture of contour lines in continuum percolation model

perimeters of percolation clusters. One is typically interested in locating percolation threshold and studying scaling behavior near the threshold.

We are going to use the percolation geometrical arguments to investigate the appearance of anomalous transport in two-dimensional chaotic flows. The percolation approach looks very attractive because it gives a simple and, at the same time, universal model related to both long-range correlation effects and complex topology. Kadomtsev and Pogutse [213] reduce the increasing of turbulent diffusion in two-dimensional chaotic flows to the problem of random contours, which are well described in the framework of percolation approach. Thus, it was supposed that the main contribution to the effective transport is related to the existence of the percolation streamline near the threshold. Here, we restrict ourselves by the single-scale approximation of the streamline function. For the steady case, the characteristic spatial scale is given by the relation

$$\lambda \approx \left| \frac{\Psi(x, y)}{\nabla \Psi(x, y)} \right|.$$
 (10.5.3)

The percolation theory requires the existence of at least one coastline of infinite length, which is given by the scaling law [103]:

$$L(\varepsilon) \propto \lambda \left(\frac{a(\varepsilon)}{\lambda}\right)^{D_h}$$
. (10.5.4)

Here,  $D_h(v) = 1 + 1/v = 7/4$  is the coastline exponent and  $\varepsilon$  is a small dimensionless quantity, which characterizes the degree of deviation of the system from the critical state (the percolation threshold),

$$\varepsilon \approx \frac{\delta \Psi}{\lambda V_0},\tag{10.5.5}$$

where  $\delta \Psi$  is the value of the streamline function  $\Psi = \Psi(x,y)$  near the percolation threshold,  $\lambda$  is the characteristic scale, and  $V_0$  is the characteristic velocity of the flow. To describe transport effects, it is necessary to employ the correlation length  $a(\varepsilon)$ , which is the main magnitude characterizing spatial scales of the system located near the percolation threshold,  $\varepsilon \to 0$ ,

$$a(\varepsilon) = \frac{\lambda}{|\varepsilon|^{\nu}}.$$
 (10.5.6)

Here,  $\lambda$  is the geometric characteristic scale.

Thus, the idea of long-range correlations was accomplished in the framework of the percolation approach. Such a critical behavior is not amenable to any kind of a conventional perturbation analysis. We discuss this problem in more detail later in the framework of small percolation parameter renormalization as well as in relation to the presence of stochastic layers in two-dimensional random flows.

On the other hand, there exists an important topological difference between two-dimensional (2D) and three-dimensional (3D) percolation problems. In the two-dimensional case, the only infinitely extended cluster may exist at a time  $(\vec{V}(\vec{r}) > h)$  or  $\vec{V}(\vec{r}) < h)$ , while in three dimensions there may exist simultaneous percolation through both clusters.

#### 10.6 Phenomenological Arguments for Percolation Parameter

We consider here a simple and effective method, which permits us to estimate the percolation parameters by using the finite value of the percolation parameter  $\varepsilon_*$  instead of  $\varepsilon \to 0$ . In fact, it is possible "to hide" singularity into a phenomenological small parameter. Thus, the correlation length is one of the most important values describing transport. However, in a system of finite size  $L_0$  we cannot consider the infinite value

$$\Delta_{COR} \approx a(\varepsilon)|_{\varepsilon \to 0} \to \infty.$$
 (10.6.1)

Here, it is relevant to introduce a new small "renormalization" parameter  $\varepsilon_*$  as the value that provides the condition

$$a(\varepsilon_*) = \frac{\lambda}{|\varepsilon|^{\nu}} \approx L_0.$$
 (10.6.2)

The simplest calculations yield a new small parameter

$$\varepsilon_*(L_0) \approx \left(\frac{\lambda}{L_0}\right)^{\frac{1}{\nu}}.$$
 (10.6.3)

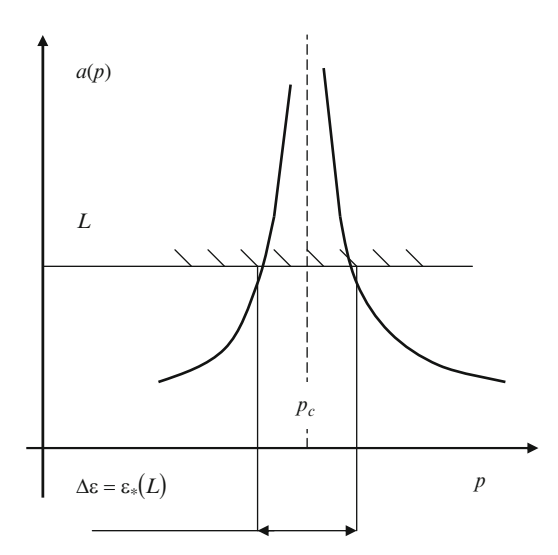
This result can be interpreted in the framework of percolation experiments with finite size samples. Under these conditions, the percolation threshold arises when the value of  $\varepsilon_*$  slightly differs from zero and is situated in an interval  $\Delta \varepsilon$ . The estimate obtained for  $\varepsilon_*$  can be considered as the characteristic width of this interval (see Fig. 10.6.1)  $\Delta \varepsilon \approx \varepsilon_*(L_0)$ . Actually, we are starting from the initial small parameter

$$\varepsilon_0(\lambda, L_0) \approx \frac{\lambda}{L_0} \ll 1,$$
(10.6.4)

which describes a real physical system with the characteristic scales  $L_0$  and  $\lambda$ . On renormalization, we obtain a new percolation parameter

$$\Delta \varepsilon pprox \varepsilon_*(\varepsilon_0) pprox \varepsilon_0^{\frac{1}{\nu}}.$$
 (10.6.5)

**Fig. 10.6.1** Sketch of renormalization procedure for a system of finite size



It is natural that the value  $\Delta \varepsilon$  decreases if the system size  $L_0$  increases.

Similar renormalization method could be applied to the transport description of two-dimensional chaotic flows, which allows us to develop the Kadomtsev–Pogutse percolation approach discussed in the previous section. The key problem is to determine a small parameter  $\varepsilon_0$  and to find an adequate renormalization condition for the finite value of  $\varepsilon_*$ . Then we can calculate the diffusion coefficient that is based on the estimate of the finite correlation length  $a(\varepsilon_*)$  and correlation time  $\tau(\varepsilon_*)$ 

$$D_{\mathrm{eff}}(\varepsilon_*) \propto \frac{a^2(\varepsilon_*)}{\tau(\varepsilon_*)}.$$
 (10.6.6)

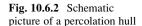
In the framework of phenomenological approach, we can estimate the correlation time  $\tau$  as

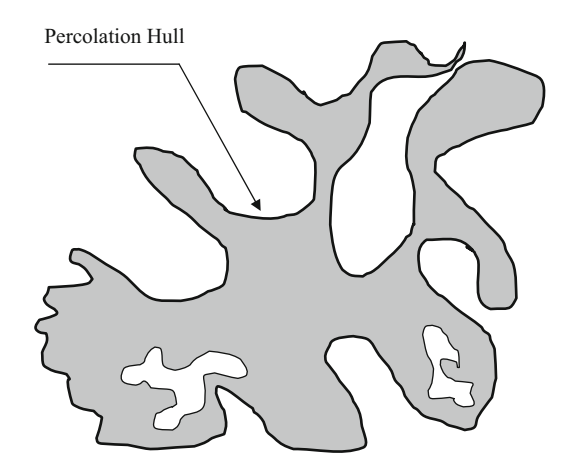
$$\tau(\varepsilon_*) \approx \frac{L(\varepsilon_*)}{V_0},$$
(10.6.7)

where L is the length of the percolation streamline. After substitution, one finds

$$\tau(\varepsilon_*) \approx \frac{\lambda}{V_0} \left(\frac{a(\varepsilon_*)}{\lambda}\right)^{D_h} \approx \frac{\lambda}{V_0} \left(\frac{1}{\varepsilon_*}\right)^{v \cdot D_h}.$$
(10.6.8)

Corresponding scaling will be obtained below on the basis of stochastic layer concept. In this percolation approach, the renormalized small percolation parameter  $\varepsilon_*$  is expressed through the characteristic random flow parameters, such as the Peclet number, the Kubo number, and the energy dissipation rate Indeed, in two dimensions we are faced with a quite different scenario. While many fractals, such





as the comb structures, are essentially loopless structures, many others, such as twodimensional percolation clusters, consist of a network of loops.

In our case, the percolation hull is the best candidate to approximate scalar ballistic path. A percolation cluster is a collection of occupied sites connected to each other by paths along nearest-neighbor pairs of sites and surrounded inside and outside by vacant sites. The perimeter of a percolation cluster is the continuous path of occupied sites at a boundary, which can be either external or internal to the cluster. The term "hull" was first used by Mandelbrot [157–161] to describe the island of points enclosed by the external boundary of a cluster, but it has been generalized to refer to the boundary as well (see Fig. 10.6.2), and that meaning will be used here.

#### 10.7 Subdiffusion and Percolation

The main specific feature of percolation media is that they consist of nonoverlapping regions (clusters) such that the transport inside each cluster is possible, whereas the passage of particles between clusters is impossible. Since only finite clusters exist in such a medium occurring in the state below the percolation threshold, the transport of particles over large distances in this state is hindered. Finite clusters possess fractal properties. Above the percolation threshold, the medium contains an infinite cluster and the transport of particles is not limited with respect to the range. A key characteristic of such a medium is the correlation length a. Below the percolation threshold, the distribution of clusters with respect to size l falls in the region l < a (the number of clusters with dimensions  $l \gg a$  is exponentially small). On approaching the percolation threshold, the correlation length exhibits unlimited growth:  $a \to \infty$ . Above the percolation threshold, this parameter becomes finite again and the distribution of finite clusters exhibits the same properties as those below the threshold. As for the infinite cluster, it possesses

(like the finite clusters) fractal properties and is scale invariant on the spatial scale  $L_0 < a$ , while being statistically homogeneous on the scale  $L_0 \gg a$ .

An important topological feature of any cluster is that it can be subdivided into two regions: backbone and a set of dead-ends, so that backbone connects remote parts of the cluster and all of them are linked to backbone, each at a single site, while being isolated from each other. It is important to note that the fractal dimension of dead-ends is greater than that of backbone (see Fig. 10.7.1). Scalar particles occurring within backbone will be called "active." The total number of active particles decreases with time, since they are lost in dead-ends and localized in small clusters. This implies that effective transport can be even subdiffusive if we consider finite time intervals.

Indeed, there exist two different time intervals. In the framework of the coastline phenomenology, the key value is the characteristic correlation time,  $\tau(\varepsilon_*) \approx \frac{L(\varepsilon_*)}{V_0}$ . The first case when

$$t > \tau(\varepsilon_*) \approx \frac{L(\varepsilon_*)}{V_0}$$
 (10.7.1)

was preliminary considered above on the basis of the conventional definition of the diffusion coefficient,

$$D_{\rm eff} \propto \frac{a^2(\varepsilon_*)}{\tau(\varepsilon_*)}$$
. (10.7.2)

The second case corresponds to the interval

$$t \ll \tau(\varepsilon_*) \approx \frac{L(\varepsilon_*)}{V_0}$$
. (10.7.3)

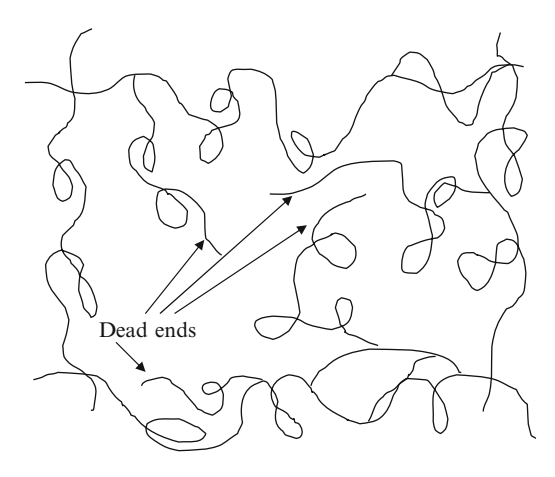


Fig. 10.7.1 Schematic diagram of a percolation network (nodes-links-blobs (NLB) model)

Here, particles are captured by dead-ends and localized in small clusters, and that is why the mean squared displacement of tracer is less than the correlation spatial scale  $R^2(t) < a^2$ . In some sense, the percolation cluster looks like a labyrinth for walking scalar particles. It is convenient to introduce the estimate of the mean squared displacement of tracer particles in the following form:

$$R^2(t) \propto a^2 P_{\infty}(t),\tag{10.7.4}$$

where  $P_{\infty}$  is an additional factor, which describes the part of space related to "active" motion of scalar particles. We expect that the effective transport will be anomalous so that

$$R^2(t) \propto t^{2H},\tag{10.7.5}$$

where H is the Hurst exponent. By establishing the relation between the phenomenological expression for  $R^2(t)$  and the conventional probabilistic representation

$$R^2(t) \propto d N(t) \Delta_{\text{COR}}^2,$$
 (10.7.6)

we conclude that the additional factor  $P_{\infty}$  introduced above could characterize the fractal dimensionality effects as well as time dependence. This is a great advantage of the two-dimensional percolation model. Here, d is the space dimensionality,  $\Delta_{\text{COR}}$  is the spatial correlation scale, and N is the number of steps. Simplified estimates of effective transport for comb structures give the value of the Hurst exponent H=1/4, which could be considered as a lower boundary. Thus, we expect that 1/4 < H < 1/2. The reader can find more discussions on this subject in the section devoted to the percolation description of transport in chaotic flows in the framework of the renormalization technique.

# **Further Reading**

# **Percolation Concept**

- A. Bunde, S. Havlin (eds.), Fractals and Disordered Systems (Springer, Berlin, 1995)
- J. Cardy, *Scaling and Renormalization in Statistical Physics* (Cambridge University Press, Cambridge, 2000)
- B. Duplantier, *Brownian Motion*, Poincare Seminar, p. 201 2005
- J. Feder, Fractals (Plenum Press, New York, 1988). Department of Physics University of Oslo, Norway
- D. Stauffer, *Introduction to Percolation Theory* (Taylor and Francis, London, 1985)
- R. Zallen, The Physics of Amorphous Solids (Wiley, New York, 1998)

Further Reading 179

#### Phase Transitions

- J. Cardy (ed.), Finite-Size Scaling (Elsevier, Amsterdam, 1988)
- L.P. Kadanoff, *Statistical Physics: Dynamics and Renormalization* (World Scientific, Singapore, 1999)
- V. Privman (ed.), Finite Size Scaling and Numerical Simulation of Statistical Systems (World Scientific Publishing, Singapore, 1990)
- H.E. Stanley, *Introduction to Phase Transitions and Critical Phenomena* (Clarendon Press, Oxford, 1971)
- J.M. Ziman, Models of Disorder: The Theoretical Physics of Homogeneously Disordered Systems (Cambridge University Press, London, 1979)

#### Percolation and Transport

- A.J. Chorin, Vorticity and Turbulence (Springer, New York, 1994)
- W.C. Conner, J. Fraisserd, *Fluid Transport in Nanoporous Materials* (Springer, Berlin, 2006)
- J.-F. Gouyet, *Physics and Fractal Structure* (Springer, Berlin, 1996)
- A. Hunt, Percolation Theory for Flow in Porous Media (Springer, Berlin, 2005)
- M.B. Isichenko, Rev. Mod. Phys. **64**, 961 (1992)
- M. Sahimi, Application of Percolation Theory (Taylor and Francis, London, 1993a)
- M. Sahimi, Rev. Mod. Phys. 65, 1393 (1993b)

# Chapter 11

# **Fractional Models of Anomalous Transport**

#### 11.1 Random Walks Generalization

In the framework of the probabilistic approach to transport in random flows, the probability density  $\rho(\vec{r},t)$  plays a central role. This is the probability to find a random walker at time t at distance r from its starting point. In a random system,  $\rho(\vec{r},t)$  contains information on both static disorder and the dynamical process. In homogenous systems, the probability density is Gaussian and does not depend on the configuration considered

$$\rho(\vec{r},t) = \frac{\delta r^d}{(4\pi D_0 t)^{d/2}} \exp\left(-\frac{r^2}{4D_0 t}\right). \tag{11.1.1}$$

Here,  $D_0$  is the seed diffusion coefficient and d is the space dimensionality.

In random systems,  $\rho(\vec{r},t)$  varies from configuration to configuration and depends on the starting point. To obtain a complete description of scalar particle diffusion in random systems, one has to study the configurational average of probability density  $\rho(r,t)$ , where the particle density is given by

$$\int_{-\infty}^{\infty} n(\vec{r}, t) d\vec{r} = N_p \int_{-\infty}^{\infty} \rho(\vec{r}, t) d\vec{r}.$$
 (11.1.2)

Here,  $N_p$  is the scalar particle number. The variance of the probability density represents the mean square displacement, from which the diffusion constant and the conductivity can be obtained. The Fourier transform of  $\rho(r,t)$  represents the scattering function, which is also experimentally accessible.

The anomalous character of transport in random systems has stimulated the search for transport equations that differ significantly from conventional diffusive description. Besides the different phenomenological methods of modification of the diffusion equation, the integral equation can be used to describe the random walk processes. As early as 1905, Albert Einstein obtained a functional equation for the

particle density solely on the basis of the general ideas about the process of random walk [214]:

$$n(x, t + \tau) = \int_{-\infty}^{+\infty} W_E(y) n(x - y, t) dy,$$
 (11.1.3)

where  $W_E(y)$  is the probability density of undergoing a jump y. This fundamentally nonlocal equation can be made local by reducing it to the conventional diffusion equation

$$\frac{\partial n(x,t)}{\partial t} = D \frac{\partial^2 n(x,t)}{\partial x^2}.$$
 (11.1.4)

Here, the diffusion coefficient is given by Brownian type formula

$$D = \frac{1}{\tau} \int_{-\infty}^{+\infty} W_E(y) \frac{y^2}{2} dy = \frac{\langle y^2 \rangle}{2\tau}.$$
 (11.1.5)

The key element in the random walk approach is Markov's postulate that the length of the jump y is independent of the prehistory of motion. By introducing the probability G for a particle at position x at time t to pass over to the interval x' + dx' during the time interval dt, one obtains the functional equation for the density of walking particles

$$\frac{\partial n}{\partial t} = \int_{-\infty}^{+\infty} G(x - x') n(t, x') dx'. \tag{11.1.6}$$

This representation demonstrates the nonlocal character of transport (see Fig. 11.1.1). Linear equation always provides the best conditions for an analysis. The Einstein functional is linear and it is more convenient here to switch to the Fourier representation for the particle density n(x, t) and the functional kernel G(x) with respect to the variable x. Formal manipulations yield the equation

$$\frac{\partial \tilde{n}_k(t)}{\partial t} = \tilde{G}_k \tilde{n}_k(t), \tag{11.1.7}$$

which indicates the absence of memory effects for the Fourier harmonics. Here,  $\tilde{G}_k$  and  $\tilde{n}_k(t)$  are the Fourier transformations of the functions G(x) and n(x, t) with respect to the variable x. The approach based on the Fourier representation of nonlocal functional equation was developed by Levy and Khintchine, who used the approximate equation of the scaling form [215]

$$\frac{\partial \tilde{n}_k(t)}{\partial t} = -\text{const}|k|^{\alpha_L} \tilde{n}_k(t); \quad 0 < \alpha_L \le 2.$$
 (11.1.8)

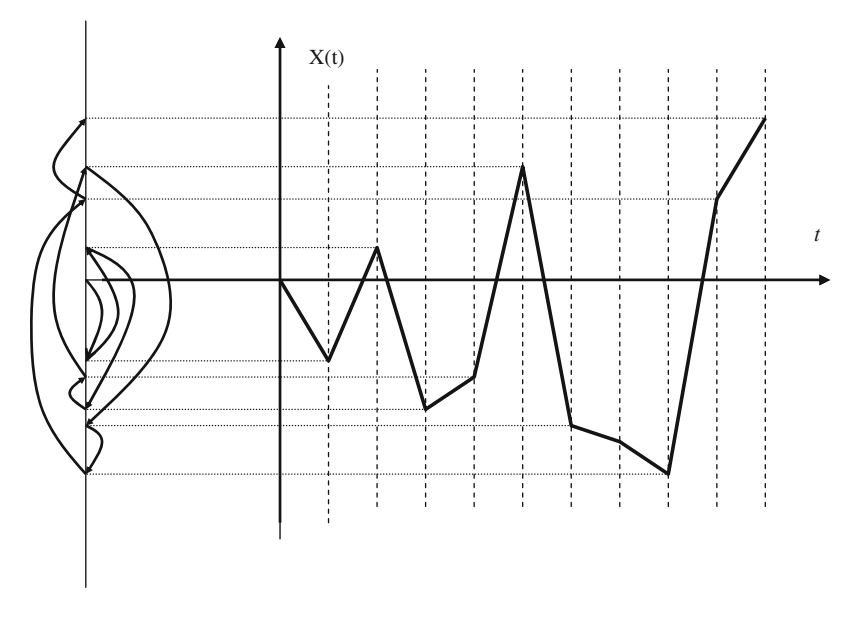


Fig. 11.1.1 Schematic diagram of Levy-Chinchine walks

It is easy to see that, for  $\alpha_L = 2$ , we are dealing with the Gaussian distribution (corresponding to a conventional diffusion equation  $\tilde{G}_k \tilde{n}_k = -D_0 k^2 \tilde{n}_k$ ). Indeed, the formal approach based on the scale-invariant behavior of the probability density leads to the relation

$$n(x,t) = t^{-\frac{1}{\alpha_{\rm L}}} g(x, \alpha_{\rm L}).$$
 (11.1.9)

Then, for the Gaussian distribution with  $\alpha_L = 2$ , we obtain

$$g(x,2) = \frac{1}{2\sqrt{\pi}} \exp\left(-\frac{x^2}{4}\right). \tag{11.1.10}$$

Some other analytic distributions are also known. For the case  $\alpha_L = 1$ , we obtain the Cauchy distribution [216]; if  $\alpha_L = 3/2$ , one arrives at the Holtsmark distribution [13]. For the case  $\alpha_L = 1/2$ , we have the Levy–Smirnov distribution [14]. All the probability densities with  $\alpha_L < 2$  have power-law tails and corresponding Levy flights differ significantly from Brownian walks. The important feature is that the second and higher order of moments of the distributions with  $1 \le \alpha_L < 2$  and all moments of the distributions with  $0 < \alpha_L < 1$  diverge. There is also an important result, which follows from the Fourier representation of density n(x, t)

$$\langle x^2 \rangle^{1/2} = -\frac{\partial}{\partial k} \left( \frac{\partial}{\partial k} \tilde{n}_k(t) |_{t=0} \right).$$
 (11.1.11)

This expression is useful for relating the transport scaling laws to probabilistic approximations. Now it is easy to find a relationship between the Hurst exponent H that describes anomalous transport and the Levy–Khintchine exponent  $\alpha_L$  that is the parameter of the kernel power approximation  $H(\alpha_L) = 1/\alpha_L$ , where  $1 \le \alpha_L < 2$ . These results were represented schematically and the reader can find more detailed information on these topics in numerous publications [13–15].

#### 11.2 Functional Equation for Return Probability

In the previous discussions, we applied the probability to return to the origin at time t using the Gaussian distribution in the form

$$P(0,t) = \frac{1}{2\sqrt{\pi \ d \ D_0 t}} \exp\left(-\frac{x^2}{4D_0 t}\right)_{x\to 0} \propto \frac{1}{\sqrt{d \ D_0 t}}.$$
 (11.2.1)

Here, d is the dimensionality of a space and  $D_0$  is the diffusion coefficient of randomly walking particle. This formula describes the probability to return without excluding that previous returns can already have occurred. To analyze transport in chaotic flows, where coherent vortices are responsible for trapping effects (see Fig. 11.2.1), it is natural to introduce the probability  $P_1(t)$  to return to the origin for the first time at the moment t.

In the framework of the continuous time approach, the functional equation for the probability to return to the origin for the first time at the moment t can be represented as the following:

$$P(0,t) = \int_0^t P(0,t')P_1(t-t')dt' + \delta(t). \tag{11.2.2}$$

Here,  $\delta(t)$  is the delta function, which describes the fact that the scalar particle that is situated at the origin at the moment under consideration corresponds to the above definition. On the other hand, the integral part of the relation is responsible for the contribution from the scalar particles, which come back to the origin at a time t' and then will return to the origin after a time interval t-t'. The functional equation obtained is linear relation and, which is more important, this equation appears to be a convolution. Therefore, it is relevant to apply the Laplace transform

$$\tilde{F}(s) = \int_0^\infty F(t) \exp(-st) dt.$$
 (11.2.3)

Upon substitution, we find the relation

$$\tilde{P}(0,s) = 1 + \tilde{P}_1(s)\tilde{P}(0,s).$$
 (11.2.4)

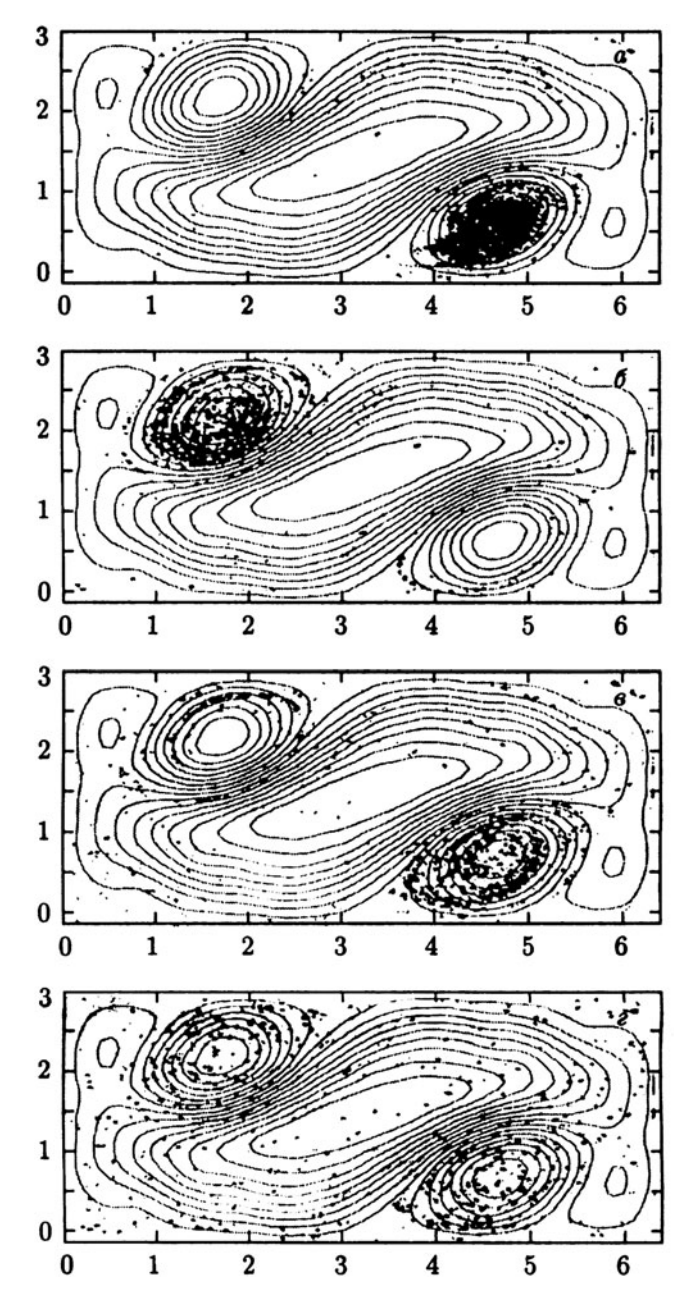


**Fig. 11.2.1** A tracer trapping by vortex structures in a two-dimensional flow (After Danilov [222] with permission)

An unknown function for us is the probability  $P_1(t)$  to return to the origin for the first time, whereas for the probability P(0,t) we can apply the Gaussian representation. In the one-dimensional case, we have

$$\tilde{P}(0,s) = \int_{t}^{\infty} \frac{\exp(-st)}{\sqrt{4\pi D_0 t}}.$$
(11.2.5)

After simple algebra, one finds

$$\tilde{P}_1(s) = \frac{\tilde{P}(0,s) - 1}{\tilde{P}(0,s)}.$$
(11.2.6)

By applying the inverse Laplace transform, one can obtain the solution for the probability  $P_1(t)$  to return to the origin for the first time at the moment t.

$$P_1(t) = \frac{\text{const}}{2\sqrt{\pi t^3}} \exp\left(-\frac{\text{const}}{4t}\right). \tag{11.2.7}$$

This is the Levy–Smirnov distribution with the asymptotic behavior,  $P_1(t)|_{t\to\infty} \propto t^{-3/2}$ . The corresponding Levy–Khintchine exponent is  $\alpha_L = 1/2$ .

Discoveries of anomalous diffusion in numerous phenomena have stimulated the search for transport equations that differ significantly from the conventional diffusive representation. An elegant integral equation corresponding to this problem was suggested by Einstein and Smoluchowski. However, trapping and memory effects were not included in that equation. To describe trapping and subdiffusive regimes, the continuous time random walk model was introduced in [13]. Fortunately, several detailed reviews [11, 14, 15] have been published recently.

# 11.3 Ensemble of Point Vortices and the Holtsmark Distribution

As early as 1919, Holtsmark founded the Levy distribution with  $\alpha_L = 3/2$  in describing the statistical properties of particle ensemble [44]. In the case of chaotic flows, we can investigate an analogous problem, where a random ensemble of point vortices can be considered. In a system of point vortices, the motion of each vortex depends on the influence of other vortices of the ensemble under consideration (see Fig. 11.3.1). However, in contrast to the Holtsmark model, here we deal with a point vortex distribution in velocities f(V). The direct use of the Holtsmark distribution for three-dimensional vortex systems was not confirmed by simulations. However, numerical simulations of point vortex ensemble on a plane allow one to consider the Levy distribution as rather correct [217, 218]. Thus, in the two-dimensional case, the velocity field from point sources is given by

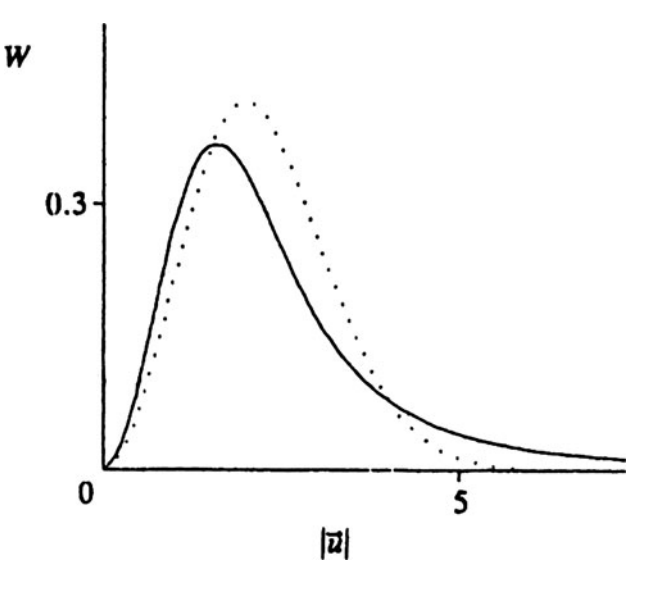


Fig. 11.3.1 The Holtsmark distribution

$$V_x(\vec{r}) = -\frac{1}{2\pi} \sum_{j=1}^{N} \frac{\Gamma_j(y - y_j)}{|\vec{r} - \vec{r}_j|^2} = \sum V_{xj}(\vec{r}_j),$$
(11.3.1)

$$V_{y}(\vec{r}) = \frac{1}{2\pi} \sum_{j=1}^{N} \frac{\Gamma_{j}(x - x_{j})}{|\vec{r} - \vec{r}_{j}|^{2}} = \sum V_{yj}(\vec{r}_{j}).$$
(11.3.2)

Below, we consider an ensemble of point vortices with the identical "charges"  $\Gamma_j = \Gamma_0$ . Let the sum N of independent random variables  $g_j$  be the expression

$$g = \sum_{j=1}^{N} g_{j}. (11.3.3)$$

Then, on the basis of the Markov method we can write the expression for the probability density

$$f(g) = \left\langle \delta \left( g - \sum_{j=1}^{N} g_j \right) \right\rangle, \tag{11.3.4}$$

where  $\langle \ \rangle$  denotes averaging over an ensemble. In our case, we are averaging over the ensemble of noncorrelated point vortices. We use here the Fourier transformation that allows us to calculate the probability density by factorization of its Fourier transform. Since the Fourier transform of delta function is given by the expression

$$\delta(\vec{r}) = \frac{1}{(2\pi)^3} \int d^3 \vec{k} \, e^{i\vec{k}\vec{r}}, \qquad (11.3.5)$$

we find the probability density as

$$f(\vec{g}) = \left\langle \frac{1}{(2\pi)^3} \int d^3 \vec{k} e^{i\vec{k} \left(\vec{G} - \sum_{j}^{N} \vec{g}_{j}\right)} \right\rangle = \frac{1}{(2\pi)^3} \int d^3 \vec{k} \ e^{i\vec{k}\vec{G}_H} \left\langle e^{i\vec{k}\sum_{j}^{N} \vec{g}_{j}} \right\rangle$$

$$= \frac{1}{(2\pi)^3} \int d^3 \vec{k} \{ e^{i\vec{k}G_H} \ \tilde{f}_{k}(\vec{k}) \}$$
(11.3.6)

In the case under consideration  $\vec{g}_j = \vec{g}_j(\vec{r}_j)$ ; therefore, using the factorization of Fourier transform of distribution function, we obtain

$$\left\langle \exp\left(-i\vec{k}\sum_{j}\vec{g}_{j}(\vec{r}_{j})\right)\right\rangle = \prod_{j}^{N}\left\{\frac{\mathrm{d}\vec{r}_{j}}{W_{V}}\exp\left[-i\vec{k}\vec{g}_{j}(\vec{r}_{j})\right]\right\} = \left\{\frac{\mathrm{d}\vec{r}}{W_{V}}\exp\left[-i\vec{k}\vec{g}(\vec{r})\right]\right\}^{N}$$
(11.3.7)

We used here an approximation of the probability function P in the form  $P = d\vec{r}/W_V$ . Here,  $W_V$  is the region volume where "sources" (vortices) creating the field under consideration are distributed. To investigate statistical properties of a random field, it is naturally to suppose a large amount of vortices. Then by applying the classical result

$$\left(1 - \frac{z}{N}\right)^N \Big|_{N \to \infty} \approx \exp(-z),$$
 (11.3.8)

we rewrite the Fourier transform of distribution density

$$\tilde{f}_{k}(\vec{k}) = \left\{ \int \frac{d\vec{r}}{W_{V}} \exp\left[-i\vec{k}\vec{g}(\vec{r})\right] \right\}^{N} = \left[\eta(\vec{k})\right]^{N}$$
(11.3.9)

in the form

$$\begin{split} \tilde{f}_{k}(\vec{k}) &= \left\{ 1 - \left[ 1 - \eta_{j}(\vec{k}) \right] \right\}^{N} = \left\{ 1 - \frac{1}{N} \int \frac{N \mathrm{d}\vec{r}_{j}}{W_{V}} \left[ 1 - \exp(-i\vec{k}\vec{g}_{j}) \right] \right\}^{N} \\ &\approx \exp\left\{ - \frac{N}{W_{V}} \int \mathrm{d}r \left( 1 - \exp\left[ -i\vec{k}\vec{g} \right] \right) \right\}. \end{split} \tag{11.3.10}$$

It is easily seen that the expression (relation)  $N/W_V$  corresponds to the spatial density of vortices  $n_V$ , which we assume a constant in order to simplify our calculations. Moreover, the condition  $N \to \infty$  allows us to use the result obtained

to analyze a field of point vortices, where the summation does not include a contribute of the vortex situated in the point under analysis. Then the expression for the Fourier transform of probability density is given by

$$\tilde{f}_k(\vec{k}) = \exp\left\{-n_V \int (1 - \exp\left[-i\vec{k}\vec{g}(\vec{r})\right]) d\vec{r}\right\}.$$
 (11.3.11)

Let the value g is approximated by

$$g(\vec{r}) = \frac{\vec{r}}{r} \left( \frac{1}{r^{\gamma_V}} \right). \tag{11.3.12}$$

Then, the formal integration over the space with *d*-dimensions, where  $d\vec{r} = r^{d-1}dr$  leads to the expression for the Fourier transform of Levy distribution

$$\tilde{f}_{k}(\vec{k}) = \exp\left\{-n_{V} \int \left[1 - \exp\left(i\frac{\vec{k}\vec{r}}{r^{\gamma_{V}+1}}\right)\right] d\vec{r}\right\} = \exp\left\{-\operatorname{const} \cdot k^{\frac{d}{\gamma_{V}}}\right\}. \quad (11.3.13)$$

The Levy exponent of the distribution  $\alpha_L$  depends on a space dimensionality d and the exponent  $\gamma_V:\alpha_L(d,\gamma_V)=\frac{d}{\gamma_V}$ . The power tail of the distribution function is given by

$$f(g) \propto \frac{1}{g^{\alpha_L + 1}}.\tag{11.3.14}$$

For the gravity case  $\gamma_V=2$  (an acceleration a is proportional inversely to the squared distance) in three-dimensional space d=3, the Holtsmark exponent is  $\alpha_L=3/2$  and  $f(a)\propto a^{-5/3}$ . In the case of the two-dimensional (d=2) point vortices system, where  $\gamma_V=1$ , we find  $\alpha_L=2$ , and hence,

$$f(V) \propto \frac{1}{V^3}.\tag{11.3.15}$$

Such a scaling for the tail of the velocity distribution function is the effective tool to investigate strongly nonequlibrium systems where stochastic mechanisms of acceleration or strong spatial gradients form nonexponential distribution [219–221].

# 11.4 Fractal Time and Scaling

Scaling concept is rather relevant to the anomalous transport problem. To interpret the scaling representation or the waiting time distribution function, it is convenient to employ the Weierstrass-like random walk [13]. Consider the effective probability distribution  $\psi(t)$ , which describes the hierarchy of independent Poisson events

$$\psi_j(t) = C(N)^j (g_0)^j \exp\left[-(g_0)^j \cdot t\right]$$
 (11.4.1)

$$\psi(t) = \sum_{j=1}^{N} \psi_{j}(t). \tag{11.4.2}$$

Here, the normalization condition is given by

$$\int_{0}^{\infty} \psi(t) \, \mathrm{d}t = 1 \tag{11.4.3}$$

In the case of g < 1 and  $N \gg 1$ , the characteristic times are expressed as  $\tau_i = 1/(q)^j$ , and hence,

$$\tau_0 < \tau_1 < \tau_2 < \dots$$
 (11.4.4)

By analyzing the expression for the probability density  $\psi$ , we see that the smallest time contributes most. For the hierarchy under consideration, we have

$$\psi_0 = C_0 \exp\left(-\frac{t}{\tau_0}\right), \quad \psi_1 = C_1 \exp\left(-\frac{t}{\tau_1}\right), \dots, \psi_j = C_j \exp\left(-\frac{t}{\tau_j}\right), \quad (11.4.5)$$

where

$$\tau_0 = 1, \ \tau_1 = \frac{1}{g_0}, \ \tau_2 = \frac{1}{g_0^2}, \ \dots \ \tau_j = \frac{1}{g_0^j}$$
 (11.4.6)

Let us build the condition to obtain the effective probability density in the scale-invariant form. After simple algebra, we derive

$$\psi(t) = \frac{1 - N}{N} \left\{ N g_0 \exp(-g_0 t) + N^2 g_0^2 \exp(-g_0^2 t) + \dots \right\}$$
 (11.4.7)

$$\psi(g_0 t) = \frac{1 - N}{N} \left\{ N g_0 \exp(-g_0^2 t) + N^2 g_0^2 \exp(-g_0^3 t) + \dots \right\} \approx \frac{\psi(t)}{N g_0} - (1 - N)g_0 \exp(-g_0 t)$$
(11.4.8)

In the case when

$$\frac{1}{N g_0} \gg (1 - N)g_0 \tag{11.4.9}$$

the effective probability density is scale-invariant and is given by the formula

$$\psi(g_0 t) = \frac{\psi(t)}{N g_0}.$$
 (11.4.10)

Now we arrive at the asymptotic representation for the waiting time distribution function  $\psi(t)$ 

$$\psi(t) \propto \frac{1}{t^{1+\gamma}}$$
 for  $t \to \infty$ , (11.4.11)

where the characteristic exponent  $\gamma$  is given by

$$\gamma = \frac{\ln N}{\ln g_0} = \frac{\ln \frac{1}{N}}{\ln \tau_0} \tag{11.4.12}$$

These calculations demonstrate how the waiting time distribution function  $\psi(t)$  can be interpreted in terms of fractal representation.

The waiting time distribution function must be the effective tool to investigate trapping effects in flows with vortex structures (see Fig. 11.4.1). Indeed, in the case of one-dimensional system of regular situated vortices (array of rolls) it is possible to find a scaling for the effective transport. Suppose that all of the tracer is initially released in a single cell. The main question is: how many cells, N(t), have been invaded by tracer at time t? In the presence of seed diffusion, we expect that

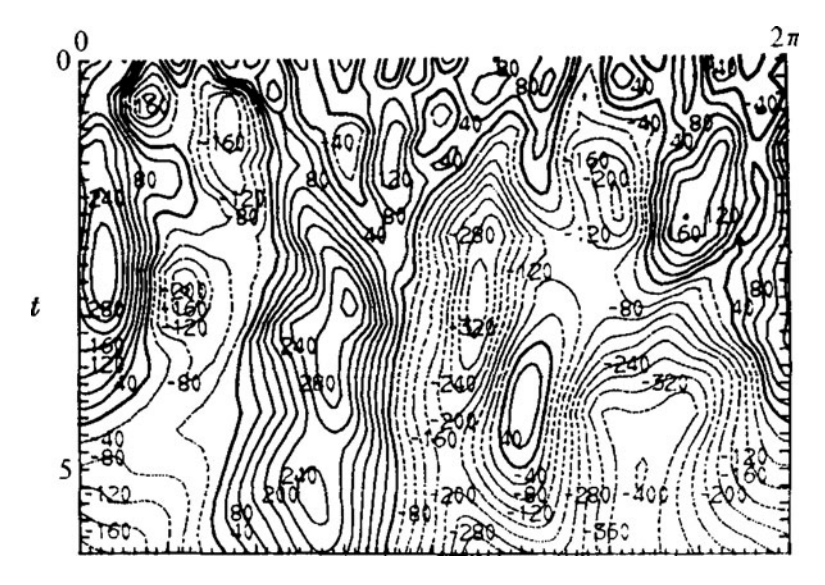
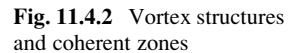
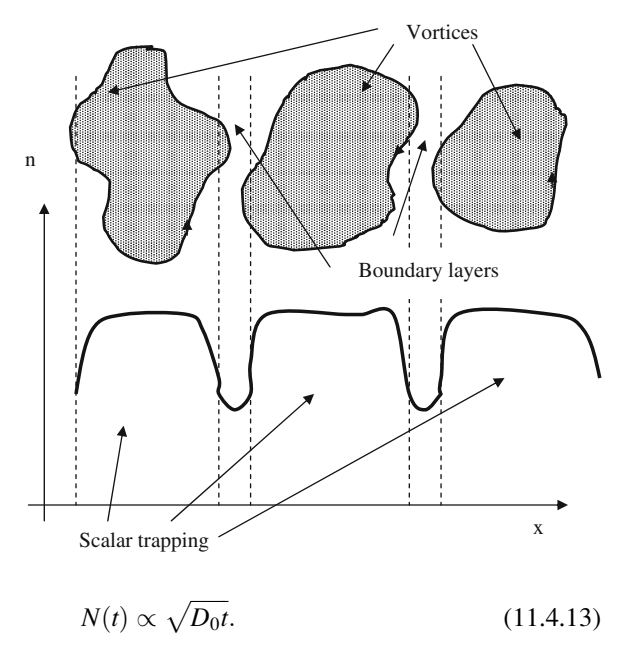


Fig. 11.4.1 The stream function of two-dimensional turbulent flow. (After Rhines [169] with permission)





With certain restriction, this  $t^{1/2}$ -law is correct. However, there is an intermediate stage

$$t \ll \frac{L_0^2}{D_0} \tag{11.4.14}$$

where the waiting time between two "jumps" is an important factor. Here,  $L_0$  is the cell characteristic scale. Below we consider the case of one-dimensional array of rolls in more details.

For the general two-dimensional case, there are anomalies if the velocity field is frozen in time. In this case, a finite fraction of the scalar particles is trapped, since the streamlines must form closed loops in the neighborhoods of local maxima and minima of the stream function. This forms trapping regions and leads to the appearance of "coherent" behavior in some spatial regions separated from each other (see Fig. 11.4.2). Such coherent structures in the form of long-living vortices considerably change the character of transport in chaotic flows in comparison with the conventional diffusion.

#### 11.5 Fractional Derivatives and Anomalous Diffusion

One of the valuable concepts used to study various transport processes is scaling. Scaling has a surprising power of prediction, simple manipulations allowing one to connect apparently independent quantities and exponents. We have seen how to

extend our ideas of using partial differential equations for the possible treatment of anomalous transport. We have looked at the nonlocal transport equation as well as the continuous time random walk approach. This allows us to apply the scaling concept to construct a generalized transport equation. Moreover, it is possible to introduce a fractional derivative when considering the conventional one-dimensional diffusion equation

$$\frac{\partial n(x,t)}{\partial t} = D_0 \frac{\partial^2 n(x,t)}{\partial x^2}$$
 (11.5.1)

for x > 0 and  $n(0, t) = n_I(t)$ ,  $n(x, 0) = n_0(x) = 0$ . By taking the Laplace transform, one obtains

$$s\tilde{n}_s(s,x) = D_0 \frac{\partial^2 \tilde{n}_s}{\partial x^2}.$$
 (11.5.2)

The solution of this equation is given by the formula

$$\tilde{n}_s(s,x) = \tilde{n}_{Is}(s,0) \exp\left\{-\sqrt{\frac{s}{D_0 x}}\right\}.$$
 (11.5.3)

The number of walking particles  $N_p$  in terms of the Laplace transformation is represented by the expression

$$\tilde{N}_{ps}(s) = \int_0^\infty \tilde{n}_s(s, x) \, \mathrm{d}x = \tilde{n}_{Is}(s) \sqrt{\frac{D_0}{s}}.$$
 (11.5.4)

Note that this leads to the relationship between the number of walking particles  $N_p(t)$  and the particle distribution function  $n(0,t) = n_I(t)$ . In the ordinary variables, this formula leads to the expression for  $N_p(t)$  in the form

$$N_p(t) = \int_0^t \frac{\sqrt{D_0}}{\sqrt{\pi(t - t')}} n_I(t') \, \mathrm{d}t'. \tag{11.5.5}$$

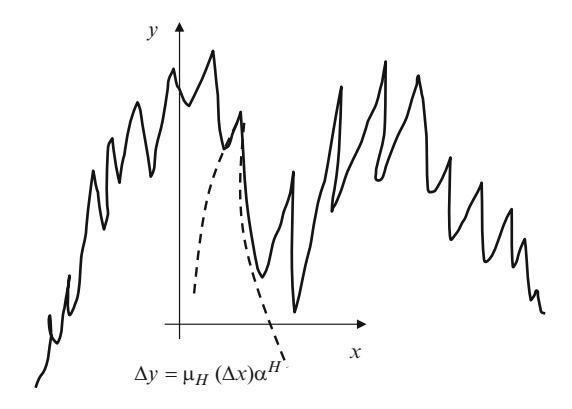
This coincides exactly with the definition of the fractional derivative of order ½ [223–226]

$$\frac{d^{1/2}f(t)}{dt^{1/2}} = \frac{1}{\Gamma(1 - 1/2)} \frac{d}{dt} \int_{-\infty}^{t} \frac{f(\tau) d\tau}{(t - \tau)^{1/2}}.$$
 (11.5.6)

The fractional representation could be also obtained for  $n(0,t) = n_I(t)$ 

$$n_I(t) = \int_0^t \frac{N(t')}{\sqrt{D_0 \pi (t - t')}} dt'.$$
 (11.5.7)

**Fig. 11.5.1** Schematic representation of the meaning of fractional derivation



Fractional derivatives provide a rather effective description of long-range correlations and memory effects. We can also use the symmetric fractional derivative of an arbitrary order  $\alpha > 0$  that can be defined, for a "sufficiently well-behaved" function f(x), where  $-\infty < x < \infty$ , as the pseudodifferential operator characterized by its Fourier representation,

$$\frac{d^{\alpha}}{d|x|^{\alpha}}f(x) = -|k|^{\alpha}\tilde{f}(k), \qquad (11.5.8)$$

where  $\alpha > 0$  and  $-\infty < k < \infty$ . Recall that the power form of the Fourier representation for the kernel of the nonlocal Einstein functional

$$\tilde{G}(k) = \text{const } |k|^{\alpha_{L}}, \tag{11.5.9}$$

where  $0 < \alpha_L < 2$ , can also be interpreted in terms of fractional derivatives.

Indeed, for the common derivative, we have, by definition  $\Delta y = \mu \Delta x$ . For a fractal function, we have (see Fig. 11.5.1)

$$\Delta y = \mu_H (\Delta x)^{\alpha_H}, \tag{11.5.10}$$

where  $\mu$  and  $\mu_H$  are the ordinary derivative and Holder derivative, respectively. More exactly, for  $\Delta x < 0$  and  $\Delta x > 0$ , the left-hand and right-hand derivatives,  $\mu_{H_-}$  and  $\mu_{H_+}$ , respectively, must be introduced [223–226]. Of course, this approach is fairly formal. The model of greatest interest for which fractional derivatives are a natural tool for investigating anomalous transport is elaborated upon in the following sections.

#### 11.6 Comb Structures and the Fractional Fick Law

Comb structures comprise of a backbone and orthogonal close-ended teeth. Diffusion processes on such structures have been studied intensively because of their potential relevance to transport processes at the threshold percolation. In this

setting, the backbone represents the connected pathway, which span the cluster, while the orthogonal close-ended teeth represent the dead-end pathways, which emanate from backbone. In the electrical analogy problem, the backbone represents the conducting pathway and the teeth dangling bonds along which current does not flow. Comb structures also provide a concrete realization of fractal diffusion equations and anomalous diffusion [210–212].

Here, transport properties of "regular" comb structures having teeth of uniform length (see Fig. 11.6.1) are identified in analytical studies. The rigorous description of a comb structure can be represented on the basis of fractional differential equation. As usual, a diffusive flux along an axis of comb structure is given by

$$q_x = -D_{xx} \frac{\partial n}{\partial x}.$$
 (11.6.1)

Here,  $D_{xx} = D_1 \delta(y)$ . The character of diffusion along the teeth is also usual. We assume that the diffusion coefficient along the teeth  $D_{yy} = D_2$  differs from the coefficient corresponding to the axis of a structure. A diffusive tensor for the whole comb structure has a form

$$D_{ij} = \begin{pmatrix} D_1 \delta(y) & 0 \\ 0 & D_2 \end{pmatrix}. \tag{11.6.2}$$

Basing on the tensor form of the Fick law  $\vec{q}_d = \hat{D} \nabla n$ , we derive a diffusive equation that takes into account anisotropy of transport

$$\left(\frac{\partial}{\partial t} - D_1 \delta(y) \frac{\partial^2}{\partial x^2} - D_2 \frac{\partial^2}{\partial y^2}\right) G(x, y, t) = \delta(x) \delta(y) \delta(t). \tag{11.6.3}$$

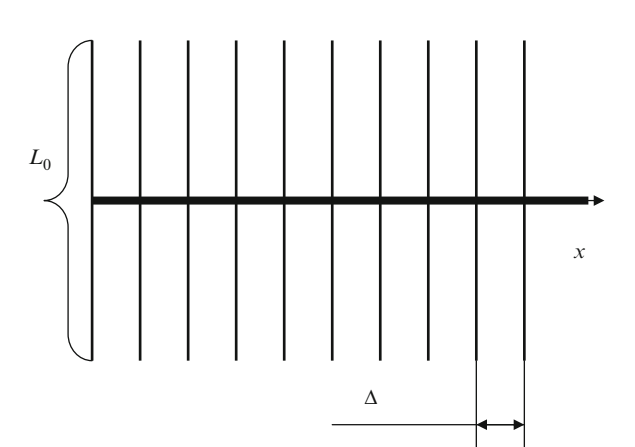


**Fig. 11.6.1** Schematic picture of regular comp structure

Here, G(x, y, t) is the Green function of the diffusion equation. By applying the Laplace transformation in time and the Fourier transformation in the longitudinal coordinate x, we find

$$\left(s + D_1 k_x^2 \ \delta(y) - D_2 \frac{\partial^2}{\partial y^2}\right) \tilde{\tilde{G}}(s, k_x, y) = \delta(y). \tag{11.6.4}$$

To simplify our analysis, let us consider a point source  $\delta(x)\delta(y)\delta(t)$  as initial data. A solution will be found in an exponential form:

$$\tilde{\tilde{G}}(s, k, y) = \tilde{\tilde{g}}(s, k) \exp(-k_0|y|).$$
 (11.6.5)

Substitution of this equation yields the following system of equations:

$$(s - D_2 k_0^2) \tilde{\tilde{G}}(s, k_x, y) = 0, (11.6.6)$$

$$(D_1k^2 + 2k_0^2D_2) \,\delta(y)\,\tilde{\tilde{g}}(s,k_x,y) = \delta(y). \tag{11.6.7}$$

The last equation includes a singular coefficient  $\delta(y)$ . The system can be easily solved after we define the value  $k_0$  from the above equation  $k_0 = \sqrt{\frac{s}{D_2}}$ . For the function g(s,k) we obtain

$$g(s, k_x) = \frac{1}{2D_2k_0^2 + D_1k_x^2}. (11.6.8)$$

Inverse Fourier transformation leads to the Green function

$$G(x, y, t) = \int_0^\infty (\tau + |y|) \exp\left(-\frac{x^2}{4D_1\tau} - \frac{D_2(\tau + |y|)^2}{4t}\right) \frac{\partial \tau \sqrt{D_2^3}}{\pi \sqrt{D_1 t^3 \tau}}, \quad (11.6.9)$$

where the following normalization was used:

$$\int_0^\infty \exp(-c\tau) \, \mathrm{d}\tau = \frac{1}{c} \tag{11.6.10}$$

Easy calculations confirm that transport along the axis of comb structure appear to be anomalous

$$\left\langle x^2(t)\right\rangle = D_1 \sqrt{\frac{t}{D_2}}.\tag{11.6.11}$$

This coincides with the elementary scaling estimates. In conformity with the initial suppositions, transport along teeth has a classical diffusive character:

 $\langle y^2(t) \rangle = 2D_2t$ . Different generalizations of this model are naturally possible due to different complications of comb structure topology.

To obtain the generalized diffusion equation in the two-dimensional case, let us consider the solution obtained in more detail. To this end, the Fourier transform of this solution in the coordinate *y* is performed:

$$G(s, k_x, k_y) = \frac{2\lambda_y}{(2D_2\lambda + D_1k^2)(\lambda^2 + k_y^2)}.$$
 (11.6.12)

Accordingly, the following diffusion equation for the anisotropic random walks on the comb structure is obtained:

$$(2D_2\lambda + D_1k^2)\left(\frac{\lambda}{2} + \frac{k_y^2}{2\lambda}\right)n(s, k_x, k_y) = 0.$$
 (11.6.13)

With the neglect of the product  $(k_x^2 \times k_y^2)$  in this equation (this is possible at large scales), the following effective equation in the  $(s, k_x, k_y)$  representation is obtained:

$$\left(s + \frac{D_1}{2}k_x^2\sqrt{\frac{s}{D_2}} + 2D_2k_y^2\right)n(s, k_x, k_y) \approx 0.$$
 (11.6.14)

In the usual (x, y, t) representation, the effective diffusion equation has the form

$$\left(\frac{\partial}{\partial t} - \frac{D_1}{2\sqrt{D_2}} \frac{\partial^2}{\partial x^2} \frac{\partial^{1/2}}{\partial t^{1/2}} - D_2 \frac{\partial^2}{\partial y^2}\right) n(t, x, y) \approx 0$$
 (11.6.15)

Thus, the operator expression for the effective diffusion tensor in the generalized Fick law is obtained:

$$\hat{D}_{\text{eff}} = \begin{pmatrix} \frac{D_1}{2\sqrt{D_2}} \frac{\partial^{1/2}}{t^{1/2}} & 0\\ 0 & D_2 \end{pmatrix}.$$
 (11.6.16)

In the case of the three-dimensional comb structure, the random walk is described by the diffusion tensor of the form

$$D_{ij} = \begin{pmatrix} \tilde{D}_1 \delta(y) \delta(z) & 0 & 0\\ 0 & \tilde{D}_2 \delta(z) & 0\\ 0 & 0 & \tilde{D}_3 \end{pmatrix}.$$
(11.6.17)

Accordingly, the diffusion equation has the form

$$\left(\frac{\partial}{\partial t} - \tilde{D}_1 \delta(y) \delta(z) \frac{\partial^2}{\partial x^2} - \tilde{D}_2 \delta(z) \frac{\partial^2}{\partial y^2} - D_3 \frac{\partial^2}{\partial z^2}\right) \times G(t, x, y, z) = \delta(x) \delta(y) \delta(z) \delta(t) \tag{11.6.18}$$

The solution of the three-dimensional problem will be represented in the form

$$G(x, k_x, y, z) = g(s, k_x) \exp(-\lambda_y |y| - \lambda_z |z|).$$
 (11.6.19)

After the substitution of this solution into the fractional differential equation, the parameters  $\lambda_y$  and  $\lambda_z$  and the function  $g(s, k_x)$  are determined in the form

$$\lambda_z = \sqrt{\frac{s}{\tilde{D}_2}}, \quad \lambda_y = \sqrt{\frac{2\tilde{D}_3\lambda_z}{\tilde{D}_2}}, \quad g(s,k) = \frac{1}{2\tilde{D}_2\lambda + \tilde{D}_1k^2}.$$
 (11.6.20)

The Fourier transform in the coordinates y and z provides the Green's function for three-dimensional case:

$$G(k_x, k_y, k_z, s) = \frac{4\lambda_y \lambda_z}{(2\tilde{D}_2 \lambda + \tilde{D}_1 k_x^2)(\lambda_y^2 + k_y^2)(\lambda_z^2 + k_z^2)}.$$
 (11.6.21)

The effective diffusion equation for the three-dimensional anisotropic case is obtained with the use of the above consideration:

$$\left(s + \frac{\tilde{D}_{1}^{3/4}\sqrt{s}}{2^{1/4}\sqrt{\tilde{D}_{3}\tilde{D}_{2}^{2}}}k_{x}^{2} + 2\tilde{D}_{2}\sqrt{\frac{s}{\tilde{D}_{3}}}k_{y}^{2} + \tilde{D}_{3}k_{z}^{2}\right) \times n(s, k_{x}, k_{y}, k_{z}) \approx 0$$
(11.6.22)

or, in the usual representation,

$$\left(\frac{\partial}{\partial t} - \frac{\tilde{D}_1}{2\sqrt{\tilde{D}_3\tilde{D}_2^2}} \frac{\partial^2}{\partial x^2} \frac{\partial^{3/4}}{\partial t^{3/4}} - \frac{2\tilde{D}_2}{\sqrt{\tilde{D}_3}} \frac{\partial^2}{\partial x^2} \frac{\partial^{1/2}}{\partial^{1/2}} - \tilde{D}_3 \frac{\partial^2}{\partial z^2}\right) \times n(s, k_x, k_y, k_z) \approx 0$$
(11.6.23)

Therefore, the effective diffusion tensor in the Fick's law for the three-dimensional anisotropic walk on the comb structure has the form

$$\hat{D}_{\text{eff}} = \begin{pmatrix} \frac{\tilde{D}_1}{2\sqrt{\tilde{D}_3}\tilde{D}_2^2} \frac{\partial^{3/4}}{\partial t^{3/4}} & 0 & 0\\ 0 & \frac{2\tilde{D}_2}{\sqrt{\tilde{D}_3}} \frac{\partial^{1/2}}{\partial t^{1/2}} & 0\\ 0 & 0 & \tilde{D}_3 \end{pmatrix}.$$
(11.6.24)

The anomalous random walk on the multidimensional comb structure in the asymptotic limit of large times (large scales) is described by the effective diffusion equations containing not only the usual spatial derivatives, but also fractional time derivatives. Such a representation is associated with the subdiffusion character of random walks on the multidimensional comb structure.

#### 11.7 Diffusive Approximation and Random Shear Flows

In the above discussion, we have seen how to construct and solve fractional differential equations modeling phenomena that have long-time memory and/or long-range interactions. We have seen that the long-range power-law correlations that characterize anomalous transport result in a non-Markovian description of the underlying process. Here, the diffusive renormalization of quasilinear equations for scalar transport is analyzed in the framework of the random shear flow model (Dreizin–Dykhne flow; Fig. 7.7.1), which is the best illustration of the above thesis.

At this stage, we are able to treat random shear flows with non-Gaussian longitudinal correlations. In the model under analysis, the transversal and longitudinal correlation effects are separated. In fact, the Eulerian correlation function could be represented by the scaling in the form

$$C(\lambda_{//}) \propto V_{\perp}^{2}(\lambda_{//}) \propto \frac{1}{\lambda_{//}^{\alpha_{E}}}.$$
 (11.7.1)

Here,  $\alpha_E$  is the correlation exponent. Such a representation allows us to consider random flows, where anisotropy effects play an important role. For the effective transverse transport, one can employ the ballistic estimate in the form

$$\lambda_{\perp}(t) \propto V_{\perp}(\lambda_{//}) t.$$
 (11.7.2)

Here,  $\lambda_{\perp}$  is the perpendicular displacement and  $\lambda_{//}$  is the longitudinal displacement. In the case under analysis, we are dealing with the diffusive character of longitudinal motion. This leads to the scaling for the longitudinal displacement  $\lambda_{//} \approx \sqrt{2D_0 t}$ . Upon substitution of this estimate into the formula for the perpendicular displacement, we find the scaling,

$$\lambda_{\perp}(t) \propto \frac{t}{\lambda_{//}^{\alpha_E}(t)} \propto t^{1-\alpha_E/4}.$$
 (11.7.3)

The expression for the Hurst exponent takes the form

$$H(\alpha_E) = 1 - \frac{\alpha_E}{4},\tag{11.7.4}$$

where  $0 \le \alpha_E \le 2$ . Note that for  $\alpha_E > 2$  this scaling yields the subdiffusive regime, which contradicts the initial assumptions about the incompressibility of the flow and using the streamline concept.

Now we obtain an equation for the passive tracer density under conditions when longitudinal correlation effects can be approximated by the longitudinal diffusive term  $D_0 \frac{\partial^2 n_1}{\partial z^2}$ . Thus, in the two-dimensional case the corresponding renormalized equations have the form

$$\frac{\partial n_0}{\partial t} = -\langle V_X(z) \frac{\partial n_1}{\partial x} \rangle; \tag{11.7.5}$$

$$\frac{\partial n_1}{\partial t} = D_0 \frac{\partial^2 n_1}{\partial z^2} - V_X(z) \frac{\partial n_0}{\partial x}.$$
 (11.7.6)

Here,  $D_0$  is the seed diffusion. The dependences  $n_0 = n_0(x, t)$  and  $n_1 = n_1(x, z, t)$  were used to describe the two-dimensional case. Using the Laplace transformation over t and the Fourier transformation over z, one obtains

$$s\tilde{n}_0(s,x) - n_0(x,0) = \tilde{D}(s)\frac{\partial^2 \tilde{n}_0}{\partial x^2},$$
(11.7.7)

$$\tilde{D}(s) = \lim_{L_0 \to \infty} \frac{1}{2L_0} \int_{-L_0}^{L_0} dz \int_{-\infty}^{\infty} dz' \left\{ \frac{\exp\left[-\sqrt{s|z-z'|^2/D_0}\right]}{\sqrt{D_0 s}} V_X(z) V_X(z') \right\}.$$
(11.7.8)

Then, one can write a diffusion equation for the model of random drift flows. Indeed, the "renormalization" of the quasilinear equations allows us to obtain the transport equations, which differ significantly from the classical diffusion equation. The correlation function  $K_C(|z-z'|) = V_X(z)V_X(z')$  can be represented in the power form

$$K_C(w) = K_C(|z - z'|) \propto \frac{V_0^2}{1 + w^{\alpha_E}}.$$
 (11.7.9)

In terms of the Laplace transformation, the renormalized transport equation takes the form

$$s\tilde{n}_0(s,x) - n_0(x,0) = \frac{V_0^2}{\sqrt{2D_0}} \left(\frac{s}{2}\right)^{\frac{x_E}{2} - 1} \frac{\partial^2 \tilde{n}_0}{\partial x^2}.$$
 (11.7.10)

By changing to the dependence in time, we obtain the fractional differential equation [188, 227]

$$\frac{\partial^{\gamma} n_0}{\partial t^{\gamma}} = V_0^2 \left( \frac{a}{\sqrt{2D_0}} \right)^{\alpha_E} \frac{\partial^2 n_0}{\partial x^2} - \frac{n_0(0, x)}{2\sqrt{\pi}t^{\gamma}}, \tag{11.7.11}$$

Further Reading 201

Here, the order of the derivative with respect to time  $\gamma$  depends on the parameter  $\alpha_E$ ,

$$\gamma(\alpha_E) = 2H(\alpha_E) = 2 - \frac{\alpha_E}{2}$$
 , (11.7.12)

which describes correlation properties in the longitudinal direction. In the case of incompressible flows, subdiffusive regimes are impossible and  $\alpha_E \leq 2$ . The special case  $\alpha_E = 1$  corresponds to a white spectrum and recovers the anomalous diffusion found previously by Dreizin–Dykhne with H = 3/4. A fractional differential equation for the Dreizin–Dykhne model is the following:

$$\frac{\partial^{3/2} n_0(t,x)}{\partial t^{3/2}} = \frac{\partial^2}{\partial t^2} \int_0^t \frac{n_0(t',x) dt'}{\sqrt{\pi(t-t')}} = \frac{V_0^2 a}{\sqrt{2D_0}} \frac{\partial^2 n_0(t,x)}{\partial x^2} - \frac{n_0(0,x)}{2\sqrt{\pi}t^{3/2}}.$$
 (11.7.13)

For  $0 \le \alpha_E \le 2$ , one has superdiffusion, while for  $\alpha_E > 2$  we arrive to the conventional diffusive behavior.

#### **Further Reading**

#### Levy Flights

- R. Balescu, Statistical Dynamics (Imperial College, London, 1997)
- R. Botet, M. Poszajczak, *Universal Fluctuations* (World Scientific, Singapore, 2002)
- G.P. Bouchaud, A. Georges, Physics Reports **195**(132–292), 1990 (1990)
- J. Bricmont et al., *Probabilities in Physics* (Springer, Berlin, 2001)
- R. Klages, G. Radons, I. Sokolov (eds.), *Anomalous Transport, Foundations and Applications*. (Wiley, New York, 2008)
- A. Pekalski, K. Sznajd-Weron (eds.), *Anomalous Diffusion. From Basics to Applications* (Springer, Berlin, 1999)
- M.F. Shiesinger, G.M. Zaslavsky, Levy Flights and Related Topics in Physics (Springer, Berlin, 1995)
- G.M. Zaslavsky, Physics Reports **371**, 461–580 (2002)
- Ya.B. Zeldovich, A.A. Ruzmaikin, D.D. Sokoloff, *The Almighty Chance* (World Scientific, Singapore, 1990)

# Continuous Time Random Walk and Scaling

- D. Ben-Avraham, S. Havlin, Diffusion and Reactions in Fractals and Disordered Systems (Cambridge University Press, Cambridge, 1996)
- J.W. Haus, K.W. Kehr, Phys. Rep. **150**, 263 (1987)

- R. Metzler, J. Klafter, Phys. Rep. 339, 1 (2000)
- E.W. Montroll, M.F. Shlesinger, *On the Wonderful World of Random Walks*. Studies in Statistical mechanics, vol. 11 (Elsevier, Amsterdam, 1984), p. 1
- E.W. Montroll, B.J. West, On an Enriches Collection of Stochastic Processes, in *Fluctuation Phenomena*, ed. by E.W. Montroll, J.L. Lebowitz (Elsevier, Amsterdam, 1979)
- V.V. Uchaikin, V.M. Zolotarev, *Chance and Stability Stable Distributions and Their Applications* (VSP, Utrecht, 1999)

#### Fractal Operators

- K. Diethelm, *The Analysis of Fractional Differential Equations. An Application-Oriented Exposition* (Springer, Berlin, 2010)
- L. Pietronero, Fractals' Physical Origin and Properties (Plenum, New York, 1988)
- D. Sornette, Critical Phenomena in Natural Sciences (Springer, Berlin, 2006)
- B.J. West, M. Bologna, P. Grigolini, *Physics of Fractal Operators* (Springer, New York, 2003)
- G. Zaslavsky, *Hamiltonian Chaos and Fractional Dynamics* (Oxford University Press, Oxford, 2005)

#### **Vortex Structures and Trapping**

- A. Crisanti, M. Falcioni, A. Vulpiani, Rivista Del Nuovo Cimento 14, 1–80 (1991)
- E. Guyon, J.-P. Nadal, Y. Pomeau (eds.), *Disorder and Mixing* (Kluwer, Dordrecht, 1988)
- P.J. Holmes, J.L. Lumley, G. Berkooz, J.C. Mattingly, R.W. Wittenberg, Physics Reports **287**, 337–384 (1997)
- A. Maurel, P. Petitjeans (eds.), *Vortex Structure and Dynamics Workshop* (Springer, Berlin, 2000)

# Part VI Isotropic Turbulence and Scaling

# Chapter 12

# **Isotropic Turbulence and Spectra**

#### 12.1 The Reynolds Similarity Law

The knowledge gained from similarity theory is applied in many fields of natural and engineering science, among others, in fluid mechanics. In this field, similarity considerations are often used for providing insight into the flow phenomenon and for generalization of results. The importance of similarity theory rests on the recognition that it is possible to gain important new insights into flows from the similarity of conditions and processes without having to seek direct solutions for posed problems. Thus, the Navier–Stokes equation of motion for a Newtonian fluid is given by

$$\frac{\partial \vec{u}}{\partial t} + (\vec{u} \nabla)\vec{u} = -\frac{1}{\rho_m} \nabla p + v_F \Delta \vec{u}, \qquad (12.1.1)$$

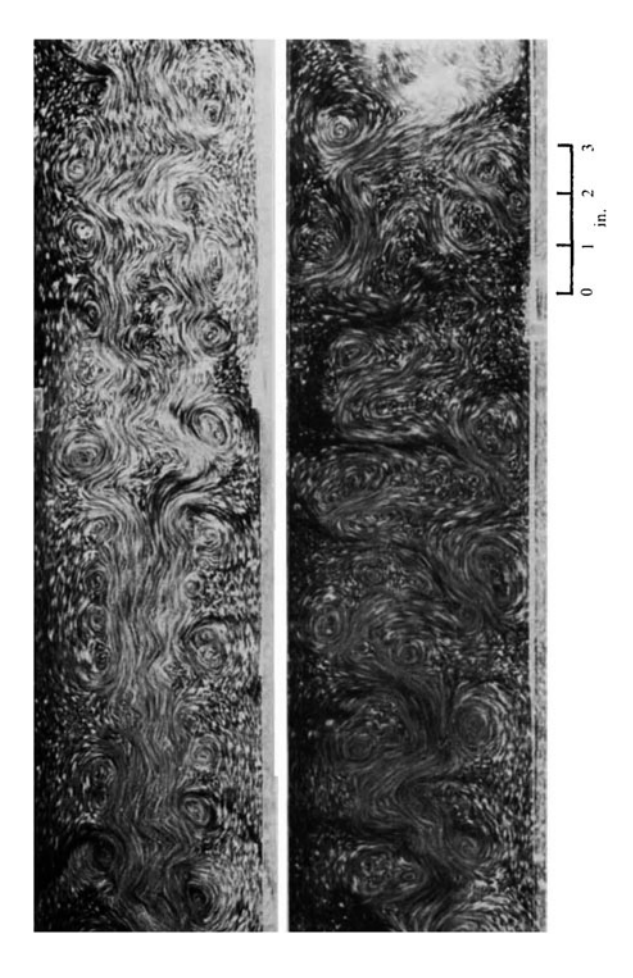
where  $\vec{u}(\vec{r},t)$  is the Eulerian velocity,  $\rho_m$  is the density, and  $v_F$  is the kinematic viscosity. It is well known that the properties of a flow on all scales depend on the Reynolds number [228–233]

$$Re = \frac{V_0 L_0}{v_E}. (12.1.2)$$

Here,  $V_0$  is a typical macroscopic velocity and  $L_0$  is a typical gradient scale length. Flows with Re < 100 are laminar. On the other hand, fluids and plasmas often exhibit a turbulent behavior. The standard criterion for turbulence to develop is that the Reynolds number must be sufficiently high (see Fig. 12.1.1). Especially in the astrophysical system, due to the large spatial scales, Reynolds numbers are in general huge and most environmental and astrophysical fluids and plasmas are therefore observed or expected to be strongly turbulent.

In similarity considerations, strictly, only quantities with the same physical units can be included. The "dimensionless proportionality factors" of the different terms

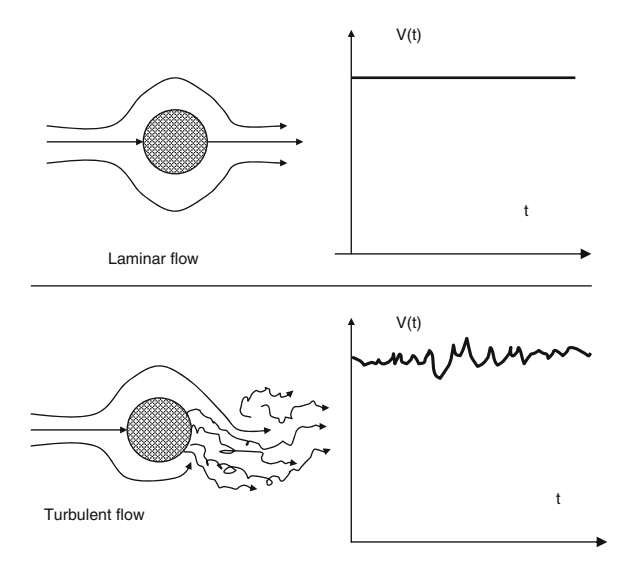
**Fig. 12.1.1** Example of a turbulent flow at about Re = 5,500 (After Papailiou and Lykoudis [234] with permission)



of a physical relationship computed from it by dividing all terms by one term in the equation are designated similarity numbers or dimensionless characteristic numbers of the physical problem. Physical processes of all kinds can thus be categorized as similar only when the corresponding dimensionless characteristic numbers, defining the physical problem, are equal. This requires, in addition, that geometric similarity exists and the boundary conditions for the considered problems are similar. The concept of similarity can therefore only be applied to physical processes of the same kind, i.e., to fluid flows or heat transport processes separately. When certain relationships apply both to flow processes and to heat transfer process, one talks of an analogy between the two processes.

In order to illustrate the sort of way in which Reynolds number can affect the flow configuration, we shall consider a specific geometry, namely an infinite circular cylinder in an otherwise unbounded fluid (see Fig. 12.1.2), the flow far from the cylinder being uniform. The Reynolds number appropriate to this problem is

Fig. 12.1.2 Flows of water past a cylinder for different values of the Reynolds number



 $Re = V_0 L_0 / v_F$ , where  $V_0$  is the velocity of the fluid far from the cylinder and  $L_0$  is the diameter of the cylinder.

To describe flow processes, it is necessary to integrate the conservation laws just derived. Since the integration of these equations in closed form is, in general, not possible because of the inherent mathematical difficulties, flows are often investigated experimentally. Fluid mechanical and thermodynamic data are measured with models geometrically similar to the full-scale configuration, for which the flow is to be determined. However, since in general the models are smaller in size, the measured data have to be applied to the full-scale configuration with the rules of the theory of similitude. This theory makes use of similarity parameters, in which the characteristic quantities with physical dimensions of the flow considered are combined to dimensionless quantities. Two flows about geometrically similar bodies are called similar, if the individual similarity parameters have the same value for both flows. The similarity parameters, which are important for the flow process considered, can either be determined with the method of dimensional analysis applied to the physical properties of the flow or by nondimensionalizing the conservation equations.

# 12.2 Cascade Phenomenology

Most of the water and air around us is in turbulent states. The complexity of the shape of cigarette smoke is also due to turbulence. On the other hand, observed features such as star-forming clouds and accretion discs are very chaotic with  $Re \ge 10^8$ . Chaotic structures develop gradually as Re increases, and those with  $Re \sim 10^3$  are appreciably less chaotic than those with  $Re \sim 10^7$ . Indeed, when the

Reynolds number is small, viscosity stabilizes the flow. When it is greater than  $10^4$ , the flow is unstable and becomes turbulent. For water at room temperature,  $v_F$  is about  $10^2$  cm<sup>2</sup>/s; hence, flow becomes turbulent for relatively small  $L_0$  and  $V_0$  – for example  $L_0 \approx 10$  cm and  $V_0 \approx 10$  cm/s. Nearly the same estimate can be made for air.

In 1941, Kolmogorov introduced a statistical theory of small-scale eddies in high Reynolds number incompressible turbulence [235, 236]. The theory was based on two fundamental hypotheses: first, the distribution of the velocity difference

$$\delta V_l(l) = \vec{l} \, \nabla \, \vec{u}(\vec{r}) \tag{12.2.1}$$

between two points in space is a universal function, depending only on the spatial separation  $|\vec{l}|$ , the kinematic viscosity  $v_F$ , and the mean energy dissipation per unit mass  $\varepsilon_K$ 

$$\varepsilon_K = \frac{v_F}{4} \sum_{i,j} \left\langle \left( \frac{\partial u_i}{\partial x_j} + \frac{\partial u_j}{\partial x_i} \right)^2 \right\rangle,$$
 (12.2.2)

where  $\langle ... \rangle$  denotes an ensemble average. For instance, the mean atmospheric dissipation rate is of order  $1.5 \times 10^{-6}$  m<sup>2</sup>/s<sup>3</sup>. Second, when the spatial separation is sufficiently large compared with the characteristic dissipation length scale, the distribution does not depend on  $v_F$ . From these hypotheses and dimensional analysis, Kolmogorov deduced that, while the stirring force that creates turbulence will surely vary from flow to flow and will affect the turbulence characteristics, the small-scale/high-wave number motions at which dissipation takes place develop a common form for all flows. If this is true, it can be argued that the equilibrium state should be scaled by the viscosity  $v_F$  and dissipation rate  $\varepsilon_K$ . In this case, the length scale and characteristic timescale are given by

$$l_{\nu} \equiv \frac{v_F^{3/4}}{\varepsilon_K^{1/4}}, \quad \tau_{\nu} = \left(\frac{v_F}{\varepsilon_K}\right)^{1/2}. \tag{12.2.3}$$

They are known as the Kolmogorov length and timescale, respectively, and they should be good yardsticks of dissipative phenomena. Typically  $l_{\nu} \approx 1/4 \, \text{mm}$  (strong wind tunnels) to 8 mm (mean atmosphere). Additionally, a velocity scale

$$V_{\nu} = \frac{l_{\nu}}{\tau_{\nu}} = (\nu_F \varepsilon_K)^{1/4}$$
 (12.2.4)

can be formed on the basis of the Kolmogorov length and timescale. Typically  $V_{\nu} \approx 60 \, \mathrm{mm/s}$  (strong wind tunnels) to 2 mm/s (mean atmosphere).

Because of additionally assumed statistical isotropy, the field increments depend solely on l, which allows one to define the characteristic eddy velocity

 $V_l = \left<\delta V_l^2\right>^{1/2}$ , or in terms of spectral terminology often used in turbulence theory  $V_k = \left<\delta V_k^2\right>^{1/2}$ , where k is the wave number,  $k \approx l^{-1}(k) = l_k$ . There are three scale ranges (see Fig. 12.2.1): the energy-containing scales, driving the flow, the inertial range, where nonlinear interactions govern the dynamics and the influence of driving and dissipation is negative, and the dissipation range at smallest scales, where dissipative effects dominate, removing energy from the system. Suppose that the fluid motion is excited at scales  $L_E$  and greater. A far-reaching idea of Kolmogorov was that of an inertial subrange ( $k_E \ll k \ll k_v$ ) consisting of a section of wave number space between  $k_E$  and  $k_v$ 

$$k_E = \frac{1}{L_E}, \quad k_v = \frac{1}{l_v} \propto Re^{3/4} k_E,$$
 (12.2.5)

where energy cascade toward small scales without significant dissipation or production. In principle, such a picture was already in the mind of Richardson about 20 years before Kolmogorov when he developed a qualitative theory of turbulence. Such a cascade in this range of wave numbers would depend on just  $\varepsilon_K$  and not  $v_F$ .

Kolmogorov argued that this has an important consequence for the form of the energy spectrum function E(k). The one-dimensional energy spectrum is the amount of energy between the wave number k and (k + dk) divided by dk

$$V_k^2 = \int_{\Delta k} E(k) \, \mathrm{d}k \approx k E(k). \tag{12.2.6}$$

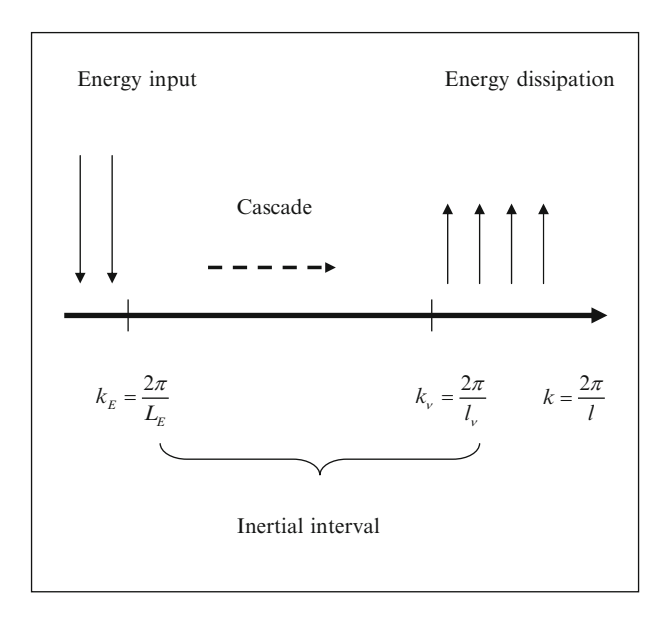
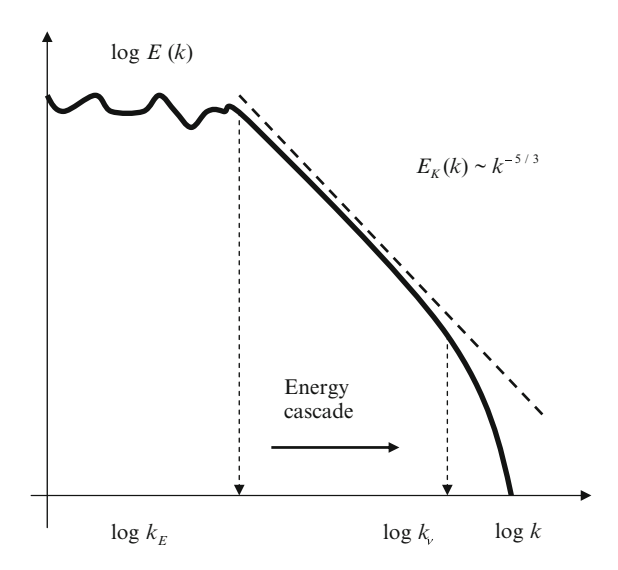


Fig. 12.2.1 Schematic picture of energy cascade in homogeneous and isotropic turbulence

Fig. 12.2.2 A typical plot of Kolmogorov energy spectra in fully developed homogeneous isotropic turbulence



Because E(k) has units of  $(length)^3/s^2$ , the only form E(k) dimensionally consistent with a scaling in terms of k and  $E_K$  is given by (see Fig. 12.2.2)

$$E_K(k) \propto C_K k^{-5/3} \varepsilon_K^{2/3},$$
 (12.2.7)

where  $C_K$  is the Kolmogorov constant and  $k_E \ll k \ll k_v$ .

Indeed, within the internal range the statistical properties of the turbulence are determined by the local wave number k and  $\varepsilon_K$ , the rate of cascade energy, which is scale-independent,

$$\varepsilon_K \propto \frac{V_k^3}{l_k} \propto \frac{V_k^2}{\tau_K(k)} \propto \frac{V_k^2}{(kV_k)^{-1}}.$$
 (12.2.8)

The energy cascades through nonlinear interactions to progressively smaller and smaller scales at the eddy turnover rate,  $\tau_K(k) \approx 1/V_k(k)k$ , with insignificant energy losses along the cascade. From this relation, we obtain

$$\tau_K(k) \approx \frac{1}{\varepsilon_K^{1/3} k^{2/3}} \tag{12.2.9}$$

$$V_k \approx (\varepsilon_K l_k)^{1/3} \approx \left(\frac{\varepsilon_K}{k}\right)^{1/3},$$
 (12.2.10)

$$E_K(k) \propto kV_k^2 \propto k^{-5/3} \varepsilon_K^{2/3}$$
. (12.2.11)

This prediction of a -5/3 spectrum is amenable to experimental verification and, in fact, has been observed to occur in a wide range of turbulent flows at high

Reynolds numbers [75–78] with the typical value  $C_K = 1.6$ . Results accumulated from many different experiments in different types of turbulent flows (particularly from atmospheric and oceanographic turbulence) and covering a very wide range of wavenumbers are shown in Fig. 12.2.3.

#### 12.3 The Taylor Microscale

The important feature, which has been realized in [235], was the idea of a virtually continuous range of eddy sizes, with turbulent energy being handed down from larger to smaller eddies and ultimately dissipated in viscous action. It is natural to employ the expression for the mean energy dissipation per unit mass  $\varepsilon_K$ 

$$\varepsilon_K = \frac{v_F}{4} \sum_{i,j} \left\langle \left( \frac{\partial u_i}{\partial x_j} + \frac{\partial u_j}{\partial x_i} \right)^2 \right\rangle,$$
 (12.3.1)

to obtain one more characteristic scale. In the framework of dimensional analysis, the mean energy dissipation can be represented as

$$\varepsilon_K = \nu_F \frac{V_0^2}{\lambda_T^2}.\tag{12.3.2}$$

Here,  $\lambda_T$  is the Taylor microscale and  $V_0$  is the turbulent fluctuation amplitude. The Taylor spatial scale is an intermediate one because it is less than macroscale  $L_0$  and greater than the Kolmogorov viscous spatial scale  $l_v \equiv \frac{v_F^{3/4}}{\epsilon_k^{1/4}}$ 

$$l_{\nu} \ll \lambda_T \ll L_0. \tag{12.3.3}$$

Initially, the Taylor microscale was introduced to characterize the Eulerian correlation function behavior

$$\lambda_T \propto -\frac{C_E(0)}{2C''_E(0)}.$$
 (12.3.4)

Here,  $C_E(\vec{r})$  is the Eulerian correlation function.

By using the estimate of the dissipation rate in the following form:

const 
$$\approx \varepsilon_K \propto \frac{V_0^3}{L_0} \propto \frac{V^3(l)}{l}$$
 (12.3.5)

one can find the relation among the characteristic scales, which are often used in cascade phenomenology

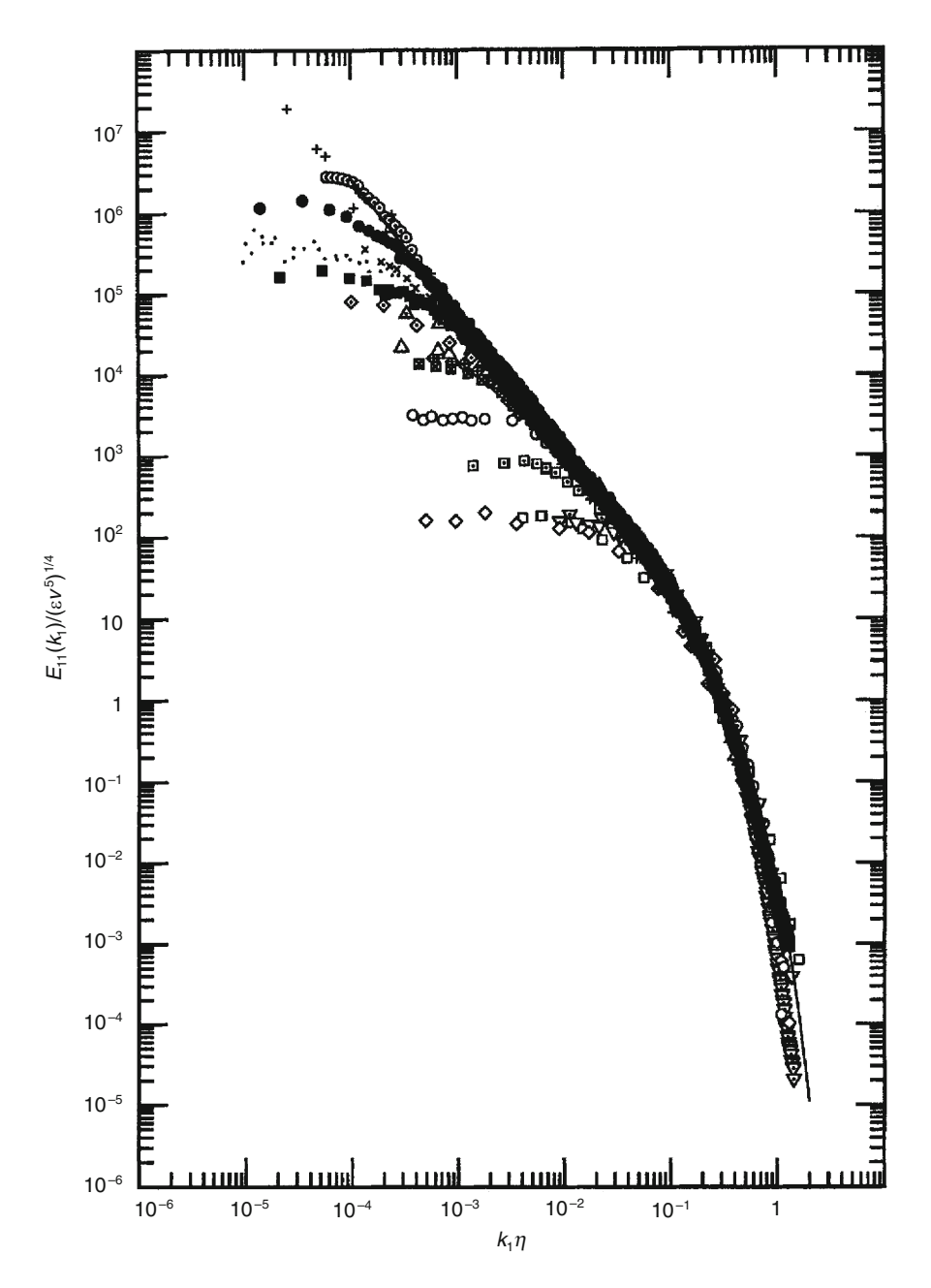


**Fig. 12.2.3** Kolmogorov's universal scaling for one-dimensional longitudinal power spectra. The present min-layer spectra for both free-stream velocities are compared with data from other experiments. (After Saddoighi and Veeravalli [237] with permission)

$$l_{\nu} \propto \frac{\lambda_T}{Re^{1/2}} \ll \lambda_T \propto \frac{L_0}{Re^{1/2}} \ll L_0.$$
 (12.3.6)

In a typical grid turbulence laboratory experiment, the large scale  $L_0$  is of order of 5 cm, whereas the Taylor microscale is approximately 2 mm and the viscous Kolmogorov spatial scale is about 0.1 mm.

The original Taylor definition is slightly different from the definition represented above. He used the formula for the isotropic turbulence in the rigorous form

$$\varepsilon_K = 15v_F \frac{\left\langle u_i^2 \right\rangle}{\lambda_T^2},\tag{12.3.7}$$

where  $u_i$  is *i*-component of the velocity fluctuation and the coefficient 15 in this representation is considerably large than one because so many components are involved. The Taylor microscale can be relatively easily experimentally measured. However, to discuss scaling arguments the simplified definition is also suitable.

### 12.4 Dissipation and Kolmogorov's Scaling

There is no commonly accepted unique definition of turbulent flow, and it is usually identified by its main features. Turbulence implies fluid motion in a broad range of spatial and temporal scales, so that many degrees of freedom are excited in the system. The viscous dissipation characteristic scale is given by the relation

$$l_{\nu} \propto \left(\frac{{\nu_F}^3}{\varepsilon_K}\right)^{1/4}$$
. (12.4.1)

By applying the Kolmogorov hypothesis

$$const \approx \varepsilon_K \propto \frac{V_k^3}{l_k} \propto \frac{V_0^2}{L_0}, \tag{12.4.2}$$

we arrive at the scaling for the characteristic length in the form

$$l_{\nu}(V_0) \propto \left(\frac{1}{V_0}\right)^{3/4}$$
. (12.4.3)

This means that the depth of the Kolmogorov cascade penetration scales inversely with the turbulent fluctuations amplitude.

Let us estimate the number of degrees of freedom excited in developed turbulence on the basis of the dissipation length scale. Since structures of size

$$l \ll l_{\nu} \propto \frac{1}{k_{\nu}} \tag{12.4.4}$$

are ironed out by viscous dissipation and slaved to larger scales, we have only to count the number of presumably independent structures of size approximately equal to  $l_v$  in a domain of volume  $L_E^3$ . This leads to the estimate of the number of degrees of freedom excited in a turbulent flow

$$N_* \propto \left(\frac{L_E}{l_v}\right)^3 \propto \left(\frac{k_v}{k_E}\right)^3 \propto k_E^3 R^{9/4}.$$
 (12.4.5)

However, nonlinear interactions are expected to reduce this number in much the same way as in weakly confined systems. Furthermore, the assumption of a constant energy transfer rate all along the cascade, which is the basis of the Kolmogorov similarity approach, implicitly contains the idea that the energy transferred was equally shared by all the daughter eddies at half scale.

The information regarding the similarity concept can be looked at from another point of view. In the inviscid limit, the Navier–Stokes equation is invariant under the rescaling,

$$x \to x' = \lambda x,\tag{12.4.6}$$

$$t \to t' = \lambda^{(1-\alpha_I/3)}t,\tag{12.4.7}$$

$$u \to u' = \lambda^{\alpha_I/3} u, \tag{12.4.8}$$

for any  $\alpha_I$ . Note that in a general case the values of the scaling exponent  $\alpha_I$  are limited by requiring that the velocity fluctuations do not break incompressibility.

In the context of the well-developed turbulence description, let us consider the local dissipation rate  $\varepsilon_r$ , which is dimensionally given by the simple estimate  $\varepsilon_r \propto \frac{u_r^3}{r}$ , and hence scales as  $\lambda^{\alpha_I-1}$ . This would mean that

$$\frac{\varepsilon_r}{\varepsilon_{L_0}} \propto \left(\frac{r}{L_0}\right)^{\alpha_I - 1}.\tag{12.4.9}$$

The constancy of  $\varepsilon_r$  in the Kolmogorov picture now suggests  $\alpha_I = 1$  in three-dimensional space.

The scaling behavior is one of the most intriguing aspects of fully developed turbulence. Indeed, this is an important property of turbulent Navier–Stokes fluids that everybody agrees on now that the dissipation rate is not determined by anything microscopic or molecular that happens. There is no parameter that governs the dissipation rate; rather the fluid dissipates whatever you throw at it. If you stir the fluid harder, the spectrum just moves a little farther out in k space until it finds a place where the energy can be dissipated at the same rate it is being injected.

#### 12.5 Acceleration and Similarity Approach

The fluid particle acceleration is among the most natural physical parameters of interest in turbulence research. The material derivative of the velocity vector is given by the Navier–Stokes equation

$$\vec{A} = \frac{D\vec{A}}{dt} = \frac{\partial \vec{u}}{\partial t} + (\vec{u} \nabla)\vec{u} = -\frac{1}{\rho_{m}} \nabla p + v_{F}\Delta \vec{u}, \qquad (12.5.1)$$

where  $\vec{A}(\vec{r},t)$  is the Eulerian acceleration, p is the pressure,  $\rho_m$  is the density, and  $v_F$  is the kinematic viscosity. In fully developed turbulence, the viscous damping term is small compared to the pressure gradient term and therefore the acceleration is closely related to the pressure gradient. Basing on the Kolmogorov theory of isotropic turbulence, it can be argued that the acceleration should be scaled by the viscosity  $v_F$  and dissipation rate  $\varepsilon_K$ . In the case under consideration, one finds [238]

$$A \propto \left(\frac{\varepsilon_K^3}{\nu_F}\right)^{1/4}.\tag{12.5.2}$$

Indeed, the acceleration must scale with the dissipation rate  $\varepsilon_K$  and it scales inversely with the viscosity  $v_F$ . In terms of dimensional arguments, this means

$$[A] = \left[\frac{\mathbf{m}^2}{\mathbf{s}^3}\right]^x \left[\frac{\mathbf{s}}{\mathbf{m}^2}\right]^y = \left[\frac{\mathbf{m}}{\mathbf{s}^2}\right]. \tag{12.5.3}$$

After simple algebra, one obtains the conditions

$$2x - 2y = 1$$
,  $2x - y = 2$ . (12.5.4)

Hence, the exponents of interests are x = 3/4, y = -1/4. The classical prediction of the variance of acceleration components (correlation function) is

$$\langle A_i A_J \rangle = \text{const} \left( \frac{\varepsilon_K^3}{v_F} \right)^{1/2} \delta_{ij}.$$
 (12.5.6)

Recent measurements indicate that this scaling is observed for the large Reynolds numbers 500 < Re < 1,000 [239]. It was found that the acceleration is a very intermittent variable with extremely large acceleration arising in structures.

The use of accelerations in a chaotic flow description possesses a large potential. Thus, it would be fruitful to employ not only the phase space, but also the acceleration space to treat nontrivial effects of turbulent transport. The situation at hand is close to that with the one-dimensional kinetic equation considered by Kramers. In order to achieve the Markovian character of the processes under the conditions of

spatial nonuniformity, he had to introduce an additional independent variable (velocity). In phase space, this made it possible to describe transport in nonuniform media, where the density gradient plays an essential role. In the anomalous transport description, applying the acceleration space could give additional degrees of freedom to treat nonlocal and memory effects [240].

## **Further Reading**

#### Hydrodynamics and Scaling

- G.I. Barenblatt, *Scaling Phenomena in Fluid Mechanics* (Cambridge University Press, Cambridge, 1994)
- G.K. Batchelor, *An Introduction to Fluid Dynamics* (Cambridge University Press, Cambridge, 1973)
- O. Darrigol, Words of Flow: A History of Hydrodynamics from the Bernoullis to Prandtl (Oxford University Press, New York, 2009)
- C.R. Doering, J.D. Gibbon, *Applied Analysis of the Navier–Stokes Equations* (Cambridge University Press, Cambridge, 1995)
- G.S. Golitsyn, Selected Papers (Moscow, Nauka, 2008)
- J. Katz, Introductory Fluid Mechanics (Cambridge University Press, Cambridge, 2010)
- J.-L. Lagrange, Mecanique Analytique (Cambridge University Press, Cambridge, 2009)
- A.J. Majda, A.L. Bertozzi, *Vorticity and Incompressible Flow* (Cambridge University Press, Cambridge, 2002)
- P. Mueller, *The Equations of Oceanic Motions* (Cambridge University Press, Cambridge, 2006)
- L. Prandtl, O.G. Tietjens, *Applied Hydro- and Aeromechanics* (McGraw Hill, London, 1953)
- M. Samimy et al., A Gallery of Fluid Motion (Cambridge University Press, Cambridge, 2003)
- P. Taberling, O. Cardoso, *Turbulence A Tentative Dictionary* (Plenum, New York, 1994)
- M. Van-Dyke, An Album of Fluid Motion (Parabolic, Stanford, CA, 1982)

#### **Turbulence**

- G.K. Batchelor, *The Theory of Homogeneous Turbulence* (Cambridge University Press, Cambridge, 1959)
- P.A. Davidson, *Turbulence, An Introduction for Scientists and Engineers* (Oxford University Press, Oxford, 2004)

Further Reading 217

U. Frisch, *Turbulence: The Legacy of A. N. Kolmogorov* (Cambridge University Press, Cambridge, 1995)

- J.R. Herring, J.C. McWilliams, *Lecture Notes on Turbulence* (World Scientific, Singapore, 1987)
- M. Lesieur, *Turbulence in Fluids* (Springer, Berlin, 2008)
- D.C. Leslie, *Developments in the Theory of Turbulence* (Clarendon, Oxford, 1973)
- W.D. McComb, *The Physics of Fluid Turbulence* (Clarendon Press, Oxford, 1994)
- A.S. Monin, A.M. Yaglom, Statistical Fluid Mechanics (MIT, Cambridge, 1975)
- K.R. Sreenivasan, Rev. Mod. Phys. 71, S 383 (1999)

#### Statistical Aspects of Turbulence

- S. Heinz, Statistical Mechanics of Turbulent Flows (Springer, Berlin, 2003)
- M. Lesieur et al. (eds.), New Trends in Turbulence (Springer, Berlin, 2001)
- J.L. Lumley (ed.), *Fluid Mechanics and the Environment. Dynamical Approaches* (Springer, Berlin, 2001)
- M. Oberlack, F.H. Busse (eds.), *Theories of Turbulence* (Springer, New York, 2002)
- J. Peinke, A. Kittel, S. Barth, M. Oberlack (eds.), *Progress in Turbulence* (Springer, Berlin, 2005)
- S.B. Pope, *Turbulent Flows* (Cambridge University Press, Cambridge, 2000)
- Y. Zhou, Phys. Rep. 488, 1 (2010)

# Simulation of Turbulent Flows

- P.S. Bernard, J.M. Wallace, *Turbulent Flow. Analysis, Measurement, and Prediction* (Wiley, New York, 2002)
- H.A. Dijkstra, Nonlinear Physical Oceanology (Springer, Berlin, 2006)
- P. Durbin, B. Pettersson-Reif, *Statistical Theory and Modeling for Turbulent Flows* (Wiley, New York, 2010)
- J. Hoffman, C. Johnson, *Computational Turbulent Incompressible Flow* (Springer, Berlin, 2007)
- M.Z. Jacobson, *Fundamentals of Atmospheric Modeling* (Cambridge University Press, Cambridge, 2005)
- P. Lynch, *The Emergence of Numerical Weather Prediction* (Cambridge University Press, Cambridge, 2006)
- R. Schiestel, *Modeling and Simulation of Turbulent Flows* (Wiley, New York, 2008)

# Chapter 13 **Turbulence and Scalar**

### 13.1 Scalar in Inertial Subrange

Velocity field generates fluctuations of various scalar quantities  $\theta$  in the turbulent flow: temperature, pressure, humidity, and so on (see Fig. 13.1.1). Soon after Kolmogorov's first seminal papers on energy spectrum of turbulence, cascade ideas were applied to passive scalars advected by turbulence [241, 242]. This is the problem of determining the statistical properties of the distribution of a scalar field that is convected and diffused within a field of turbulence of known statistical properties. The advection–diffusion equation is given by

$$\frac{\partial \theta}{\partial t} + \vec{u} \cdot \nabla \theta = D_0 \nabla^2 \theta, \tag{13.1.1}$$

where  $D_0$  is the molecular diffusivity and  $\vec{u}$  is the advection velocity, which is nondivergent. The dissipation rate of the scalar 'energy'  $\langle \theta^2 \rangle$  can be described by the equation, which is similar to the energy conservation law

$$\frac{\partial \langle \theta^2 \rangle}{\partial t} = -2D_0 \langle |\nabla \theta|^2 \rangle. \tag{13.1.2}$$

Fourier component of the spectrum of  $\theta$  is changed by the interaction between  $\theta$  and  $\vec{u}$ ; other Fourier components are changed simultaneously in such a way that the sum of the contributions to  $\langle \theta^2 \rangle$  from all Fourier components remains the same. This shows that  $\theta$  variance is simply transferred from small to large wave numbers in the advection subrange and  $\varepsilon_{\theta}$  is a given constant quantity. The dissipation rate of the scalar 'energy'  $\langle \theta^2 \rangle$  is also the spectral transfer rate. By following the line of argument of Obukhov and Corrsin, we suppose that the seed diffusivity  $D_0$  is so small as to make the effect of diffusion appreciable only at the large wave number end of the spectrum. By keeping the Kolmogorov estimate for the characteristic time of nonlinear interaction in the case of scalar cascade

220 13 Turbulence and Scalar

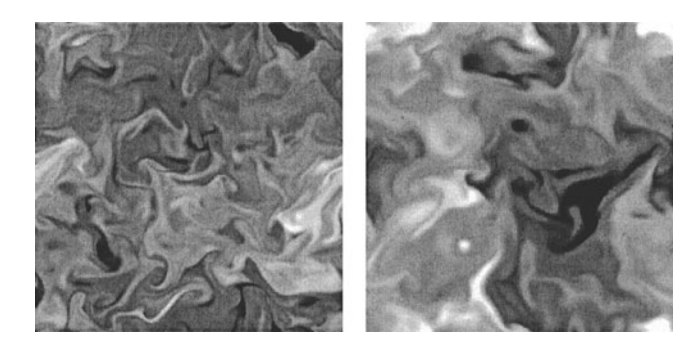


Fig. 13.1.1 The scalar distribution on a two-dimensional plane (After Brethouwer et al. [2] with permission)

$$\tau_K(k) \approx \frac{l}{V(l)} \propto \frac{l}{(\varepsilon_K l)^{1/3}} \propto \frac{1}{\varepsilon_K^{1/3} k^{2/3}},$$
(13.1.3)

one can obtain the expression for a scalar flux in the following form:

$$\varepsilon_{\theta} \propto \frac{\theta_k^2}{\tau_K(k)} = \frac{\theta_k^2}{(kV_k)^{-1}}.$$
 (13.1.4)

The scalar spectrum is given by the relation

$$E_{\theta}(k) = \int |\theta_k|^2 dW_k \tag{13.1.5}$$

In the inertial-convective subrange, where neither viscosity nor diffusion is important the scaling of interest takes the form (see Fig. 13.1.2)

$$E_{\theta}(k) = \frac{\theta_k^2}{k} \propto \frac{\varepsilon_{\theta} \tau_K(k)}{k} \propto C_{\theta} \varepsilon_{\theta} \varepsilon_{K}^{-1/3} k^{-5/3}, \tag{13.1.6}$$

where

$$k > k_{\nu} \propto 1/l_{\nu} \propto \left(\frac{\varepsilon_K}{\nu_F^3}\right)^{1/4}$$
 (13.1.7)

In this range of wave numbers, the Fourier components of  $\vec{u}$  are independent of viscosity (inertial subrange) and the Fourier components of  $\theta$  are independent of molecular diffusion (convective subrange). The  $k^{-5/3}$  temperature spectrum has been observed experimentally in turbulence of sufficiently high Reynolds number (see Fig. 13.1.3). The parameter  $C_{\theta}$ , called the Obukhov–Corrsin constant, is found in the range  $C_{\theta} \approx 0.45 - 0.55$  [75–78].

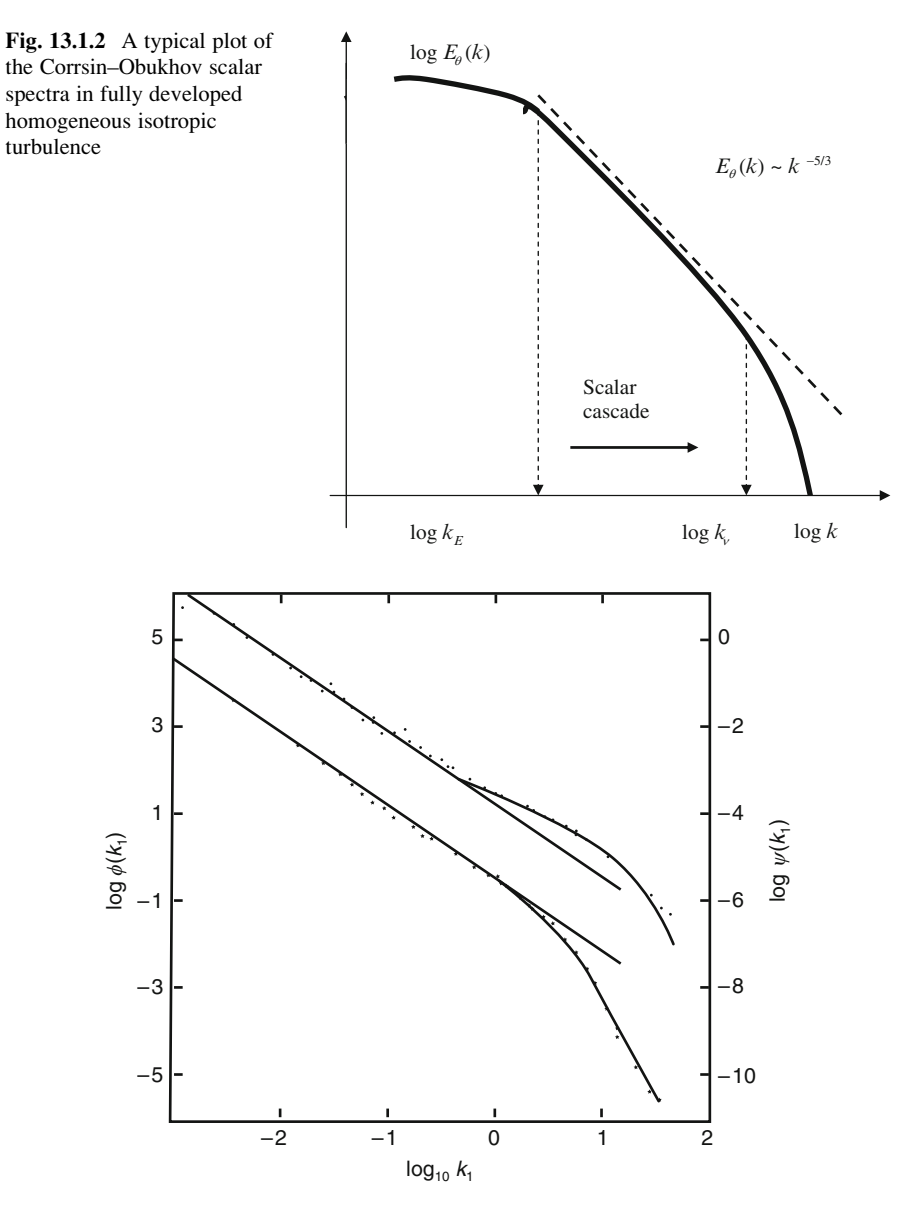


Fig. 13.1.3 Temperature and velocity spectra at a depth of 15 m near Cape Mudge. (After Grant [243] with permission)

The scaling for the scalar perturbation on scales of order l is given by the formula

$$\delta\theta(l) \propto \sqrt{\varepsilon_{\theta}\tau_{K}(l)} \propto \sqrt{\frac{\varepsilon_{\theta}l}{(\varepsilon_{K}l)^{1/3}}} \propto l^{1/3},$$
 (13.1.8)

222 13 Turbulence and Scalar

which leads to estimate for the scalar gradient as follows:

$$\nabla \theta \propto \frac{\delta \theta(l)}{l} \propto \frac{1}{l^{2/3}}.$$
 (13.1.9)

We see that decreasing spatial scales leads to increasing scalar gradients and creating fascinating pictures (see Fig. 13.1.1).

In contrast to the Kolmogorov phenomenological arguments for the energy spectrum where only two relations were used

$$const = \varepsilon_K \propto \frac{V_k^2}{\tau_K(k)}, \qquad (13.1.10)$$

$$\tau_K(k) \approx \frac{1}{V_k(k)k}.\tag{13.1.11}$$

In the case of scalar spectrum, one more supposition was applied. Indeed, we save the condition const  $= \varepsilon_{\theta}$  as well as the estimate for the characteristic time  $\tau_K(k)$ , but we extract the scaling for the velocity  $V_k \approx \left(\frac{\varepsilon_K}{k}\right)^{1/3}$  directly from the Kolmogorov analysis.

In this sense, this approach loses its "universality", but when we are dealing with the problem of scalar transport, extra arguments are often a necessary part of description. Indeed, the appearance of additional degrees of freedom allows one to describe numerous regimes of turbulent transport. However, such mobility makes us hesitant in choosing appropriative solution.

# 13.2 The Batchelor Scalar Spectrum

Batchelor [39, 152] recognized the critical importance of the dissipation region  $l < l_{\nu} \approx \left(\frac{v_F^3}{\varepsilon_K}\right)^{1/4}$  to describe small-scale turbulence. In this range of scales, the Kolmogorov scaling for the velocity  $V(l) \propto (\varepsilon_K l)^{1/3}$ should be replaced by the linear dependence (see Fig. 13.2.1)

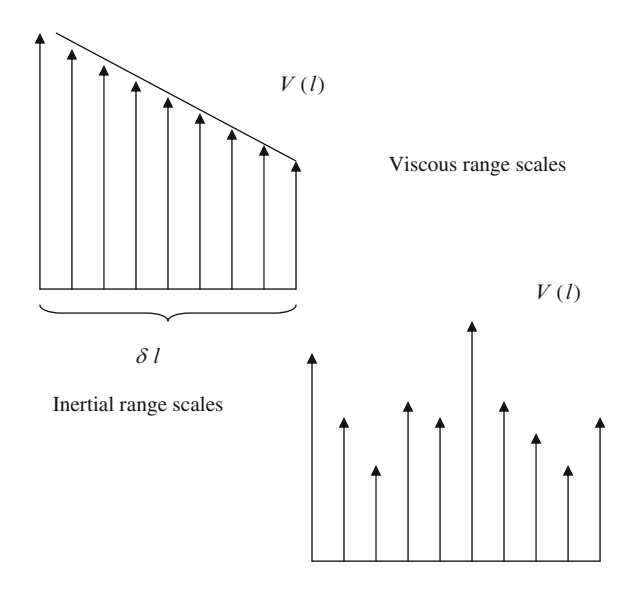
$$V(l) \propto {\rm const} \ l \propto \left(\frac{\varepsilon_K}{v_F}\right)^{1/2} l.$$
 (13.2.1)

Here, we use the viscous characteristic time  $\tau_{\nu}$ .

We derive now the spectrum for the viscous–convective range of scales. The boundary of this region is given by the diffusive estimate

$$l_B^2 \propto D_0 \tau_v \propto \left(\frac{D_0 v_F^2}{\varepsilon_K}\right)^{\frac{1}{2}}$$
 (13.2.2)

Fig. 13.2.1 Schematic picture of the velocity differences on the distance for laminar and turbulent flow



If the Prandtl number

$$Pr = \frac{v_{\rm F}}{D_0} \tag{13.2.3}$$

is large, the Batchelor scale is small compared with the Kolmogorov scale  $l_{\nu}$ 

$$l_B \approx \left(\frac{D_0 v_F^2}{\varepsilon_K}\right)^{\frac{1}{4}} < < \left(\frac{v_F^3}{\varepsilon_K}\right)^{\frac{1}{4}} \approx l_v.$$
 (13.2.4)

On scales between the Kolmogorov scale and the Batchelor scale, the velocity gradient is approximately uniform. On these grounds, it is possible to determine the spectrum of fluctuations of the scalar field in the viscous—convective subrange. The expression for a scalar flux is given by

$$\varepsilon_{\theta} \propto \frac{\theta_{k}^{2}}{\tau_{\text{CASC}}(k)} \propto \frac{\theta_{k}^{2}}{(kV_{k}(k))^{-1}} \propto \frac{\theta_{k}^{2}}{\tau_{v}} \propto \left(\frac{\varepsilon_{K}}{v_{\text{F}}}\right)^{2} \theta_{k}^{2}.$$
(13.2.5)

Here, we apply the linear approximation for the velocity  $V(l) \propto \left(\frac{\varepsilon_K}{v_F}\right)^{1/2} l$ . This yields the scaling of interest

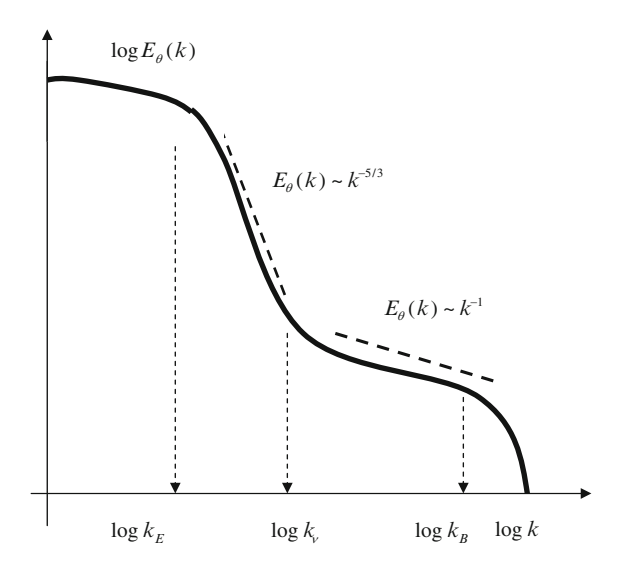
$$E_{\theta}(k) = \frac{\theta_k^2}{k} \propto \frac{\varepsilon_{\theta} \tau_{\nu}}{k}$$
 (13.2.6)

Finally, one obtains (see Fig. 13.2.2)

$$E_{\theta}(k) \propto \text{const } \varepsilon_{\theta} \left(\frac{v_F}{\varepsilon_K}\right)^{1/2} \frac{1}{k},$$
 (13.2.7)

224 13 Turbulence and Scalar

Fig. 13.2.2 Idealized Batchelor scalar spectra in fully developed homogeneous isotropic turbulence



where

$$l_{\nu}^{-1} = k_{\nu} < k < k_B = l_B^{-1}. \tag{13.2.8}$$

We stress that Batchelor succeeded in describing the exponential instability effects in terms of cascade phenomenology. Indeed, in the viscous range of scales we are dealing with the exponential stretching

$$\frac{\mathrm{d}}{\mathrm{d}t}l \propto V(l) \propto \mathrm{const}\ l. \tag{13.2.9}$$

The value  $l_B \approx \left(\frac{D_0 v_F^2}{\varepsilon_K}\right)^{\frac{1}{4}}$  describes the depth of the scalar cascade penetration and at the same time this is the stretching characteristic scale (see Fig. 13.2.3). In contrast to the single-scale approximation here, we are dealing with the hierarchy of scales. Using the Kolmogorov assumption

const 
$$\approx \varepsilon_K \propto \frac{V_k^3}{l_k} \propto \frac{V_0^2}{L_0}$$
, (13.2.10)

one finds the scaling for the characteristic length in terms of the Peclet number

$$l_B \approx \left(L_0 \frac{D_0 v_F^2}{{V_0}^3}\right)^{\frac{1}{4}} \propto \frac{1}{Pe^{3/4}},$$
 (13.2.11)

which differs from the single-scale approximation.

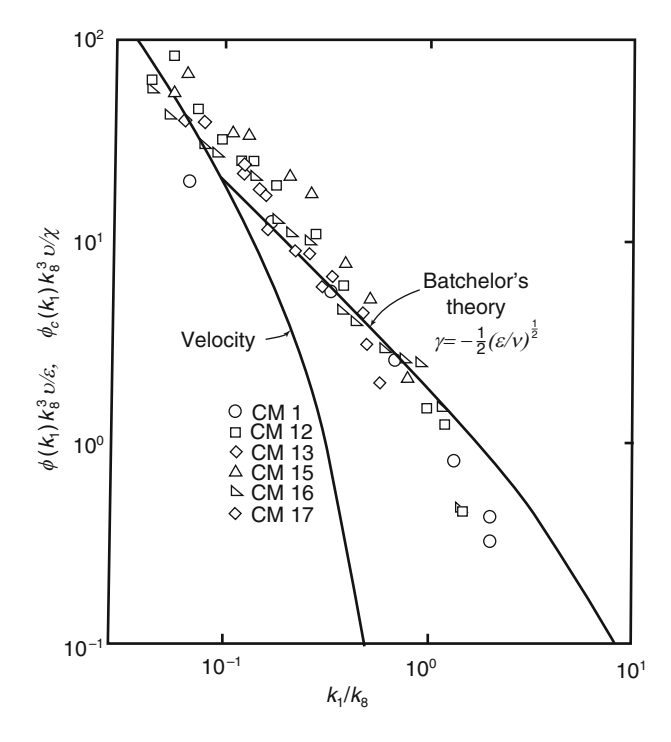


Fig. 13.2.3 Viscous—convective subrange spectra (After Gibson and Schwarz [244] with permission)

# 13.3 The Small Prandtl Number and Scalar Spectrum

Batchelor also considered the opposite case of the small Prandtl number

$$Pr = \frac{v_{\rm F}}{D_0} \ll 1.$$
 (13.3.1)

Here, the "conduction cutoff" occurs at the wave number

$$l_{\theta} = \left(\frac{D_0^3}{\varepsilon_K}\right)^{\frac{1}{4}} = l_{\nu} P r^{-3/4}, \quad Pr < 1.$$
 (13.3.2)

To obtain the scalar spectrum, it is convenient to consider the balance between advection and diffusion

$$\vec{u} \nabla \theta = D_0 \Delta \theta. \tag{13.3.3}$$

The scalar perturbations in the range between the conduction cutoff and the viscous cutoff are described by the estimate

$$V(l)\frac{\theta_0}{L_0} \approx D_0 \frac{\theta_k}{l^2}.$$
 (13.3.4)

By applying the Kolmogorov scaling for the velocity  $V(l) \propto (\varepsilon_K l)^{1/3}$ , we arrive at

$$\delta\theta(l) \propto (\varepsilon_K l)^{1/3} l^2 \frac{\theta_0}{D_0 L_0} \propto \varepsilon_K^{1/3} l^{7/3}. \tag{13.3.5}$$

Now the scalar spectrum in the range of wave numbers between the conduction cutoff and the viscous cutoff is given by

$$E_{\theta}(k) \propto \frac{\theta_k^2}{k} \propto \varepsilon_{\theta} \varepsilon_K^{2/3} k^{-17/3},$$
 (13.3.6)

where

$$l_{\theta}^{-1} = k_{\theta} < k < k_{\nu} = l_{\nu}^{-1}, \tag{13.3.7}$$

This is the internal-diffusive-range spectrum (see Fig. 13.3.1). Experimentally, such a range could be expected to exist for turbulence in liquid metals. A numerical simulation of a passive scalar convected by a frozen velocity field presented in [245–248] confirms the 17/3 exponent.

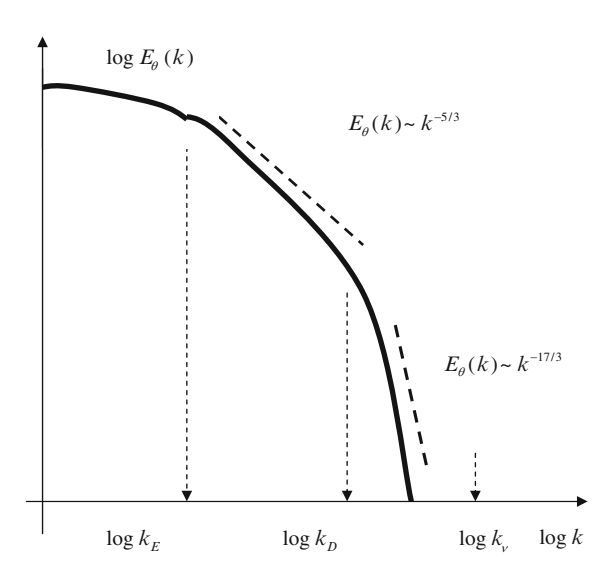


**Fig. 13.3.1** Idealized Batchelor scalar spectra in fully developed homogeneous isotropic turbulence for the small Prandtl numbers (*Pr*<1)

#### 13.4 Seed Diffusivity and Turbulent Transport

On the basis of the Kolmogorov phenomenology, it is possible to introduce a "self-consistent" diffusion coefficient that describes both the Lagrangian contribution and molecular diffusion effects [73, 249]. The quasilinear scaling for the turbulent diffusion coefficient in terms of the Lagrangian correlation function,

$$D_{\rm T} = \int \langle V(0)V(t)\rangle dt \propto \langle V\rangle^2 \tau, \qquad (13.4.1)$$

points to the relation between the diffusivity and the turbulent energy spectrum E(k). To establish the direct relationship between the turbulent diffusion coefficient  $D_{\rm T}$  and the energy spectrum E(k), let us consider a "local" diffusion coefficient  $\delta D(k)$ [186] related to the specific scale length  $l_k \approx 1/k$  of eddies with the characteristic velocity  $V_k$ . Thus, the velocity and scalar fields are decomposed into ingredients. Here, the smallest spatial scale corresponds to the Batchelor dissipative scale  $l_B$ . Now the diffusion equation for the scale k is given by

$$V_k \nabla \theta_k = D_0 \nabla^2 \theta_k, \tag{13.4.2}$$

where

$$\theta_k = \theta_{k-1} + \dots + \theta_2 + \theta_1. \tag{13.4.3}$$

After averaging, we obtain the relation

$$\langle V_k \theta_k \rangle = -D_0 \nabla \theta_k. \tag{13.4.4}$$

Thus, we derive the expression that is differential in the form:

$$\delta D(k) = \frac{2}{3} \frac{E(k)}{k^2 D_0} \delta k. \tag{13.4.5}$$

Note that the value of D(k) should be taken into account along with molecular diffusion  $D_0$ . Upon solving this differential equation, we obtain the expression for the turbulent diffusion coefficient

$$(D(k) + D_0)^2 = \int_k^\infty \frac{E(k)}{k^2} dk + D_0^2, \tag{13.4.6}$$

where by assumption,  $D(\infty)=0$ . In this formula, the integral term plays the main role for scales that are larger than the characteristic turbulent scale  $l_T$  that enters into the expression for the Reynolds number:  $Re=\frac{V_0 l_T}{v_F}$ . By neglecting the molecular diffusion effects, we derive the Howells expression

$$D_H = \sqrt{\int_k^\infty \frac{E(k)}{k^2} \mathrm{d}k}$$
 (13.4.7)

which differs significantly from the quasilinear scaling  $D_{\rm T} \propto V_0^2 \tau$ . The new scaling yields a different type of estimate for the diffusion coefficient,

$$D_H(V_0) \propto V_0 \lambda \propto D_0 P e, \tag{13.4.8}$$

where  $\lambda$  is the characteristic spatial scale. Of course, there is no unique recipe to obtain the estimates of turbulent transport and the best way depends on a flow character. Nevertheless, the diffusive renormalization considered above was confirmed by the direct calculation of the correlation function and repeatedly used to describe scalar transport in chaotic flows.

#### 13.5 Fluctuation–Dissipative Relation and Cascade Arguments

It is interesting to incorporate the Kolmogorov scaling arguments in the fluctuation—dissipative relationship for scalar density fluctuations

$$\frac{1}{2}\frac{\mathrm{d}}{\mathrm{d}t}\int_{W}\langle n\rangle^{2}\mathrm{d}W + \frac{1}{2}\frac{\mathrm{d}}{\mathrm{d}t}\int_{W}(\delta n)^{2} = -\int_{W}D_{0}(\nabla n)^{2}\,\mathrm{d}W. \tag{13.5.1}$$

Thus, for the case of quasi-steady flows, we can write the Zeldovich expression in the following form:

$$D_0 \int_W (\nabla n)^2 dW \propto Q(n_1 - n_2),$$
 (13.5.2)

where the flux Q through a boundary is estimated in terms of the mixing length  $L_0$  and the velocity fluctuations  $V_0$ 

$$Q \approx S \langle V_0 \cdot L_0 \rangle \nabla n \approx S D_{\rm T} \left( \frac{\Delta n}{L_0} \right)_{\rm macro}.$$
 (13.5.3)

The Zeldovich expression is valid even for the high Peclet numbers  $Pe = \frac{V_0 L_0}{D_0} \gg 1$ . Simple calculations yield the fluctuation–dissipative relation [37]

$$\left\langle \left(\nabla n\right)^{2}\right\rangle = \left(\frac{V_{0}L_{0}}{D_{0}}\right)\frac{\left(\Delta n\right)^{2}}{L_{0}^{2}}.$$
 (13.5.4)

In terms of the Peclet number, one can rewrite this formula for turbulent flows

Further Reading 229

$$\nabla n|_{\text{local}} \approx \left(\frac{D_{\text{T}}}{D_0}\right)^{1/2} \frac{(\Delta n)^2}{L_0^2} \approx Pe^{1/2} \left. \nabla n \right|_{\text{macro}}.$$
 (13.5.5)

This means that when  $Pe \gg 1$ , two fluid elements having substantially different scalar densities (or temperatures) can appear side by side, which was confirmed by numerous experiments and numerical simulations [250–257].

Let us express the local density perturbations  $\delta n|_{\text{turb}}$  on scales  $\lambda$ 

$$\delta n|_{\text{turb}} \propto \nabla n|_{\text{local}} \lambda \approx P e^{1/2} |\nabla n|_{\text{macro}} \lambda.$$
 (13.5.6)

We can estimate the scale  $\lambda$  basing on the Kolmogorov phenomenology as

$$\lambda \approx l_{\nu} \propto \frac{L_0}{Re_{\nu}^{3/4}} \propto \frac{L_0}{Pe_{\nu}^{3/4}}, \text{ where } Pe \propto Re \gg 1.$$
 (13.5.7)

Then, the expression for the amplitude of scalar density perturbation on spatial scales of order  $l_v$  is given by the scaling

$$\delta n|_{\text{turb}} \approx P e^{-1/4} \delta n|_{\text{macro}} \approx R e^{-1/4} \delta n|_{\text{macro}}.$$
 (13.5.8)

This scaling obtained for the cascade case (strong turbulence) differs remarkably from the quasilinear limit (week turbulence where  $Pe \ll 1$ )

$$\delta n(Pe) \propto n_0 Pe, \quad Pe \ll 1.$$
 (13.5.9)

It is possible to estimate the convective contribution to turbulent transport as  $q \propto \delta nV_0$ , which leads to the expecting flat scaling for the effective diffusivity in the following form:

$$D_{\rm eff}(Pe) \propto \frac{q(Pe)}{n_0} L_0 \propto D_0 P e^{3/4}.$$
 (13.5.10)

This differs considerably from weak turbulence case (Pe < < 1) where quasilinear regimes of transport are described by scaling  $D_{\rm eff}(Pe) \propto D_0 Pe^2$ .

## **Further Reading**

#### Scalar and Cascade

T. Cebeci, Analysis of Turbulent Flows (Elsevier, Amsterdam, 2004)

K.R. Sreenivasan, Annu. Rev. Fluid Mech. 29, 435 (1997)

K.R. Sreenivasan, Rev. Mod. Phys. **71**, S 383 (1999)

230 13 Turbulence and Scalar

H. Tennekes, J.L. Lumley, A First Course in Turbulence (MIT, New York, 1970)

- A. Tsinober, An Informal Introduction to Turbulence (Kluwer, Amsterdam, 2004)
- J.C. Vassilicos (ed.), *Intermittency in Turbulent Flows* (Cambridge University Press, Cambridge, 2001)
- Z. Warhaft, Annu. Rev. Fluid Mech. 32, 203–240 (2000)

### Scalar and Turbulent Transport

- L. Biferale, I. Procaccia, Phys. Rep. 254, 365 (2005)
- J. Cardy et al., Non-Equilibrium Mechanics and Turbulence (Cambridge University Press, Cambridge, 2008)
- A. Crisanti, M. Falcioni, A. Vulpiani, Rivista Del Nuovo Cimento 14, 1–80 (1991)
- G. Falkovich, K. Gawedzki, M. Vergassola, Rev. Mod. Phys. 73, 913 (2001)
- J.C.R. Hunt, Annu. Rev. Fluid Mech. 17, 447 (1985)
- H.K. Moffatt, J. Fluid Mech. 106, 27 (1981)
- H.K. Moffatt, Rep. Prog. Phys. **621**, 3 (1983)
- F.T.M. Nieuwstadt, H. Van Dop (eds.), *Atmospheric Turbulence and Air Pollution Modeling* (D. Reidel, Dordrecht, 1981)
- E.D. Siggia, Annu. Rev. Fluid Mech. 26, 137 (1994)

# **Chapter 14 Relative Diffusion and Scaling**

### 14.1 The Richardson Law and Anomalous Transport

In this chapter, we consider the dispersion of pairs of particles passively advected by homogeneous, isotropic, fully developed turbulent type. Due to the incompressibility of the velocity field the particle will, on average, separate one from another. There are important differences between the diffusion from a continuous source, in which particles are released in sequence at a fixed position, and that of a single puff of particles (see Fig. 14.1.1). Indeed, the measure of a dispersant that is required in observation or in a predictive model will often depend on whether the dispersant is introduced into a chaotic flow continuously from a location or the dispersant is released at some particular time as a patch or group of particles, an 'instantaneous release'. In the last case, the size of the patch and its mean or maximum concentration as function of time provide useful measure.

Thus, one can employ dimensional arguments to estimate the effective concentration in a patch of particles of size  $L_0$ 

$$n_{\rm eff}(t) \propto \frac{N}{L_0^d(t)}.$$
 (14.1.1)

Here, N is the total number of particles in this patch and d is the dimensionality of the space. For instance, in three-dimensional space the diffusive estimate of the patch size  $L_0^2 \propto D_0 t$  leads to the scaling

$$n_{\rm eff}(t) \propto \frac{N}{(D_0 t)^{3/2}} \propto t^{-3/2},$$
 (14.1.2)

whereas the Richardson formula,  $L_0^2 \propto l_R^2 \propto t^3$ , gives considerably different estimate for the effective concentration

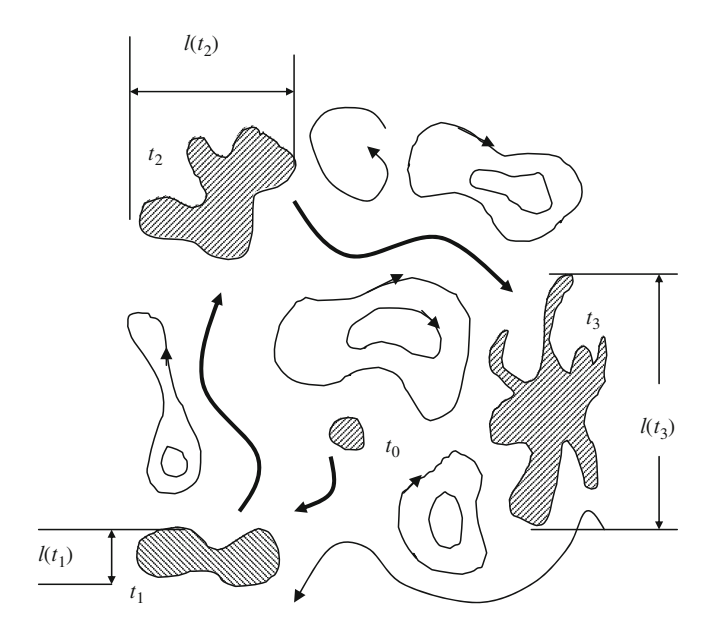


Fig. 14.1.1 Schematic picture of the relative dispersion

$$n \, \text{eff}(t) \propto \frac{N}{l_R^3(t)} \propto t^{-9/2}.$$
 (14.1.3)

The relative dispersion of two fluid material points is a direct generalization of single particle dispersion. The results of various experiments on diffusion in atmosphere lead to the Richardson law [258]

$$\frac{1}{2} \frac{\mathrm{d} \langle l_R^2(t) \rangle}{\mathrm{d}t} = \mathrm{const} \langle l_R^2(t) \rangle^{\frac{2}{3}}.$$
 (14.1.4)

Here,  $l_R$  is the separation of two scalar particles. This means that the spread of a large cloud of particles could not be built up by superimposing the growths of component elements of the cloud treated separately. In terms of the relative diffusion coefficient, this result can be presented as

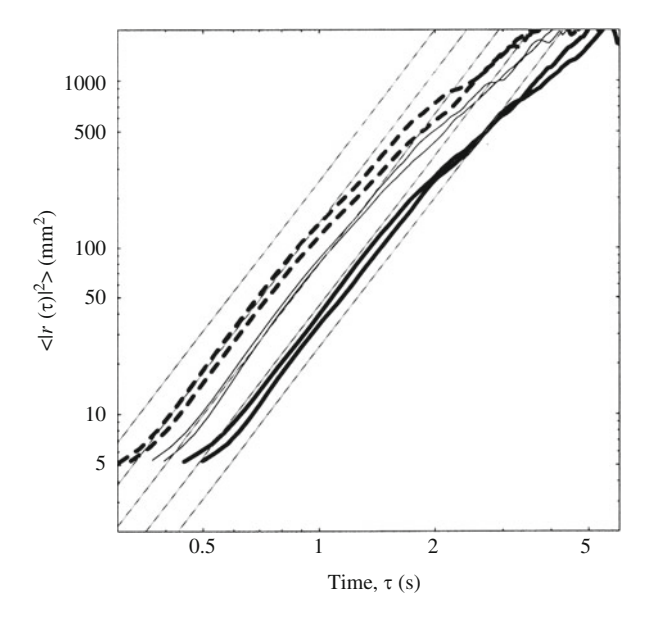
$$D_R(l_R) = C_R \ l_R^{\frac{4}{3}},\tag{14.1.5}$$

where  $C_R \approx 0.2$  is the Richardson constant. Moreover, by integrating once, we can write the mean square separation of the particle as (see Fig. 14.1.2)

$$\langle l_R^2(t) \rangle \propto t^3,$$
 (14.1.6)

where  $l_R$  ranges from  $10^2$  to  $10^6$  cm. This scaling for the separation of two scalar particles differs significantly even from the ballistic estimate.

Fig. 14.1.2 The Richardson scaling. The thin straight lines are  $\propto \tau^3$ . (After Ott and Mann [259] with permission)



The unique nature of the relative diffusion was recognized by Richardson at a very early stage (1926). Indeed, from the conventional point of view, we can consider that particle 1 and particle 2 are released simultaneously at time t = 0 and at positions  $x_1$  and  $x_2$ , respectively. Let the distance between the two particles be l(t). Then we shall put

$$Y(t) = x_2(t) - x_1(t), (14.1.7)$$

and the mean square separation is given by the relation

$$\langle Y^2(t) \rangle = \langle x_1^2(t) \rangle - 2\langle x_1(t)x_2(t) \rangle + \langle x_2^2(t) \rangle. \tag{14.1.8}$$

Destroying correlations in time,  $\langle x_1(t)x_2(t)\rangle = 0$ , leads to the result that is in accord with the following estimate:

$$\langle Y^2(t) \rangle \approx 2(2D_{\rm T})t.$$
 (14.1.9)

The mechanism behind pair separation  $\langle l_R^2(t)\rangle \propto t^3$  in turbulent flows has been a puzzle since it was reported and understanding the particle pair dispersion in turbulent velocity fields is of great interest for both theoretical and practical implications. Based on the theory of phenomenological turbulence, Obukhov suggested [236] a theoretical interpretation of the Richardson law for relative diffusion. Indeed, it is possible to compose the scaling for the diffusion coefficient based on the dimensional character of the value  $\varepsilon_K = [L^2/T^3]$  and the variable k that characterizes the spatial scale  $k \approx 1/l(k) = [1/L]$ . Then, simple calculations yield the dimensional estimate for the Richardson coefficient:

$$D_R(l) = \left[\frac{L^2}{T}\right] \approx \frac{(k^2 \varepsilon_{\rm K})^{1/3}}{k^2} \approx \varepsilon_{\rm K}^{1/3} l^{4/3} \propto l^{4/3}$$
 (14.1.10)

or in terms of the mean square relative separation

$$\langle l_R^2(t) \rangle \propto \text{const } \varepsilon_{\text{K}} t^3,$$
 (14.1.11)

where const  $\approx 3$ . This coincides exactly with the Richardson predictions. Thus, the idea of describing turbulence by the hierarchy of eddies of different scales has obtained its first experimental confirmation in the framework of the scalar transport.

## 14.2 The Batchelor Intermediate Regime

Richardson's scaling has been explained in the framework of the Kolmogorov–Obuchov phenomenology fruitfully applied in the inertial range of spatial scales. However, there are several stages in the process of relative diffusion. At the first stage, the particles are initially close together and only the smallest eddied can increase their separation. At the next stage particles move further apart, a greater range of eddy sizes become important, with, at all times, the eddies comparable in size to the interparticle separation having the dominant effect (see Fig. 14.2.1). The last stage is when the distance between particles becomes greater than the largest turbulent eddy, and the motion of each particle becomes independent of the other. The separation between them is then determined by their own individual random walks. This stage is characterized by the largest energy-containing eddies.

In context of the transport description, we should also analyze a character of relative motion of scalar particles on scales essentially less than inertial ones. Thus, mechanisms responsible for forming anomalous character of relative diffusion are switched on viscous scales. Beyond the inertial range, there is no synergetics of nonlinear vortices interaction and that is why it is impossible to apply the turbulent cascade concept. However, we have an advantage in using intriguing physical mechanisms such as exponential stretching of fluid elements and memory effects related to quasiballistic motion of scalar particles. The pioneering works in this field were done by Batchelor who developed scaling ideas and discovered several new turbulent transport regimes.

The scaling suggested by Richardson,

$$D_R(l_R) \propto l_R^{\frac{4}{3}},$$
 (14.2.1)

corresponds to his notion of the hierarchical character of turbulent transport. Thus, he related the acceleration effect to increasing in the scale of eddies taking part in transport processes. Therefore, in his approach the diffusion coefficient  $D_R$  is the function of the interparticle distance  $l_R$ .

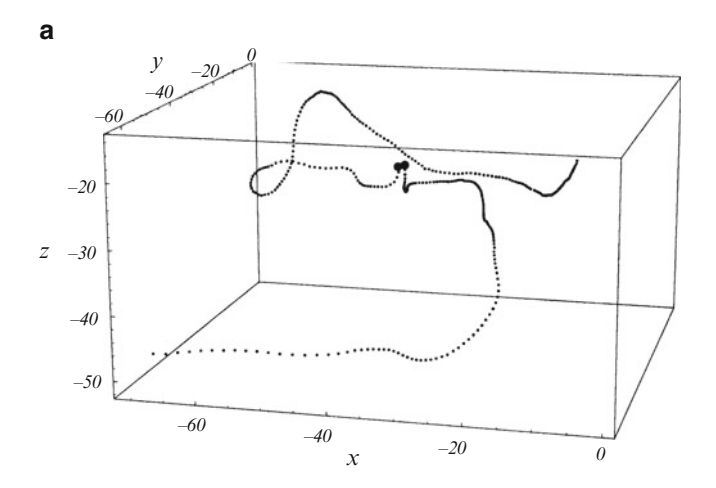


**Fig. 14.2.1** Traces of pairs of particles that are initially within 2 mm of each other. (After Ott and Mann [259] with permission)

Batchelor [260] considered the problem from a different point of view. In his model, the diffusion coefficient  $D_R$  is the result of statistical averaging over the ensemble of different scales. Batchelor argued, to the contrary, that relative diffusivity  $D_R$  should be independent of  $l_R$ ; on dimensional grounds, this implies that  $D_R$  scales with squared time

$$D_R(t) \propto t_R^{4/3}(t) \propto \varepsilon_{\rm K} t^2.$$
 (14.2.2)

It is natural to suppose that there exists an intermediate regime corresponding to the initial stage of separation process where the dependence of the relative diffusivity  $D_R(t)$  has a linear form

$$D_R(t) \propto V_*^2 t. \tag{14.2.3}$$

Here,  $V_*$  is the characteristic velocity scale, which is not universal parameter but depends on the initial separation  $l_*$  of scalar particles under consideration. In such regimes, the dissipation rate  $\varepsilon_{\rm K}$  is still the key value and we could construct the relation for  $V_*$  basing on dimensional arguments

$$V_* \propto (l_* \varepsilon_{\rm K})^{1/3},\tag{14.2.4}$$

where  $l_*$  is the parameter. After substitution, one obtains

$$D_R(t) \propto \frac{l_R^2(t)}{t} \propto (l_* \varepsilon_{\rm K})^{2/3} t,$$
 (14.2.5)

or for the relative distance in the intermediate range

$$\langle l_R^2(t) \rangle \propto l_*^2 + \text{const} \cdot (l_* \varepsilon_K)^{2/3} t^2,$$
 (14.2.6)

where

$$t < \tau_* \approx \left(\frac{l_*^2}{\varepsilon_{\rm K}}\right)^{1/3}.\tag{14.2.7}$$

Such a quasiballistic behavior is rather adequate for the problem under analysis, but the main feature of this consideration is the physical meaning of the characteristic length  $l_*$  and the characteristic timescale  $\tau_*$  introduced by Batchelor. Thus,  $\tau_*$  may be identified as the scale for which the two scalar particles "remember" their initial relative velocity while they move in the same eddy of size  $l_*$ . Here, we are dealing with the Lagrangian nature of initial stage of dispersion, which leads to the appearance of nontrivial memory effects.

At times of the order of  $\tau_*$ , this eddy breaks up, and the growth of the pair separation will undergo a transition to the classical Richardson scaling

$$l_*^2(\tau_*) \propto \varepsilon_{\rm K} \tau_*^3. \tag{14.2.8}$$

Here, the characteristic viscous time,  $\tau_{\nu} = (\nu_F/\varepsilon_K)^{1/2}$ , is a good approximation for the characteristic time  $\tau_*$ , because on the "viscous boundary" the Richardson law is automatically valid

$$l_{\nu}^2 \propto \varepsilon_{\rm K} \tau_{\nu}^3$$
. (14.2.9)

Here,  $l_{v}$  is the Kolmogorov microscale  $l_{v} = (v_{F}^{3}/\varepsilon_{K})^{1/4}$ .

Indeed, in the intermediate range of scales we are faced with a new scenario. By following the Batchelor–Townsend [261] line of arguments, it is natural to build the approximation equation, which can connect the ballistic mode and the Richardson law. On the basis of dimensional arguments, it is possible to rewrite the Richardson equation for the interparticle distance in the form

$$\frac{\mathrm{d}\langle l_R^2(t)\rangle}{\mathrm{d}t} = \varepsilon_{\mathrm{K}} t^2 \Omega(t) = \varepsilon_{\mathrm{K}} t^2 \Omega\left(\frac{t}{\tau_{\mathrm{v}}}, \frac{l_*}{\sqrt{\varepsilon_{\mathrm{K}} t^3}}\right). \tag{14.2.10}$$

In the framework of scaling concept, a power form is appropriative approximation of the function  $\Omega$ . Thus, we arrive at

$$\frac{\mathrm{d}\langle l_R^2(t)\rangle}{\mathrm{d}t} = \varepsilon_\mathrm{K} t^2 \left(\frac{t}{\tau_\mathrm{v}}\right)^\varsigma \left(\frac{l_*}{\sqrt{\varepsilon_\mathrm{K} t^3}}\right)^\zeta. \tag{14.2.11}$$

In the ballistic mode, the separation  $l_R$  has to be independent of the viscosity, but the memory effects are essential. This leads to the formula

$$\frac{\mathrm{d}\langle l_R^2(t)\rangle}{\mathrm{d}t} = \varepsilon_{\mathrm{K}} t^2 \left(\frac{l_*}{\sqrt{\varepsilon_{\mathrm{K}} t^3}}\right)^{2/3} = (\varepsilon_{\mathrm{K}} l_*)^{2/3} t, \tag{14.2.12}$$

where the characteristic exponents are  $\zeta = 0$ ,  $\zeta = 2/3$ . On the other hand, when we are dealing with the large times, the separation  $l_R(t)$  has to be independent of the initial particle separation  $l_*$ , which yields the relation

$$\frac{\mathrm{d}\langle l_R^2(t)\rangle}{\mathrm{d}t} = \varepsilon_{\mathrm{K}} t^2,\tag{14.2.13}$$

where the characteristic exponents are  $\zeta = 0$ ,  $\varsigma = 0$ .

Batchelor's quasiballistic regime has been observed in numerical experiments [262], where it was shown measurements of relative dispersion for turbulence levels up to  $\text{Re} \approx 800$ . For experimentally accessible initial separations, these data scale as  $t^2$  for more than two decades in time, with no hint of classical Richardson  $t^3$  scaling. This behavior holds throughout the entire inertial range, even for large initial separations. This demonstrates once again that the initial separation is an important parameter for relative dispersion in turbulent flow and cannot be neglected.

# 14.3 Dissipation Subrange and Exponential Regime

The description of relative diffusion in a dissipative interval of isotropic turbulence was first introduced by Batchelor in his analysis of exponential stretching of fluid element in a chaotic flow on small scales [263]. Such an exponential stretching of fluid element obviously leads to exponential growth of the distance between two scalar particles placed inside this element and separated by a small distance. The fruitful approach to analyze this initial stage of dispersion is to use the linear dependence for fluctuations of velocity

$$V(l) \propto \text{const} \cdot l.$$
 (14.3.1)

This is natural approximation for the viscous subrange because it provides correct transition to the Kolmogorov dependence

$$V(l) \propto (\varepsilon_{\rm K} \cdot l)^{1/3}$$
. (14.3.2)

The modified scaling for relative diffusion takes the form

$$D_R(l) \propto V(l)l \propto \text{const } l^2.$$
 (14.3.3)

This relation implies an exponential growth of pair separation. Indeed, the modified scaling  $D_R(l) \propto l^2$  can be applied to obtain the average relative distance between two scalar particles  $\langle l(t) \rangle$  if we use the Taylor definition of the diffusion coefficient

$$D_R(t) \propto \frac{\mathrm{d}\langle l_R^2(t)\rangle}{\mathrm{d}t}.$$
 (14.3.4)

Then we can write the differential equation

$$\frac{\mathrm{d}}{\mathrm{d}t} \langle l_R^2(t) \rangle = \mathrm{const} \langle l_R^2(t) \rangle. \tag{14.3.5}$$

Its exponential solution describes relative diffusion on scales where viscosity effects are important

$$\left\langle l_R^2(t) \right\rangle = l_0^2 \exp\left(\frac{t}{\tau_v}\right).$$
 (14.3.6)

Here,  $l_0$  is the initial distance between scalar particles in the dissipative interval of scales and  $\tau_{\nu} = (\nu_{\rm F}/\epsilon_{\rm K})^{1/2}$  is the characteristic temporal scale related to the dissipation range.

This result brings out the essentially accelerative nature of the relative diffusion, which occurs as long as the separations involved are small compared with the viscous scale. The initial separation of scalar particles must be less than the Kolmogorov dissipative spatial scale

$$l_0 \ll l_R \ll l_v = \left(\frac{v_F^3}{\varepsilon_K}\right)^{1/4}.$$
 (14.3.7)

The corresponding applicability condition for times is given by

$$t \ll \tau_{\nu} = \left(\frac{\nu_{\rm F}}{\varepsilon_{\rm K}}\right)^{1/2}.\tag{14.3.8}$$

Often, recourse is made of the simplified approximation formula to connect the exponential regime with the Richardson one

$$l_R \propto V(r + l_R, t)\delta t - V(r, t)\delta t \approx \delta V(r)\delta t.$$
 (14.3.9)

Thus, for the small values of  $l_R$ ,  $l_R < l_\nu$ , the estimate  $V(r) \propto \mathrm{const} \cdot r$  leads to the exponential regime, whereas in the case of  $l_R \gg l_\nu$  we arrive at the Richardson scaling with the estimate  $V(r) \propto (\varepsilon_\mathrm{K} \cdot r)^{1/3}$ . However, such an approach ignores the ballistic mode,  $\left\langle l_R^2(t) \right\rangle \propto (l_* \varepsilon_\mathrm{K})^{2/3} t^2$ ; therefore, it is rather superficial.

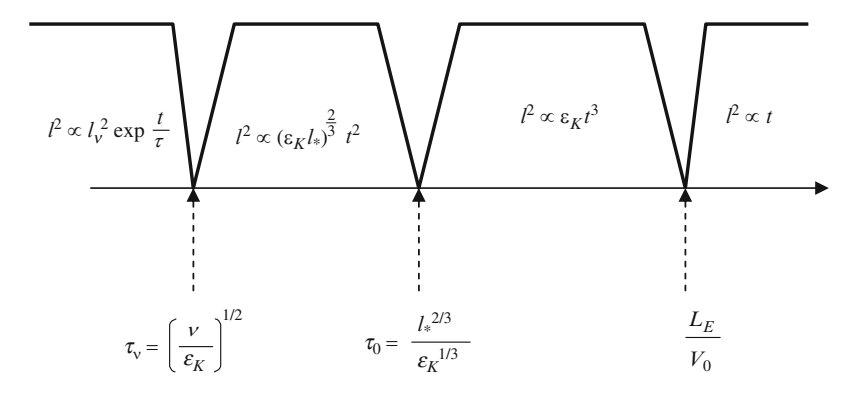


Fig. 14.3.1 Schematic diagram of Batchelor and Richardson relative dispersion regimes

Batchelor distinguished four regimes: an exponential regime, a regime dominated by the initial velocity difference, the inertial range regime (Richardson regime), and a normal diffusion regime at large separation (see Fig. 14.3.1). Papers by Batchelor considered above have provided the starting point for many subsequent treatments of the scalar transport, a problem that has attracted renewed attention, with respect to dynamical chaos and anomalous diffusion, in recent years.

# 14.4 Gaussian Approximations and Relative Dispersion

It is natural to make an attempt to find adequate differential equations, which provide precise description of different stages of complex chaotic mixing phenomena, instead of several scaling models discussed above. Thus, the analysis of the dispersion process by means of a conventional diffusion equation is based on two important physical assumptions, which can be verified a posteriori. The first one is that the dispersion process is self-similar in time, which is probably true in nonintermittent velocity field; the second one is that the velocity field is short correlated in time.

Approximation  $\langle l_R^2(t) \rangle \propto t^3$  suggested by Richardson corresponds to his notion of the hierarchical character of turbulent transport. Thus, he related essentially accelerative nature of the relative distance growth to increasing in the scale of eddies taking part in transport processes. Therefore, in his approach the diffusion coefficient  $D_R$  is the function of the interparticle distance  $l_R$ .

Richardson was concerned with finding a diffusion equation to describe the concentration field relative to the center of mass of a moving cloud. To treat the shape characteristics of a spreading cloud, he introduced the distance-neighbor function F, the probability density, to find two initially close particles at the distance  $l_R$  from one another at the moment t

$$\frac{\partial F(l_R, t)}{\partial t} = \frac{\partial}{\partial l_R} C_R l^{4/3} \frac{\partial F(l_R, t)}{\partial l_R}.$$
 (14.4.1)

Batchelor [263] considered the problem from a different point of view. In his model, the diffusion coefficient  $D_R$  is the result of statistical averaging over the ensemble of different scales and he proposed using the temporal dependence for the definition of  $D_R(t) \approx \left\langle l_R^2(t) \right\rangle^{2/3} \propto \mathrm{const}\, \varepsilon_K t^2$ . Then, the equation for the probability density takes the following form, which is similar to the Richardson equation but with the time-dependent coefficient of diffusion:

$$\frac{\partial F(l_R, t)}{\partial t} = \operatorname{const} \varepsilon_K t^2 \frac{\partial}{\partial l_R} \frac{\partial F}{\partial l_R}.$$
 (14.4.2)

Note that the arguments in favor of one type or another of the diffusion coefficient have a qualitative character in both these cases. These pioneering models lead to different results in spite of the underlying law  $\langle l_R^2(t)\rangle \propto t^3$ . However, the distribution function F is different in these cases. It is easy to see this difference when we employ the Fourier transform

$$\tilde{F}_k(t) = \int_{-\infty}^{\infty} F(x, t) e^{ikx} dx.$$
 (14.4.3)

Thus, in the conventional diffusive equation, the law of temporal relaxation of the function F in the Fourier form corresponds to the relation

$$\tilde{F}_k(t) \propto \exp(-t),$$
 (14.4.4)

whereas in the case of the time-dependent diffusion coefficient we deal with stronger decay:

$$\tilde{F}_k(t) \propto \exp(-t^3). \tag{14.4.5}$$

Here,  $\tilde{F}_k(t)$  is the Fourier transformation of the function F(x,t) over the variable x. It is obvious that the characters of those solutions describing the probability density evolution are also different. Thus, for the Richardson model, we find

$$\langle l_R^2(t) \rangle = \frac{35}{9} \left( \frac{2}{3} C_R t \right)^3,$$
 (14.4.6)

whereas the Batchelor equation yields the different result

$$\left\langle l_R^2(t) \right\rangle = \left(\frac{2}{3}C_R t\right)^3. \tag{14.4.7}$$

The same situation we have when comparing the distance-neighbor function F at zero point. For the Richardson model, one obtains

$$F(0,t) = \frac{3}{\sqrt{6\pi}} \frac{1}{\left(\frac{2}{3}C_R t\right)^{3/2}},$$
(14.4.8)

whereas the Batchelor representation gives the dependence as follows (see Fig. 14.4.1):

$$F(0,t) = \frac{1}{\sqrt{2\pi} \left(\frac{2}{3} C_R t\right)^{3/2}}$$
 (14.4.9)

Unfortunately, it is impossible to decide what is a correct equation, if one looks at this problem from the conventional diffusion point of view, because the physical arguments from Kolmogorov and Obukhov lead to an explanation in terms of the hierarchy of scales, whereas Richardson and Batchelor deal with the local diffusive equation with partial differentials.

The development of Batchelor's ideas concerning relative diffusion has led to new approaches where nontrivial mixing effects were described in more detail. In the conventional transport theory, diffusive models are grounded on kinetic equations. Transition from a configuration space to a phase-space allows one to describe both ballistic and nonlocal effects. Kinetic approximation was used in the second Obukhov work on relative diffusion [265]. In spite of some critical

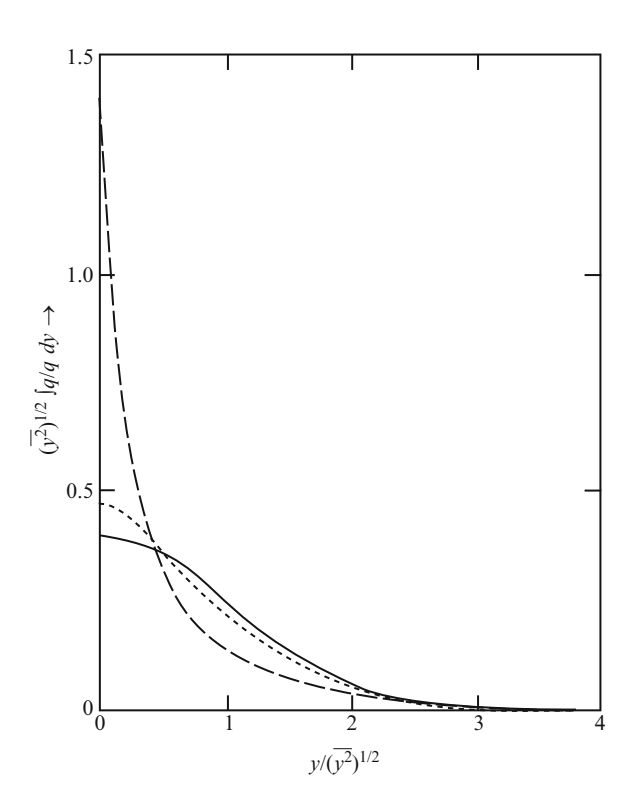


Fig. 14.4.1 Average distance-neighbor function from 209 realizations of C compared with suggestions of Batchelor and Richardson. Continuous line Batchelor; N dash lines empirical; M dash lines Richardson (After Sullivan [264] with permission)

comments on such an approach, here again, however, Obukhov has made what appears to me to be an observation of great interest. Thus, he recognized the perspective of using a velocity space in the analysis of statistical properties of turbulent pulsations and suggested to use an approximative kinetic equation for the velocity distribution function  $F_V(V,x,t)$ 

$$\frac{\partial F_V}{\partial t} + \vec{V} \nabla F_V = \varepsilon_K \frac{\partial^2 F_V}{\partial V^2}.$$
 (14.4.10)

Here,  $\varepsilon_{\rm K}$  plays the role of the diffusive coefficient in a velocity space  $D_V$ . Indeed, Yaglom [266, 267] found that the correlation function of accelerations related to turbulent pulsations of velocity is given by the expression

$$C_A(t) = \langle A(0)A(t)\rangle = \varepsilon_K \delta(t),$$
 (14.4.11)

where A(t) is an acceleration, which can be treated as a white noise in an impulse space. Such a form of the correlation function permits describing a random process on the basis of the Fokker–Plank equation in phase-space with the constant diffusion coefficient  $D_V = \varepsilon_{\rm K}$ .

By considering the evolution of the theoretical models describing complex transport effects, we can note an interesting tendency. Initially, new ideas arise when transport phenomenon is studied in a usual (configuration) space. Then, they penetrate into kinetic theory, where problems are related to the analysis of a velocity space or a phase space. Thus, relative diffusion models were developed in a similar manner.

## 14.5 Fractional Equation Approach

Fractional differential equations are an especially effective tool for investigating anomalous transport. These equations allow us to obtain scalar probability density functions based on the scaling representation of characteristic parameters of the model. Thus, the Einstein functional equation for the particle density

$$\frac{\partial n}{\partial t} = \int_{-\infty}^{+\infty} G(x - x') n(t, x') dx'$$
 (14.5.1)

could be applied to describe nonlocal effects of turbulent diffusion. Such an approach was realized by Monin who was guided by ideas about the hierarchical properties of well-developed isotropic turbulence [268]. In the corresponding formulation of the problem, all statistical parameters are determined exclusively by the scale length  $l_k \approx 1/k$  and the mean energy dissipation rate  $\varepsilon_K$ . In the framework of Fourier's representation for the Einstein functional

$$\frac{\partial \tilde{n}_k(t)}{\partial t} = \tilde{G}(k)\tilde{n}_k, \tag{14.5.2}$$

where the functional kernel is given by scaling  $\tilde{G}(k) = \text{const } k^{\alpha_L}$ , there is only the "uncertain parameter"  $\alpha_L$ . By following the Kolmogorov phenomenology, it is natural to compose  $\tilde{G}(k)$  as

$$\tilde{G}(\varepsilon_{K}, k) = \varepsilon_{K}^{\frac{1}{3}} k^{\frac{2}{3}} \propto \frac{1}{\tau_{\text{rel}}(\varepsilon_{K}, k)}.$$
(14.5.3)

Note, the kernel dimensionality is inversely proportional to the relaxation time. Thus, we obtain the equation for the particle density with fractional derivatives:

$$\frac{\partial n}{\partial t} = \varepsilon_{\text{K}}^{1/3} \frac{\partial^{2/3} n}{\partial x^{2/3}}.$$
 (14.5.4)

Here, the Levy–Khinchine exponent is  $\alpha_L = 2/3$  (see Fig. 14.5.1). In an effort to derive a conventional differential equation, one can differentiate the fractional differential equation twice with respect to time

$$\frac{\partial^3 n}{\partial t^3} = \varepsilon_{\rm K} \frac{\partial^2 n}{\partial x^2}.$$
 (14.5.5)

The solution in terms of the Whittaker functions behaves asymptotically as  $n(\to\infty)\propto x^{-11/13}$  [268]. The fractional equation obtained differs significantly from the conventional diffusive equation suggested by the Richardson, Batchelor, Okubo, and others [269–272]. This new equation allows one to incorporate the Kolmogorov hierarchy of spatial scales, which, in our case, is related to the hierarchy of relaxation times.

On the other hand, applying the continuous time random walk approach makes it possible to consider both spatial nonlocality and memory effects [11, 12]. Blumen,

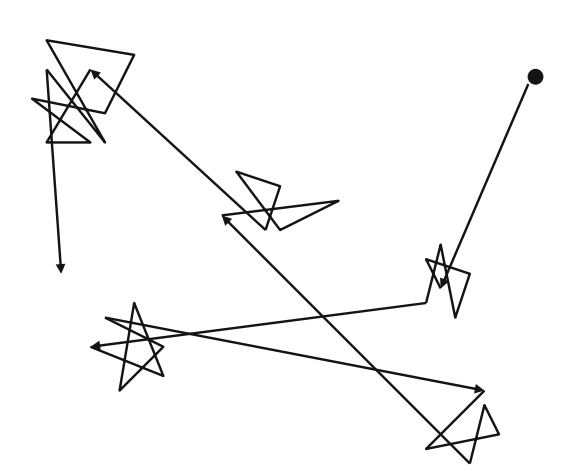


**Fig. 14.5.1** Schematic illustration of a Levy flight

Klafter, and Shlesinger [273] employed the advantages of this method to describe the Richardson relative diffusion  $R^2(t) \propto t^3$ . It is natural that the use of the nonlocal operator leads to the distribution function, which differs significantly from the conventional diffusion models. Nevertheless, convincing arguments in favor of choice of the specific type of equation describing the behavior of the distribution function are absent and the search for adequate theoretical models and experimental proofs has been continued.

#### 14.6 Turbulence Scaling and Fractality

In the above discussions, we have implicitly assumed that  $\varepsilon_K$  is spatially homogeneous and not fractal. However, the Kolmogorov theory fails to describe intermittency effects. Landau noted that theory does not take proper account of spatial fluctuations of local dissipation rates. In fact, high Reynolds number turbulence is intermittent with regions of high turbulence activity separated by regions of very low turbulence. The correlation of energy dissipation rate,  $\varepsilon_D(x)$ , at x is given by the often-studied function [17, 62]

$$K_{\varepsilon\varepsilon}(l) = \langle \varepsilon'_{\mathbf{D}}(x+l,t)\varepsilon'_{\mathbf{D}}(x,t)\rangle,$$
 (14.6.1)

where  $\varepsilon'_{D}$  is the fluctuation of the energy dissipation

$$\varepsilon_{\rm D}(\vec{r},t) \propto v_{\rm F} |\nabla u(\vec{r},t)|^2.$$
 (14.6.2)

The dimensional arguments lead to the scaling

$$K_{\varepsilon\varepsilon}(l) = \varepsilon_{\rm D}(l)^2 \propto \left(\frac{V(l)}{l}\right)^2 \propto \frac{1}{l^{8/3}}$$
 (14.6.3)

where the Kolmogorov scaling was applied,  $V(l) \propto l^{1/3}$ . However, experiments have confirmed that the energy dissipation region of isotropic turbulence in three-dimensional space has a fractal structure and the correlation of energy dissipation rate is given by

$$K_{\varepsilon\varepsilon}(l) \propto \frac{1}{l_i^u},$$
 (14.6.4)

which decays as the power law, where the intermittency exponent is  $\mu_i = 0.25 \pm 0.05$  [17, 78]. On the other hand, it was found in [219] that data are best fitted by a relation

$$D_R(l) \propto l^{\left(\frac{4}{3} + \frac{2}{3}\mu_i\right)}$$
 (14.6.5)

with the same intermittency exponent  $\mu_i \approx 0.2$ . One can see that the correlation term  $2\mu_i/3$  is approximately ten times less than the Richardson 4/3 exponent, but the physical meaning of the fractal representation of intermittency phenomena is of great importance. The above scaling indicates that the velocity field has fractal properties with the dimensionality  $d_F = 3 - \mu_i$ .

Mandelbrot [274] and then Fricsh, Sulem, and Nelkin [275] have renormalized the Kolmogorov–Obukhov spectrum using the fractal representation of energy dissipation regions. The fraction of the volume corresponding to "one dissipation center" can be represented in the form:

$$Q_{\rm F}(l) \approx \frac{W_d}{N(l)} \approx \frac{l^d}{l^{d_{\rm F}}} \approx l^{d-d_{\rm F}}.$$
 (14.6.6)

Here, N(l) is the number of "dissipation centers" in the region of size l,  $W_d \approx l^d$  is the volume of this region, d is the dimensionality of Euclidean space, and  $d_F$  is the fractal dimensionality of the "cluster" consisted of "dissipation centers". The Kolmogorov–Obukhov expression for  $\varepsilon_K$  can be rewritten in the renormalized form:

const = 
$$\varepsilon_{\rm F} \approx \frac{V(l)^3}{l} Q_{\rm F}(l)$$
. (14.6.7)

Then, upon performing calculations, we arrive at the formula in terms of the wave number  $k \propto 1/l$ :

$$E_{\rm F}(k) \propto \frac{{V_k}^2}{k} Q_{\rm F}(k) \propto E_{\rm K}(k) k^{-\frac{d-d_{\rm F}}{3}} \approx \frac{1}{k^{5/3}} \frac{1}{k^{(d-d_{\rm F})/3}}.$$
 (14.6.8)

The last factor is the correction factor caused by the fractal nature of energy dissipation regions. Experiments are satisfactorily described by the value  $d_F \approx 2.8$  [17, 22].

The similar analysis has led to the modification of the Richardson scaling

$$D_{\rm F}(l) \propto V_l l Q_{\rm F}(l) \propto V_l(l) l l^{\mu_i} \propto l^{\frac{4}{3} + \frac{2}{3}\mu_i}.$$
 (14.6.9)

The Kolmogorov idea partially loses its initial universality after we introduce a new parameter  $d_F$ . However, at the same time, such corrections essentially increase the possibilities to fit theory and experiment.

On the other hand, in [273] the modified continuous time random walk model was considered, where the intermittency effects are included by scaling

$$V(x) \propto x^{\gamma_R}, \quad \gamma_R = \frac{1}{3} + \frac{d - d_F}{6} = \frac{1}{3} \left( 1 + \frac{\mu_i}{2} \right).$$
 (14.6.10)

Then, the mean square separation of two particles is given by

$$R^2(t) \propto t^{\frac{12}{4-\mu_i}}, \quad \beta_R \le \frac{1-\mu_i}{3}.$$
 (14.6.11)

Note that this scaling for the modified Richardson law has been obtained independently by Hentschel and Procaccia [276], who used a much different approach. Hundreds of research papers have been written on the application of the continuous time random walk approach to turbulent diffusion basing on fractal concept, but we shall not go into detail here. For a fuller treatment of this exciting subject, we refer the reader to [17, 22, 77, 78].

#### **Further Reading**

#### Relative Dispersion

- G.T. Csanady, Turbulent Diffusion in the Environment (D. Reidel, Dordrecht, 1972)
- P.A. Davidson, Turbulence, an Introduction for Scientists and Engineers (Oxford University Press, Oxford, 2004)
- N.F. Frenkiel (ed.), Atmospheric Diffusion and Air Pollution (Academic, New York, 1959)
- M. Lesieur, Turbulence in Fluids (Kluwer, Dordrecht, 1997)
- W.D. McComb, The Physics of Fluid Turbulence (Clarendon Press, Oxford, 1994)
- A.S. Monin, A.M. Yaglom, Statistical Fluid Mechanics (MIT, Cambridge, 1975)
- F.T.M. Nieuwstadt, H. Van Dop (eds.), Atmospheric Turbulence and Air Pollution Modeling (D. Reidel, Dordrecht, 1981)
- H.A. Panofsky, I.A. Dutton, Atmospheric turbulence, Models and Methods for Engineering Applications (Wiley Interscience, New York, 1970)
- F. Pasquill, F.B. Smith, Atmospheric Diffusion (Ellis Horwood, New York, 1983)
- L. Richardson, Weather Prediction by Numerical Process (Cambridge University Press, Cambridge, 2007)

#### Environmental Flows

- C.D. Ahrens, Meteorology Today, 9th edn. (Brooks Cole, Pacific Grove, CA, 2008)M.J.P. Cullen, A Mathematical Theory of Large-scale Atmosphere ocean Flow (Imperial College, London, 2006)
- B. Cushman-Roisin, Introduction to Geophysical Fluid Dynamics (Prentice Hall, Englewood Cliffs, NJ, 1994)

Further Reading 247

- C. Egbers, G. Pfister (eds.), Physics of Rotating Fluids (Springer, Berlin, 1999)
- D.L. Hartmann, Global Physical Climatology (Academic, San Diego, CA, 1994)
- J. Marshall, R.A. Plumb, Atmosphere, Ocean and Climate Dynamics (Academic, San Diego, CA, 2007)
- R.K. Zeytounian, Meteorological Fluid Dynamics (Springer, Berlin, 1991)

#### Environmental Turbulence

- S.A. Thorpe, Introduction to Ocean Turbulence (Cambridge University Press, Cambridge, 2007)
- J.S. Turner, Buoyancy Effects in Fluid (Cambridge University Press, Cambridge, 1973)
- J.C. Wyngaard, Turbulence in the Atmosphere (Cambridge University Press, Cambridge, 2010)

#### Turbulent Diffusion in the Environment

- H. Burchard, Applied Turbulence Modelling in Marine Waters (Springer, Berlin, 2002)
- G.T. Csanady, Turbulent Diffusion in the Environment (D. Reidel, Dordrecht, 1972)
- N.F. Frenkiel (ed.), Atmospheric Diffusion and Air Pollution (Academic, New York, 1959)
- C.J. Hearn, The Dynamics of Coastal Models (Cambridge University Press, Cambridge, 2008)
- A. Majda, X. Wang, Non-linear Dynamics and Statistical Theories for Basic Geophysical Flows (Cambridge University Press, Cambridge, 2006)
- F.T.M. Nieuwstadt, H. Van Dop (eds.), Atmospheric Turbulence and Air Pollution Modeling (D. Reidel, Dordrecht, 1981)
- H.A. Panofsky, I.A. Dutton, Atmospheric Turbulence, Models and Methods for Engineering Applications (Wiley Interscience, New York, 1970)
- F. Pasquill, F.B. Smith, Atmospheric Diffusion (Ellis Horwood, New York, 1983)

# Chapter 15

# **Two-Dimensional Turbulence and Transport**

### 15.1 Two-Dimensional Navier-Stokes Equation

The Navier-Stokes equation is an equation of the motion of a fluid element in the absence of a pressure-gradient force and viscosity. In an incompressible fluid, the fluid mass density  $\rho_{\rm m}$  is constant. If we further assume that  $\rho_{\rm m}$  is uniform, the equation may be expressed as

$$\frac{d\vec{u}}{dt} = \frac{\partial \vec{u}}{\partial t} + (\vec{u}\,\nabla)\vec{u} = -\nabla T + v_{\rm F}\nabla^2\vec{u},\tag{15.1.1}$$

$$\nabla \cdot \vec{u} = 0. \tag{15.1.2}$$

Here,  $T = P/\rho_{\rm m}$  is the temperature, in units of energy, and  $v_{\rm F}$  is the kinematic viscosity. In a two-dimensional fluid, the viscosity  $v_{\rm F}$  has components only in the x-y plane, and these components are functions of x, y, and t. Here,  $\nabla T$  can be eliminated by taking the curl of equation (15.1.1). In two dimensions

$$\nabla \times [(\vec{u} \cdot \nabla)\vec{u}] = \nabla \times \left(\frac{1}{2}\nabla u^2 - \vec{u} \times \vec{\Omega}\right)$$

$$= (\vec{u} \cdot \nabla)\vec{\Omega} + \vec{\Omega}\nabla \cdot \vec{u}.$$
(15.1.3)

where  $\vec{\Omega} = \nabla \times \vec{u}$  is the vorticity vector, which lies in the z direction. Equations (15.1.1) and (15.1.2) reduce to the equation of vorticity,

$$\frac{d\vec{\Omega}}{dt} = \frac{\partial \vec{\Omega}}{dt} + (\vec{u} \cdot \nabla)\vec{\Omega} = v_F \nabla^2 \vec{\Omega}.$$
 (15.1.4)

Furthermore, in two dimensions  $\vec{u}$  may be expressed by a scalar stream function  $\Psi$ :

$$\vec{u} = -\nabla \times \Psi \vec{e}_z = -\nabla \Psi \times \vec{e}_z, \tag{15.1.5}$$

$$\vec{\Omega} = \nabla^2 \Psi \ \vec{e}_z, \tag{15.1.6}$$

where  $\vec{e}_z$  is the unit vector in the z direction. Equations (15.1.1) and (15.1.2) can then be written in terms of the function  $\Psi$  only:

$$\frac{\partial}{\partial t} \nabla^2 \Psi - (\nabla \Psi \times \vec{e}_z) \cdot \nabla (\nabla^2 \Psi) - \nu_F \nabla^4 \Psi = 0, \tag{15.1.7}$$

where  $\nabla$  is the two-dimensional gradient operator. If the viscosity is small, the mode excited in this system is highly nonlinear. The Reynolds number  $\text{Re} = V_0 L_0 / v_F$  gives a measure of the "nonlinearity" of the system. Here,  $V_0$  is a typical macroscopic velocity,  $L_0$  is a typical gradient scale length, and  $v_F$  is the kinematic viscosity. If the Reynolds number is large, spatial Fourier modes rapidly cascade two-dimensionally to other Fourier modes, and a turbulent state results. The equation for mode coupling between different spatial Fourier modes can be obtained from (15.1.7) by expressing  $\Psi$  in terms of its Fourier amplitude:

$$\Psi = \frac{1}{2} \left( \sum_{\vec{k}} \Psi_k(t) \exp(i\vec{k} \cdot \vec{x}) + c.c \right), \tag{15.1.8}$$

where  $\vec{k}$  is the two-dimensional wave vector and  $\Psi_k$  is the corresponding Fourier amplitude. Equation (15.1.7) then reduces to

$$\frac{d\Psi_k}{dt} + k^2 v_F \Psi_k = \frac{1}{2} \sum_{k=k',k''} \Lambda_{k',k''}^k \Psi_{k'} \Psi_{k''}, \qquad (15.1.9)$$

where the matrix elements  $\Lambda^k_{k',k''}$  are given by

$$\Lambda_{k',k''}^k = \frac{1}{k^2} (\vec{k'} \times \vec{k''}) \cdot \vec{e_z} (k''^2 - k'^2). \tag{15.1.10}$$

This equation shows that the coupling coefficient  $\Lambda$  has a large value when  $\vec{k}$ ,  $\vec{k'}$ , and  $\vec{k''}$  have comparable magnitudes, which indicates that the modal cascade is dominated by local interactions in  $\vec{k}$  space.

That the total energy and enstrophy are conserved is easily shown from (15.1.1), (15.1.2), and (15.1.3). By taking the scalar product of the velocity field  $\vec{u}$  with (15.1.1) and noting that

$$(\vec{u} \cdot \nabla)\vec{u} = \frac{1}{2}\nabla u^2 - \vec{u} \times \vec{\Omega}, \qquad (15.1.11)$$

as well as

$$\nabla^2 \vec{u} = -\nabla \times \vec{\Omega} + \nabla \nabla \cdot \vec{u}, \tag{15.1.12}$$

$$\frac{\partial}{\partial t} \left( \frac{u^2}{2} \right) + \nabla \cdot \left( \vec{u} \frac{u^2}{2} + \vec{u} T \right) = v_F \nabla \cdot \left( \vec{u} \times \vec{\Omega} \right) - v_F \Omega^2. \tag{15.1.13}$$

If the fluid is surrounded by either a periodic boundary or a rigid boundary, so that the perpendicular component of the velocity field  $u_n$  vanishes on the boundary, this equation gives the conservation of the total energy as

$$\frac{\partial E}{\partial t} = \frac{\partial}{\partial t} \int \frac{u^2}{2} dW = \oint v_F \left( \vec{u} \times \vec{\Omega} \right) \cdot d\vec{S} - \int v_F \Omega^2 dW.$$
 (15.1.14)

Similarly, if we take the scalar product of equation (15.1.3) with  $\vec{\Omega}$ , noting that

$$\vec{\Omega} \cdot (\vec{u} \cdot \nabla) \vec{\Omega} = -\vec{\Omega} \cdot \left( \vec{u} \times \left( \nabla \times \vec{\Omega} \right) \right) = \vec{u} \cdot \left( \vec{\Omega} \times \left( \nabla \times \vec{\Omega} \right) \right) = \vec{u} \cdot \nabla \left( \frac{\Omega^2}{2} \right), \quad (15.1.15)$$

then one finds the equation

$$\frac{\partial}{\partial t} \left( \frac{\Omega^2}{2} \right) + \nabla \cdot \left( \frac{\Omega^2}{2} \vec{u} \right) = v_F \nabla \cdot \left( \vec{\Omega} \times \left( \nabla \times \vec{\Omega} \right) \right) - v_F (\nabla \times \vec{\Omega})^2, \quad (15.1.16)$$

For the same boundary condition, the conservation of enstrophy is obtained as

$$\frac{\partial}{\partial t} \int \frac{\Omega^2}{2} dW = \oint v_F \vec{\Omega} \times \left( \nabla \times \vec{\Omega} \right) \cdot d\vec{S} - \int v_F (\nabla \times \vec{\Omega})^2 dW. \tag{15.1.17}$$

Let us consider the integral

$$\int \vec{\Omega} \cdot \left( \vec{\Omega} \cdot \nabla \right) \vec{u} dW. \tag{15.1.18}$$

One can see that in three-dimensional space there is an additional term on the right-hand side, which invalidates the enstrophy conservation.

The enstrophy conservation leads to the emergence of isolated vortex structures, which is a fascinating aspect of two-dimensional turbulence. This phenomenon has been obtained in many numerical computations (see Fig. 15.1.1). Most vortices are monopoles but some dipoles, and even tripoles, can be formed. Such vortex formation has been observed as well in laboratory experiments with thin water layer and more spectacularly in electron plasma experiments. Such kind of organization can be explained in the framework of statistical mechanics as a local equilibrium around an initial vorticity maximum.

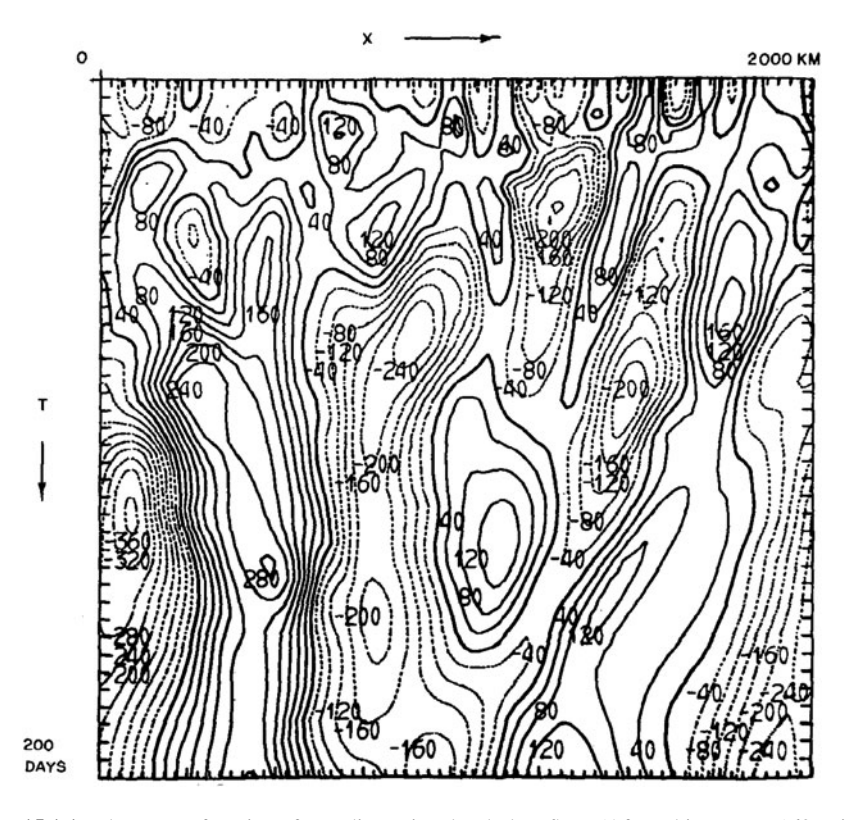


Fig. 15.1.1 The stream function of two-dimensional turbulent flow. (After Rhines P.B. [169] with permission)

#### 15.2 Inverse Cascade

The mathematical description of a fully developed turbulent state is difficult, if not impossible. However, the turbulent spectrum may be obtained by using arguments similar to the Kolmogorov phenomenological approach, which was applied to the inertial range.

Recall that the inertial range is a range in wave number space where there is neither a source nor a sink (dissipation) and where the wave number spectrum is assumed to cascade smoothly in a stationary state. If we write the Fourier amplitude of the velocity field as  $V_k$ , the rate at which the spectrum case is given by  $kV_k$ . The omnidirectional energy spectrum E(k) is defined such that  $\int E(k) dk$  gives the total energy, where

$$k = (\vec{k} \cdot \vec{k})^{1/2}. \tag{15.2.1}$$

Hence, E(k)k has the dimension of  $V_k^2$ . Kolmogorov argues that, in a quasi-steady state, there should be a stationary flow of energy in  $\vec{k}$  space from the source to the

15.2 Inverse Cascade 253

sink. This means that the energy density flow  $\rho_m k V_k V_k^2$  should be constant and given by the dissipation rate of the energy density  $\varepsilon_K$  at the sink:

$$\rho_{\rm m}kV_k^3 = \varepsilon_K. \tag{15.2.2}$$

Now, in two-dimensional turbulence there is an additional conserved quantity, the enstrophy. Hence, two types of inertial range are expressed: one for energy and the other for enstrophy. Since the enstrophy density is given by  $k^2V_k^2$ , the inertial range of enstrophy requires that

$$\rho_{\rm m}kV_kk^2V_k^2 = \varepsilon_{\Omega} = \text{const.}$$
 (15.2.3)

Thus, by writing the estimate

$$V_k = (kE_{\Omega}(k))^{1/2}, \tag{15.2.4}$$

the energy spectrum in this range is given by

$$E_{\Omega}(k) = C' \left(\frac{\varepsilon_{\Omega}}{\rho_{\rm m}}\right)^{2/3} k^{-3}. \tag{15.2.5}$$

This equation shows an energy spectrum of  $k^{-3}$  (see Fig. 15.2.1), in contrast to the Kolmogorov spectrum of  $k^{-5/3}$ , which is obtained from the inertial range of energy.

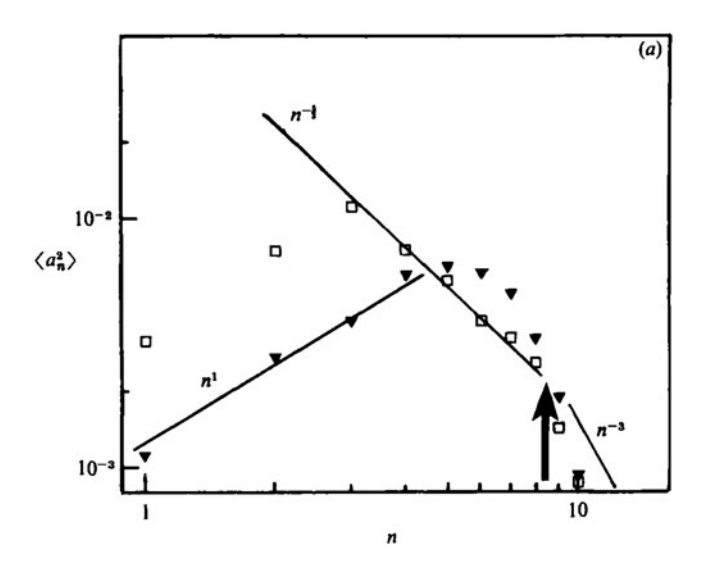


Fig. 15.2.1 One-dimensional spectra of transverse velocity component in  $\log - - \log$  coordinates. (After Sommeria J. [277] with permission)

Kraichnan [278] showed that if  $E_{\Omega}(k) \propto k^{-3}$  there is no energy cascade, while if  $E(k) \propto k^{-5/3}$  there is no enstrophy cascade. Hence, a source at  $k = k_{\rm S}$  will set up two inertial ranges:  $k > k_{\rm S}$  and  $k < k_{\rm S}$ . Since the enstrophy, because of its larger k dependence, is dissipated at large wave numbers at a rate faster than the energy,  $k > k_{\rm S}$  region is expected to be the inertial range for enstrophy, which implies that the  $k < k_{\rm S}$  region would be the inertial range for energy.

Thus, the energy spectrum has two parts:

$$E_{\Omega}(k) \propto k^{-3}, k > k_{\rm S},$$
 (15.2.6)

$$E(k) \propto E_K(k) \propto k^{-5/3}, k < k_S.$$
 (15.2.7)

Kraichnan argues that since there is no energy cascade for  $k > k_S$ , the energy should cascade toward the smaller wave numbers for  $k < k_S$ ; in other words, an inverse cascade is expected (see Fig. 15.2.2). On the other hand, the enstrophy cascades toward the large wave number regime at  $k > k_S$ .

Strictly two-dimensional (2D) turbulence is idealization, since natural flows have a 3D aspect to them. Nevertheless, understanding the simplest 2D case gives a good grasp of more complicated systems that occur in the atmosphere and oceans. Examples of quasi-2D flow where the mixing and dispersion of passive tracers are important are easily found in the atmosphere and in oceanic flows where a combination of geometry, stratification, and rotation acts to suppress motion in the vertical direction. In a similar way, the magnetic field lines can constrain charged particles in plasma confinement devices and astrophysical flows to quasi-2D behavior [279–293].

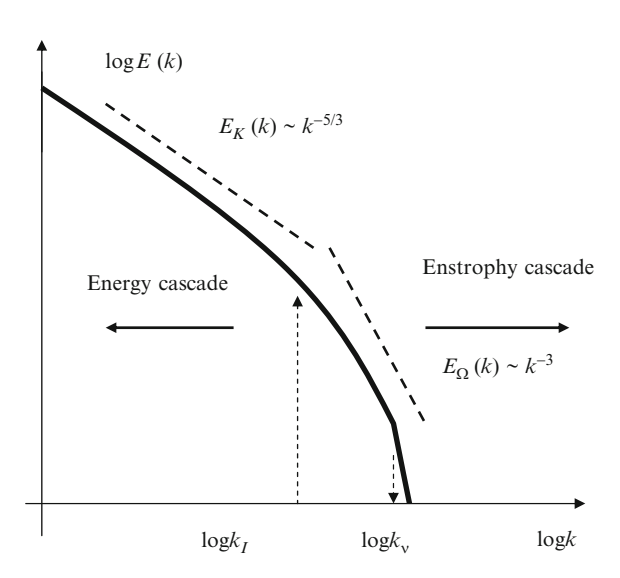


Fig. 15.2.2 Idealized Kraichnan energy spectra for two-dimensional forced turbulent flow

#### 15.3 Freely Evolving Two-Dimensional Turbulence

Basing on the scaling arguments, it is possible to treat the behavior of freely (no forcing) evolving two-dimensional turbulent flow. Of course, there is a big difference between freely evolving and forced turbulence. Thus, as early as 1969 Batchelor [294] assumed a self-similar character of evolution of freely evolving two-dimensional turbulence.

The Navier–Stokes equation for the two-dimensional case gives the rate of decay of the mean kinetic energy in the form

$$\frac{\mathrm{d}W_{\mathrm{E}}}{\mathrm{d}t} = -2\Theta v_{\mathrm{F}} = -\varepsilon_{\mathrm{K}},\tag{15.3.1}$$

where  $v_F$  is the kinematic viscosity,  $\Theta = \langle \Omega^2 \rangle$  is the enstrophy, and  $\vec{\Omega} = \nabla \times \vec{u}$  is the vorticity vector, which lies in the z direction. One can see that this rate is always negative. The vorticity equation considered above leads to the enstrophy evolution equation described by the relation

$$\frac{\mathrm{d}\Theta}{\mathrm{d}t} = -v_{\mathrm{F}} |\nabla\Omega|^2 = -\varepsilon_{\Theta}. \tag{15.3.2}$$

We see that the rate of enstrophy decay is also negative.

Viscous effects are negligible for finite time. By taking into account this set of equations, one can suppose the self-similar form for the energy spectrum

$$E(k,t) = U_0^3 t Z(V_0 kt). (15.3.3)$$

Here,  $U_0$  is the characteristic velocity and Z is an arbitrary function. Indeed, there are only two relevant dimensional parameters,  $U_0$  and t to describe the energy spectrum evolution of freely evolving two-dimensional turbulence. On the other hand, this means that in this single-scale approximation the characteristic spatial size scales with time as

$$l_*(t) \propto 1/k_* \propto U_0 t. \tag{15.3.4}$$

This means that spectral peak migrates to small k.

The enstrophy dimensional representation in the integral form

$$\Theta(t) = \int_0^\infty E(k, t) k^2 \mathrm{d}k,\tag{15.3.5}$$

allows one to solve the equation for the mean kinetic energy. By introducing a new dimensionless variable,  $z = U_0 k t$ , we easily find the relation for the enstrophy evolution

$$\Theta(t) = \int_0^\infty U_0^3 t Z(U_0 k t) k^2 dk = \frac{1}{t^2} \int_0^\infty Z(z) dz = \frac{C_z}{2t^2}.$$
 (15.3.6)

Here,  $C_z$  is the constant. Upon substitution, we find the equation for the mean kinetic energy in the following form:

$$\frac{\mathrm{d}W_E(t)}{\mathrm{d}t} = -v_\mathrm{F} \frac{C_z}{t^2}.\tag{15.3.7}$$

The solution of this differential equation is given by the form

$$W_E(t) = W_E(0) - v_F \frac{C_z}{t}.$$
 (15.3.8)

The expression for the enstrophy evolution in the inertial subrange takes the following form:

$$\Theta(t) = -\frac{1}{2v_E} \frac{dW_E}{dt} = \frac{C_z}{t^2}.$$
 (15.3.9)

This simplified single-scale approximation describes a growth of the integral scale and decay of the total enstrophy as  $\Theta(t) \propto 1/t^2$ . The rate of enstrophy decay is described by the scaling

$$\varepsilon_{\Theta} = -\frac{\mathrm{d}\Theta}{\mathrm{d}t} = 2\frac{C_z}{t^3}.\tag{15.3.10}$$

The energy flux is everywhere toward small k, while enstrophy flows in both directions.

These results could be valid for the build-up period of the enstrophy cascade. However, the scaling law obtained,  $\Theta(t) \propto 1/t^2$ , has only a methodological value, because the laboratory measurements give different exponents ranging from 0.29 to 1.12 [279–281].

## 15.4 Scalar Spectra in Two-Dimensional Turbulence

In this section, we apply the cascade ideas to passive scalar problem. We suppose that tracer is advected by two-dimensional well-developed turbulence [279–281]. In the inertial range, the scalar spectrum  $E_{\theta}(k)$  will be defined, in general, by three important parameters  $\varepsilon_{\theta}$ ,  $\varepsilon_{K}$ , and  $\varepsilon_{\Omega}$ . Here,  $\varepsilon_{\theta}$  is the scalar flux,  $\varepsilon_{K}$  is the dissipation rate of the energy, and  $\varepsilon_{\Omega}$  is the dissipation rate of the enstrophy. It is convenient to introduce an additional spatial scale

$$L_{\Omega} \approx \left(\frac{\varepsilon_K}{\varepsilon_{\Omega}}\right)^{1/2}$$
. (15.4.1)

Then from the dimensional point of view, one can build a scalar power spectrum basing on the expression

$$E_{\theta}(k) = \frac{\theta_k^2}{k} \propto f(kL_{\Omega}) \varepsilon_{\theta} \varepsilon_{K}^{-1/3} k^{-5/3}, \qquad (15.4.2)$$

where f is an arbitrary function, which will be defined below from the physical arguments. Thus, in the inverse cascade subrange  $(k < k_S)$  the parameter  $\varepsilon_{\Omega}$  characterizing the dissipation rate of the enstrophy density is inessential. This leads to f = const. Now one obtains the scalar power spectrum in the form

$$E_{\theta}(k) = \operatorname{const} \varepsilon_{\theta} \varepsilon_{K}^{-1/3} k^{-5/3}. \tag{15.4.3}$$

On the contrary, for the direct cascade subrange  $(k>k_S)$  the parameter  $\varepsilon_K$ , which characterizes the dissipation rate of the energy density, is inessential. On these grounds, we approximate an arbitrary function f by the formula

$$f(kL_{\Omega}) = \operatorname{const}(kL_{\Omega})^{-2/3}. \tag{15.4.4}$$

The corresponding scaling for the scalar power spectrum is given by

$$E_{\theta}(k) = \operatorname{const} \varepsilon_{\theta} \varepsilon_{\Omega}^{-1/3} k^{-1}. \tag{15.4.5}$$

Indeed, in the direct cascade subrange  $(k>k_S)$  the velocity fluctuations are estimated as

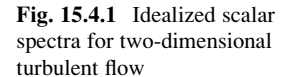
$$V_k \propto \frac{\varepsilon_{\Omega}^{1/3}}{k},\tag{15.4.6}$$

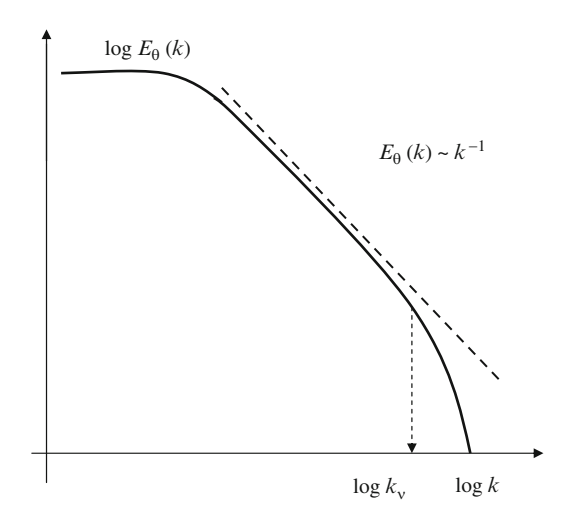
which follows from the conservation of the enstrophy density  $\rho_m k V_k k^2 V_k^2 = \varepsilon_\Omega = {\rm const.}$  To define the scalar perturbation amplitude, one should employ the expression for a scalar flux

$$\varepsilon_{\theta} \propto \frac{\theta_k^2}{\tau_{\text{CASC}}(k)} = \frac{\theta_k^2}{(kV_k)^{-1}}.$$
 (15.4.7)

This leads to the formula for the scalar perturbation in the form

$$\theta_k \propto \frac{\varepsilon_\theta^{1/2}}{\varepsilon_\Omega^{1/6}},$$
(15.4.8)





and hence, one obtains scaling for the scalar spectrum

$$E_{\theta}(k) \propto \frac{\theta_{\rm k}^2}{k} \propto \frac{\varepsilon_{\theta}}{\varepsilon_0^{1/3}} \frac{1}{k},$$
 (15.4.9)

The scalar power spectra obtained for the inertial range of spatial scales are represented in Fig. 15.4.1. For a deeper discussion of scalar power spectra problem in two-dimensional turbulent flows, we refer the reader to [287–290].

## 15.5 Atmospheric Turbulence and Relative Dispersion

By considering the relative diffusion in two dimensions, we are faced with a quite different scenario. It is believed that in this case there exists the direct relationship (based on dimensional estimates) between the relative displacement of two particles in a turbulent flow and the expression for a spectrum E(k)

$$D_{\rm R}(l) \propto V(l)l \propto l\sqrt{E(k)k}\Big|_{k \approx \frac{1}{l}},$$
 (15.5.1)

which in the case of the spectrum  $E(k) \propto k^{-5/3}$  yields the Richardson scaling  $D_{\rm R} \propto l_{\rm R}^{4/3}$ .

In the case of two-dimensional turbulence, one can use the Kraichnan spectra for the inverse cascade  $E(k) \propto k^{-3}$ . Unlike with three-dimensional turbulence, where energy is transported via nonlinear interactions from the large scales to the small dissipative scales, energy in two-dimensional turbulence moves from small to large scales. This "inverse cascade" thereby shifts energy away from the dissipative

scales, requiring a large-scale dissipation mechanism. At the same time, enstrophy, the squared vorticity, is transferred downscale. So if energy is injected at a single scale  $l_{\rm I} \propto 1/k_{\rm I}$ , there will be two different inertial ranges. The Kraichnan approach leads to the modified formula for relative diffusivity

$$D_{\rm R}(l_{\rm R}) \propto {\rm const}\ l_{\rm R}^2.$$
 (15.5.2)

This means that one can obtain the differential equation for a relative displacement. According to the theory of Lin [296], one expects a variation of  $d\langle l_R^2 \rangle/dt$  as  $\langle l_R^2 \rangle$  in the enstrophy range.

$$\frac{\mathrm{d}\langle l_{\mathrm{R}}^{2}(t)\rangle}{\mathrm{d}t} = \mathrm{const} \cdot \langle l_{\mathrm{R}}^{2}(t)\rangle. \tag{15.5.3}$$

These results are similar to the expressions describing the Batchelor viscous regime and that is why one obtains the exponential dependence for relative distance

$$\langle l_{\rm R}^2(t) \rangle = \text{const } \exp\left(\frac{t}{\tau_0}\right).$$
 (15.5.4)

Thus, a pair of particles with an initial separation smaller than the injection scale  $l_{\rm I}$  would experience exponential growth until the separation reached the injection scale  $l_{\rm I}$ , after which the square separation would grow cubically in time, up to the scale of the largest eddies  $l_{\rm E}$ .

Unique results of observations have been published by Morel and Larcheveque [295] based on the so-called EOLE experiment with 480 balloons distributed over the Southern Hemisphere at the 200 mb level. It was found that the eddy dispersion process is homogeneous, isotropic, and stationary up to scales of the order of 1,000 km. Thus, the mean square relative separation  $\langle l_{\rm R}^2(t) \rangle$  increases exponentially with time up to 6 days (see Fig. 15.5.1), which is in agreement with the Lin predictions [296], whereas  $\langle l_{\rm R}^2(t) \rangle = 80$  km,  $T_1 = 1.35$  days, and more slowly like  $t^{1/2}$  later. The relative diffusivity coefficient is saturated at  $t \to \infty$  and its estimate is  $D_{\rm R} \approx 1.6 \times 10^6 {\rm m}^2 {\rm s}^{-1}$ . These measurements show the expected dependences. For spatial scales between 100 and 1,000 km, good agreement is found with the theory based on a cascade enstrophy in 2D turbulence.

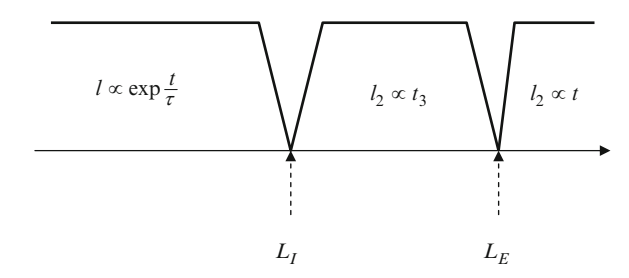


Fig. 15.5.1 Schematic diagram of relative dispersion regimes for two-dimensional turbulent flow

There are important distinctions between the atmospheric and ocean turbulence. Motions of the air in the atmosphere and that of seawater in the oceans that fall under the scope of environmental fluid dynamics occur on spatial scales of several kilometers up to the size of the ears. Generally, the oceanic motions are slower than their atmospheric counterparts. Moreover, the ocean tends to evolve more slowly than the atmosphere. For instance, a number of oceanic processes are caused by the presence of continents and islands, which is not so essential for the atmosphere. Below we consider significant differences between relative dispersion in the atmosphere and in the ocean.

#### 15.6 Rough Ocean and Richardson's Scaling

Besides significant scale disparities, the earth's atmosphere and oceans also have their own peculiarities. Flow patterns in the atmosphere and oceans are generated by vastly different mechanisms. The atmosphere is thermodynamically driven by the solar radiation, whereas oceans are forced by periodic gravitational forces and its surface is subjected to a wind stress that drives most ocean currents (see Fig. 15.6.1). That is why relative diffusion in the ocean could be different from the atmospheric one. Indeed, the exceptional universality of Richardson's scaling could be comparable to the universality of the Kolmogorov and Obuchov spectrum and numerous experiments confirm that this scaling correctly describes the relative diffusion in the ocean, in spite of the large-scale ocean turbulence that cannot be analyzed in terms of three-dimensional isotropic turbulence. Indeed, the investigation of scalar scattering in ocean verifies well the validity of "4/3 law" ranging from 10 m to 10<sup>3</sup> km (see Fig. 15.6.2). It was calculated that on the scales 10–10<sup>3</sup> m, the magnitude of  $\varepsilon_K \approx 10^{-4} \text{cm}^2/\text{c}^3$ , whereas on the scales 10–1,000 km, the value of  $\varepsilon_K$  is much lower,  $\varepsilon_K \approx 10^{-5} \text{cm}^2/\text{c}^3$ . This intriguing fact for the range of 10–10<sup>3</sup> m was recently explained by Golitsyn [298] based on the consideration of spectral characteristics of both hydrodynamical and wave turbulence.

By analyzing the relation between Lagrangian characteristics and spectral one, we have to take into consideration the expression

$$\left\langle \left( z(t') - z(t) \right)^2 \right\rangle = 2 \int_{-\infty}^{\infty} \left( 1 - e^{i\omega(t - t')} E_z(\omega) d\omega \right). \tag{15.6.1}$$

For example, using velocity as a Lagrangian characteristic z leads to

$$\left\langle \frac{V^2}{2} \right\rangle = \int_{-\infty}^{\infty} E_V(\omega) d\omega.$$
 (15.6.2)



Fig. 15.6.1 Schematic picture of float trajectories in the North Atlantic. The motion caused by mean currents and mesoscale eddies

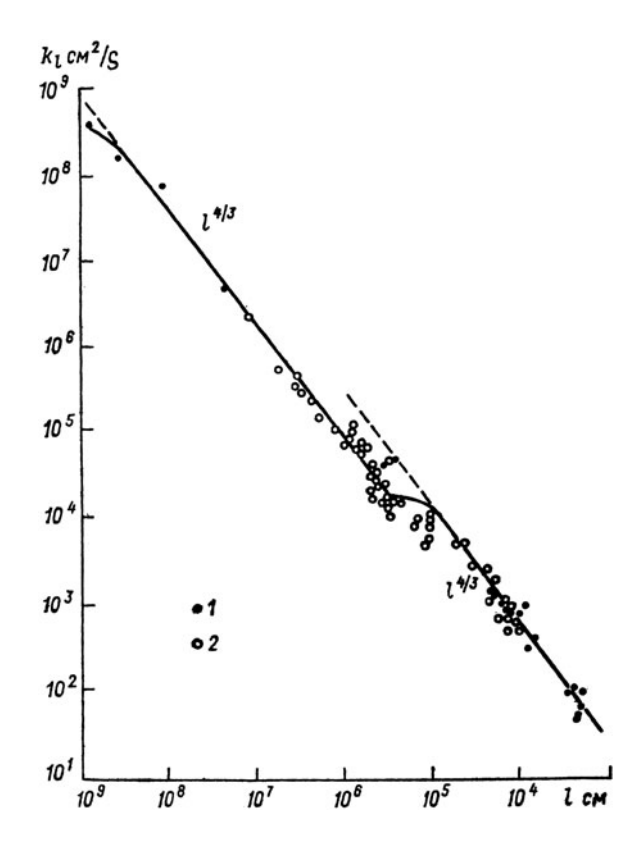


Fig. 15.6.2 The plot of sizerelated dispersion for different horizontal scales (After Okubo A. Ozmidov R.V [297] with permission)

Then, the Richardson law

$$\langle l_{\rm R}^2(t) \rangle \propto {\rm const} \cdot \varepsilon_K t^3,$$
 (15.6.3)

can be treated as a white noise in an impulse space, where the energy flux over the spectrum,  $D_V \propto \varepsilon_K$ , plays the role of the diffusive coefficient

$$\frac{(\Delta V)^2}{t} = \varepsilon_K = \text{const.}$$
 (15.6.4)

Calculations yield the estimate of the frequency spectrum  $E_V(\omega)$  in the scaling form

$$E_V(\omega) \propto \frac{\langle V^2 \rangle}{\omega} \propto \frac{\varepsilon_K}{\omega^2} \propto \frac{1}{\omega^2}.$$
 (15.6.5)

On the other hand, we can derive the expression

$$\frac{1}{2} \left\langle \left(\frac{\mathrm{d}z}{\mathrm{d}t}\right)^2 \right\rangle = \int_0^\infty \omega^2 E_z(\omega) \mathrm{d}\omega, \tag{15.6.6}$$

which leads to the relationship between the spectra  $E_V(\omega)$  and  $E_r(\omega)$  in the form

$$E_{\rm r}(\omega) \propto E_V(\omega) \frac{1}{\omega^2} \propto \frac{1}{\omega^4}.$$
 (15.6.7)

Thus, the realization of Richardson's law implies the specific form for the frequency spectrum  $E_r(\omega) \propto \omega^{-4}$ .

A similar spectrum was found in both the theory and experiments on investigation of spectral properties of sea-waves by Zakharov [299] and Toba [300]

$$E_{\rm h}(\omega) \propto \frac{1}{\omega^4}.$$
 (15.6.8)

Using this, Golitsyn pointed out that due to the fluid incompressibility

$$div \, \vec{u} = 0, \tag{15.6.9}$$

vertical and horizontal displacements have the same frequency spectrum; hence, the main reason for Richardson's law to be valid in describing relative diffusion in oceanology is the existence of the inertial interval in the turbulent spectrum of seawaves predicted by Zakharov. Undoubtedly, this is a highly significant example of the interaction between wave turbulence and vortex turbulence.

Further Reading 263

In conclusion, we recall Taylor's words [301]: "Since the curve shown when here seems to contain all the observational data that Richardson had when he announced the remarkable Richardson law, it reveals a well-developed physical intuition that he chose as his index 4/3 instead of, say, 1.3 or 1.4 but he had the idea that the index was determined by something connected with the was energy was handed down from larger to smaller and smaller eddies. He perceived that this is a process which, because of its universality, must be subject to some simple universal rule."

#### **Further Reading**

#### Two-Dimensional Turbulence

- D. Biskamp, *Magnetohydrodynamic Turbulence* (Cambridge University Press, Cambridge, 2004)
- S. Kida, M. Takaoka, Annu. Rev. Fluid Mech. **26**, 169 (1994)
- R.H. Kraichnan, D. Montgomery, Rep. Prog. Phys. 43, 547 (1980)
- J. Sommeria, Les Houches Series (Nova Science publisher, New York, 2010)
- P. Tabeling, Phys. Rep. **362**, 1–62 (2002)

## Magnetized Plasma Physics

- R. Dandy, *Physics of Plasma* (Cambridge University Press, Cambridge, 2001)
- P.H. Diamond, S.-I. Itoh, K. Itoh, *Modern Plasma Physics*, vol. 1 (Cambridge University Press, Cambridge, 2010)
- W. Horton, Y.-H. Ichikawa, *Chaos and Structures in Nonlinear Plasma* (Word Scientific, Singapore, 1994)
- B.B. Kadomtsev, *Tokamak Plasma: A Complex System* (IOP Publishing, Bristol, 1991)
- J.A. Krommes, Phys. Rep. **360**, 1–352 (2002)
- M. N. Rosenbluth, R. Z. Sagdeev (eds.) *Handbook of Plasma Physics*, (North-Holland, Amsterdam 1984)
- Toscani Boffi, Rionero (eds) Mathematical Aspects of Fluid and Plasma Dynamics. Proc. Salice Terme 1988, (Springer, 1991)
- J.A. Wesson, *Tokamaks* (Oxford University Press, Oxford, 1987)

## Magnetohydrodynamic Turbulence and Dynamo

S. Childress, A.D. Gilbert, *Stretch, Twist, Fold: The Fast Dynamo* (Springer, Berlin, 1995)

- E. Falgarone, T. Passot (eds.), *Turbulence and Magnetic Fields in Astrophysics* (Springer, Berlin, 2003)
- E. Parker, Cosmical Magnetic Fields (Oxford University Press, Oxford, 1980)
- E. Priest, T. Forbes, *Magnetic Reconnection* (Cambridge University Press, Cambridge, 2000)
- J.E. Pringle, A. King Astrophysical Flows (Cambridge University Press, Cambridge)
- A. Ruzmaikin, A. Shukurov, D. Sokoloff, *Magnetic Fields of Galaxies* (Springer, Berlin, 1988)
- D. D. Schnack Lectures in Magnetohydrodynamics. With an Appendix on Extended MHD (Springer, 2009)
- A.M. Soward et al. (eds.), Fluid Dynamics and Dynamos in Astrophysics (CRC, FL, USA, 2002)
- YaB Zeldovich et al., Magnetic Fields in Astrophysics (Springer, Berlin, 2005)

# Part VII Convection and Scaling

# Chapter 16

# **Convection and Rayleigh Number**

#### **16.1** Buoyancy Forces

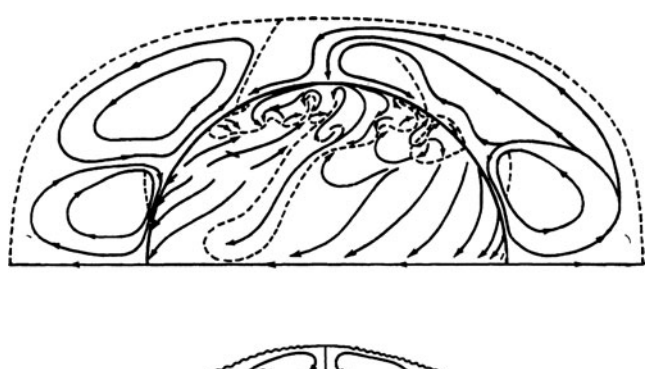
Convection may be considered as a part of fluid turbulence and recent research has many parallels with studies of turbulence. For instance, there is considerable interest in coherent structures and intermittency effects. Convection in the environment is almost always a turbulent flow, characterized by unsteady motions over a range of length and timescales [302–306]. Indeed, most of the motion in the Earth atmosphere takes the form of convection, caused by warming of the planet by the Sun: heat absorbed by the surface of the Earth is transmitted to the lower layers of the atmosphere; warmer air being lighter, it rises, leaving surface for downward currents of cold air see Fig. 16.1.1.

The upthrust on a body submerged in water is equal to the weight of water it displaces that was discovered by Archimedes. Indeed, a body of volume W and density  $\rho_T$  have a weight  $g\rho_T W$ , where g is the acceleration due to gravity. In water of density  $\rho_m$ , the body displaces a weight of water  $g\rho_m W$ . The net buoyancy force on the body submerged in water is  $g(\rho_m - \rho_T)W$ . By applying the Newton second law, one easily obtains the vertical acceleration in the form  $g(\rho_m - (\rho_T/\rho_T))$ . The body referred to may itself be a volume of water. Let us suppose that this volume of water has the density  $\rho_T$  and it is surrounded by water of density  $\rho_m$ . The buoyancy of such a volume is given by the expression

$$B_{\rho} = g \frac{\rho_{\rm m} - \rho_{\rm T}}{\rho_{\rm m}}.$$
 (16.1.1)

The buoyancy is positive if the density of the volume is less than that of its surroundings.

Consider a small volume of water of density  $\rho_T$ , which is displaced upward by a small displacement l. Then, the density difference between it and its new surroundings is  $-l(d\rho_T/dz)$ . Here, we suppose that there exists a uniform density gradient  $d\rho_T/dz$ , with the z coordinate in the vertically upward direction. If it is released, its upward acceleration will be of order



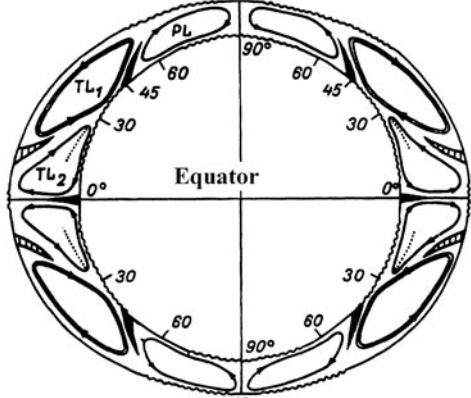


Fig. 16.1.1 Sketch of the general atmospheric circulation composed of direct and indirect cells

$$B_{\rho} = \frac{gl}{\rho_{\rm T}} \frac{\mathrm{d}\rho_{\rm T}}{\mathrm{d}z}.\tag{16.1.2}$$

When density increasing upward

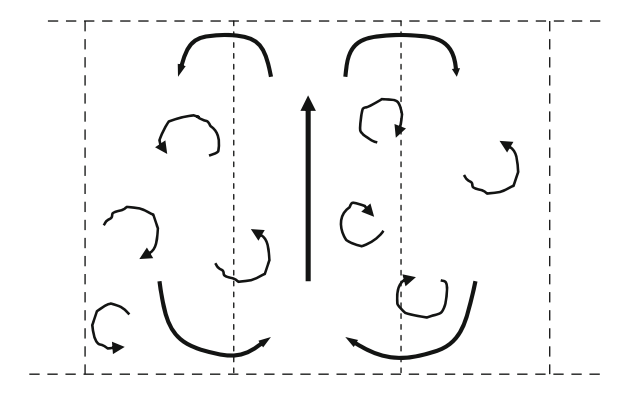
$$\frac{\mathrm{d}\rho_{\mathrm{T}}(z)}{\mathrm{d}z} > 0,\tag{16.1.3}$$

the net force is upward and the acceleration is positive. This means that the volume of water will move away from its initial position (see Fig. 16.2.1).

The basic destabilizing force is the differential buoyancy experienced by a fluid particle subjected to a temperature fluctuation. Let us estimate the typical acceleration due to this differential buoyancy:  $\alpha_\rho$  being the thermal expansion coefficient (i.e.,  $-(1/\rho_{\rm m})(\partial\rho_{\rm T}/\partial T)),\,g$  is the acceleration due to gravity,  $\rho_{\rm m}$  is some average density, and the order of magnitude of density fluctuations is  $\rho_{\rm m}\alpha_\rho\Delta T,$  where  $\Delta T$  is the temperature difference between the top (cold) and the bottom (hot) plates. The potential buoyancy force per unit volume is then  $\rho_{\rm m}\alpha_\rho g\Delta T,$  which allows the definition of the characteristic time  $\tau_{\rm B}$  through

$$\rho_{\rm m} \alpha_{\rho} g \Delta T = \text{force} = \rho_{\rm m} \times \text{acceleration} = \rho_{\rm m} \frac{L_0}{\tau_{\rm B}^2}.$$
 (16.1.4)

**Fig. 16.2.1** Schematic illustration of a convective flow cell



Apart from numerical factors,  $\tau_B$  is the time required for a hot bubble to rise, or a cold bubble to sink over the distance  $L_0$ .

Damping is expected from the irreversible trend to uniformity: relaxation of velocity gradients via viscous friction and relaxation of temperature gradients via heat diffusion. Both processes are governed by a law of the diffusive form. Here, we have two diffusivities: the kinematic viscosity  $v_F = \eta_F/\rho_m$ , where  $\eta_F$  is the dynamical viscosity, and the heat diffusivity  $\chi_q = \chi_Q/C_q$ , where  $\chi_Q$  is the heat conductivity and  $C_q$  is the hear capacity per unit volume.

The viscous characteristic time  $\tau_{\nu}$  is given by the relation  $\nu_{\rm F} = L_0^2/\tau_{\nu}$  and the diffusive characteristic time  $\tau_{\rm D}$  is then defined as follows:  $k_q = L_0^2/\tau_{\rm D}$ . The Rayleigh number

$$Ra = \frac{\alpha_{\rho} g \Delta T L_0^3}{k_{\rm T} v_{\rm F}},\tag{16.1.5}$$

can then be understood as the ratio  $\tau_{\nu}\tau_{D}/\tau_{B}^{2}$ , where  $\tau_{B}$  contains explicitly the control parameter  $\Delta T$ .

When  $Ra \ll 1$ , i.e.,  $\tau_B \gg \tau_\nu \tau_D$ , the buoyancy force is insufficient to make the hot (cold) bubble rise (sink) sufficiently quickly. Damping process, especially thermal diffusion, irons out the fluctuation so that the layer remains at rest. On the contrary, when  $Ra \gg 1$ , i.e.,  $\tau_B \ll \tau_\nu \tau_D$ , the buoyancy is expected to be strong enough to overturn the layer. The convection threshold should then correspond to some "intermediate" value of Ra that remains to be estimated.

## 16.2 The Oberbeck-Boussinesq Equations

The Boussinesq approximation is basically an assumption of moderate heating reasonably valid in usual experimental situations. Thermodynamic properties of the fluid are considered in a state equation that simply reads:

$$\rho_{\rm T}(T) = \rho_{\rm m}(1 - \alpha_{\rm o}(T - T_{\rm m})), \tag{16.2.1}$$

where  $T_{\rm m}$  is a reference temperature,  $\rho_{\rm m}$  is the density at that temperature, and  $\alpha_{\rho}$  is the coefficient of thermal expansion (most of the time we will take  $T_{\rm m}$  at the bottom plate:  $y_{\rm m}=0$ ). Mechanically, the fluid can be treated as incompressible and all density fluctuations are neglected except in the buoyancy term.

The incompressibility condition (continuity of matter) reads

$$\vec{V} \cdot \nabla \vec{V} = \frac{\partial V_x}{\partial x} + \frac{\partial V_y}{\partial y} + \frac{\partial V_z}{\partial z} = 0, \qquad (16.2.2)$$

The Navier-Stokes equations in our case is given by

$$\rho_{\rm m} \left( \frac{\partial}{\partial t} + \vec{V} \cdot \nabla \right) \vec{V} = -\nabla P + \eta_{\rm F} \nabla^2 \vec{V} + \rho_{\rm T}(z) \vec{g}. \tag{16.2.3}$$

It contains the buoyancy term (the dynamical viscosity  $\eta_F = \rho_m \nu_F$  is assumed independent of the local temperature). According to our qualitative understanding of the instability mechanism, we know that the vertical direction is singled out.

The heat equation reads

$$C_q \left(\frac{\partial}{\partial t} + \vec{V} \cdot \nabla\right) T = \chi_Q \nabla^2 T,$$
 (16.2.4)

where the heat capacity per unit volume  $C_q$  and the thermal conductivity  $\chi_{\varrho}$  are assumed constant (heating due to viscous dissipation is also neglected).

We shall generally assume that the fluid layer is of infinite horizontal extent. The horizontal boundaries are either rigid walls or free surfaces. The case of the no-slip condition yields a velocity of zero at the respective boundary. Such boundary conditions at free surfaces are given by  $V_z = 0$ , where we have applied the continuity equation.

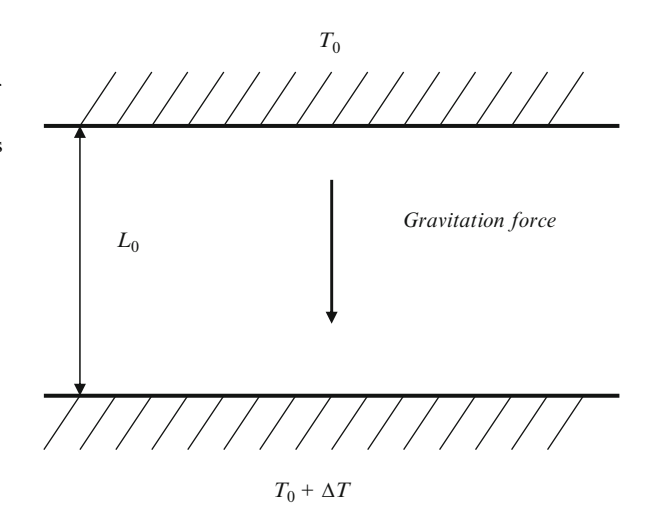
In the case of rigid walls, with the effect of capillarity neglected, both the normal stress and the shearing stress are zero at the free surface. Summarized, the boundary conditions at rigid walls are given by  $\partial V_z/\partial z=0$ . Besides, the boundaries will usually be assumed to be perfect heat conductors.

The validity of these approximations is discussed here. We just note that simplifications introduced above are generally supported by order of magnitude estimates but may be insufficient in certain cases, e.g., for water around 4° where it presents a density maximum, thus calling for "non-Boussinesq correction".

## 16.3 The Rayleigh-Benard Instability

Rayleigh–Benard instability arises when a thin layer of fluid is suggested to heat fluxes at the top and/or bottom of the layer (see Fig. 16.3.1). The motion that results from this type of instability is referred to as Rayleigh–Benard convection, and it is

Fig. 16.3.1 Schematic diagram of the Rayleigh–Benard problem of convection between two infinite horizontal boundaries



manifested in certain types of stratocumulus, altocumulus, and cirrocumulus, which exhibit substructure in the form of rolls and cells (see Fig. 16.3.2). An instability theory to explain the phenomenon was provided by Rayleigh. This type of convection was described by Thomson (1881), who observed a pattern of cells of overturning fluid in a barrel of warm soapy water behind an inn used for cleaning glasses. His theory is based on the Boussinesq equations applied to an incompressible fluid that expands as its temperature is increased. For such a fluid, the buoyancy is given by  $B_{\rho} = g\alpha_{\rho}T'$ , where  $\alpha_{\rho}$  is the expansion coefficient, defined such that  $\rho'/\rho_{\rm m} = -\alpha_{\rho}T'$ . Friction and heat conductivity are parameterized in terms of a constant viscosity  $\nu_{\rm F}$  and thermal conductivity  $\chi_Q$ . The equations are linearized about a state of zero mean motion and horizontally uniform temperature [307–311]. Perturbations are then governed by the equation of motion,

$$\frac{\partial \vec{V}'}{\partial t} = -\frac{1}{\rho_{\rm m}} \nabla P' + \vec{g} \alpha_{\rho} T + \nu_{\rm F} \nabla^2 \vec{V}', \qquad (16.3.1)$$

the continuity equation,

$$\nabla \cdot \vec{V}' = 0, \tag{16.3.2}$$

and the thermodynamic equation,

$$\frac{\partial T'}{\partial t} - V_z \beta_q = \chi_q \nabla^2 T', \qquad (16.3.3)$$

where  $\chi_q = \chi_Q/\rho C_q$ ,  $C_q$  is the specific heat of the homogeneous fluid, and  $\beta_q = -\partial T/\partial z$  is maintained by heating below and/or cooling above. Substitution of solutions of the form

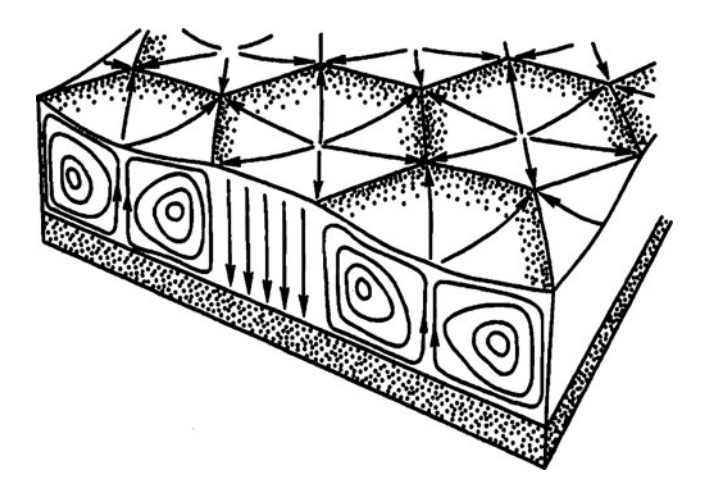


Fig. 16.3.2 Sketch of the Rayleigh-Benard cells

$$V_{\tau}', T' \propto \sin k_y z e^{i(k_x x + k_y y)} e^{\gamma_{RB} t}, \qquad (16.3.4)$$

$$V'_{\nu}, V'_{\nu}P' \propto \cos k_{\nu}ze^{i(k_{\nu}x+k_{\nu}y)}e^{\gamma_{\rm RB}t}, \qquad (16.3.5)$$

into equations for perturbation  $\vec{V}'$ , T' leads to the dispersion relation

$$\gamma_{\text{RB}}^{2}(k_{x}^{2} + k_{y}^{2} + k_{z}^{2}) + \gamma_{\text{RB}}(\chi_{q} + \nu_{\text{F}})(k_{x}^{2} + k_{y}^{2} + k_{z}^{2})^{2} + \nu_{\text{F}}\chi_{q}(k_{x}^{2} + k_{y}^{2} + k_{z}^{2})^{3} - \beta_{q}g\alpha_{\rho}(k_{x}^{2} + k_{y}^{2}) = 0.$$
(16.3.6)

Solving this quadratic equation leads further to the conclusion that unstable solutions ( $\gamma_{RB}$  positive and real) occur when

$$\beta_q g \alpha_\rho (k_x^2 + k_y^2) + \nu_F \chi_q (k_x^2 + k_y^2 + k_z^2)^3 < 0.$$
 (16.3.7)

If there is no friction ( $v_F = 0$ ), this relation reduces to simply  $\beta_q > 0$ . That is, the lapse rate must be positive to get unstable growth. If both friction and conduction are finite, then terms in the dispersion relation can be rearranged to

$$Ra > \frac{(k_x^2 + k_y^2 + k_z^2)^3 L_0^4}{k_x^2 + k_y^2},$$
(16.3.8)

where Ra is the Rayleigh number, defined as

$$Ra \equiv \frac{L_0^3 \nabla T g \alpha_{\rho}}{\chi_{\alpha} v_{\rm F}},\tag{16.3.9}$$

and  $L_0$  is the depth of the fluid. The expression for the Rayleigh number contains all of the prescribed characteristics of the fluid. If it is assumed that the vertical wave number is related to  $L_0$  by  $k_z = \pi/L_0$ , then it is clear that instability can occur for any number of combinations of  $k_x$  and  $k_y$ , including both cells  $(k_x = k_y)$  and rolls  $(k_x = 0, k_y \neq 0)$ ; and the value which Ra must exceed, according to the dispersion relation obtained above, is a function of horizontal wave number  $\sqrt{k_x^2 + k_y^2}$ , as shown in Fig. 16.3.3.

In order to be unstable at all, the Rayleigh number characterizing the fluid must exceed the minimum value:

$$Ra_* = \frac{27\pi^4}{4} \approx 657.5,$$
 (16.3.10)

which is found from the dispersion relation by differentiating the right-hand side of it with respect to  $(k^2+l^2)$ . The most unstable solution for the special case of  $\chi_q=\nu_F$  is obtained by differentiating the dispersion relation with respect to  $(k_x^2+k_y^2+k_z^2)$  (or  $(k_x^2+k_y^2)$ ) and setting

$$\frac{d\gamma_{\text{RB}}}{d(k_x^2 + k_y^2 + k_z^2)} = 0,$$
(16.3.11)

to find the condition of maximum  $\gamma_{RB}$ . A second equation in  $\gamma_{RB}$  is given by

$$\frac{k_z^2}{k_x^2 + k_y^2 + k_z^2} = 1 - \frac{Ra}{L_0^4} \left(\frac{k_z}{k_x^2 + k_y^2 + k_z^2}\right)^4,$$
 (16.3.12)

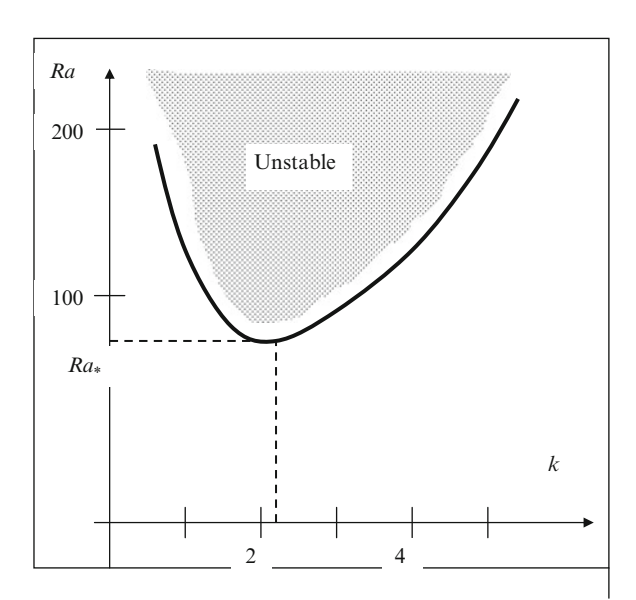


Fig. 16.3.3 Schematic diagram of stable and unstable regions for the Rayleigh–Benard problem

which is the relation among the wave numbers when  $\gamma_{RB}$  has its maximum value. If we again assume that  $k_z = \pi/L_0$  and that we have square cells such that  $k_x = k_y = 2\pi/S$ , where S is the spacing of the cells.

The critical value of the Rayleigh number  $Ra_*$  depends on the boundary conditions. In the case of more realistic boundary conditions [308–311], we have larger values than  $Ra_* \approx 657.5$ , but still of the same order of magnitude. For a layer of water 10 cm deep, a Rayleigh number of 1,000 is achieved with a temperature difference  $10^{-4}$  K and that is why any realistic unstable temperature distribution will produce Rayleigh numbers that far exceed critical values. Because Rayleigh number increases rapidly with  $L_0$ , deeper layers produce even higher values of Ra.

#### 16.4 The Lorenz Model and Strange Attractor

There is another line of attack, which could be used to consider the Rayleigh–Benard convection. We start from the Boussinesq approximation, which assumes that the density variations are incorporated only in the buoyancy term. Perturbations are then governed by the equation of motion, the continuity equation, and the thermodynamic equation, respectively

$$\frac{\partial \vec{V}'}{\partial t} = -\frac{1}{\rho_{\rm m}} \nabla P' + \vec{g} \alpha_{\rho} T + v_{\rm F} \nabla^2 \vec{V}', \qquad (16.4.1)$$

$$\nabla \cdot \vec{V}' = 0, \tag{16.4.2}$$

$$\frac{\partial T'}{\partial t} + V_z \frac{\partial T}{\partial z} = \chi_q \nabla^2 T'. \tag{16.4.3}$$

Taking the curl of the motion equation yields an equation for the vorticity,

$$\frac{d\vec{\Omega}}{dt} + (\vec{u} \cdot \nabla)\vec{\Omega} = (\vec{\Omega} \cdot \nabla)\vec{u} + v_F \nabla^2 \vec{\Omega} - \alpha_\rho \nabla \times (g\Delta T), \tag{16.4.4}$$

which is given by the conventional relation  $\vec{\Omega}(x,y,z,t) = \nabla \times \vec{u}$ . The velocity is zero in the z direction, i.e.  $\vec{u} = (u_x, u_y, 0)$ . The assumption of two-dimensionality eliminates the term, which describes vortex stretching in the equation of motion. The vorticity has a nonzero component only in the z direction,  $\vec{\Omega} = (0,0,\Omega)$ , and the previous equation takes the form

$$\frac{d\vec{\Omega}}{dt} + (\vec{u} \cdot \nabla)\vec{\Omega} = v_F \nabla^2 \vec{\Omega} - g\alpha_\rho \frac{\partial \nabla T}{\partial r}.$$
 (16.4.5)

Two-dimensional incompressible flow may be expressed by the scalar stream function  $\psi$ :

$$u_x = \frac{\partial \psi(x, y, t)}{\partial y}, u_y = -\frac{\partial \psi(x, y, t)}{\partial x}.$$
 (16.4.6)

The vorticity is related to the stream function  $\psi$  by the Poisson equation

$$\vec{\Omega}(x, y, z, t) = \nabla^2 \psi, \tag{16.4.7}$$

and the vorticity equation could be written in terms of stream function  $\psi$  as follows:

$$\frac{\partial}{\partial t} \nabla^2 \psi - \left[ \psi, \nabla^2 \psi \right] = \nu_F \nabla^4 \psi - g \alpha_\rho \frac{\partial \Delta T}{\partial x}. \tag{16.4.8}$$

Here, the conventional relation for the two-dimensional Jacobian operator is used

$$[f,g] \equiv \frac{\partial f}{\partial x} \frac{\partial g}{\partial z} - \frac{\partial f}{\partial z} \frac{\partial g}{\partial x}.$$
 (16.4.9)

We now write the temperature field T in terms of a background profile  $\langle T \rangle$ , which depends only on y and the temperature perturbation T'

$$T(x, y, t) = \langle T(y) \rangle + T'(x, y, t).$$
 (16.4.10)

The equation for the temperature perturbation T' takes the following form:

$$\frac{\partial T'}{\partial t} - [\psi, T'] - \frac{\partial \psi}{\partial x} \frac{\partial \langle T \rangle}{\partial y} = \chi_q \nabla^2 T' + \chi_q \frac{\partial^2 \langle T \rangle}{\partial y^2}.$$
 (16.4.11)

Boundary conditions of no normal flow and no slip at the upper and lower boundaries imply that:

$$\psi|_{y=0} = \nabla^2 \psi|_{y=0} = 0, \psi|_{y=L_0} = \nabla^2 \psi|_{y=L_0} = 0.$$
 (16.4.12)

The temperature at the top and bottom boundaries is fixed, so

$$T'|_{y=0} = 0, T'|_{y=L_0} = 0.$$
 (16.4.13)

Lorenz took the system of equations obtained by truncating the original infinite system to only three variables [313]. This corresponds to looking for solutions of the form

$$\psi(x, y, t) \frac{a_{\rm R}}{\sqrt{2}(1 + a_{\rm R}^2)\chi_q} = X(t)\sin\left(\frac{\pi a_r}{L_0}x\right)\sin\left(\frac{\pi}{L_0}y\right),\tag{16.4.14}$$

$$T'(x,y,t)\frac{\pi Ra}{Ra_*\Delta T} = \sqrt{2}Y(t)\cos\left(\frac{\pi a_r}{L_0}x\right)\sin\left(\frac{\pi}{L_0}y\right) + Z(t)\sin\left(\frac{2\pi}{L_0}x\right). \quad (16.4.15)$$

By substituting the truncated Fourier expansions of  $\psi$  and T' into the governing equations, we find three coupled ordinary differential equations for the coefficients X(t), Y(t), and Z(t):

$$\dot{X} = -\Pr X + \Pr Y,$$
 (16.4.16)

$$\dot{Y} = -XZ + R_I X - Y$$
, and (16.4.17)

$$\dot{Z} = XY - b_R Z.$$
 (16.4.18)

To obtain this system, one also rescales time

$$\tau_0 = \frac{\pi^2 (1 + a_{\rm R}^2) \chi_q t}{H^2}.$$
 (16.4.19)

Here, the normalized Rayleigh number is  $R_L = Ra/Ra_*$ , the parameter  $b_R$  is related to the aspect ratio of convective cells  $b_R = 4/1 + a_R^2$ , and the Prandtl number is  $\Pr = v_F/\chi_q$ . The coefficient X is proportional to the intensity of the convective motion. The coefficient Y is proportional to the difference in temperature between the upgoing and downgoing currents. The coefficient Z describes the horizontally averaged deviation from the linear temperature profile. This is a dissipative system, since its divergence is negative:

$$\frac{\partial \dot{X}}{\partial x} + \frac{\partial \dot{Y}}{\partial y} + \frac{\partial \dot{Z}}{\partial z} = -\Pr(-1) - b_{R} < 0. \tag{16.4.20}$$

Fixed points are given by the system:

$$X - Y = 0, (16.4.21)$$

$$-XZ + (R_{L} - 1)X = 0, (16.4.22)$$

$$XY - b_{R}Z = 0, (16.4.23)$$

For  $R_L < 1$ , there is only one fixed point  $\vec{S_0}$ ,  $X_0 = Y_0 = Z_0 = 0$ , corresponding to a linear (conductive) temperature profile, with no convection. For  $R_L > 1$ , there are two additional fixed points  $\vec{S_1}$  and  $\vec{S_2}$ ,

$$X_1 = Y_1 = \sqrt{b_R(R_L - 1)}, \quad Z_1 = R_L - 1,$$
 (16.4.24)

$$X_2 = Y_2 = -\sqrt{b_R(R_L - 1)}, \quad Z_2 = R_L - 1,$$
 (16.4.25)

corresponding to steady convection in parallel rolls.

By a linear stability analysis, it can be shown that  $\vec{S_0}$  is the only stable fixed point for  $R_L < 1$ . At  $R_L = 1$ , there is a pitchfork bifurcation in which  $\vec{S_0}$  becomes unstable and  $\vec{S_1}$  and  $\vec{S_2}$  appear as new, stable equilibria. If  $\Pr > b_R + 1$ ,  $\vec{S_1}$  and  $\vec{S_2}$  become unstable through a subcritical Hopf bifurcation at

$$R_{\rm L} = R_{**} = \frac{\Pr(\Pr + b_{\rm R} + 3)}{\Pr - b_{\rm P} - 1}.$$
 (16.4.26)

The consequence of the disappearance of the stable fixed point is chaotic motion [313–317]. In the phase space, the attractor of the system (see Fig. 16.4.1) is a "strange" object, with a fractal dimension.

The trajectory of the solution follows a part in phase space that spirals away from one unstable fixed point and then loops in close to the other unstable fixed

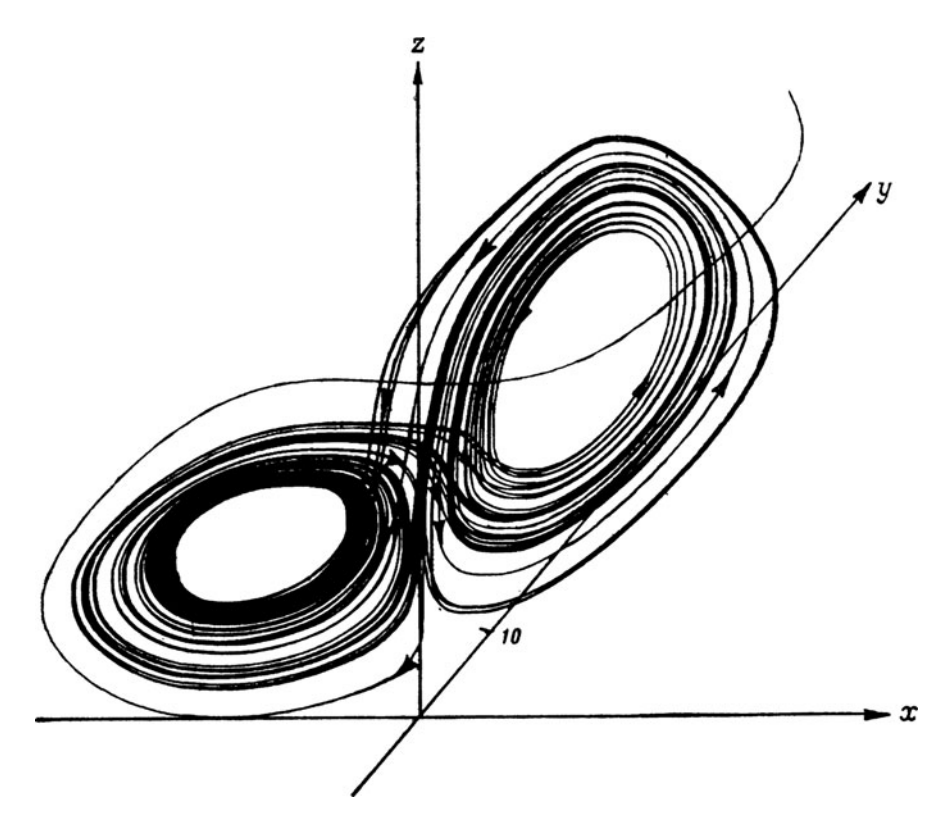


Fig. 16.4.1 The Lorenz attractor

point. It then spirals away from this second unstable focus until it loops back to the neighborhood of the first unstable fixed point. The switching between orbiting around one unstable fixed point and the other follows an irregular, aperiodic sequence. Trajectories started from nearby points on the strange attractor diverge rapidly from one another, though they remain on the attractor. Such a sensitivity to initial conditions makes the prediction of the trajectory impossible even though the system is deterministic. Strange attractors are intimately associated with chaotic dynamics and unpredictability in dissipative systems.

Detailed understanding of the processes involved in the transition to turbulence requires more sophisticated theory. In this chapter, the Rayleigh–Benard convection has served as a pretext for a detailed presentation of some technicalities involved in convective turbulence analysis. It will now serve us to introduce both the quasilinear approach and scaling to describe complex convective structures, at a phenomenological level.

### **Further Reading**

#### Convection

- P. Berge, Y. Pomeau, C. Vidal, *L'ordre dans le chaos* (Hermann, Editeurs des sciences et des arts, 1988)
- A. Boubnov, G. Golitsyn, Convection in Rotating Fluids (Springer, Berlin, 1995)
- J. G. Knudsen, D. L. Katz Fluid dynamics and heat transfer, MGH, (1958)
- Palmen, C.W. Newton, *Atmospheric Circulation Systems* (Academic, London, 1969)
- R.S. Scorer, *Environmental Aerodynamics* (Wiley, New York, 1978)
- T. Zhao, Convective and advective heat transfer in geological science (Springer, Berlin, 2008)

## Cloud Dynamics

- D. G. Andrews, *An Introduction to Atmospheric Physics* (Cambridge University Press, Cambridge, 2010)
- R. G. Fleagle, J.A. Businger, *An Introduction to Atmospheric Physics* (Academic, London, 1980)
- R. A. Houze, *Cloud Dynamics* (Academic, London, 1993)
- R. R. Rogers, A Short Course in Cloud Physics (Pergamon, Oxford, 1976)
- H. U. Roll, *Physics of the Marine Atmosphere* (Academic, London, 1965)
- A. Tsonis, *An Introduction to Atmospheric Thermodynamics* (Cambridge University Press, Cambridge, 2007)

# Chapter 17

## **Convection and Turbulence**

#### 17.1 The Obukhov–Golitsyn Scaling for Turbulent Convection

In this section, we establish the relationship between the classical Zeldovich and Kolmogorov results of turbulent transport of scalar particles and the theory of turbulent convection. Let us consider the simplified balance of energy in a convective flow. In the steady case, the rate of kinetic energy generation,

$$E_{(+)} = \alpha_{\rho} \rho g \int_{0}^{L_{0}} \langle V_{Z} T' \rangle dz, \qquad (17.1.1)$$

must be equal to the rate of energy dissipation of convective motions due to the viscous effects:

$$E_{(-)} = -\rho v_{\rm F} \int_0^{L_0} \langle \vec{V} \Delta \vec{V} \rangle dz. \tag{17.1.2}$$

Here,  $L_0$  is the fluid layer depth.

In order to write a heat balance equation, we have to take into account the heat flux  $q_T$  to a lower boundary of fluid. This flux is the sum of the heat conduction contribution and the convective motion term

$$q_{\rm T} = q_0 + q_{\rm conv} = -\rho C_p \chi_q \frac{dT}{dz} + \rho C_p \langle V_Z \delta T \rangle. \tag{17.1.3}$$

Finally, the heat balance in the absence of internal sources has the form

$$q_{\rm T}L_0 = q_0L_0 + E_{(+)}H_B. (17.1.4)$$

When convection occurs the heat transfer is greater than that by conduction. It is convenient to measure this increase by the dimensionless Nusselt number

$$Nu = \frac{q_{\rm T}}{q_0} = \frac{q_{\rm T}}{\left(\frac{\chi_q \Delta T}{\lambda}\right)}.$$
 (17.1.5)

Here, the denominator is the heat flux that would result from the steady conduction. This means that the Nusselt number is the dimensionless value of the actual heat flux, and when we are dealing with the conductive regime, one obtains Nu = 1. For regimes where convection is presented, we have Nu > 1.

Now, by taking into account the energy balance, we can write the expression

$$q_{\rm T} = \frac{q_{\rm T}}{Nu} + E_{(+)} \frac{H_B}{L_0},\tag{17.1.6}$$

which allows us to estimate the efficiency of heat power convertation brought into the convective layer

$$\gamma = \frac{E_{(+)}}{q_{\rm T}} = \left(\frac{L_0}{H_B}\right) \left(1 - \frac{1}{Nu}\right) \approx \frac{L_0}{H_B},$$
 (17.1.7)

where we suppose that  $Nu \gg 1$ . This expression allows the heat flux to be determined in terms of the external parameters of convective flows  $L_0$  and  $H_B$  and so is of considerable practical as well as conceptual value.

On the other hand, we can easily evaluate the energy dissipation for the quasisteady case

$$E_{(-)} \approx E_{(+)} = \gamma q_{\rm T} \approx \frac{L_0}{H_R} \left( 1 - \frac{1}{Nu} \right) q_{\rm T} \approx \frac{L_0}{H_R} q_{\rm T},$$
 (17.1.8)

where  $Nu \gg 1$ .

At this stage, it is natural to apply the Kolmogorov–Obukhov concept of well-developed turbulence to the turbulent convection in the horizontal infinite layer of a fluid. Thus, we can estimate the Kolmogorov constant  $\varepsilon_{\rm K}$ . Indeed, using an expression for the kinetic energy dissipation in a flat layer  $E_{(-)}$ , we find the Golitsyn formula [318] for an energy flux

$$\varepsilon_{\rm K} = \frac{E_{(-)}}{\rho L_0} = \frac{q_{\rm T}}{\rho H_B} \frac{Nu - 1}{Nu}.$$
 (17.1.9)

In the case of the high Nusselt number  $Nu \gg 1$   $(q_T \gg q_0)$ , we deal with the well-developed convective turbulence. This allows us to introduce the scaling for the energy flux

$$\varepsilon_{\rm K} = \frac{q_{\rm T}}{\rho H_B} = \left(\frac{\alpha_\rho g}{\rho c_p}\right) q_{\rm T}.$$
 (17.1.10)

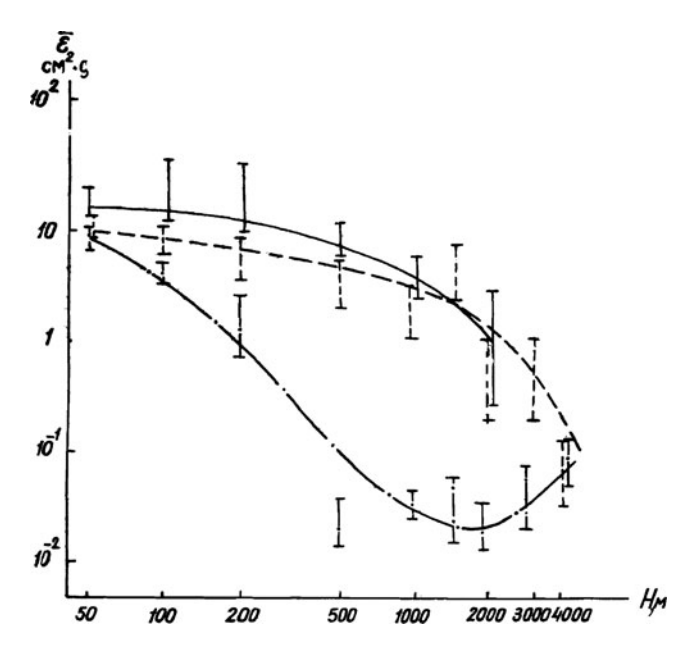


**Fig. 17.1.1** The mean profile of the energy dissipation rate for different values of height (After Koporov B.M. Tsvang L.R. [319] with permission)

For modeling the turbulent convection in the atmospheric boundary layer, this scaling was applied by Obuchov [241]. From this experiment, the order of the magnitude of  $\varepsilon_K$  was experimentally defined in conditions of clear sky in a steppe on different levels. Data obtained (see Fig. 17.1.1) allow one to consider the estimate of  $\varepsilon_K \approx 5 \, \text{cm}^2/\text{s}^3$  as rather correct ranging from 50 to 1,000 m.

# 17.2 Quasilinear Regimes of Turbulent Convection

We turn our attention to different aspects of the model under analysis. In the turbulent convection regimes, where the Nusselt numbers are high, the formula  $\varepsilon_{\rm K} = (\alpha_\rho g/\rho c_p)q_{\rm T}$  leads to Zeldovich's quasilinear scaling obtained from the general analysis of scalar transport equations

$$D_{\rm eff} \propto D_0({\rm const} + Pe^2). \tag{17.2.1}$$

Let us calculate the characteristic velocity of convective motions basing on the dimensional estimate of viscous dissipation

$$\varepsilon_{\rm K} \propto v_{\rm F} \frac{V_0^2}{L_0}.\tag{17.2.2}$$

In the case of  $Nu \gg 1$ , one can find the scaling for the characteristic velocity

$$V_0 \propto \left(\frac{\varepsilon_{\rm K}}{v_{\rm F}}\right)^{1/2} L_0. \tag{17.2.3}$$

This estimate of the characteristic velocity can be rewritten in terms of the Rayleigh number and the Nusselt number

$$V_0^2 \propto L_0^2 \left(\frac{\varepsilon_{\rm K}}{\nu_{\rm F}}\right) \propto \left(\frac{q_{\rm T}}{\Delta T}\right) \left(\frac{\Delta T}{\nu_{\rm F}}\right) \propto Nu \cdot Ra.$$
 (17.2.4)

The author of [318] used this expression to analyze the energy balance in the case of convection in water. The experimental results were obtained,  $V_0 \approx 2.6\,\mathrm{mm/s}$  for  $\varepsilon_\mathrm{K} \approx 3 \times 10^{-3}\,\mathrm{cm^2/s^3}$ , which coincide with the results of independent experimental data.

Basing on linear dependence between the energy flux  $\varepsilon_{\rm K}$  and the convective heat flux  $q_{\rm T}$ 

$$\varepsilon_{\rm K} = \left(\frac{\alpha_{\rho}g}{\rho c_p}\right) q_{\rm T} \propto q_{\rm T},$$
(17.2.5)

it is easy to obtain a quasilinear scaling for a heat flux in terms of the Peclet number *Pe*:

$$q_{\rm T}(Pe) \propto Nu \propto V_0^2 \propto {\rm Re}^2 \propto Pe^2.$$
 (17.2.6)

On the other hand, on the basis of the transport equation,

$$(\vec{V}\nabla)T \approx -\frac{1}{\rho c_p} \nabla \vec{q}_{\mathrm{T}},$$
 (17.2.7)

we find an estimate of temperature fluctuations

$$\delta T(Pe) \approx \frac{q_{\rm T}(Pe)}{V_0} \frac{1}{\rho c_p} \propto V_0 \propto {\rm Re} \propto Pe.$$
 (17.2.8)

Note that both estimates obtained for the temperature fluctuation  $\delta T$  and convective heat flux  $q_{\rm T}$  coincide exactly with Zeldovich's predictions for a quasilinear case,  $Pe \ll 1$ . Indeed, such turbulent convective regimes are occurred in the regimes where viscosity effects are essential.

#### 17.3 Strong Convective Turbulence

For fixed fluid properties, which in our case are described by dimensionless Prandtl number, scaling analysis of turbulent transport suggests that

$$Nu = Nu(Ra), (17.3.1)$$

and much attention has been given to the form of this functional relationship, particularly at high Rayleigh number (see Fig. 17.3.1). The nature of dependence Nu(Ra) for the Rayleigh number  $Ra > Ra_*$  was investigated theoretically long ago by Kraichnan [320], and his work has stimulated the search for ways to explore this high Rayleigh number regime because it is related to fundamental change in the heat transport mechanism.

Note that near the boundaries heat is transferred by conduction since the vertical velocities are zero at the boundaries. The heat flux  $q_T$  across each layer is

$$q_{\rm T} = \chi_q \frac{\delta T}{\delta_{\rm T}},\tag{17.3.2}$$

where  $\delta T$  is the temperature difference across the boundary layer of thickness  $\delta_T$ . Thus, estimate for the Nusselt number is given by

$$Nu = \frac{\delta T \cdot L_0}{\Delta T \cdot \delta_T}. (17.3.3)$$

Observations show that as the Rayleigh number increases, the boundary layers become thinner and the temperature drop across them increases until

$$\delta T \approx \frac{1}{2}\Delta T,\tag{17.3.4}$$

and hence finally, one obtains the estimate in the form

$$Nu(\delta_{\rm T}) \approx \frac{L_0}{2\delta_{\rm T}}.$$
 (17.3.5)

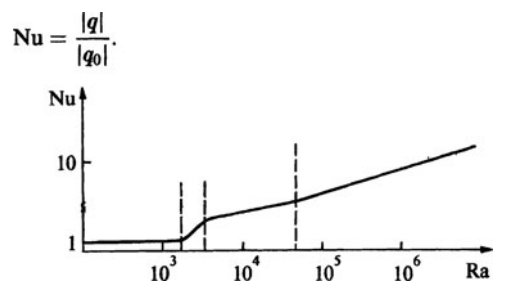


**Fig. 17.3.1** A typical plot of the dependence of the Nusselt number on the temperature difference

In the case of  $Nu \gg 1$ , the interior of the fluid has almost uniform temperature and all the temperature drop occurs across the boundary layers, which are thin compared to the fluid depth (see Fig. 17.3.2).

On the other hand, we can estimate a boundary layer width  $\delta_T$  responsible for the conduction in the steady case from the heat transport equation. In the simplified dimensional form, we find

$$V_0 \frac{T}{L_0} \approx \chi_q \frac{T}{\delta_T^2}.$$
 (17.3.6)

Then, we obtain the scaling for the layer width in terms of the Peclet number:

$$\delta_{\rm T}(Pe) \propto \frac{L_0}{\sqrt{Pe_{\rm T}}} \propto L_0 \sqrt{\frac{\chi_q}{V_0 L_0}}.$$
 (17.3.7)

Indeed, when  $Ra \gg 1$ , the buoyancy forces dominate and, when the stratification is unstable, convection will ensue. For turbulent flows (for instance, environmental) Ra is large, but near any boundary the scale of the motion is small and heat enters the fluid by conduction, through a thin boundary layer. Now, it is easy to calculate an expression for the Nusselt number

$$Nu \propto \frac{\delta_{\rm T}}{L_0} \propto \sqrt{Pe_{\rm T}} \propto \sqrt{V_0}$$
 or  $V_0^2 \propto Nu^4$ . (17.3.8)

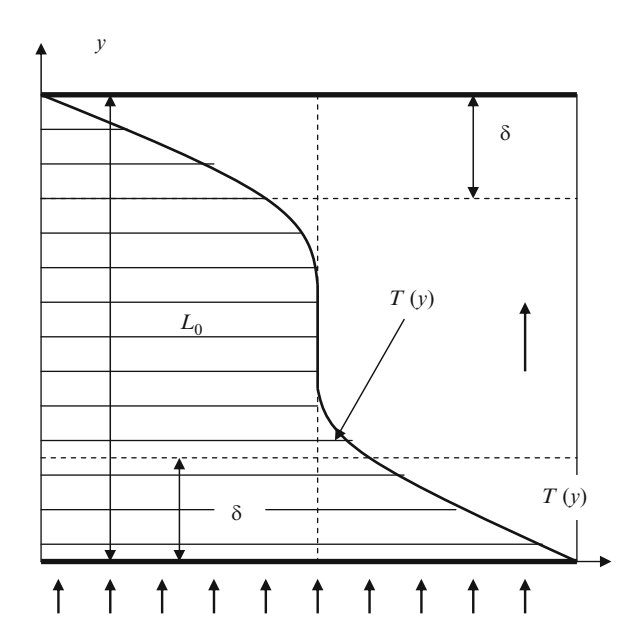


**Fig. 17.3.2** A typical plot of the temperature profile in the Rayleigh–Benard convection

By comparing this expression for  $V_0 = V_0(Nu)$  with the previous one

$$V_0^2 \propto L_0^2 \left(\frac{\varepsilon_{\rm K}}{v_{\rm F}}\right) \propto Nu \cdot Ra,$$
 (17.3.9)

we can draw the well-known scaling in the theory of turbulent convection

$$Nu(Ra) \propto Ra^{1/3},\tag{17.3.10}$$

where  $Ra \gg 1$ , which corresponds to regimes of strong convective turbulence. The corresponding heat flux is given by the expression

$$q_{\rm T} \propto \rho C_p \left(\frac{\alpha_\rho g \chi_q^2}{\nu_{\rm F}}\right)^{1/3} \Delta T^{4/3}.$$
 (17.3.11)

It is interesting that the estimate of temperature fluctuations obtained on the basis of these formulas is less than the Zeldovich classical result for the case of very strong turbulence (when  $Pe \approx \text{Re} \gg 1$ ) demonstrated before:

$$\delta T(Pe) \propto \frac{q_{\rm T}(Pe)}{V_0} \propto \frac{Nu}{V_0} \propto \frac{1}{\sqrt{V_0}} \propto \frac{1}{\sqrt{Pe}} \ll \frac{1}{Pe^{1/4}}.$$
 (17.3.12)

On the other hand, in regimes with  $Ra \propto Pe \gg 1$ , the heat transport  $q_T$  depends, in general, on the condition near boundaries  $\delta_T \propto \frac{1}{V_0} \ll L_0$  and is independent of the layer depth  $L_0$ 

$$q_{\rm T} = \chi_q \frac{\Delta T}{L_0} Nu(Ra) \propto \frac{Ra(L_0)^{1/3}}{L_0} \propto \frac{(L_0^3)^{1/3}}{L_0}.$$
 (17.3.13)

This, obviously, also leads to the scaling  $Nu \propto Ra^{1/3}$ .

In the conditions of very strong turbulence, the dependence of the Nusselt number on the Rayleigh number Nu = Nu(Ra) still remains unsolved both experimentally and theoretically.

## 17.4 Diffusive Growth of Boundary Layer

The experimental data have showed that in the case of the high Rayleigh numbers there are regimes where a convective flow is not steady. To explain the mechanism of unsteadiness, we represent a phenomenological approach, which was introduced by Howard [321]. He considered high Rayleigh number convection to consist of the

temporal development and subsequent breakdown of the boundary layers to release buoyant fluid (see Fig. 17.4.1).

Let us suppose that heat is conducted from the boundary into a layer with thickness

$$\delta_{\rm T}(t) \propto \sqrt{\chi_q t} \propto \frac{1}{Pe^{1/2}}.$$
 (17.4.1)

The value of  $\delta_T$  will grow diffusively until it reaches a critical thickness at which a local boundary layer Rayleigh number  $Ra(\delta)$  is given by the relation

$$Ra(\delta) = \frac{g\alpha_{\rho}\delta T\delta_{\mathrm{T}}^{3}}{v_{\mathrm{F}}\chi_{a}} = Ra_{*} \approx O(10^{3}).$$
 (17.4.2)

This local Rayleigh number  $Ra(\delta)$  is based on the boundary layer scale  $\delta_T$  and temperature drop  $\delta T$ . At this point, the boundary layer is assumed to break away at  $t \approx t_c$  and the process repeats. This leads to the instability as convection tends to increase the boundary layer thickness that in turn increases the rate of growth.

The critical Rayleigh number defines a critical boundary layer thickness  $\delta_c$ , which is given by

$$\delta_c = L_0 \left( \frac{2Ra_*(\delta)}{Ra} \right)^{1/3} = \frac{L_0}{Nu}.$$
 (17.4.3)

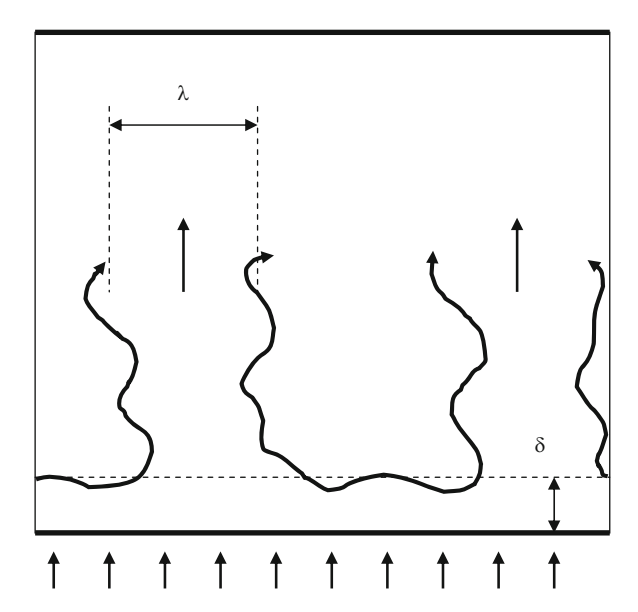


**Fig. 17.4.1** Sketch of the thermal boundary layer destruction

Note that the value of  $Ra_* \approx 1,000$  corresponds to rigid boundary conditions. Now, one obtains the scaling for high Rayleigh number regimes

$$Nu(Ra) = 0.077Ra^{1/3}. (17.4.4)$$

It is possible to estimate the characteristic time of delay needed to renovate boundary layer based on relation

$$\delta_c^3(t)\Delta T \approx (\chi_d t)^{3/2}\Delta T \approx 1.$$
 (17.4.5)

This yields the expression

$$t_c(\Delta T) \propto \Delta T^{-2/3}$$
. (17.4.6)

This phenomenological model of turbulent convection has provided insight into the boundary layer evolution in the presence of time dependence effects.

Concerning the nature of the dependence of Nu(Ra) at the high Rayleigh number, note that there exists a famous theoretical Kraichnan prediction for a system without boundary layers

$$Nu(Ra) \propto Ra^{1/2}. (17.4.7)$$

This theoretical result is based on the mixing-length theory. This means that the Nusselt number increases much more rapidly with Ra than it does below  $Ra_*$ . Indeed, recently, the author of [322] achieved larger Ra in helium and for  $Ra > 10^{10}$  he found that the dependence of Nu(Ra) becomes steeper. Thus  $Ra > 10^{14}$  it is consistent with  $Nu \propto Ra^{1/2}$ . The Reynolds number at the onset of this asymptotic regime is  $Re \approx 10^4$ .

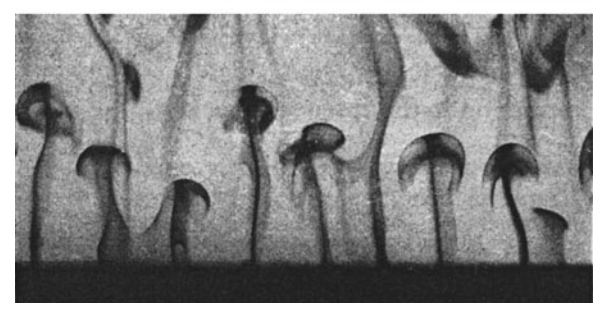
However, to theoretically analyze turbulent convection at the high Rayleigh number, it is necessary to apply more complex methods, which allow one to take into account the nontrivial topology of conductive boundary layer (see Fig. 17.4.2).

## 17.5 Chicago Scaling

In the context of complex structures formation in chaotic flow, we consider the experimental works [324] showing that at Rayleigh numbers between about  $5 \times 10^5$  and  $4 \times 10^7$ , conventional scaling  $Nu \propto Ra^{1/3}$  applies quite well. But at about  $Ra = 4 \times 10^7$  another distinct transition in the character of the convection occurs, so that above this transition (see Fig. 17.5.1)  $Nu(Ra) \propto Ra^{2/7\pm0.006}$ . In addition, the experiments show that the nondimensional magnitude of the temperature fluctuations is related to Ra by

Fig. 17.4.2 Buoyant plumes or thermals. The plumes or thermals, made visible by dye in the two photographs, rise from a heated surface in the laboratory in the absence of shear. (After Sparrow E.M. et al. [323] with permission)





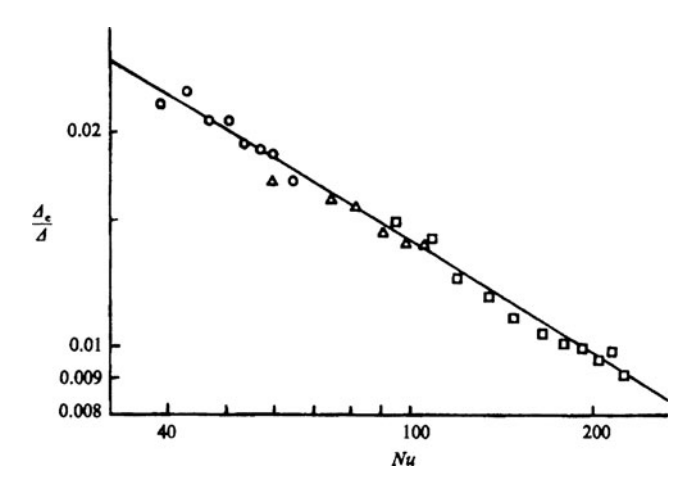


Fig. 17.5.1 The dependence of the characteristic temperature  $\Delta_c$  on Nu.  $\Delta_c$  is proportional to a r.m.s. temperature fluctuation and is measured at the center probe. The different symbols indicate different pressure in the helium. (After Castaing B. et al. [324] with permission)

$$\frac{\left(\langle \delta T \rangle^2\right)^{1/2}}{\Delta T} \propto Ra^{-\frac{1}{7}},\tag{17.5.1}$$

while the dimensional velocity fluctuations are given by

$$\frac{\left(\langle \delta V \rangle^2\right)^{1/2} L_0}{v_{\rm E}} \propto R a^{\frac{3}{7}}.\tag{17.5.2}$$

Kadanoff and associates at the University of Chicago have provided a rationalization for these observations. First of all, assume that the Nusselt number and the dimensionless temperature and velocity fluctuations all go as some power of *Ra* 

$$\frac{\left(\langle \delta T \rangle^2\right)^{1/2}}{\Delta T} \propto R a^{m_1},\tag{17.5.3}$$

$$\frac{\left(\langle \delta V \rangle^2\right)^{1/2} L_0}{\nu_{\rm F}} \propto R a^{m_2},\tag{17.5.4}$$

$$Nu \propto Ra^{m_3}$$
. (17.5.5)

We next note that the heat flux in the interior is carried by the convection itself, so that

$$Nu \propto \delta T \delta V \propto \left( \langle \delta T \rangle^2 \right)^{1/2} \left( \langle \delta V \rangle^2 \right)^{1/2} \propto Ra^{m_2 + m_1}.$$
 (17.5.6)

By comparing last equations, one obtains,

$$m_3 = m_2 + m_1. (17.5.7)$$

It is also true that away from the boundaries, the individual convective elements are accelerated by buoyancy so that the main balance in the vertical momentum equation is between acceleration and buoyancy:

$$\frac{dV}{dt} \propto V \frac{\partial V}{\partial \tau} \propto g \alpha_{\rho} \, \delta T. \tag{17.5.8}$$

This gives the scaling relation for the velocity fluctuation amplitude

$$\left(\langle \delta V \rangle^2\right) \propto g \alpha_{\rho} L_0 \left(\langle \delta T \rangle^2\right)^{1/2}.$$
 (17.5.9)

After substitution, we have the estimate

$$Ra^{2m_2} \propto \frac{L_0^3}{v_F^2} g \alpha_\rho \Delta T R a^{m_1} \propto R a^{m+1}.$$
 (17.5.10)

Then, one obtains the formula

$$2m_2 = m_1 + 1. (17.5.11)$$

Now the critical assumption made by the Chicago group is that the velocity achieved by buoyant elements traversing the boundary layers is determined by a balance between buoyancy and dissipation:

$$g\alpha_{\rho}\Delta T \propto \frac{v_{\rm F} \left(\langle \delta V \rangle^2\right)^{1/2}}{\lambda^2},$$
 (17.5.12)

where  $\lambda$  is the dept of the boundary layers. Now,  $\lambda$  is related to the Nusselt number by  $\lambda(Nu) = L_0/Nu$  that allows us to find the relationship

$$g\alpha_{\rho}\Delta T \propto \frac{Nu^2 v_{\rm F}^2 Ra^{m_2}}{L_0^3}.$$
 (17.5.13)

Now, we can rewrite the formula for the Rayleigh number

$$Ra \propto Ra^{2m_3+m_2},$$
 (17.5.14)

or in terms of characteristic exponents

$$1 = 2m_3 + m_2. (17.5.15)$$

Solving equations obtained for the characteristic exponents yields

$$m_3 = \frac{2}{7}, \quad m_2 = \frac{3}{7}, \quad m_1 = -\frac{1}{7},$$
 (17.5.16)

which is in agreement with the experiments.

What is remarkable about both the 2/7 and 1/3 power laws is that they predict a dependence of the dimensional heat flux on molecular diffusion in the limit of high Rayleigh number. Thus, for example, the scaling  $Nu \propto Ra^{m_3}$  implies that

$$q_{\rm T} \propto \langle \delta V \rangle \langle \delta T \rangle \propto v_{\rm F}^{1-2m_3}$$
. (17.5.17)

Thus, only if  $m_3$  were equal to 1/2 would the dimensional heat flux be independent of viscosity. This indicates that no matter how turbulent the actual convection is, there is still a dependence on molecular fluxes. This makes application to geophysical fluids highly problematic, since other influences are bound to dominate the convective heat flux [325–327].

#### 17.6 Turbulent Thermal Convection and Spectra

In concluding this chapter, we briefly consider the power spectra for heat convection. Obukhov and Bolgiano [328, 329] applied the analogy of the cascade scalar description in turbulent flows on turbulent thermal convection. In the steady case, we rewrite the Boussinesq equation in the simplified form

$$(\vec{V}\nabla)\vec{V} = \alpha_{\rho} \, \vec{g}(T - T_0), \tag{17.6.1}$$

The basic equations to analyze power spectra of heat convection are related to the scalar flux conservation

$$\varepsilon_{\rm T} \propto \frac{\delta T_l^2}{\tau_{\rm CASC}(l)} \propto \frac{\delta T_l^2 V_l}{l} = {\rm const},$$
 (17.6.2)

and the balance between acceleration and buoyancy

$$\frac{V_l^2}{l} \propto g \alpha_\rho \delta T_l, \tag{17.6.3}$$

that is true away from the boundaries. Here, we apply the dimensional estimate for the cascade characteristic time  $\tau_{\text{CASC}} \propto l/V_l(l)$ .

In the simplified case, it is possible to employ the Kolmogorov scaling for velocity fluctuation amplitude

$$V_l \propto (\varepsilon_{\rm K}^l)^{1/3} \propto \frac{\varepsilon_{\rm K}^{1/3}}{k^{1/3}} \propto V_{\rm k},$$
 (17.6.4)

that allows us to solve this basic system of equations. For the velocity fluctuation amplitude, we have

$$V_l \propto (\varepsilon_{\rm T} \alpha_{\rho}^2 g^2)^{1/5} l^{3/5}.$$
 (17.6.5)

For the temperature fluctuation amplitude, one obtains

$$\delta T_l \propto \left(\frac{\varepsilon_{\rm T}^{2/5}}{\alpha_{\rho}^{1/5} g^{1/5}}\right) l^{1/5}.$$
 (17.6.6)

We now calculate power spectra for inertial range of spatial scales of turbulent convective flow basing on the conventional definitions

$$E(k) \propto \frac{V_k^2}{k} \propto \left(\varepsilon_T \alpha_\rho^2 g^2\right)^{2/5} k^{-11/5}, \tag{17.6.7}$$

$$E_{\rm T}(k) \propto \frac{\delta T_{\rm k}^2}{k} \propto \left(\frac{\varepsilon_{\rm T}^2}{\alpha_{\rho}g}\right)^{2/5} k^{-7/5}.$$
 (17.6.8)

These are the energy spectrum and the scalar spectrum, respectively (see Fig. 17.6.1). Such a consideration is valid when

$$\Pr = \frac{Pe}{\text{Re}} = \frac{v_{\text{F}}}{\chi_a} \approx 1. \tag{17.6.9}$$

It is natural to estimate the rate of energy dissipation, which is related to the buoyancy effects

$$\varepsilon_{\rho} \approx (g\alpha_{p})\delta V_{l}\delta T_{l} \propto \varepsilon_{T}^{3/5} (g\alpha_{p})^{6/5} l^{4/5}.$$
(17.6.10)

Note, that  $\varepsilon_{\rho}$  scales as  $l^{4/5}$ . This means that in case of small spatial scales this rate of dissipation will be less than the Kolmogorov rate of dissipation  $\varepsilon_{\rm K} \propto V_l^3/l$ . By comparing the rate of energy dissipation which is related to the buoyancy effects and the Kolmogorov rate of dissipation

$$\varepsilon_{\rm T}^{3/5} \left( g \alpha_p \right)^{6/5} L_{Bo}^{4/5} \approx \varepsilon_{\rm K}, \tag{17.6.11}$$

one can find the Bolgiano spatial scale

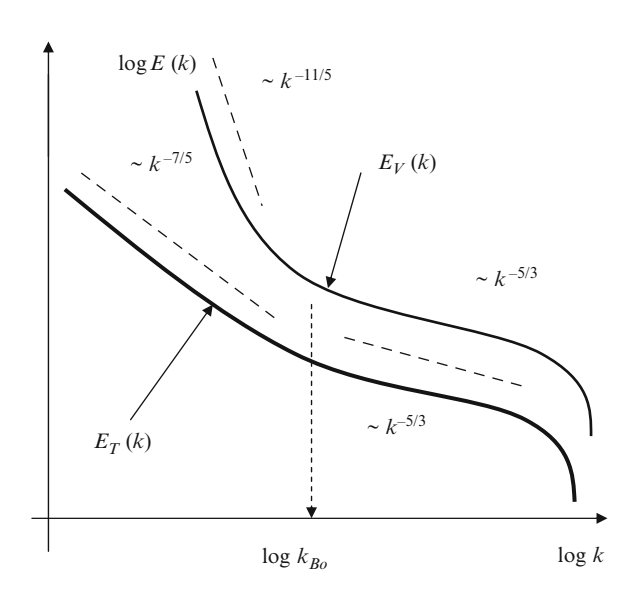


**Fig. 17.6.1** Idealized energy and scalar spectra for convective turbulence

Further Reading 293

$$L_{Bo} \propto \frac{\varepsilon_{\rm K}^{5/4}}{\left(g\alpha_p\right)^{3/2}\varepsilon_{\rm T}^{3/4}},\tag{17.6.12}$$

which characterizes the low boundary of the Bolgiano-Obukhov regime.

For scales less than the Bolgiano spatial scale,  $l < L_{Bo}$ , we shall apply Kolmogorov kind of spectra for both energy spectrum and scalar spectrum

$$E(k) \propto E_{\rm K}(k) \propto k^{-5/3},$$
 (17.6.13)

$$E_{\rm T}(k) \propto k^{-5/3}$$
. (17.6.14)

Since Bolgiany's and Obukhov's articles, tremendous progress in the understanding of the turbulent convection has been achieved by experiment, theory, and numerical simulation. However, it has also become clear that our understanding is far from complete. The key problem of the turbulent convection description is closely related to the existence of coherent structures as a part of the turbulence itself. We look at this aspect of the theory below.

#### **Further Reading**

#### Convective Turbulence

- G.I. Barenblatt, *Scaling Phenomena in Fluid Mechanics* (Cambridge University Press, Cambridge, 1994)
- G.K. Batchelor, H.K. Moffat, M.G. Worster, *Perspectives in Fluid Dynamics* (Cambridge University Press, Cambridge, 2000)
- S.B. Pope, *Turbulent Flows* (Cambridge University Press, Cambridge, 2000)
- A. Tsinober, *An informal Introduction to Turbulence* (Kluwer Academic Publishers, The Netherlands, 2004)
- J.S. Turner, Buoyancy Effects in Fluid (Cambridge University Press, Cambridge, 1973)

#### **Environmental Convection**

- F.T.M. Nieuwstadt, H. Van Dop (eds.), *Atmospheric Turbulence and Air Pollution Modeling* (D. Reidel Publishing Company, Dordrecth, 1981)
- R.S. Scorer, Environmental Aerodynamics (Wiley, New Jersey, 1978)
- G. Schubert, D.L. Turcotte, P. Olson, *Mantle Convection in the Earth and Planets* (Cambridge University Press, Cambridge, 2008)

#### Pattern Formation

- Y. Kuramoto, *Chemical Oscillations*, *Waves and Turbulence* (Springer, Berlin, 1984)
- P. Manneville, *Instabilities, Chaos and Turbulence. An Introduction to Nonlinear Dynamics and Complex Systems* (Imperial College Press, London, 2004)
- A. Mikhailov, *Introduction to Synergetics*, *Part 2* (Springer, Berlin, 1995)
- L. M. Pismen, *Patterns and Interfaces in Dissipative Dynamics* (Springer, Berlin, 2006)

# Part VIII Structures and Complex Flow Topology

## Chapter 18

## **Coherent Structures and Transport**

#### **18.1 Regular Structures**

Until now we have discussed aspects of transport in chaotic flows ignoring, on most occasions, the existence of coherent structures. However, the crucial issue of the modern theory of anomalous transport is related to the formation of complex structures in turbulent flows. Here, we are concerned with simplified models of complex structures that are present in hydrodynamic system, magnetized plasma, etc. In this context, a coherent structure is, for instance, a vortex system that persists for a long time. Environmental and plasma-physical examples of complex vortex structures include Gulf Stream rings, the Great Red Spot on Jupiter, and convective cells systems in high temperature tokamak plasma (see Fig. 18.1.1). Thus, in the framework of the geophysical fluid dynamics the analysis of complex structures evolution could provide insight into the processes involved in the transformation from a line of convective cells to an organized mesoscale system.

For the sake of simplicity first we discuss the regular structures. Such an approach is an attractive one, which could possibly provide an alternative starting point for the description of anomalous transport in complex system. Moreover, of particular importance to us is the case of two-dimensional incompressible flows, with

$$\operatorname{div} \vec{u} = \frac{\partial u_x}{\partial x} + \frac{\partial u_y}{\partial y} = 0. \tag{18.1.1}$$

Both the oceans and the atmosphere (for velocities much smaller than the speed of sound) can be regarded as incompressible and can in many situations be considered two-dimensional systems as well [302–306]. In this simplified case, there exists a stream function  $\Psi(x, y, t)$  whose derivatives give the velocity components of the flow:

$$u_x(x, y, t) = -\frac{\partial \Psi(x, y, t)}{\partial y},$$
(18.1.2)

$$u_{y}(x, y, t) = -\frac{\partial \Psi(x, y, t)}{\partial x}.$$
 (18.1.3)

By substituting the above equations in the equation of motion, one obtains the equation of motion for an advected particle in terms of the stream function:

$$\dot{x} = -\frac{\partial \Psi(x, y, t)}{\partial y},\tag{18.1.4}$$

$$\dot{y} = \frac{\partial \Psi(x, y, t)}{\partial x}.$$
(18.1.5)

The simplest example of the velocity field of interest is given by the streamline function  $\Psi(x) = \Psi_0 \sin(x)$ . Here,  $\Psi_0$  is an arbitrary stream function amplitude. The velocity field for this streamline function is represented as follows:

$$\vec{u}(x) = \begin{pmatrix} 0 \\ \Psi_0 \cos(x) \end{pmatrix}. \tag{18.1.6}$$

This is a simple shear flow. Randomization of this sinusoidal velocity field leads to the Dreizin–Dyhne random shear flow. More interesting example arises when one considers a superposition of two independent sinusoidal shear flows:

$$\Psi(x, y) = \Psi_0[\sin(x) + \sin(y)]. \tag{18.1.7}$$

The corresponding velocity field for this streamline function is given by

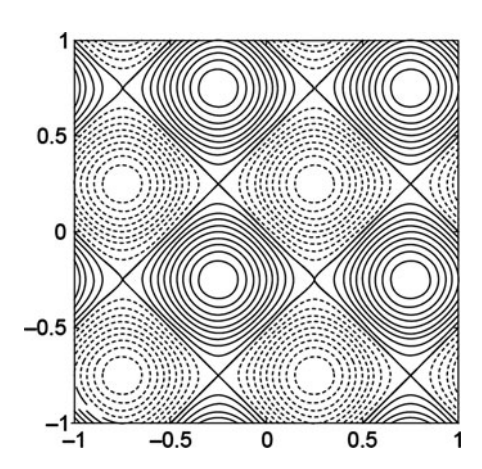
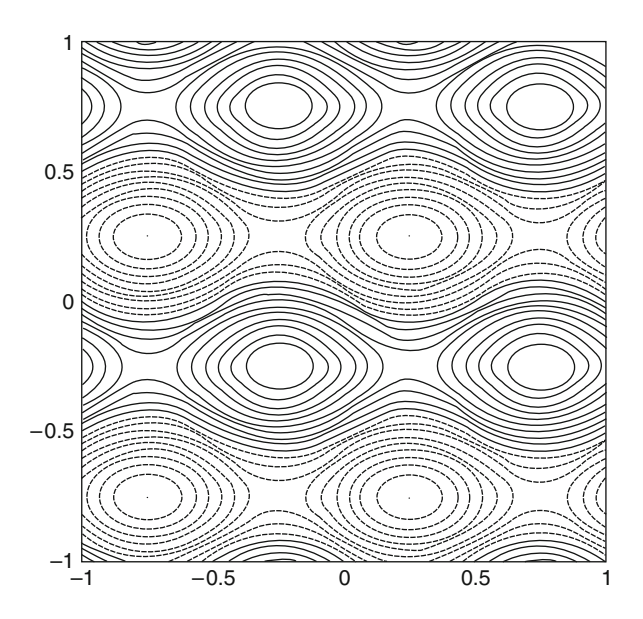


**Fig. 18.1.1** Stremlines of a two-dimensional cellular flow

Fig. 18.1.2 Twodimensional array of swirling eddies



$$\vec{u}(x) = \begin{pmatrix} -\Psi_0 \cos y \\ \Psi_0 \cos(x) \end{pmatrix}. \tag{18.1.8}$$

This is a periodical two-dimensional system of swirling eddies (cell system) rotating in clockwise as well as counterclockwise fashion (see Fig. 18.1.1). Randomization of this cell velocity field leads to the Manhattan random flow.

The two-dimensional array of swirling eddies can be obtained by the superposition of a sinusoidal shear flow on a periodical system of swirling eddies

$$\Psi(x,y) = \Psi_0[\sin(x) + \sin(y)] + \Psi_1 \sin(y). \tag{18.1.9}$$

Here,  $\Psi_1$  is an arbitrary stream function amplitude (see Fig. 18.1.2). The most often recourse is made of the Taylor vortices stream function

$$\Psi(x, y) = \Psi_0 \sin(x) \sin(y). \tag{18.1.10}$$

Thus, we obtain a periodical two-dimensional system of swirling eddies (aligned with the x and y direction) that are rotating in clockwise as well as counterclockwise fashion (see Fig. 18.1.3). The Taylor vortices system satisfies the free-slip boundary condition as well as the no-penetration condition. This simple model of the streamline topology is able to capture the essential features of Rayleigh—Benard convection as well as two-dimensional symmetric square-cell convective system.

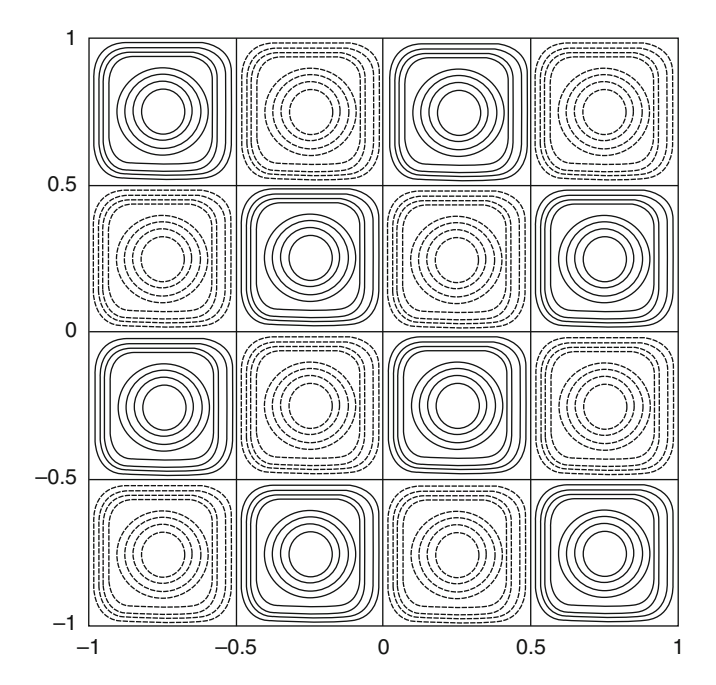


Fig. 18.1.3 Streamlines of the Taylor vortices

## 18.2 Scaling for Diffusive Boundary Layer

This section considers the dispersion of a passive scalar in a periodic system of convective cells. The complete evolution of the tracer concentration n is determined by the advection—diffusion equation.

$$\frac{\partial n}{\partial t} + \vec{u} \times \nabla n = D_0 \nabla^2 n, \qquad (18.2.1)$$

where  $D_0$  is the molecular diffusivity and  $\vec{u}$  is the advection velocity. For the sake of simplicity, we treat a convection cell whose horizontal length is much larger than its height and where the convective rolls are aligned along the *z*-axis. In this situation, the flow could be considered as two-dimensional.

Assuming stress-free boundary conditions and single-mode convection, an explicit form for the velocity field is given by:

$$\Psi(x,y) = \Psi_0 \sin(k_x x) \sin(k_y y). \tag{18.2.2}$$

Here, the supposition is made that

$$\Psi_0 = \lambda V_0 \text{ and } k_x = k_y = \frac{2\pi}{\lambda},$$
 (18.2.3)

where  $\lambda$  is the cell size.

It is natural to set up a transport model in the form of a random walk between cells. Here, the diffusive boundary layer is responsible for transport among cells (see Fig. 18.2.1). The molecular diffusivity  $D_0$  is assumed to be very small or, more precisely, the Peclet number is large

$$Pe = \frac{\lambda V_0}{D_0} > 1. \tag{18.2.4}$$

Here,  $\lambda$  is the cell size and  $V_0$  is the characteristic velocity of the convective flow. In our case, an estimation of the width of diffusive boundary layer  $\Delta$  could be obtained on the basis of the advection–diffusion equation by comparison of diffusive and convective terms

$$V_0 \frac{\partial n}{\partial x} \approx D_0 \frac{\partial^2 n}{\partial y^2}.$$
 (18.2.5)

On the basis of dimensional arguments, we arrive at the relation

$$V_0 \frac{n}{\lambda} \approx D_0 \frac{n}{\Lambda^2}.$$
 (18.2.6)

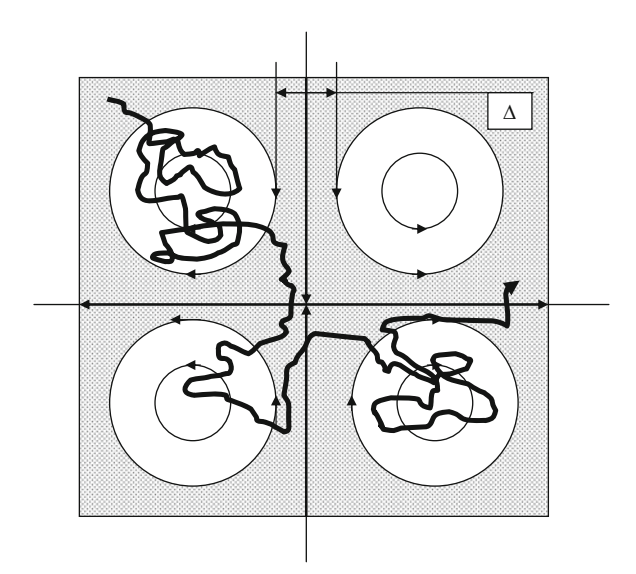


**Fig. 18.2.1** A system of convective cells

This relation establishes the importance of boundary layer scale  $\Delta(V_0)$  throughout a domain where a steady flow operates. Now one obtains the formula for the boundary layer width [330, 331],

$$\Delta(V_0) \propto \sqrt{D_0 \tau} \propto \sqrt{\frac{D_0 \lambda}{V_0}} \propto \frac{1}{\sqrt{Pe}} \propto \frac{1}{\sqrt{V_0}}.$$
 (18.2.7)

This result is fairly predictable. Indeed, the thickness of almost all the boundary layers goes like  $1/\sqrt{Pe}$ ,  $1/\sqrt{Re}$ , etc.

The correlation timescale is given by

$$\tau(V_0) \approx \frac{\lambda}{V_0} \approx \frac{\Delta^2(V_0)}{D_0}.$$
 (18.2.8)

By estimating the fraction of space responsible for the convective contribution to effective transport as  $\lambda \Delta/\lambda^2 \approx \Delta/\lambda$ , we obtain the transport scaling

$$D_{\rm eff} \approx V_0^2 \tau \left(\frac{\Delta \lambda}{\lambda^2}\right) \approx V_0^2 \tau \frac{\Delta}{\lambda}.$$
 (18.2.9)

This is the quasilinear expression, which is corrected (renormalized) by the geometrical factor  $\Delta/\lambda$  to account for the fraction of space that is responsible for the convection. Here,  $\lambda$  is the cell size and  $V_0$  is the characteristic velocity of the convective flow.

By taking into account the expressions for the correlation time  $\tau(V_0)$  and diffusive layer width  $\Delta(V_0)$ , we arrive at the following estimate for the turbulent diffusion coefficient:

$$D_{\text{eff}} \approx \sqrt{D_0 V_0 \lambda} \approx D_0 P e^{1/2} \propto V_0^{1/2}$$
. (18.2.10)

This representation of the result in terms of the Peclet number differs significantly from both the quasilinear,  $D_{\rm eff} \propto V_0^2$ , and the Howells linear estimates,  $D_{\rm eff} \propto V_0$ . The scaling  $D_{\rm eff} \propto V_0^{1/2}$  was anticipated in a related problem in [250] and the proportionality constant has been calculated in [330]. Note that using very tricky singular perturbation techniques it is possible to solve the advection–diffusion equation in order to obtain the formal solution for the scalar diffusive flux and the result coincides with the scaling obtained above. Note that the study of the influence of particle inertia in cellular flow showed that particles in a random convective cell systems may settle out even more rapidly than in still fluid [332].

The stream function terminology is fairly effective in considering turbulent transport in the presence of structures. Thus, the transport scaling obtained can also be interpreted in terms of a stream function perturbation,

$$D_{\rm eff} \approx V_0 \Delta(\varepsilon) \approx \Delta \Psi,$$
 (18.2.11)

where  $\Delta\Psi$  is the change in the stream function amplitude across a diffusive boundary layer  $\Delta$ . The subsequent progress of research on diffusion processes in systems with convective cells has led us to the understanding of the importance of the stochastic layer width  $\Delta$  in analyzing the convective fraction of the transport.

#### 18.3 Anomalous Transport in a Roll System

Subdiffusive scalar transport can occur in regular steady flows as well as in random velocity fields. The basic mechanism responsible for this slow diffusion is trapping, which caused the existence of complex vortex structures. Thus, the subdiffusive motion of a tracer particle in the array of convective rolls is related to both the convection along streamlines and the molecular diffusion, which allows "jumps" between streamlines [332–340]. Note that without compressibility in two-dimensional flows the subdiffusion mechanism cannot be realized.

We could generalize the diffusive model of transport in convective roll system because each roll acts as a trap. We obtain not only effective diffusion coefficient but also the scalar distribution function. The key element of such a consideration is the waiting time distribution function decaying as

$$\psi(t) \propto \frac{1}{t^{1+\mu_{\rm p}}} \tau^{-(1+\mu_{\rm p})}.$$
 (18.3.1)

Here,  $\mu_{\rm p}$  is the waiting time characteristic exponent. This scaling representation is valid for times  $t_*$ 

$$t_*(L_0, D_0) \le \frac{L_0^2}{D_0},$$
 (18.3.2)

where  $L_0$  is the diameter of a roll. The scalar particle distribution function corresponding to the scaling representation of the waiting time distribution is given by the formal expression [333]

$$P(x,t) = \frac{1}{t^{\mu_{\rm p}/2}} f_{\mu_{\rm p}/2} \left( \frac{|x|}{t^{\mu_{\rm p}/2}} \right). \tag{18.3.3}$$

The aim of our investigation is a relationship between the characteristic exponent  $\mu_p$ , which characterizes the rate of decay of the waiting time distribution, and the parameter, which describes the velocity field in a system of convection rolls. Indeed, to specify the convective flow under consideration, we can assume that for small distances from the wall the velocity scales with the distance as follows:

$$V(y) \propto V_0 \left(\frac{y}{L_0}\right)^{\beta_p}.$$
 (18.3.4)

Here, the boundary conditions imposed by the horizontal plates are given by the simple relations: the exponent  $\beta_p=0$  corresponds to "free" boundary condition, whereas the value  $\beta_p=1$  describes "no-slip" boundary conditions.

The particle experiences molecular diffusion  $D_0$ , which allows "jumps" between different streamlines as well as moves along the streamlines. This permits us to obtain a relationship between the characteristic exponent  $\mu_p$  and the parameter  $\beta_p$  by estimating the waiting time distribution  $\psi(t)$  through the scaling for the probability of leaving the roll  $P_1$ . Indeed, in terms of probabilistic approach, one has the balance relations

$$\psi(t)dt = P_1(N)dN. \tag{18.3.5}$$

It is convenient to pass to discrete representation of rolls. One can analyze the streamlines as a numbered set, where  $i=1,...i_{\max}$ . The particle thus makes a one-dimensional random walk on this numbered set. The circular convective motion is superimposed by definition. The probability of leaving the roll is proportional to the probability of first return to the site i=1, which, after N steps, could be represented as the power law

$$P_1(N) \propto N^{-3/2}$$
. (18.3.6)

Here, the supposition is made  $N^2 \ll i_{\rm max}$ . Since different visits to a given roll lead to different diffusion histories, the total time t will again be the sum of independent, broadly distributed variables. The number of visited rolls after a time t thus reads

$$N_I(t) \propto t^{\frac{\mu_p}{2}}, \text{ for } \mu_p < 1.$$
 (18.3.7)

Now, if  $\tau(i)$  represents the time needed to make a closed loop on the *i*th streamline, the total time spent by the particle in the cell is given by the formula

$$t(N) = \sum_{j=1}^{N} \tau(i(j)).$$
 (18.3.8)

Note that flux conservation condition imposes that the *i*th streamline is situated at some distance from the horizontal plate, which can be expressed as follows:

$$\left(\frac{i}{i_{\text{max}}}\right)^{\frac{1}{\beta_{\text{p}}+1}} L_0. \tag{18.3.9}$$

In this context, the transit time is given by the formula

$$\tau(i) \propto \left(\frac{L_0}{V_0}\right) \left(\frac{i_{\text{max}}}{i}\right)^{\frac{\beta_p}{\beta_p+1}}.$$
 (18.3.10)

It is natural to employ the Gaussian distribution function to define the probability to be on the *i*th line after *j* steps. This leads to the formula

$$P(i,j) \propto j^{-1/2} e^{-i^2/j}$$
. (18.3.11)

Averaging leads to the relation for the mean transit time  $\langle \tau(j) \rangle$  in the following form:

$$\langle \tau(j) \rangle \equiv \sum_{i} \tau(i) P(i,j) \propto j^{-\frac{\beta_{\rm p}}{2(\beta_{\rm p}+1)}},$$
 (18.3.12)

and thus one obtains the formula for the total time spent by the particle in the cell

$$t = \sum_{i=1}^{N} \langle \tau(j) \rangle \propto N^{\frac{\beta_{p}+2}{2(\beta_{p}+1)}}.$$
 (18.3.13)

This expression shows that time and number of steps are not proportional to one another, except the case where  $\beta_p = 0$ . Indeed, the first loop passage takes a long time since the particle gets close to the wall where the velocity is vanishing. The upper bound on t is given by the scaling:

$$t_{\text{max}} \propto \left(\frac{L_0}{V_0}\right) \left(\frac{V_0 L_0}{D_0}\right)^{\frac{\beta_p}{2+\beta_p}} \propto P e^{\frac{\beta_p}{2+\beta_p}}.$$
 (18.3.14)

To obtain the characteristic exponent  $\mu_p$ , which characterizes the rate of decay of the waiting time distribution, we apply the probabilistic arguments considered above

$$\psi(t)\frac{dt}{dN}dN = P_1(N)dN, \qquad (18.3.15)$$

This yields the relationship between exponents  $\mu_p$  and  $\beta_p$  [332, 333]

$$\mu_{\rm p} = \frac{1 + \beta_{\rm p}}{2 + \beta_{\rm p}}.\tag{18.3.16}$$

Now one can find the number of "invaded" rolls  $N_I(t)$  as well as the full diffusive front in terms of the Levy laws P(x,t). In particular, for stress-free boundary

condition  $\beta_p = 0$ ,  $\mu_p/2 = 1/4$ , that, initially, gives the number of invaded rolls grew as  $N_I(t) \propto t^{1/4}$ . For rigid boundary condition  $\beta_p = 1$ ,  $\mu_p/2 = 1/3$ , that, initially, gives the number of invaded rolls grew as  $N_I(t) \propto t^{1/3}$ . In this case, one obtains

$$P(X,t) = \sqrt{\frac{|X|}{t}} K_{1/3} \left( \frac{|X|^{3/2}}{t^{1/2}} \right).$$
 (18.3.17)

This well-known result by Cardoso and Tabeling [333] reproduces quite well the experimental data. At a later time when the effects of molecular diffusion become dominant, the number of invaded rolls grew as  $N_I(t) \propto t^{1/2}$ , which coincides with the conventional diffusive representation.

Chaotic flows often contain ordered regions (vortex structures) that hamper mixing. The transport barriers they present can be overcome by frequency-driven reconstruction of flow topology.

#### 18.4 Convection Towers and Thermal Flux

Topological peculiarities of a flow could be used to analyze strong-turbulent regimes. As a simple example, we can derive scaling estimates of atmospheric convection related to the beginning of hurricanes. The initial stage of tornado beginning is characterized by the existence of narrow convective flows (see Fig. 18.4.1). In such a formulation of the problem, it is possible to use, as a key geometric characteristic, the width of the "percolation" convective flow  $\delta$  instead of

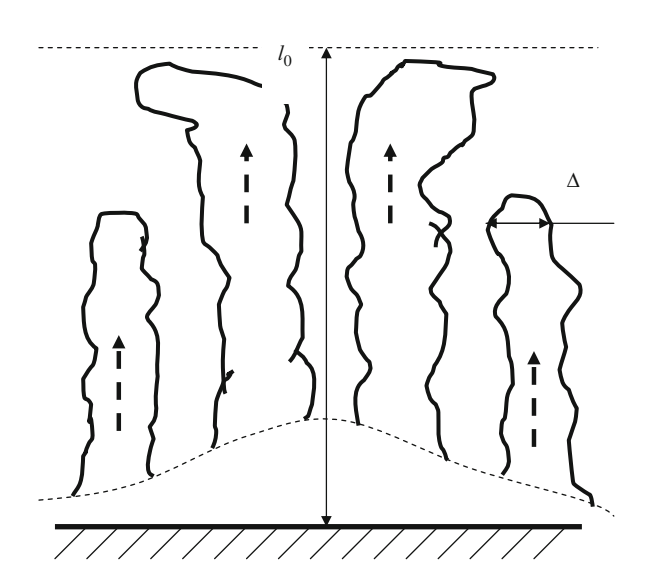


Fig. 18.4.1 Schematic illustration of convective towers

the classical width of a boundary layer. Then, on the one hand, for a thermal flow we obtain an expression in terms of  $\delta$ 

$$q_T \approx \chi_T \frac{T_0}{\lambda} \approx (V_0 \delta) \frac{T_0}{\lambda},$$
 (18.4.1)

where  $V_0$  is the characteristic velocity of a convective flow,  $\lambda$  is the characteristic geometric size, and  $T_0$  is the characteristic temperature. On the other hand, the geometry of the model under consideration leads to the estimate

$$q_T = \frac{Q_T}{\delta^2 N(\delta)} \propto \frac{Q_T}{\delta^2},\tag{18.4.2}$$

where  $Q_T$  (Dg/s) is the supplied power,  $\delta^2$  is the convective current cross section, and  $N(\delta)$  is the number of convective channels. By comparing these two equations, we obtain

$$V_0 \approx \frac{Q_T \lambda}{T_0} \times \frac{1}{\delta^3} \propto \frac{1}{\delta^3},$$
 (18.4.3)

or in terms of the Peclet number

$$\delta(Pe) \propto \frac{1}{P_{\rho}^{1/3}}.\tag{18.4.4}$$

The fast rotation in our simplified model of hurricane structures is obviously related to the narrow convective channels. Let us consider a balance of characteristic times. Suppose that in our case (see Fig. 18.4.2), the rotation frequency  $\omega$  scales inversely with the characteristic time  $\tau_Q \approx L_0/V_0$ 

$$\frac{1}{\omega(V_0)} \approx \frac{L_0}{V_0}.\tag{18.4.5}$$

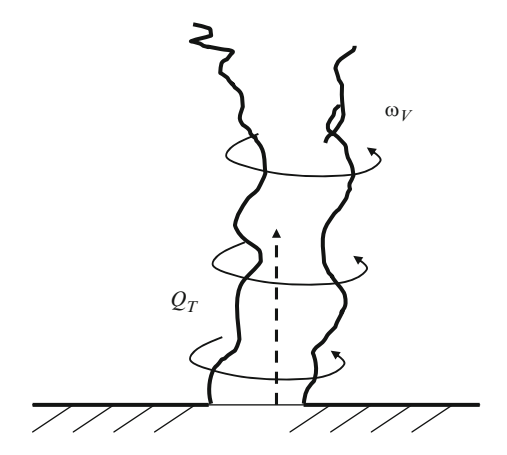
With allowance for the scaling for  $V_0 \propto 1/\delta^3$ , we find

$$\omega(\delta) \propto \left(\frac{Q_T}{T_0} \frac{\lambda}{H}\right) \frac{1}{\delta^3} \propto \frac{1}{(\delta T)^3}.$$
 (18.4.6)

For the sake of simplicity, we suppose that  $\delta \propto \delta T$ . Now, the scaling for the thermal flux is given by

$$q_T \approx V_0 \delta T \approx (V_0 \delta) \frac{T_0}{\lambda} \propto V_0^{2/3}.$$
 (18.4.7)

**Fig. 18.4.2** Sketch of the vortex structure of convective towers



This result agrees well with the Zeldovich prediction for the case of strong turbulence. We see that narrow convective (percolation) channels could lead to considerable rotation frequencies at the initial stage of hurricane structure formation. Hurricane structure models are quite beyond our scope and we shall just put forward the analogy between convective cell system and our simplified problems. Similar problem arises in the framework of turbulent diffusion description in the presence of coherent structures where narrow stochastic layers are responsible for main contribution to effective transport.

### 18.5 Random Flow Landscape and Transport

Above we analyzed the transient regimes of anomalous transport in the array of convective rolls in the framework of continuous time random walks. The main feature of that case was particle trapping by vortices. The model of regular convective cells is correct when every single vortex is separated from all others by a separatrix.

On the contrary, when we are dealing with random two-dimensional flows such a "small-scale" division of flow domain is unlikely. Here, the considerable contribution to transport will be related to tracer ballistic motion along streamlines, which embraces a flow domain. For instance, by considering cellular structures of stratocumulus and small cumulus over oceans in terms of global climatology, we can see that there exist simultaneously both regions where closed cells predominate and regions where currents are more common. On the other hand, the Gulf Stream is one of the famous examples of similar organized mesoscale system. It is difficult to decide whether flights related to currents or trapping by vortices will define the effective transport in such complex flows.

The appearance of advective currents could be related to distortion of initially symmetric patterns by a small fluctuation field. In a simplified form, such an example was considered in [341] on the basis of the steady velocity field

$$\Psi(x,y) = \Psi_0 \sin(x) \sin(y) + \varepsilon_S \cos(x) \cos(ky), \qquad (18.5.1)$$

Here, the one-parameter perturbation field

$$\Psi_{\rm p}(x,y) = \varepsilon_{\rm S}\cos(x)\cos(y) \tag{18.5.2}$$

is superimposed on the Roberts symmetric square-cell stream function  $\Psi_0$ . Here,  $\varepsilon_S$  is the fluctuation amplitude. This is the extension of the convective cells model. If the parameter  $\varepsilon_S > 0$ , the streamlines  $\Psi = \text{const}$  form a periodic array of oblique cat's-eyes separated by continuous channels carrying finite fluid flux (see Fig. 18.5.1). Here, channels traversing the flow domain as well as a periodic pattern of regions of closed streamlines are presented. In this case, advection dominates molecular diffusion  $D_0$ , and tracer is transported both in thin boundary layers and within the channels. Note that steady random flows cannot diffuse a passive scalar in the absence of molecular diffusivity. For the large Peclet number,  $Pe \gg 1$ , the separation of the cat's-eyes thus locates the boundary layers of thickness order

$$\Delta(V_0) \propto \frac{1}{\sqrt{Pe}} \propto \frac{1}{\sqrt{V_0}}$$
 (18.5.3)

The parameter that measures the ratio of channel to boundary layer width is given by

$$\varepsilon_S \sqrt{\frac{\lambda V_0}{D_0}} = \varepsilon_S \sqrt{Pe}. \tag{18.5.4}$$

Here,  $D_0$  is the seed diffusivity and  $Pe = \lambda V_0/D_0$  is the Peclet number. The kinematic dynamo problem provided the original motivation for cat's-eyes model of scalar transport.

The landscape considered above is spatially periodic and has very symmetric streamline pattern. More interesting situation arises when we apply random separatrix splitting (see Fig. 18.5.2). This landscape reconstruction of initially symmetric topology of two-dimensional flow allows us to treat transport and correlation effects in terms of the continuum percolation approach. We consider a two-dimensional zero-average-velocity steady flow specified by the bounded "common position" stream function  $\Psi(x,y)$ . We also imply an isotropic-on-average oscillating function with a quasi-random location of saddle points along its height.

In a general case, one can represent such one-scale chaotic flow as

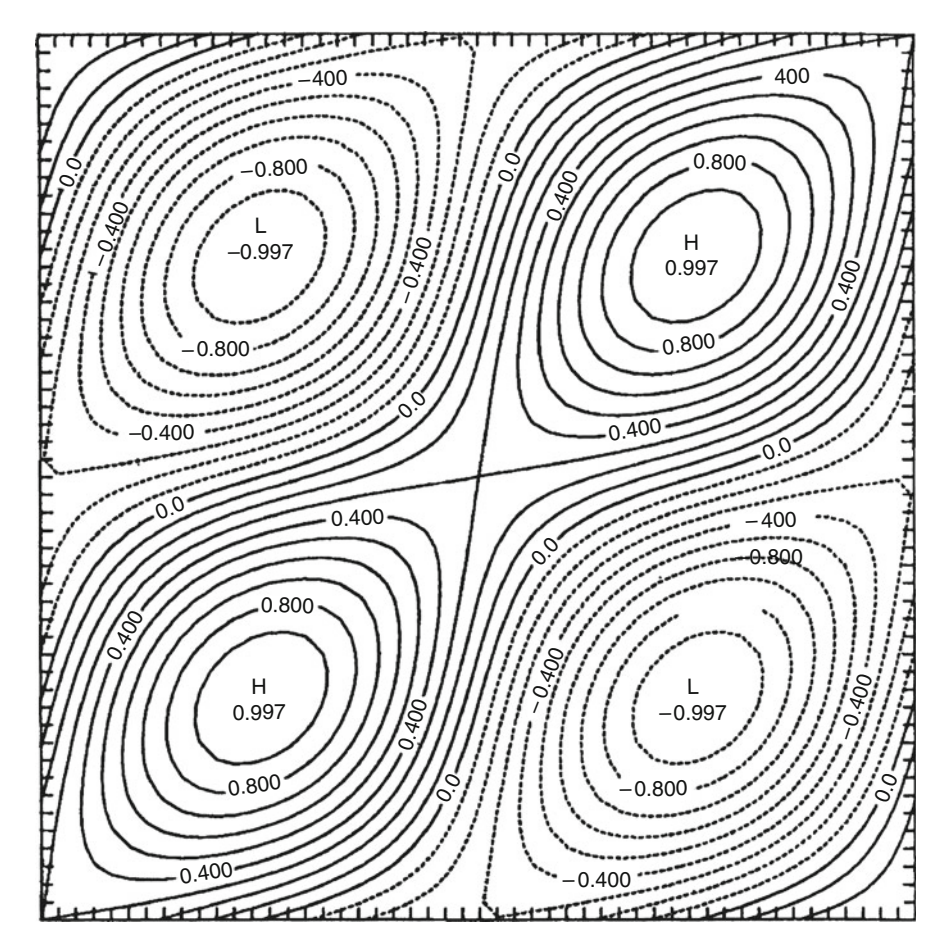


**Fig. 18.5.1** Streamlines of the flow for  $\delta=0.3$ . The channel is bounded by the streamlines  $\psi=\pm0.3$  (After Childress S. and Soward A.M. [341] with permission)

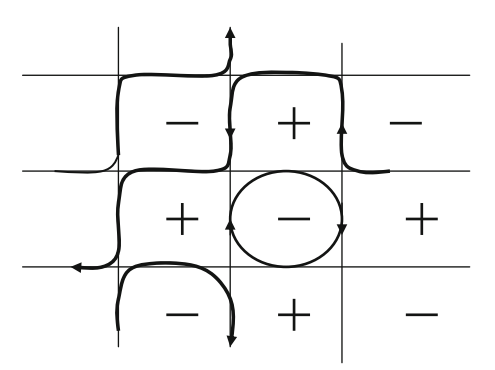


**Fig. 18.5.2** Schematic diagram of separatrix random splitting

$$\Psi(\vec{r}) = \sum_{i}^{N} \Psi_{i} \sin\left(\vec{k}_{i} \vec{r} + \phi_{i}\right), \tag{18.5.5}$$

where  $N \gg 1$ . To treat such a random velocity field, we introduce the following scales:  $\Psi_0 \approx \lambda V_0$ ,  $\lambda \approx \left|\frac{\Psi}{\nabla \Psi}\right|$ . Here,  $V_0$  is the characteristic velocity scale and  $\lambda$  is the spatial scale.

Here, we represent the percolation method that provides to be fruitful [213, 342, 343] to describe turbulent transport in two-dimensional random flows. In such an approach, the percolation streamline (percolation hull) contributes most to turbulent transport near the threshold. Thus, the value  $\delta\Psi_p=\epsilon\lambda V_0$  is the percolation scale of the stream function near the percolation threshold, where  $\epsilon$  is the small percolation parameter. Similar to the convective cell model, one can find the diffusive boundary layer width by the relation

$$V_0 \frac{n}{L(\varepsilon)} \approx D_0 \frac{n}{\Delta^2(\varepsilon)},$$
 (18.5.6)

where we use the percolation streamline length  $L(\varepsilon)$  instead of the spatial scale  $\lambda$  (see Fig. 18.5.3). However, we shall establish a relation between the diffusive boundary layer width  $\Delta$  and the small percolation parameter  $\varepsilon$ . Let us identify the small "width" of a percolation streamline with the small parameter of the percolation theory by the formula

$$\Delta(\varepsilon) = \lambda \varepsilon. \tag{18.5.7}$$

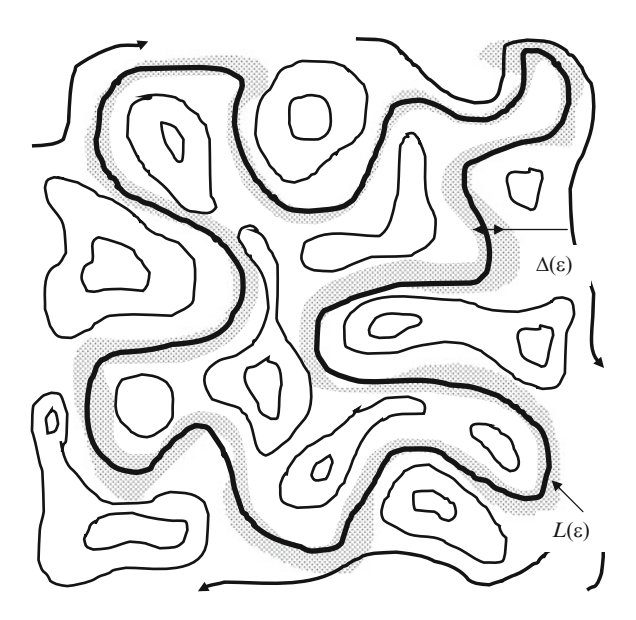


Fig. 18.5.3 Percolation streamline and stochastic layer in a two-dimensional chaotic flow

Now, we obtain the equation for the determination of the "universal" value of  $\varepsilon_*$ , as a function of the flow parameters  $D_0, V_0, \lambda$ ,

$$\sqrt{\frac{D_0 L(\varepsilon)}{V_0}} = \varepsilon \lambda. \tag{18.5.8}$$

The specific calculations can be completed by using the rigorous scaling results of the percolation theory obtained for the correlation scale a and the length of the fractal streamline L,

$$a(\varepsilon) = \frac{\lambda}{|\varepsilon|^{\nu}}, L(\varepsilon) = \lambda \left(\frac{a(\varepsilon)}{\lambda}\right)^{D_{h}},$$
 (18.5.9)

as functions of  $\varepsilon$  for the two-dimensional case, where the correlation exponent v and the Hull exponent  $D_{\rm h}$  are given by v=4/3,  $D_{\rm h}=1+1/v=7/4$ . The functional form of these dependencies reflects the fractal and percolation behavior of streamlines. The solution of the renormalization equation in terms of the Peclet number  $Pe=\lambda V_0/D_0$  leads to the scaling,

$$\varepsilon_* = \left(\frac{1}{Pe}\right)^{\frac{1}{3+\nu}} = \left(\frac{1}{Pe}\right)^{\frac{3}{13}}.$$
 (18.5.10)

In order to calculate the effective diffusion coefficient, we consider the renormalized random walk representation of the diffusion coefficient

$$D_{\rm eff}(\varepsilon) \approx \frac{a^2(\varepsilon)}{\tau} P_{\infty}(\varepsilon).$$
 (18.5.11)

Here, a is the spatial correlation scale, the correlation time is

$$\tau(\varepsilon) \approx \frac{\Delta^2(\varepsilon)}{D_0} \approx \frac{L(\varepsilon)}{V_0},$$
(18.5.12)

and  $P_{\infty}$  is the fraction of a space occupied by the percolation streamline. Effects of "long range correlations" enter into the expression for the diffusion coefficient precisely through  $a(\varepsilon)$ . By following the ideas of the convective nature of the flow along the percolation streamline, we estimate  $P_{\infty}$  in terms of the length of the percolation streamline  $L(\varepsilon)$  and the stochastic layer width  $\Delta(\varepsilon)$ 

$$P_{\infty}(\varepsilon) \approx \frac{L(\varepsilon)\Delta(\varepsilon)}{a^2(\varepsilon)}$$
. (18.5.13)

The expression derived

$$D_{\rm eff}(\varepsilon) \approx \frac{a^2}{\tau} \frac{L(\varepsilon)\Delta(\varepsilon)}{a^2} \approx V_0\Delta(\varepsilon),$$
 (18.5.14)

is similar to the formula for the effective diffusivity in the convective cell system  $D_{\rm eff} \approx V_0 \Delta$ , but here we deal with the percolation kind of dependence  $\Delta = \Delta(\varepsilon)$ . After substitution, one obtains

$$D_{\rm eff} \approx V_0 \Delta(\varepsilon_*) \approx V_0 \lambda \left(\frac{1}{Pe}\right)^{\frac{1}{3+\nu}} \approx D_0 P e^{10/13} \propto V_0^{10/13}.$$
 (18.5.15)

This expression allows the scalar flux to be determined in terms of the external parameters of the random flows  $D_0, V_0, \lambda$  and so is of considerable practical as well as conceptual value. From the point of view of the renormalization of the initial small parameter  $\varepsilon_0 = 1/Pe$ , the expression for the effective percolation parameter can be obtained:

$$\varepsilon_* = (\varepsilon_0)^{\frac{1}{3+\nu}} \gg \varepsilon_0. \tag{18.5.16}$$

In this approach, the length of the fractal percolation line is not infinitely large, because the small parameter  $\varepsilon_*$  does not tend to zero, but has a finite value,

$$\varepsilon_* = \frac{\delta \Psi_*}{\lambda V_0},\tag{18.5.17}$$

for all types of flows with the characteristics  $D_0, V_0, \lambda$ . Therein lies the universality of the formula  $\Delta(\varepsilon) = \lambda \varepsilon$ . We can also estimate the range of the percolation scaling applicability in terms of spatial scales. It is necessary to take into account the finite size  $L_0$  of a real system. By analogy with the system size renormalization, we can consider the estimate

$$a(\varepsilon_*) = \lambda P e^{\frac{\nu}{\nu+3}} \le L_0. \tag{18.5.18}$$

Then, calculations yield the inequality for the Peclet number in the form

$$1 < Pe < \left(\frac{L}{\lambda}\right)^{(\nu+3)/\nu}. \tag{18.5.19}$$

Note that the simplicity of the percolation estimate of turbulent transport is elusive. It will suffice to recall in this connection the "hierarchy" of scales used here

$$\lambda \left(\frac{a}{\lambda}\right)^{D_h} \approx L \approx \frac{a}{\varepsilon_*} \gg a \approx \frac{\lambda}{\varepsilon_*^{\nu}} \gg \lambda \gg \Delta \approx \lambda \varepsilon_*.$$
 (18.5.20)

This four-level spatial hierarchy of scales opens wide possibilities to obtain new scalings in the framework of the percolation method.

#### 18.6 Transient Percolation Regime

In a percolation cluster walking scalar particles are captured by dead-ends and localized in small clusters, and that is why the mean squared displacement of tracer could be much less than the correlation spatial scale  $R^2(t) < a^2$ , when considering the initial stage of tracer evolution. We already introduced above the effective formula to estimate the mean squared displacement of tracer particles in the following form:

$$R^2(t) \propto a^2 P_{\infty}(t),\tag{18.6.1}$$

where  $P_{\infty}$  is an additional factor, which describes the part of space related to "active" motion of scalar particles. Isichenko [103] considered an intermediate percolation regime with the motion of scalar particles along the percolation streamline at the initial stage. Here, we are dealing with the tracer transport on timescales of order

$$t < \tau_B \approx \frac{L(t)}{V_0},\tag{18.6.2}$$

This case differs significantly from the percolation model of turbulent diffusion considered in the previous section, where

$$t \ge \tau_B \approx \tau_D \approx \frac{\Delta^2}{D_0}.$$
 (18.6.3)

For the initial stage of evolution of tracer, we used the estimate of the correlation spatial scale in the following form:

$$a_I(t) \approx \lambda \left(\frac{L(t)}{\lambda}\right)^{1/D_h} \approx \lambda \left(\frac{V_0 t}{\lambda}\right)^{1/D_h},$$
 (18.6.4)

where  $D_h = 1 + 1/v$  and v = 4/3. Here, the supposition was made that the test particle path at this stage is approximately ballistic  $L(t) \approx V_0 t$ . Let us apply the renormalized expression for the mean free path of scalar particle in the general form

$$R^2(t) \approx D_{\text{eff}} t \approx a_I^2(t) P_{\infty}.$$
 (18.6.5)

where the part of space responsible for the main contribution to transport  $P_{\infty}$  is estimated on the basis of the geometrical arguments

$$P_{\infty} \approx \frac{L\Delta}{a_I^2} \approx \frac{\Delta}{\varepsilon a_I} \approx \frac{\lambda}{a_I}.$$
 (18.6.6)

After substitution, one obtains the anomalous diffusion scaling in the following form:

$$R^2(t) \approx a_I^2 P_\infty \approx \lambda^2 \left(\frac{V_0 t}{\lambda}\right)^{1/D_h}$$
 (18.6.7)

This relation describes the subdiffusive regime at the initial period of advection when the scalar particle moves along a fractal streamline.

$$R(t) \propto t^{1/2D_{\rm h}} \propto t^{2/7}$$
. (18.6.8)

The Hurst exponent or this case is given by

$$H(D_{\rm h}) = \frac{1}{2D_{\rm h}} = 2/7.$$
 (18.6.9)

The model of the evolution of correlation scale  $a_I(t)$  can be used to interpret and to analyze another percolation regime [344]. Thus, simultaneously with increasing the correlation scale  $a_I(t) \approx (L(t)/\lambda)^{1/D_h}$ , it is necessary to take into account the decreasing stochastic layer width  $\Delta = \Delta(t)$ , which, in the framework of percolation models of turbulent diffusion, is related to the value of the small parameter  $\varepsilon_* \approx \Delta/\lambda$  and hence to the correlation scale  $a(t) \approx \lambda/\varepsilon^{\nu} \propto \Delta^{-\nu}(t)$ . We consider this problem below in the context of the turbulent transport description in the presence of flow topology reconstruction (see Fig. 18.6.1).

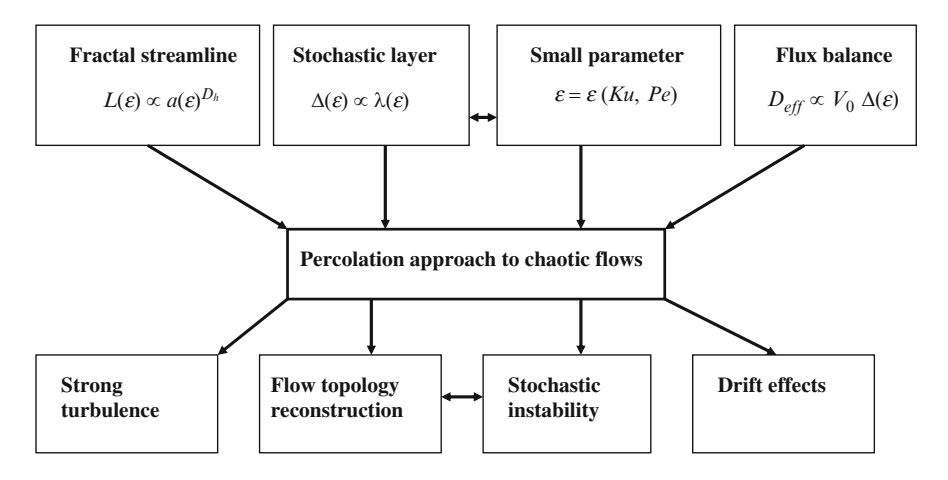


Fig. 18.6.1 Percolation approach to chaotic flows

#### **Further Reading**

#### **Vortex Structures and Transport**

- A. Crisanti, M. Falcioni, A. Vulpiani, Rivista Del Nuovo Cimento **14**, 1–80 (1991) G.S. Golitsyn, *Selected papers* (Nauka, Moscow, 2004)
- E. Guyon, J.-P. Nadal, Y. Pomeau (eds.), *Disorder and Mixing* (Kluwer Academic Publishers, Dordrecht, 1988)
- Holmes PJ, Lumley JL, Berkooz G, Mattingly JC and Wittenberg RW Phys. Rep. 337–384. (1997)
- A. Maurel, P. Petitjeans (eds.), *Vortex Structure and Dynamics Workshop* (Springer, Berlin, 2000)
- H.K. Moffatt, Rep. Prog. Phys. 621, 3 (1983)

#### Two-Dimensional Turbulence and Complex Structures

- D. Biskamp, *Magnetohydrodynamic Turbulence* (Cambridge University Press, Cambridge, 2004)
- R.H. Kraichnan, D. Montgomery, Rep. Prog. Phys. 43, 547 (1980)
- Y. Kuramoto, *Chemical Oscillations*. Waves and Turbulence (Springer, Berlin, 1984)
- P. Manneville, *Instabilities, Chaos and Turbulence. An Introduction to Nonlinear Dynamics and Complex Systems* (Imperial College Press, London, 2004)
- A. Mikhailov, *Introduction to Synergetics*, *Part 2* (Springer, Berlin, 1995)
- L.M. Pismen, *Patterns and Interfaces in Dissipative Dynamics* (Springer, Berlin, 2006)

## Percolation and Anomalous Diffusion

- O.G. Bakunin, Rep. Prog. Phys. 67, 965 (2004)
- R. Balescu, *Aspects of Anomalous Transport in Plasmas* (IOP Bristol, Philadelphia, 2005)
- R. Balescu, Statistical Dynamics (Imperial College Press, London, 1997)
- J.-P. Bouchaund, A. Georges, Phys. Rep. **195**, 127 (1990)
- A. Bunde, S. Havlin, Fractals and Disordered Systems (Springer, Berlin, 1995)
- A. Bunde, S. Havlin, Fractals in Science (Springer, Berlin, 1996)
- P.H. Diamond, S.-I. Itoh, K. Itoh, *Modern Plasma Physics*, vol. 1 (Cambridge University Press, Cambridge, 2010)
- M.B. Isichenko, Rev. Mod. Phys. 64, 961 (1992)
- M. Sahimi, Rev. Mod. Phys. 65, 1393 (1993)

Further Reading 317

J.M. Ziman, Models of Disorder: The Theoretical Physics of Homogeneously Disordered Systems (Cambridge University Press, London, 1979)

#### Coherent Structures in Turbulent Plasma

- A. Dinklage, T. Klinger, G. Marx, L. Schweikhard, *Plasma Physics, Confinement, Transport and Collective Effects* (Springer, Berlin, 2005)
- W. Horton, Y.-H. Ichikawa, *Chaos and Structures in Nonlinear Plasmas* (Word Scientific, Singapore, 1994)
- M.B. Isichenko, Rev. Mod. Phys. **64**, 961 (1992b)
- K. Itoh et al., Transport and Structural Formation in Plasmas (IOP, London, 1999)
- B.B. Kadomtsev, Collective Phenomena in Plasma (Nauka, Moscow, 1976)
- B.B. Kadomtsev, *Tokamak Plasma: A Complex System* (IOP Publishing, Bristol, 1991)
- A.S. Kingsep, *Introduction to the Nonlinear Plasma Physics Mosk* (Fiz.-Tekh. Inst, Moscow, 1996)
- J.A. Krommes, Phys. Rep. **360**, 1–352 (2002)
- M.N. Rosenbluth, RZ Sagdeev (eds) *Handbook of Plasma Physics*, North-Holland, Amsterdam (1984)
- J.A. Wesson, *Tokamaks* (Oxford University Press, Oxford, 1987)

## Chapter 19

## Flow Topology Reconstruction and Transport

#### 19.1 High-Frequency Regimes

Steady incompressible two-dimensional flows are integrable and cannot exhibit chaotic behavior of streamlines. However, steady three-dimensional flows and time-dependent two-dimensional flows can have chaotic streamlines. The time dependence of a flow is an important factor that leads to a reconstruction of the streamline topology and has a significant influence on transport processes. For instance, environmental flows often exhibit the transformation of line of convective cells to organized coherent structures even at mesoscale level. To describe such complicated regimes in frequency-driven flows, we have to take into account the characteristic time  $T_0 \approx 1/\omega$ , which becomes the key parameter among other timescales. The analysis of hierarchy of timescales in a problem under consideration is an important part of the description of transport in chaotic flows. Thus, even dimensional arguments allow one to find a characteristic time, which have to be applied as a correlation scale.

For instance, one can obtain the Kolmogorov scaling for well-developed turbulence by the analysis of characteristic timescales. Thus, dimensional estimates resulting from the Kolmogorov hypothesis about the energy flux over a spectrum give

$$\frac{V^2(l)}{\tau(l)} \propto \varepsilon_{\rm K} = {\rm const.}$$
 (19.1.1)

There are two ways to choose characteristic times  $\tau$ . The first follows from the formula describing viscosity effects:  $\tau_{\nu}(l) \propto l^2/\nu_{\rm F}$ . The second way is based on the Kolmogorov dimensional estimate:  $\tau_{\rm K}(l) \propto l/V(l)$ . At high Reynolds number,

$$Re = \frac{\tau_{\nu}}{\tau_{K}} = \frac{V(l)l}{\nu_{F}} > 1, \tag{19.1.2}$$

the choice of the lowest time  $\tau_{\rm K}$  leads to the classical Kolmogorov result for well-developed turbulence,  $V^2(l) \propto (\epsilon_{\rm K} l)^{2/3}$ . In the scaling description of turbulent convection, such phenomenology (fastest response principle) was successfully applied to the forced turbulent flows whose total kinetic energy is determined by the total power brought into the fluid [318].

It is possible to apply such an approach to the turbulent transport description. However, one should account for numerous factors such as the seed (molecular) diffusion, streamlines reconnection, stochastic instability, and others. We already discussed the quasilinear transport regime, where the characteristic time is given by the estimate  $1/\omega$ . When the Kubo number is small, the scalar particle cannot "feel" the structure of velocity field. The path of a test particle can be estimated by the ballistic way as

$$l_{\omega} \approx \frac{V_0}{\omega} \approx V_0 T_0.$$
 (19.1.3)

Here,  $l_{\omega}$  is the frequency path. In this connection, it is convenient to introduce the dimensionless Kubo number

$$Ku = \frac{l_{\omega}(V_0)}{\lambda} \approx \frac{V_0}{\omega \lambda},\tag{19.1.4}$$

which characterizes the turbulent transport in the presence of time-dependence effects. Here,  $\lambda$  is the spatial scale of the flow under consideration and  $V_0$  is the characteristic velocity scale. One can obtain the scaling for the diffusion coefficient on the basis of simple estimates of the correlation time  $\tau_{\rm COR} \approx 1/\omega$  and the correlation length  $\Delta_{\rm COR} \approx l_\omega$  as follows:

$$D_{\rm eff} \approx \frac{\Delta_{\rm COR}^2}{\tau_{\rm COR}} \approx V_0^2 \tau_{\rm COR} \approx \frac{{V_0}^2}{\omega} \approx \lambda^2 \omega \ Ku^2.$$
 (19.1.5)

To pass from the high-frequency mode to the regimes with strong turbulence, one can take into account the appearance of coherent structures. In this case, the characteristic time depends on the characteristic velocity  $V_0$  and the typical structure size  $\lambda$ . By following the fast mode selection principle, we have to apply a new kind of estimate for the correlation time  $\lambda/V_0$ . In the case of low-frequency regime, a scalar explores the structure of a velocity field. If the characteristic velocity is large enough, it is obviously that

$$\tau_{\lambda}(V_0) \approx \frac{\lambda}{V_0} < \frac{1}{\omega},$$
(19.1.6)

and the effective diffusivity takes the Howells form with the linear dependence on the turbulence amplitude,  $D_{\rm eff} \propto V_0 \lambda$ . In the low-frequency regimes, where  $\omega \to 0$  and  $Ku \gg 1$ , the real correlation scale  $\Delta_{\rm COR}$  could be much less than the formally defined frequency path  $l_{\omega}$ ,

$$\Delta_{\rm COR} \ll l_{\omega} \approx \frac{V_0}{\omega}|_{\omega \to 0} \to \infty.$$
(19.1.7)

This also leads to the invalid scaling for the effective diffusivity

$$D_{\rm eff} \approx V_0^2 \tau_{\rm COR} \approx \frac{{V_0}^2}{\omega}|_{\omega \to 0} \to \infty.$$
 (19.1.8)

From the general consideration, it is clear that in the low-frequency region the effective diffusion coefficient has to increase with the frequency:

$$D_{\rm eff}(\omega) \propto \omega^{\eta_{\rm T}},$$
 (19.1.9)

since a slow reorganization of the flow topology does not lead to considerable transport increasing. Indeed, simulations [345–351] confirm this supposition.

The description of transport in a flow with symmetric convective cells could be also interpreted on the basis of the fastest mode rule. When the amplitude of turbulent pulsations increases, the effective correlation time sharply decreases,

$$\tau \approx \frac{(D_0 \lambda)^{1/2}}{V_0^{3/2}} \ll \frac{\lambda}{V_0} \approx \tau_{\lambda},$$
(19.1.10)

and one obtains the expected flat scaling

$$D_{\text{eff}}(V_0) \propto V_0^2 \frac{(D_0 \lambda)^{1/2}}{{V_0}^{3/2}} \propto \sqrt{V_0}.$$
 (19.1.11)

The principle of fastest mode selection is also realized in percolation models of turbulent transport. In the framework of steady percolation, the characteristic correlation time is also much less than formal timescale

$$\tau(\varepsilon) \approx \frac{\Delta^2(\varepsilon)}{D_0} \approx \varepsilon^2 \frac{\lambda^2}{D_0} \ll \frac{\lambda^2}{D_0}.$$
(19.1.12)

In our consideration, all the temporal scales were constructed from the external parameters of the problem and this phenomenological approach to the analysis of the hierarchy of temporal scales allows us to treat long-range correlation effects in terms of simple scaling. Thus, fastest mode rule can have a heuristic value.

## 19.2 Time Dependence and the Taylor Shear Flow

The conventional description of transport in chaotic flows has an averaged character. At the same time, it is clear that the local characteristics such as frequency-driven flows fluctuate. The question arises as to how these fluctuations influence the

transport processes and how the corresponding effects can be taken into account. Here, it is convenient to employ the advection-diffusion equation for the passive scalar density

$$\frac{\partial n}{\partial t} + u_X(z, t) \frac{\partial n}{\partial x} = D_0 \left( \frac{\partial^2 n}{\partial x^2} + \frac{\partial^2 n}{\partial z^2} \right), \tag{19.2.1}$$

with the expression for the longitudinal velocity in the form

$$u_X(z,t) = \omega_V z \cos(\omega t). \tag{19.2.2}$$

Here,  $\omega_V$  is the dimensional parameter and  $\omega$  is the characteristic frequency. For the initial condition

$$n(x, z, 0) = \sin(kx),$$
 (19.2.3)

the exact solution is given by the formula

$$n(x, z, t) = \sin\left(kx - k\omega_V z \frac{\sin(\omega t)}{\omega}\right)$$

$$\times \exp\left\{-k^2 D_0 \left[t + \frac{\omega_V^2}{2\omega^2} \left(t - \frac{\sin(2\omega t)}{2\omega}\right)\right]\right\}. \tag{19.2.4}$$

In the most interesting low-frequency case,  $Ku \gg 1$  and  $\omega \ll \omega_V$ , the asymptotic solution,  $t \gg 1/\omega$ , takes the following form:

$$n(x,z,t) = \sin\left(kx - k\omega_V z \frac{\sin(\omega t)}{\omega}\right) \exp\left\{-k^2 t D_0 \left[1 + \frac{\omega_V^2}{2\omega^2}\right]\right\}, \quad (19.2.5)$$

which allows one to define the effective longitudinal diffusivity as

$$D_{\text{eff}} = D_0 \left( 1 + \frac{\omega_V^2}{2\omega^2} \right) \propto \frac{1}{\omega^2}. \tag{19.2.6}$$

Actually, here the influence of time dependence on the scalar transport is analyzed in terms of the Taylor method for the longitudinal dispersion in shear flows [352, 353]. The general scheme of the averaged description of transport in frequency-driven flows can also be formulated in terms of the advection—diffusion equation. To treat time-dependence effects, the author of [353] considered turbulent diffusion in the two-dimensional system of regular but time-periodic flows. To represent this general method and verify the result obtained above, we consider more complex expression for the longitudinal velocity of flow

$$V_X(z,t) = 2V_0 \cos(kz) \cos(\omega t). \tag{19.2.7}$$

By applying the decomposition method, one can represent the solution of the advection–diffusion equation in the following form:

$$n(z,t) = n_0 + n_1 = n_0 + \sin(kz)(n_S \sin \omega t + n_C \cos \omega t + \dots).$$
 (19.2.8)

The amplitudes of the harmonics  $n_S$ ,  $n_C$  can be defined as a result of the solution of the diffusion equation. The averaging method will be applied. Let us represent the mean density of tracer as

$$n_0 = \langle n \rangle = c_a + c_b x. \tag{19.2.9}$$

The values  $V_0$ ,  $c_a$ , and  $c_b$  are the external flow characteristics. The substitution, with allowance for the assumption  $n_1 \ll n_0$ , yields the equation for the average scalar density  $n_0$  in the form

$$\frac{\partial n_0}{\partial t} = -\left\langle V_X \frac{\partial n_1}{\partial x} \right\rangle + D_0 \frac{\partial^2 n_0}{\partial x^2}.$$
 (19.2.10)

The equations for the amplitudes of the harmonics  $n_S$ ,  $n_C$  are given by the relations

$$n_{\rm S} + \frac{2V_0}{w} \frac{\partial n_0}{\partial x} = -\frac{D_0 k^2}{\omega} n_{\rm C},\tag{19.2.11}$$

$$n_{\rm C} = \frac{D_0 k^2}{\omega} n_{\rm S}.$$
 (19.2.12)

Simple calculations lead to the diffusive equation

$$\frac{\partial n_0}{\partial t} = D_0 \left[ \frac{V_0^2 k^2}{\omega^2 + D_0^2 k^4} \right] \frac{\partial^2 n_0}{\partial x^2} + D_0 \frac{\partial^2 n_0}{\partial x^2}, \tag{19.2.13}$$

where the effective diffusivity is given by the formula

$$D_{\text{eff}}(k,\omega) = D_0 \left[ \frac{Ku^2}{1 + (\omega \tau_D)^{-1}} + 1 \right],$$
 (19.2.14)

Here, the characteristic time is  $\tau_D = 1/(D_0 k^2)$ .

For high frequencies,  $\omega > 1/\tau_D$ , we arrive at the quasilinear formula:

$$D \approx D_0 \left[ \frac{V_0^2 k^2}{\omega^2} \right] \approx D_0 K u^2 \propto \omega^{-2}. \tag{19.2.15}$$

A realistic application of the above solution to turbulent flow could be possible only if one considers the Kolmogorov cascade. It is convenient to rewrite the Taylor equation, considering first the cascade  $l_{n-1}$ ,  $l_n$ ,  $l_{n+1}$ ; the transport at each next (larger) scale is calculated by substituting into the formula for the turbulent diffusivity at the smaller scale in place of the molecular transport:

$$D_{n+1} = D_n \left[ 1 + \frac{V_n^2}{V_n^2 + D_n^2 / l_n^2} \right]. \tag{19.2.16}$$

One can replace the difference equation by a differential one. Finally, we obtain the differential equation in the following form:

$$\frac{\mathrm{d}\ln D}{\mathrm{d}\ln \lambda} = \mathrm{const} \frac{V^2(\lambda)}{V^2(\lambda) + \frac{D^2}{\lambda^2}},\tag{19.2.17}$$

Here, it is supposed that  $D = D_0$  at  $\lambda = 0$ . This equation can be exactly solved and with the power dependence  $V(\lambda) \propto \lambda^{\kappa}$ . Here,  $\kappa$  is the characteristic exponent. By performing all the calculations for the Kolmogorov scaling, one finds

$$D_{\text{eff}} = D_0 \sqrt{\text{const} \frac{V_0^2 \lambda^2}{D_0^2} + O(1)}.$$
 (19.2.18)

The important fact here is that the expression obtained has the correct transformation properties under  $t \to -t$  – the same properties as those possessed by the molecular-diffusion coefficient. By the meaning of the derivation, the square root here is just an approximation of a function that always remains positive.

By concluding this section, we note that in the general case of the time-dependent Taylor shear flow with many harmonics in the velocity profile the effective diffusivity is described by the integral form

$$D_{\text{eff}} = D_0 \left[ 1 + \iint \frac{\tilde{V}(k,\omega)dkd\omega}{\omega^2 + D_0^2 k^4} \right]. \tag{19.2.19}$$

Despite this expression formally allows the estimate for  $\omega \to 0$  to be obtained, it appears to be only an intermediate asymptotic and does not take into account effects related to the flow topology reconstruction, which are significant for Ku >> 1. Below the reader will find more detailed analysis of turbulent transport processes in low-frequency regimes (Fig. 19.2.1).

## 19.3 Oscillatory Rolls and Lobe Transport

In the framework of time-periodic velocity fields, the case of greatest interest is the transport in the presence of flow topology reorganization. In this context, let us discuss the Solomon–Gollub model that mimics the Rayleigh–Benard convection

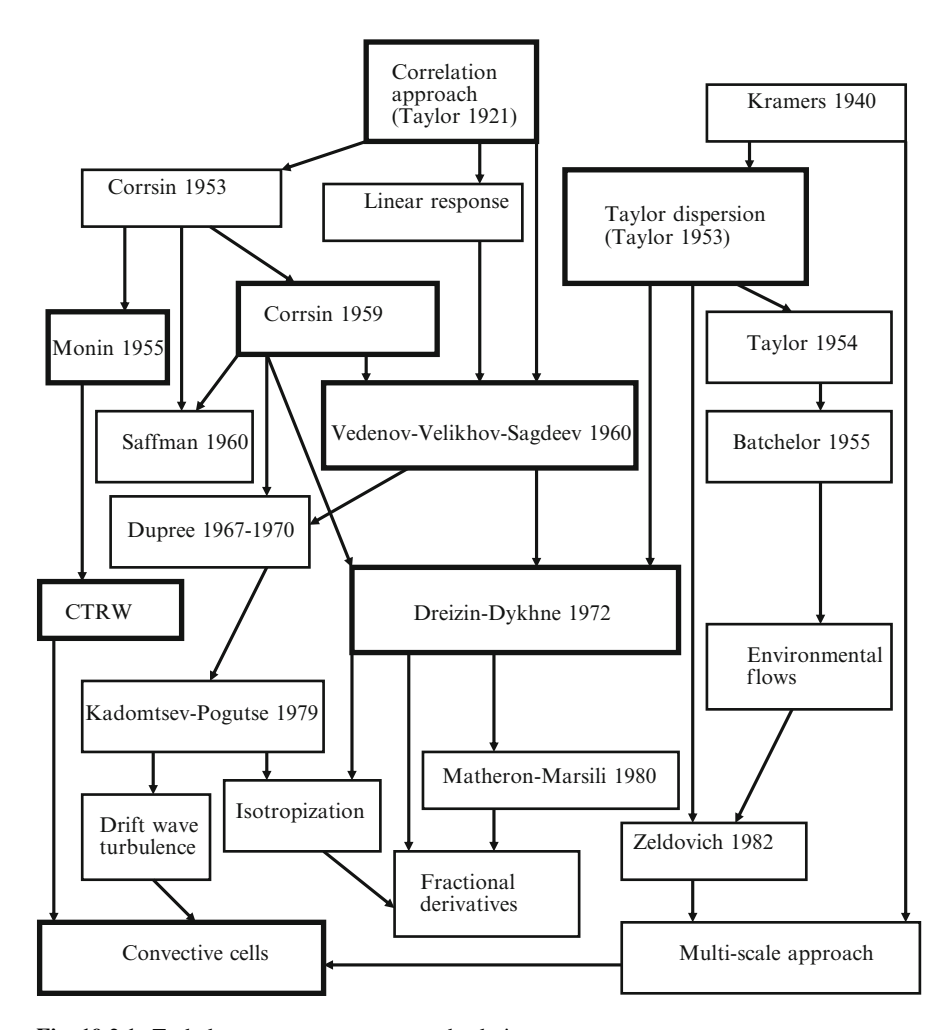


Fig. 19.2.1 Turbulent transport concepts and solutions

[339, 340]. If the temperature difference between the top and bottom of the convective cell is increased, an additional time-periodic instability occurs, resulting in a time-periodic velocity field. Instead of steady symmetric roll stream function, the following form of the velocity field was applied

$$\Psi(x, y, t) = \Psi_0 \sin \left[ \frac{2\pi}{\lambda} (x + B_{\psi} \sin \omega t) \right] \sin \left[ \frac{2\pi}{\lambda} y \right], \tag{19.3.1}$$

where  $\lambda$  is the characteristic spatial scale and  $B_{\psi}$  is the temporal perturbation amplitude proportional to  $(Ra-Ra_*)^{1/2}$ , where Ra is the Rayleigh number and  $Ra_*$  is the critical Rayleigh number at which the time-periodic instability occurs. The stream function amplitude  $\Psi_0$  is given by the relation

$$\Psi_0(V_0, \lambda) = \frac{V_0 \lambda}{2\pi},\tag{19.3.2}$$

where  $V_0$  is the characteristic velocity scale.

This simple model is able to capture the essential features of convective cell system in the presence of the oscillatory instability because the term  $B_{\psi}\sin(\omega t)$  represents the lateral oscillation of the rolls. For fixed values of the temporary perturbation amplitude  $B_{\psi}$ , it is convenient to introduce the Kubo number in the form

$$Ku = \frac{\Psi_0(V_0, \lambda)}{\lambda^2 \omega} = \frac{V_0}{\lambda \omega},\tag{19.3.3}$$

which plays the role of dimensionless control parameter that allows one to analyze different turbulent transport regimes taking place for different values of the Kubo number. In the case of large Ku, we are dealing with very strong Lagrangian correlations.

The streamline approximation under consideration ignores three-dimensional effects as well as higher-order modes, but it nicely illustrates the qualitative features. It was experimentally observed the dramatic enhancement in the effective diffusivity as compared to the case of steady convection and the flux across the roll boundaries scales linearly with the amplitude of the oscillatory instability  $(Ra - Ra_*)^{1/2}$ .

In order to explain these features, it is convenient to employ the dynamics of Hamiltonian system. In our two-dimensional model, there exists a stream function  $\Psi(x, y, t)$ 

$$u_x(x, y, t) = -\frac{\partial \Psi(x, y, t)}{\partial y}, \quad u_y(x, y, t) = -\frac{\partial \Psi(x, y, t)}{\partial x},$$
 (19.3.4)

One immediately notices that the pair of equations of motion for an advected particle has a Hamiltonian structure and the stream function  $\Psi(x, y, t)$  is the Hamiltonian

$$\dot{x} = -\frac{\partial \Psi(x, y, t)}{\partial y}, \quad \dot{y} = \frac{\partial \Psi(x, y, t)}{\partial x}.$$
 (19.3.5)

The dynamics of a passively advected scalar is, in our two-dimensional incompressible flow, a one-degree-of-freedom Hamiltonian system. It is well known that phase space of such a Hamiltonian system coincides with the configuration domain in which flow occurs.

In the case of steady flow under consideration, the stream function is independent on time and the scalar trajectories coincide with the level curves of  $\Psi$ . Moreover, such Hamiltonian systems are always integrable. On the contrary, one-degree-of-freedom Hamiltonian systems with a time-dependent Hamiltonian

$$\Psi(x, y, t) = \Psi_0(x, y) + \varepsilon_\omega \Psi_1(x, y, t), \tag{19.3.6}$$

typically exhibit non-integrable dynamics, or chaos [89–92]. In such driven system, an advected scalar particle moves unpredictably and this advective dynamics is referred to Lagrangian chaos (see Fig. 19.3.1). Note that the mechanism of scalar transport for time-dependent Hamiltonian systems is related to separatrix splitting and it is fundamentally different from that occurs in the steady case in the presence of the molecular (seed) diffusion.

As soon as time dependence sets in by  $B_{\psi} \neq 0$ , chaos in the convective rolls system is observed because one expects the heteroclinic trajectories which create the roll boundaries in the steady case to break up, giving rise to wildly oscillation lobes (see Fig. 19.3.2). In the case under consideration (one-degree-of-freedom Hamiltonian systems with a time-dependent Hamiltonian), we expect lobe transport to dominate. Recall that as one approaches the boundary  $\delta_{\psi} \to 0$ , the period of rotation diverges logarithmically

$$T_{\rm Sep} \propto \frac{1}{\omega} \ln \frac{{\rm const}}{\delta \psi},$$
 (19.3.7)

where  $\delta_{\psi}$  is the relative stream function amplitude at the edge of the stochastic layer. This corresponds exactly to the well-known result for the period of a true pendulum that follows a trajectory very close to the separatrix [89–92].

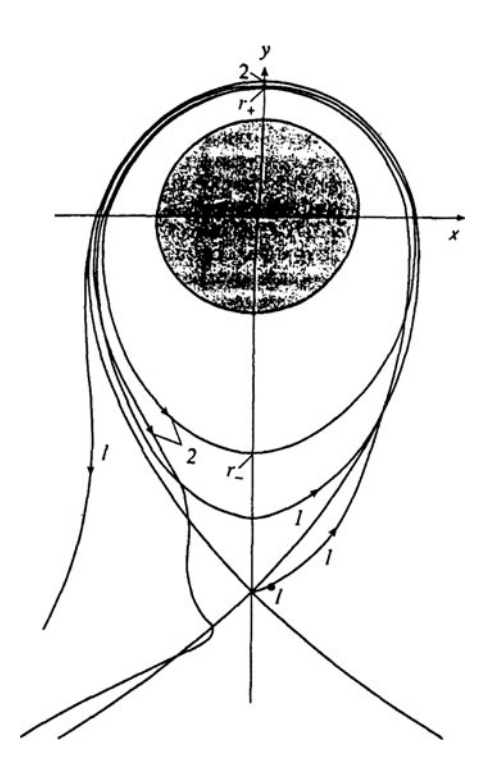
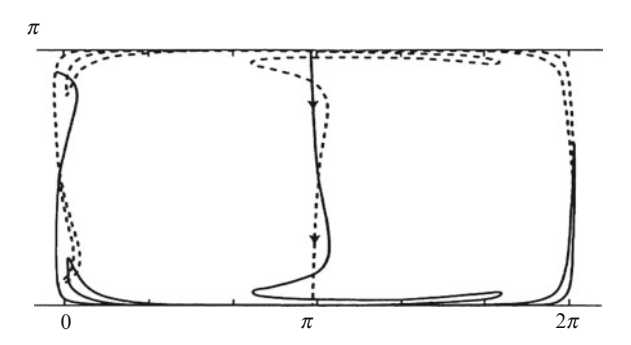


Fig. 19.3.1 The trajectories of particles near separatrix of vortex structure (After Gledzer A.E. [354] with permission)

**Fig. 19.3.2** Sketch of perturbated separatrix in a cellular flow



To set up a transport model in terms of a stream function perturbation, which is similar to the steady percolation approach, where  $D_{\rm eff} \approx V_0 \Delta(\varepsilon) \approx \delta \Psi$ , we have to calculate the Melnikov function, which gives the change in stream function amplitude  $\delta \Psi_0$  due to the separatrix splitting

$$\delta\psi_0(t_0) = \int dt \frac{d\Psi_0(x(t,t_0), y(t,t_0))}{dt}.$$
 (19.3.8)

By taking into account the advection equation, one obtains the integral over Lagrangian trajectory of tracer in the following form:

$$\delta\Psi_0(t_0) = \int dt \varepsilon_\omega \vec{V} \nabla\Psi_0 = \varepsilon_\omega \int dt \left\{ \frac{\partial \Psi_1(t)}{\partial x} \frac{\partial \Psi_0}{\partial y} - \frac{\partial \Psi_1(t)}{\partial y} \frac{\partial \Psi}{\partial x} \right\}. \tag{19.3.9}$$

Here, the trajectory of scalar particle can be represented as the asymptotic expansions

$$x(t,t_0) \approx x(t_0) + \varepsilon_{\omega} x_1(t), \qquad (19.3.10)$$

$$y(t, t_0) \approx y(t_0) + \varepsilon y_1(t),$$
 (19.3.11)

where  $\varepsilon$  is the perturbation amplitude and  $(x(t_0),y(t_0))$  are the initial points of the particle. For the regular cell structure under consideration, the Melnikov function may be carried out exactly. By omitting very complicated calculations given in numerous textbooks and monographs on this subject [92–95, 345], we represent only the final result

$$\delta\Psi_0(t_0) = \frac{\pi D_S}{2} \varepsilon_\omega \sin(\omega t_0). \tag{19.3.12}$$

Here,  $D_{\rm S}$  is the diffusivity related to the separatrix splitting

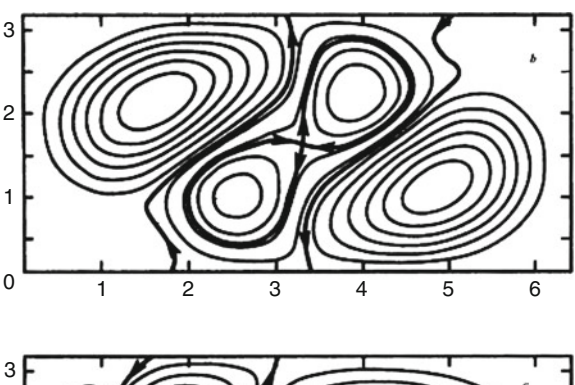
$$D_{\rm S} \approx \frac{\varepsilon_{\omega} \omega}{\pi \sinh(\frac{\pi \omega}{2})}$$
 (19.3.13)

The use of the Melnikov method allows us to study how the transport depends upon the frequency of the perturbation. These results were obtained for the regular system of convective rolls, but our interest is centered on the models of transport in periodically driven random flows, which are developed in the next section.

### 19.4 Flow Topology Reconstruction and Scaling

The reorganization of flow topology, where long streamlines play an important role, is a factor that significantly impacts on transport processes (see Fig. 19.4.1). In the low-frequency case,  $\omega \ll V_0/\lambda$ , the correlation scale is much less than the frequency path  $l_\omega$ . As we saw in the previous section, the description of separatrix deformation (reconnection) could provide highly significant information to obtain effective diffusivity. The Hamiltonian description of streamlines makes the two-dimensional model the most efficient one. In this relation, it is convenient to consider a two-dimensional percolation chaotic flow, which permits analyzing the spatial and temporal hierarchy of scales and extracting scales responsible for the critical streamline evolution. Indeed, in the framework of the single-scale approach, we have the following hierarchy of spatial scales:

$$\lambda \left(\frac{a}{\lambda}\right)^{D_h} \approx L \approx \frac{a}{\varepsilon_*} \gg a \approx \frac{\lambda}{\varepsilon_*} \gg \lambda \gg \Delta \approx \lambda \varepsilon_*.$$
 (19.4.1)



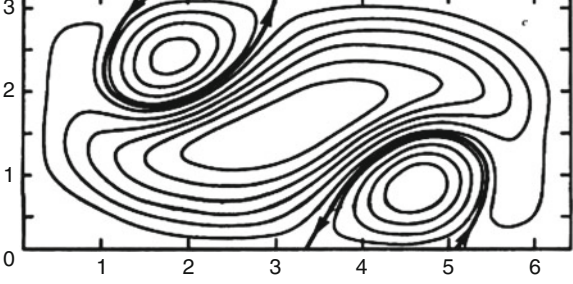


Fig. 19.4.1 Two-dimensional flow topology reconstruction (After Danilov S.D., Dovgenko V.A., and Yakushkin I.G. [222] with permission)

Here,  $a(\varepsilon)$  is the percolation correlation length,  $\lambda$  is the spatial scale, and L is the length of the percolation streamline:

$$a(\varepsilon) = \lambda \varepsilon^{-\nu}, L(\varepsilon) = \lambda \left(\frac{a}{\lambda}\right)^{D_h}, \nu = 4/3, D_h = 1 + \frac{1}{\nu}.$$
 (19.4.2)

From the point of view of probabilistic description, we have to define a geometric factor, which would be responsible for separatrix evolution. The natural estimate for the fraction of space where the reconnection process can occur is  $S_{\rm per} \propto \lambda^2$ . However, as it was discussed before, the description of a single streamline (single trajectory) does not give enough information to obtain transport coefficient, because the measured quantities are always the result of averaging over an ensemble. That is why we must pass from the single percolation streamline description to the analysis of a stochastic layer. Note that in two-dimensional case the fraction of space corresponding to the stochastic layer is

$$S_{\text{layer}} \propto L(\varepsilon)\Delta(\varepsilon) = \frac{\lambda^2}{\varepsilon^{\nu}},$$
 (19.4.3)

and hence,  $S_{\text{layer}} \gg S_{\text{per}}$ , as was expected.

Let us consider now the evolution aspects of the percolation structure growth. At the initial stage of the evolution of the correlation length a(t) scales with the scalar particle path L(t) as

$$a_{\rm I}(t) \approx \left(\frac{L(t)}{\lambda}\right)^{1/D_{\rm h}}.$$
 (19.4.4)

On the other hand, simultaneously with increasing the correlation scale, it is necessary to take into account the increasing stochastic layer width  $\Delta = \Delta(t)$ , which, in the framework of percolation models of turbulent diffusion, is related to the value of the small parameter  $\varepsilon \approx \Delta/\lambda$  and hence to the correlation scale  $a \approx \lambda/\varepsilon^{\nu}$ . Trivial calculations allow one to obtain the expression describing the decrease in correlation scale  $a_{\rm D}(t)$  due to the increase in the stochastic layer width

$$a_{\rm D}(t) \approx \frac{\lambda^{\nu+1}}{\Delta^{\nu}(t)}.$$
 (19.4.5)

In the framework of the mean field theory, the consideration of the balance between  $a_{\rm D}(t)$  and  $a_{\rm I}(t)$  enables us to estimate the characteristic time  $t_0$  that has to be used to define the effective diffusion coefficient  $D_{\rm eff}$ .

In the context of the reconstruction of chaotic flow topology, one can establish the relationship between the stochastic layer width and the parameter responsible for streamline reorganization. Thus, in the Hamiltonian dynamics the linear estimate of the stochastic layer width  $\Delta(t) \propto t$  is widely used [89–92]. Now it is easy to represent this expression in the form

$$\Delta(t) = (\lambda \omega)t, \tag{19.4.6}$$

where  $\omega$  is the characteristic frequency of the model under consideration. Then, the correlation scales balance

$$\lambda \left(\frac{V_0 t_0}{\lambda}\right)^{\frac{1}{D_h}} \approx \frac{\lambda}{(\omega t_0)^{\nu}},$$
 (19.4.7)

allows the estimate of the characteristic time  $t_0$  to be obtained

$$t_0 \approx \frac{1}{\omega} \left(\frac{\lambda \omega}{V_0}\right)^{\frac{1}{\nu+2}} \approx \frac{1}{\omega} \left(\frac{1}{Ku}\right)^{\frac{1}{\nu+2}},$$
 (19.4.8)

and hence, the estimate of the turbulent diffusion coefficient is given by expression [342]

$$D_{\text{eff}} \approx V_0 \Delta(\varepsilon_*) \approx V_0 \Delta(t_0) \approx \lambda V_0 \left(\frac{1}{Ku}\right)^{\frac{1}{v+2}} \propto V_0^{\frac{7}{10}} \omega^{\frac{3}{10}}.$$
 (19.4.9)

Here, the lifetime of the individual percolation streamline  $t_0$  is the main parameter and that is why it is rather natural to employ the fast mode selection principle. Let us estimate the time it takes the flow pattern to change completely as  $T_0 \approx 1/\omega$ . We consider the low-frequency case  $\lambda \ll V_0 T_0$ . In the context of this problem, the relation

$$t_0(\varepsilon_*) \approx \frac{L(\varepsilon_*)}{V_0} \approx \varepsilon_* \frac{1}{\omega},$$
 (19.4.10)

can be used as the renormalization equation to obtain the small parameter of the problem  $\varepsilon_*$ . In the time-dependent flow under consideration, one would also expect a universal result for a specific "universal" value of the small percolation parameter  $\varepsilon_*$ . For this purpose, one can use the above expression accounting for the convective nature of motion along the percolation streamline during the lifetime of this streamline. This equation also enables one to find the small percolation parameter  $\varepsilon_*$  in terms of the time-dependent flow parameters:  $\omega$ ,  $V_0$ ,  $\lambda$ .By assuming the percolation parameter to be small

$$\varepsilon_*(Ku) \approx \frac{\Delta}{\lambda} \approx \frac{\Delta(t_0)}{\lambda} \approx \left(\frac{1}{Ku}\right)^{\frac{1}{v+2}} < 1,$$
 (19.4.11)

and by accounting for the finite size of the system that the correlation scale must be less than the flow domain scale  $L_0$ 

$$a(\varepsilon_*) = \frac{\lambda}{\left|\varepsilon_*(Ku)\right|^{\nu}} = \lambda K u^{\frac{\nu}{\nu+2}} \le L_0, \tag{19.4.12}$$

we can find an inequality for the Kubo number, which corresponds to timedependent percolation models of turbulent transport in the presence of the flow topology reconstruction

$$1 < Ku < \left(\frac{L}{\lambda}\right)^{\frac{\nu+2}{\nu}} = Ku_{\text{max}}.$$
 (19.4.13)

The correlation scale in the low-frequency regime under consideration  $a(\varepsilon_*)$  is really much less than the frequency pass  $l_{\omega}$  for  $\varepsilon_* < 1$ :

$$a(\varepsilon_*) \approx \varepsilon_* L(\varepsilon_*) \approx \varepsilon_* V_0 t_0(\varepsilon_*) \approx \varepsilon_*^2 V_0 / \omega \approx \varepsilon_*^2 l_\omega \ll l_\omega,$$
 (19.4.14)

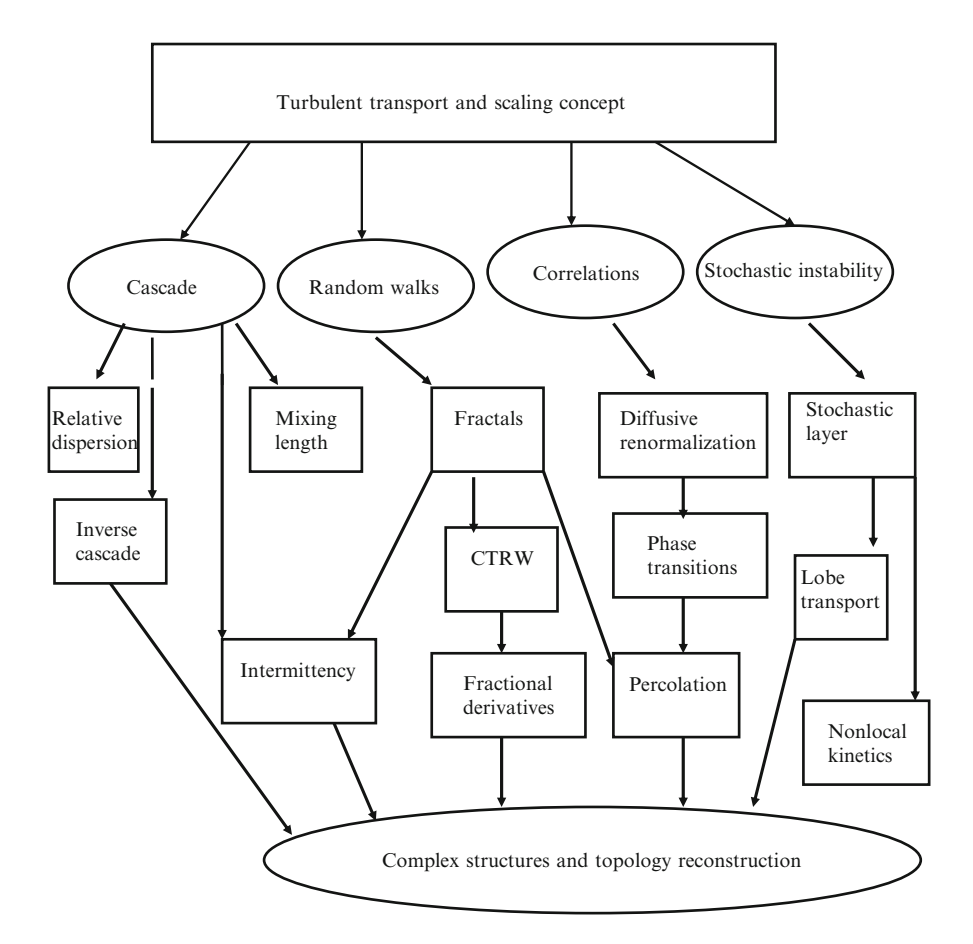


Fig. 19.4.2 Turbulent transport and scaling concept

Further Reading 333

which demonstrates the correctness of the assumptions made. The percolation scaling has been checked to hold the low-frequency domain for guiding centers in a  $k^{-3}$  turbulent spectrum simulated by a large number of randomly phased waves and this has been confirmed at very high amplitudes [346–351].

On the other hand, the fastest mode principle discussed above is also suitable for turbulent transport in low-frequency regimes. Indeed, taking the characteristic correlation time in the scaling form

$$\tau(V_0) \approx \frac{L}{V_0^{\chi}} \ll \frac{1}{\omega},\tag{19.4.15}$$

in the case of strong turbulence (Re  $\gg$  1), the correlation time will be less than characteristic frequency. Here, the supposition was made that the characteristic exponent  $\chi$ >0. This estimate can also be interpreted in terms of the correlation path  $L_{\tau}$  for an arbitrary frequency-driven flow as follows:

$$L_{\tau} \propto V_0 \tau \propto \frac{V_0}{V_0^{\chi}} \ll \frac{V_0}{\omega} \approx l_{\omega}.$$
 (19.4.16)

Here,  $l_{\omega}$  is the frequency path. One can expect that the correlation path in the case of strong turbulence scales with the velocity fluctuation amplitude  $V_0$ . This leads to the double inequality  $1>\chi>0$  and hence to the flat scaling for the correlation path

$$\Delta_{\text{COR}}(V_0) \le L_{\tau}(V_0) \propto V_0^{1-\chi}, 1 > \chi > 0.$$
 (19.4.17)

Thus, we obtain one more tool to treat transport in chaotic flows where the reconstruction of the flow topology is essential.

The approach considered makes it possible to use the correlation scale balance as the basis for constructing new turbulent transport models based on the model approximations for the growth of the stochastic layer width  $\Delta(t)$ . Repeat that the evolution of a single percolation streamline does not provide all necessary information to describe turbulent transport effects. Specifically stochastic layer that arises around a percolation streamline is responsible for the effective transport in chaotic flows Fig. 19.4.2

# **Further Reading**

# Flow Reconstruction and Transport Scaling

- O.G. Bakunin, *Turbulent and Diffusion. Scaling Versus Equations* (Springer, Berlin, 2008)
- R. Balescu, *Aspects of Anomalous Transport in Plasmas* (IOP Bristol, Philadelphia, 2005)

- P. Castiglione et al., *Chaos and Coarse Graining in Statistical Mechanics* (Cambridge University Press, Cambridge, 2008)
- A. Crisanti, M. Falcioni, A. Vulpiani, Rivista Del Nuovo Cimento 14, 1–80 (1991)
- P.H. Diamond, S.-I. Itoh, K. Itoh, *Modern Plasma Physics*, vol. 1 (Cambridge University Press, Cambridge, 2010)
- W. Horton, Y.-H. Ichikawa, *Chaos and Structures in Nonlinear Plasmas* (Word Scientific, Singapore, 1994)
- M.B. Isichenko, Rev. Mod. Phys. **64**, 961 (1992)
- H.K. Moffatt, Rep. Prog. Phys. **621**, 3 (1983)
- H.K. Moffatt, G.M. Zaslavsky, P. Comte, M. Tabor, *Topological Aspects of the Dynamics of Fluids and Plasmas* (Kluwer Academic Publishers, Dordrecht, 1992)
- T. Tel, Phys. Rep. 413, 91 (2005)
- G.M. Zaslavsky, Phys. Rep. 371, 461–580 (2002)

#### Lobe Transport

- H. Aref, M.S. El Naschie, Chaos Applied to Fluid Mixing (Pergamon, Oxford, 1994)
- S. Childress, A.D. Gilbert, *Stretch, Twist, Fold: The Fast Dynamo* (Springer, Berlin, 1995)
- J. Ottino, *The Kinematics of Mixing* (Cambridge University Press, Cambridge, 1989)
- E. Ott, *Chaos in Dynamical Systems* (Cambridge University Press, Cambridge, 1993)
- R. Samelson, S. Wiggins, Lagrangian Transport in Geophysical Jets and Wves. The Dynamical System Approach (Springer, New York, 2006)
- S. Wiggins, Chaotic Transport in Dynamical Systems (Springer, New York, 1990)
- S. Wiggins, Introduction to Applied Nonlinear Dynamical Systems and Chaos (Springer, New York, 1999)

- 1. M. Van-Dyke, An Album of Fluid Motion (Parabolic, Stanford, CA, 1982)
- 2. G. Brethouwer, J.C.R. Hunt, F.T.M. Nieuwstadt, J. Fluid Mech. 474, 193–225 (2003)
- 3. B. Castaing et al., J. Fluid Mech. 204, 1-30 (1989)
- 4. H.C. Berg, Random Walks in Biology (Princeton University Press, Princeton, NJ, 1969)
- YaB Zeldovich, A.A. Ruzmaikin, D.D. Sokoloff, *The Almighty Chance* (World Scientific, Singapore, 1990)
- 6. H. Carslaw, Mathematical Theory of Conduction of Heat in Solids (Macmillan, London, 1921)
- 7. L. Dresner, Similarity Solutions of Nonlinear Partial Differential Equations (Longman, London, 1983)
- 8. G.I. Barenblatt, Scaling Phenomena in Fluid Mechanics (Cambridge University Press, Cambridge, 1994)
- 9. J.M. Burgers, *The Nonlinear Diffusion Equation* (D. Reidel, Dordrecht, 1974)
- R.M. Mazo, Brownian Motion, Fluctuations, Dynamics and Applications (Clarendon, Oxford, 2002)
- 11. G.H. Weiss, Aspects and Applications of the Random Walk (Elsevier, Amsterdam, 1994)
- 12. A.P.S. Selvadurai, Partial Differential Equations in Mechanics (Springer, Berlin, 2000)
- 13. E.W. Montroll and M. F., *Shlesinger on the Wonderful World of Random Walks*, in Studies in Statistical Mechanics, vol 11 (Elsevier Science Publishers, Amsterdam 1984), p. 1
- 14. A. Pekalski, K. Sznajd-Weron (eds.), *Anomalous Diffusion. From Basics to Applications* (Springer, Berlin, 1999)
- M.F. Shiesinger, G.M. Zaslavsky, Levy Flights and Related Topics in Physics (Springer, Berlin, 1995)
- 16. D. Sornette, Critical Phenomena in Natural Sciences (Springer, Berlin, 2006)
- F.U. Turbulence, The Legacy of A.N. Kolmogorov (Cambridge University Press, Cambridge, 1995)
- 18. U. Frisch, in: J.R. Herring and J.C. McWilliams Lecture Notes on Turbulence (World Scientific, Singapore, 1987)
- 19. L. Biferale et al., Phys. Fluids **7**, 2725 (1995)
- 20. M.J. Ringuette et al., J. Fluid Mech. **594**, 59–69 (2008)
- 21. D.W. Hughes, J. Fluid Mech. 594, 445 (2008)
- 22. K.R. Sreenivasan, Rev. Mod. Phys. 71, S383 (1999)
- 23. L.M. Pismen, Patterns and Interfaces in Dissipative Dynamics (Springer, Berlin, 2006)
- 24. W. Horton, Rev. Mod. Phys. 71, 735 (1999)
- 25. P.W. Terry, Rev. Mod. Phys. 72, 109 (2000)
- 26. J.A. Wesson, Tokamaks (Oxford University Press, Oxford, 1987)
- 27. O.G. Bakunin, Reviews of Plasma Physics, vol. 24 (Springer, Berlin, 2008)

References References

 P.H. Diamond, S.-I. Itoh, K. Itoh, Modern Plasma Physics (Cambridge University Press, Cambridge, 2010)

- 29. G.P. Bouchaud, A. Gorges, Phys. Rep. 195, 132–292 (1990)
- 30. J.W. Haus, K.W. Kehr, Phys. Rep. 150, 263 (1987)
- 31. D. Ben-Avraham, S. Havlin, *Diffusion and Reactions in Fractals and Disordered Systems* (Cambridge University Press, Cambridge, 1996)
- 32. W. Horton, Y.-H. Ichikawa, *Chaos and Structures in Nonlinear Plasmas* (Word Scientific, Singapore, 1994)
- 33. A. Scott, Nonlinear Science (Oxford University Press, Oxford, 2003)
- 34. G.B. Whitham, Linear and Nonlinear Waves (Wiley, New York, 1974)
- 35. R.T. Foister, T.G.M. Van de Ven, J. Fluid Mech. 96(1), 105 (1980)
- 36. YaB Zeldovich, A.D. Myshkis, Principles of Mathematical Physics (Nauka, Moscow, 1973)
- 37. YaB Zeldovich, Zg Eksp, Teoret. Fiz. **7**(12), 1466 (1937)
- 38. P.C. Chatwin, P.J. Sullivan, J. Fluid Mech. 91(2), 337 (1979)
- 39. G.K. Batchelor, J. Fluid Mech. 5, 113 (1959)
- 40. P. Langeven, Comptes Rendues 146, 530 (1908)
- 41. B. Duplantier Brownian Motion, Poincare Seminar (2005)
- 42. C.W. Gardiner, Handbook of Stochastic Methods (Springer, Berlin, 1985)
- 43. L.E. Reichl, A Modern Course in Statistical Physics (Wiley-Interscience, New York, 1998)
- 44. S. Chandrasekhar, Rev. Mod. Phys. 15, 1 (1943)
- W.T. Coffey, Y.P. Kalmykov, J.T. Waldron, The Langevin Equation (World Scientific, Singapore, 2005)
- K. Jacobs, Stochastic Processes for Physicists Understanding Noisy Systems (Cambridge University Press, Cambridge, 2010)
- 47. K. Sekimoto, Stochastic Energetics (Springer, Berlin, 2010)
- 48. H. Kramers, Physica 7, 284 (1940)
- 49. G.M. Zaslavsky, M. Edelman, Chaos 10, 135 (2000)
- 50. O.G. Bakunin, S.I. Krasheninnikov, Plasma Phys. Rep. 21, 502 (1995)
- 51. P. Hanggi, H. Thomas, Phys. Rep. 88, 207 (1982)
- 52. P. Hanggi, M. Borkovec, P. Talkner, Rev. Mod. Phys. **62**, 251 (1990)
- 53. O.G. Bakunin, Phys. Lett. A **322**, 105–110 (2004)
- 54. H. Malchow, L. Schimansky-Geier, *Noise and Diffusion in Bistable Nonequilibrium Systems* (Teuber, Leipzig, 1985)
- 55. K.S. Garcia et al., Phys. Rep. 465, 149 (2008)
- 56. O.G. Bakunin, Plasma Phys. Rep. **29**(9), 847 (2003)
- 57. H. Risken, *The Fokker–Planck Equation* (Springer, Berlin, 1989)
- 58. N.G. Van Kampen, Stochastic Processes in Physics and Chemistry (North Holland, Amsterdam, 1984)
- 59. G.I. Taylor, Proc. London Math. Soc. Ser. **20**, 196 (1921)
- G.K. Batchelor (ed.), The Scientific Papers of Sir G.I. Taylor. Meteorology, Oceanology, Turbulent Flow, vol. 2 (Cambridge University Press, Cambridge, 1960)
- 61. W.D. McComb, The Physics of Fluid Turbulence (Clarendon, Oxford, 1994)
- 62. A.S. Monin, A.M. Yaglom, Statistical Fluid Mechanics (MIT, Cambridge, 1975)
- 63. H. Tennekes, J.L. Lumley, A First Course in Turbulence (MIT, Cambridge, 1970)
- 64. Y. Sato, K. Yamamoto, J. Fluid Mech. **175**, 183 (1987)
- 65. L. Zeng, J. Fluid Mech. 594, 271 (2008)
- 66. Corrsin S, in *Proceedings of Iowa Thermodynamics Symposium*, 1953, pp. 5–30
- 67. G.T. Csanady, Turbulent Diffusion in the Environment (D. Reidel, Dordrecht, 1972)
- 68. N.F. Frenkiel (ed.), Atmospheric Diffusion and Air Pollution (Academic, New York, 1959)
- F.T.M. Nieuwstadt, H. Van Dop (eds.), Atmospheric Turbulence and Air Pollution Modeling (D. Reidel, London, 1981)
- H.A. Panofsky, I.A. Dutton, Atmospheric Turbulence Models and Methods for Engineering Applications (Wiley Interscience, New York, 1970)

71. F. Pasquill, F.B. Smith, *Atmospheric Diffusion, Ellis Horwood Limited* (Ellis Horwood Limited, Halsted Press: a Division of Willey, New York, 1983)

- J.C. Wyngaard, Turbulence in the Atmosphere (Cambridge University Press, Cambridge, 2010)
- 73. S. Corrsin, in N.F. Frenkiel (ed.) *Atmospheric Diffusion and Air Pollution* (Academic, New York, London 1959)
- 74. J.S. Hay, F. Pasquill, Adv. Geophys. **6**, 345 (1959)
- 75. P. Bernand, J.M. Wallace, Turbulent Flow (Wiley, Hoboken, NJ, 2002)
- 76. T. Cebeci, Analysis of Turbulent Flows (Elsevier, Amsterdam, 2004)
- P.A. Davidson, Turbulence. An Introduction for Scientists and Engineers (Oxford University Press, Oxford, 2004)
- A. Tsinober, An Informal Introduction to Turbulence (Kluwer Academic Publishers, Amsterdam, 2004)
- 79. U. Marconi, A. Vulpiani, Phys. Rep. **461**, 111 (2008)
- 80. O.G.J. Bakunin, Plasma Phys. 72, 647-670 (2006)
- 81. Y. Kaneda, T. Ishida, J. Fluid Mech. 402, 311 (2000)
- 82. C. Cambon, F.S. Godeferd, F. Nicolleau, J.C. Vassilicos, J. Fluid Mech. 499, 231 (2004)
- 83. V.I. Arnold, Ann. Inst. Fourier 16, 316-361 (1966)
- 84. M.M. Henon, Acad. Sci. Paris **262**, 312–314 (1966)
- 85. S. Childress, A.D. Gilbert, Stretch, Twist, Fold: The Fast Dynamo (Springer, Berlin, 1995)
- 86. G.M. Zaslavsky, The Physics of Chaos in Hamiltonian Systems (ICP, London, 2007)
- 87. V.I. Arnold, B.A. Khestin, Topological Methods in Hydrodynamics (Springer, Berlin, 2006)
- 88. H.K. Moffatt, G.M. Zaslavsky, P. Comte, M. Tabor, *Topological Aspects of the Dynamics of Fluids and Plasmas* (Kluwer Academic Publishers, Dordrecht, 1992)
- 89. A.J. Lichtenberg, M.A. Liberman, Regular and Stochastic Motion (Springer, Berlin, 1983)
- 90. MacKay R.S., Meiss J.D. Hamiltonian Dynamical Systems. A Reprint Selection Hilger, 1987
- 91. E. Ott, Chaos in Dynamical Systems (Cambridge University Press, Cambridge, 1993)
- S. Wiggins, Introduction to Applied Nonlinear Dynamical Systems and Chaos (Springer, New York, 1999)
- 93. H. Aref, M.S. El Naschie, Chaos Applied to Fluid Mixing (Pergamon, Oxford, 1994)
- 94. J. Ottino, The Kinematics of Mixing (Cambridge University Press, Cambridge, 1989)
- 95. S. Wiggins, Chaotic Transport in Dynamical Systems (Springer, New York, 1990)
- 96. M.V. Budyansky et al., J. Exp. Theor. Phys. 99, 1018–1027 (2004)
- 97. N.S. Krylov, Selected Papers (Nauka, Moscow, 1950)
- 98. J.R. Dorfman, An Introduction to Chaos in Nonequilibrium Statistical Mechanics (Cambridge University Press, Cambridge, 1999)
- 99. C. Beck, F. Schlogl, *Thermodynamics of Chaotic Systems* (Cambridge University Press, Cambridge, 1993)
- 100. V. Berdichevski, *Thermodynamics of Chaos and Order* (Longman, London, 1998)
- P. Castiglione et al., Chaos and Coarse Graining in Statistical Mechanics (Cambridge University Press, Cambridge, 2008)
- 102. P. Gaspard, *Chaos, Scattering and Statistical Mechanics* (Cambridge University Press, Cambridge, 2003)
- 103. M.B. Isichenko, Rev. Mod. Phys. 964, 961 (1992)
- 104. O.G. Bakunin, Nucl. Fusion 47, 1857–1876 (2005)
- 105. C. Eckart, J. Mar. Res. 7, 265-275 (1948)
- 106. P. Welander, Tellus 7, 141–156 (1955)
- 107. J.M. Ottino, Phys. Fluids 22, 021301 (2010)
- 108. A.D. Stroock, G.J. McGraw, Philos. Trans. R. Soc. Lond. A 362, 971–986 (2004)
- 109. T.M. Squires, S.R. Quake, Rev. Mod. Phys. 77, 977 (2005)
- 110. G.M. Zasavsky, B.V. Chirikov, Sov Phys Uspekhy 14, 549 (1972)
- 111. A.B. Rechester, M.N. Rosenbluth, Phys. Rev. Lett. 40, 38 (1978)
- 112. V.S. Ptuskin, Astrophys. Space Sci. **61**, 251 (1979)

References References

- 113. A.B. Rechester, M.N. Rosenbluth, R.B. White, Phys. Rev. Lett. 42, 1247 (1979)
- 114. T.X. Stix, Nucl. Fusion 18, 353 (1978)
- 115. J.-L. Thiffeault, M.D. Finn, Philos. Trans. R Soc. A 364, 3251-3211 (2006)
- 116. K. Horiuti, T. Fujisawa, J. Fluid Mech. **595**, 341 (2008)
- 117. L.I. Pitterbarg, S.V. Semovsky, Dokladi Akademii Nauk 285, 589–593 (1985)
- 118. R. Narayan, Phys. Rev. Lett. 42, 1247 (1999)
- 119. B.I. Davydov, Dokl Akad Nauk SSSR 2, 474 (1934)
- 120. G.H. Weiss, Aspects and Applications of the Random Walk (Elsevier, Amsterdam, 1994)
- 121. A. Cattaneo, Atti Semin Mat Fis Univ Modena 3, 83 (1948)
- 122. S. Goldstein, Quart. J. Mech. Appl. Math. 4(4.1), 129 (1951)
- 123. R.W. Davies, Phys. Rev. 93, 1169 (1954)
- 124. D.D. Joseph, L. Prezioso, Rev. Mod. Phys. 61, 41 (1989)
- 125. R. Ferrari et al., Physica D **154**, 111–137 (2001)
- 126. O.G. Bakunin, Physics-Uspekhi 46, 323 (2003)
- 127. V. Uchaikin, Physics-Uspekhi 173, 765 (2003)
- 128. M.R. Maxey, J. Fluid Mech. **174**, 441–465 (1987)
- 129. A. Vedenov, E.P. Velikhov, R.Z. Sagdeev, Plasma Phys. Control. Nucl. Fusion Res. 2, 82 (1962)
- 130. W.E. Drummond, D. Pines, Plasma Phys. Control. Nucl. Fusion Res. 3, 1049 (1962)
- 131. B.B. Kadomtsev, Collective Phenomena in Plasma (Nauka, Moscow, 1976)
- 132. A.S. Kingsep, *Introduction to the Nonlinear Plasma Physics Mosk* (Fiz.-Tekh. Inst, Moscow, 1996)
- 133. V.N. Tsytovich, Theory of Turbulent Plasma (Plenum, New York, 1974)
- 134. M.N. Rosenbluth, R.Z. Agdeev (eds.) *Handbook of Plasma Physics* (North-Holland, Amsterdam 1984)
- 135. T.H. Dupree, Phys. Fluids 9, 1773 (1966)
- 136. T.H. Dupree, Phys. Fluids **10**, 1049 (1967)
- 137. T.H. Dupree, Phys. Fluids **15**, 334 (1972)
- 138. O. Ishihara, A. Hirose, Comments on Plasma, Phys. Control. Fusion 8, 229 (1984)
- 139. A. Salat, Naturforsch Z. Teil A 38, 1189 (1983)
- 140. O. Ishihara, A. Hirose, Phys. Fluids 28, 2159 (1985)
- 141. A. Salat, Phys. Fluids **31**, 1499 (1988)
- 142. O. Ishihara, H. Xia, A. Hirose, Phys. Fluids B 4, 349 (1992)
- 143. G.I. Taylor, Proc. R. Soc. London Ser. A 219, 186 (1953)
- B. Cushman-Roisin, J.-M. Beckers, Introduction to Geophysical Fluid Dynamics (Academic, New York, 2010)
- S.A. Thorpe, Introduction to Ocean Turbulence (Cambridge University Press, Cambridge, 2007)
- C.J. Hearn, The Dynamics of Coastal Models (Cambridge University Press, Cambridge, 2008)
- 147. R. Ferrari, W. Young, J. Mar. Res. 55, 1069 (1997)
- 148. G.I. Taylor, Proc. R. Soc. London, Ser. A 223, 446 (1954)
- 149. J.W. Elder, J. Fluid Mech. 5, 544–560 (1959)
- 150. H.B. Fischer, J. Hydraul, Div. Proc. ASCE 93, 187 (1967)
- 151. P.C. Chatwin, C.M. Allen, Annu. Rev. Fluid Mech. 17, 119 (1985)
- 152. G.K. Batchelor et al., Proc. Phys. Soc. 68, 1095 (1955)
- 153. J.L. Lumley, J. Math. Phys **3**(2), 309–312 (1962)
- L.C. Van Rijn Principles of Sediment Transport in Rivers, Estuaries and Coastal Seas Aqua, 1993
- 155. C. Ancey et al., J. Fluid Mech. **595**, 83–114 (2008)
- 156. A. Dreizin Yu, A.M. Dykhne, Sov. Phys. J. Exp. Theor. Phys. 36, 127 (1973)
- 157. B.B. Mandelbrot, The Fractal Geometry of Nature (Freemen, San Francisco, 1982)
- 158. A. Bunde, S. Havlin (eds.), Fractals and Disordered Systems (Springer, Berlin, 1995)

- 159. A. Bunde, S. Havlin (eds.), Fractals in Science (Springer, Berlin, 1996)
- J. Feder, Fractals, Department of Physics University of Oslo, Norway (Plenum, New York, 1988)
- 161. J.-F. Gouyet, *Physics and Fractal Structure* (Springer, Berlin, 1996)
- 162. H.M. Hastings, G. Sugihara, Fractals (Oxford University Press, Oxford, 1993)
- L.S. Liebovitch, Fractals and Chaos Simplified for the Life Sciences (Oxford University Press, Oxford, 1998)
- 164. M. Schroeder, Fractals, Chaos, Power Laws. Minutes from an Infinite Paradise (W.H. Freeman and Company, New York, 2001)
- 165. P.G. De Gennes, Introduction to Polymer Dynamics (Cambridge, 1990)
- 166. P.G. De Gennes, Scaling Concepts in Polymer Physics, (Cornell University Press, 1979)
- 167. M. Kleman, O.D. Lavrentovich, Soft Matter Physics (Springer, Berlin, 2003)
- 168. V.E. Kravtsov, I.V. Lerner, V.I. Udson, J. Exp. Theor. Phys. 91(2(8)), 569 (1986)
- 169. P.B. Rhines, J. Fluid Mech. 69(Part 3), 417-443 (1975)
- 170. M.B. Isichenko, J. Kalda, J. Nonlinear Sci. 1, 255 (1991)
- 171. M.B. Isichenko, J. Kalda, J. Nonlinear Sci. 1, 375 (1991)
- 172. M. Mitsugu, S. Ouchi, K. Honda, J. Phys. Sos. Japan 60, 2109 (1991)
- 173. S. Isogami, M. Matsushita, J. Phys. Sos. Japan 61, 1445 (1992)
- 174. A. Bunde, J.F. Gouet, J. Phys. A: Math. Gen. 18, L285 (1985)
- 175. H. Saleur, B. Duplantier, Phys. Rev. Lett. 58, 2325 (1987)
- 176. B. Sapoval, B. Rosso, J. Gouyet, J. Phys. Lett. 46, 149 (1985)
- 177. J. Kondev, C.L. Henley, Phys. Rev. Lett. **74**, 4580 (1995)
- 178. J. Kondev, C.L. Henley, D.G. Salinas, Phys. Rev. E 61, 104 (2000)
- 179. J. Kondev, Phys. Rev. Lett. 86, 5890 (2001)
- 180. J. Kalda, Phys. Rev. E 64, 020101(R) (2001)
- 181. J. Kalda, Phys. Rev. Lett. 90, 118501-1 (2003)
- 182. O.G. Bakunin, Chaos Solitons & Fractals 23, 1703 (2005)
- 183. P. Resibois, M. Leener, De Classical Kinetic Theory (Wiley, New York, 1977)
- 184. B. Berne, J. Chem. Phys. 56, 2164 (1972)
- 185. G. Matheron, G. De Marsily, Water Resour. Res. 16, 901 (1980)
- 186. I.D. Howells, J. Fluid Mech. 9, 104 (1960)
- 187. M. Avellaneda, A. Majda, J. Phys. Fluids 4, 41 (1992)
- 188. O.G. Bakunin, T. Schep, J. Phys. Lett. A 322, 105 (2004)
- 189. S. Redner, Physica D 38, 287 (1989)
- 190. J.-P. Bouchaud, A. Georges, Phys. Rev. Let. 64, 2503 (1990)
- 191. D.L. Koch, J.F. Brady, Phys. Fluids A 1, 47 (1990)
- A.J. Majda, A.L. Bertozzi, Vorticity and Incompressible Flow (Cambridge University Press, Cambridge, 2002)
- 193. E. Ben-Naim, S. Redner, Phys. Rev. A 45, 7207 (1992)
- 194. M.E. Fisher, J. Chem. Phys. 44, 616 (1966)
- 195. S.R. Broadbent, J.M. Hammersley, Proc. Camb. Phil. Soc. 53, 629 (1957)
- 196. D. Stauffer, Introduction to Percolation Theory (Taylor and Francis, London, 1985)
- 197. H.E. Stanley, J.Stat. Phys. 34, 843 (1984)
- 198. I.M. Sokolov, Sov. Phys. Usp. 29, 924 (1986)
- 199. D. Stauffer, Phys. Rep. 2, 3 (1979)
- H.E. Stanley, Introduction to Phase Transitions and Critical Phenomena (Clarendon, Oxford, 1971)
- 201. A. Hunt, Percolation Theory for Flow in Porous Media (Springer, Berlin, 2005)
- 202. M. Sahimi, Application of Percolation Theory (Taylor&Francis, New York, 1993)
- 203. R. Zallen, The Physics of Amorphous Solids (Wiley, New York, 1998)
- 204. L.P. Kadanoff, *Statistical Physics: Dynamics and Renormalization* (World Scientific Publishing, Singapore, 1999)

References References

205. J.M. Ziman, Models of Disorder: The Theoretical Physics of Homogeneously Disordered Systems (Cambridge University Press, London, 1979)

- 206. R.A. Fisher, Statistical Methods and Scientific Inference (Hafner, New York, 1973)
- J. Cardy, Scaling and Renormalization in Statistical Physics (Cambridge University Press, London, 2000)
- 208. J. Cardy (ed.), Finite-Size Scaling (Elsevier, Amsterdam, 1988)
- V. Privman (ed.), Finite Size Scaling and Numerical Simulation of Statistical Systems (World Scientific Publishing, Singapore, 1990)
- 210. E. Montroll, G. Weiss, J. Math. Phys. 6, 178 (1965)
- 211. E. Montroll, H. Scher, Phys. Rev. Ser. B 12, 2455 (1972)
- 212. Lubashevskiy I.A. and Zemlianov, JETF, 114, 1284 1998
- 213. B.B. Kadomtsev, and O.P. Pogutse, Plasma Physics and Controlled Nuclear Fusion Research. In: Proceedings of the 7-th International Conference, IAEA Vienna, 1, 649 1978
- 214. A. Einstein, Ann. Physik 17, 549 (1905)
- 215. AYa Khintchine, P. Levy, Compt. Rend. 202, 274 (1936)
- 216. A. Cauchy, Comptes Rends 37, 292 (1853)
- 217. A. Leonard, I. Mizic, Phys. Fluid. (1994)
- 218. B. Kuvshinov, T. Schep, Phys. Rev. Lett. 215, 3675 (1998)
- 219. G.M. Zaslavsky, Chaos 4, 253 (1994)
- 220. A.V. Chechkin, V.Y. Gonchar, J. Exp. Theor. Phys. 91, 635 (2000)
- 221. O.G. Bakunin, Plasma Phys. Rep. 16, 529 (1990)
- 222. S.D. Danilov, V.A. Dovgenko, I.G. Yakushkin, J. Exp. Theor. Phys. 91, 423–432 (2000)
- 223. K. Diethelm, *The Analysis of Fractional Differential Equations. An Application-Oriented Exposition* (Springer, Berlin, 2010)
- 224. L. Pietronero, Fractals' Physical Origin and Properties (Plenum, New York, 1988)
- B.J. West, M. Bologna, P. Grigolini, *Physics o Fractal Operators* (Springer, New York, 2003)
- G. Zaslavsky, Hamiltonian Chaos and Fractional Dynamics (Oxford University Press, Oxford, 2005)
- 227. O.G. Bakunin, Physica A **337**, 27–35 (2004)
- 228. G.I. Barenblatt, Scaling Phenomena in Fluid Mechanics (Cambridge University Press, Cambridge, 1994)
- 229. G.K. Batchelor, An Introduction to Fluid Dynamics (Cambridge University Press, Cambridge, 1973)
- 230. O. Darrigol, Words of Flow: A History of Hydrodynamics from the Bernoullis to Prandtl (Oxford University Press, New York, 2009)
- 231. L. Prandtl, O.G. Tietjens, Applied Hydro- and Aeromechanics (McGraw-Hill, London, 1953)
- 232. M. Samimy et al., A Gallery of Fluid Motion (Cambridge University Press, Cambridge, 2003)
- 233. P. Taberling, O. Cardoso, *Turbulence*. A Tentative Dictionary (Plenum, New York, 1994)
- 234. D.P. Papailiou, P.S. Lyykoudis, J. Fluid Mech. 62, 11–31 (1974)
- 235. N. Kolmogorov, Dokl. Akad Nauk SSSR 30, 299 (1941)
- 236. A.M.C.R. Obukhov, Acad. Sci. U.R.S.S 32, 19 (1941)
- 237. S.G. Saddoughi, S.V. Veeravally, J. Fluid Mech. 268, 333–372 (1994)
- 238. A.M. Yaglom, Dokl. Akad Nauk SSSR **67**, 795 (1949)
- A. La Porta et al., Fluid particle accelerations in fully developed turbulence. Lett. Nat. 409, 1017 (2001)
- 240. O.G. Bakunin, Plasma Phys. Control. Nucl. Fusion 45, 1909 (2003)
- 241. A. Obuchov, M. Izvestia, S.S.S.R. Akad Nauk, Geophysics 13, 58 (1949)
- 242. S. Corrsion, J. Appl. Phys. 22, 469 (1951)
- 243. H. Grant, J. Fluid Mech. 34, 423 (1968)
- 244. C.H. Gibson, W.H. Schwarz, J. Fluid Mech. 16, 365 (1963)
- 245. M.-C. Jullien, P. Castiglione, Phys. Rev. Lett. **85**, 3636 (2000)

- 246. P. Vaishnavi et al., J. Fluid Mech. 596, 103 (200)
- A. Grosman, V. Steinberg, Elastic turbulence in a polymer solution flow. Lett. Nat. 405, 53 (2000)
- 248. D.R. Fereday, Phys. Fluids 16, 4359 (2004)
- 249. P.G. Saffman, Fluid Mech. 8, 18 (1959)
- 250. H.K. Moffatt, J. Fluid Mech. 106, 27 (1981)
- 251. H.K. Moffatt, Rep. Prog. Phys. 621, 3 (1983)
- 252. K.R. Sreenivasan, Rev. Mod. Phys. 71, 383 (1999)
- 253. P.G. Mestayer, J. Fluid Mech. 125, 475 (1982)
- 254. S. Chen, R.H. Kraichnan, Phys. Fluids 68, 2867 (1998)
- 255. G. Falkovich, K. Gawedzki, M. Vergassola, Rev. Mod. Phys. 73, 913 (2001)
- 256. Z. Warhaft, Annu. Rev. Fluid Mach. 32, 203–240 (2000)
- 257. B.I. Shraiman, E.D. Siggia, Nature **405**, 639 (2000)
- 258. L.F. Richardson, Proc. R. Soc. London, Ser. A 110, 709 (1926)
- 259. S. Ott, J. Mann, J. Fluid Mech. 422, 207 (2000)
- 260. G.K. Batchelor, Q. J. R. Meteor. Soc 76, 133 (1950)
- G.K. Batchelor, A.A. Townesend, In Surveys in Mechanics (Cambridge University Press, Cambridge, 1956), pp. 352–99
- 262. M. Bourgoin et al., Science **311**, 835–838 (2006)
- 263. G.K. Batchelor, Proc. CambridgePhylor. Soc 48, 345 (1952)
- 264. P.J. Sullivan, J. Fluid Mech. 20, 606 (1971)
- A.M. Obuchov, in N.F. Frenkiel (ed) Atmospheric Diffusion and Air Pollution (Academic, New York, 1959)
- A.M. Yaglom, Correlation Theory of Time-Independent Random Functions Gosmeteoizdat, Leningrad (1981)
- 267. B. Sawford, Annu. Rev. Fluid Mech. 33, 289-317 (2001)
- 268. A.S. Monin, Dokl. Akad. Nauk SSSR 105, 256 (1955)
- 269. A. Okubo, Oceanol. J. Soc. Jpn. 20, 286 (1962)
- 270. G. Boffetta, I.M. Sokolov, Phys. Fluids 14, 3224 (2002)
- 271. L. Biferale and I. Procaccia Phys. Rep. 254, (2005)
- 272. Transport and mixing in geophysical flows. Springer LNP-744 (2008)
- 273. G. Zumofen, A. Blumen, J. Klafter, M.F. Shlesinger, J. Stat. Phys. **54**, 1519 (1989)
- 274. B.B. Mandelbrot, J. Fluid Mech. 72, 401 (1975)
- 275. U. Frisch, P.-L. Sulem, M.A. Nelkin, J. Fluid Mech. 87, 719 (1978)
- 276. H.G.E. Hentschel, I. Procaccia, Phys. Rev. A 29, 1461 (1984)
- 277. J. Sommeria, J. Fluid Mech. **170**, 139–168 (1986)
- 278. R.H. Kraichnan, J. Fluid Mech. 47(3), 525–535 (1971)
- 279. R.H. Kraichnan, D. Montgomery, Rep. Prog. Phys. 43, 547 (1980)
- 280. J. Sommeria, Les Houches Series (Nova Science Publisher, New York, 2010)
- 281. P. Tabeling, Phys. Rep. 362, 1-62 (2002)
- 282. D.L. Rudnick, R. Ferrari, Science 283, 526–529 (1999)
- 283. W.J. McKiver, J. Fluid Mech. 596, 201 (2008)
- 284. B.B. Kadomtsev, Tokamak Plasma: A Complex System (IOP Publishing, Bristol, 1991)
- 285. J.A. Wesson, *Tokamaks* (Oxford University Press, Oxford, 1987)
- 286. S.R. Keating, P.H. Diamond, J. Fluid Mech. 595, 173 (2008)
- D. Biskamp, Magnetohydrodynamic turbulence (Cambridge University Press, Cambridge, 2004)
- 288. E. Falgarone, T. Passot (eds.), *Turbulence and Magnetic Fields in Astrophysics* (Springer, Berlin, 2003)
- 289. J.E. Pringle, A. King, Astrophysical Flows (Cambridge University Press, Cambridge, 2005)
- A. Ruzmaikin, A. Shukurov, D. Sokoloff, Magnetic Fields of Galaxies (Springer, Berlin, 1988)
- 291. C. Pasquero, J. Fluid Mech. **439**, 279 (2001)

 D.D. Schnack, Lectures in Magnetohydrodynamics. With an Appendix on Extended MHD. (Springer, Berlin, 2009)

- 293. YaB Zeldovich et al., Magnetic Fields in Astrophysics (Springer, Berlin, 2005)
- 294. G.K. Batchelor, Phys. Fluids Suppl. II. 12(12), 233-239 (1969)
- 295. P. Morel, M. Larcheveque, J. Atmos. Sci 31, 2189 (1974)
- 296. J.T. Lin, J. Atmos. Sci 29, 394 (1972)
- 297. A. Okubo, R.V. Ozmidov, Fizika atmosfery i okeana 1, 643 (1965)
- 298. G.S. Golitsyn, Dokl. Akad. Nauk SSSR 433(4), 231 (2010)
- 299. B.E, Zacharov, N.I. Filinenko Dokl. Akad. Nauk SSSR, 170, 6, (1966)
- 300. K. Toba, Oceanogr. Soc. Japan 29, 56 (1973)
- 301. J.I. Taylor, in N.F. Frenkiel (ed) Atmospheric Diffusion and Air Pollution (Academic, New York, 1959)
- 302. D.G. Andrews, An Introduction to Atmospheric Physics (Cambridge University Press, Cambridge, 2010)
- 303. E. Palmen, C.W. Newton, Atmospheric Circulation Systems (Academic, London, 1969)
- 304. R.S. Scorer, Environmental aerodynamics (Wiley, New Jersey, 1978)
- 305. R.A. Houze, Cloud Dynamics (Academic, London, 1993)
- 306. H.U. Roll, *Physics of the Marine Atmosphere* (Academic, London, 1965)
- P. Berge, Y. Pomeau and C. Vidal. L'ordre dans le chaos, Hermann, Editeurs des sciences et des arts (1988)
- 308. G.K. Batchelor, H.K. Moffat, M.G. Worster, *Perspectives in Fluid Dynamics* (Cambridge University Press, Cambridge, 2000)
- 309. P. Manneville, *Instabilities. Chaos and Turbulence. An Introduction to Nonlinear Dynamics and Complex Systems* (Imperial College Press, London, 2004)
- 310. L.M. Pismen, Patterns and Interfaces in Dissipative Dynamics (Springer, Berlin, 2006)
- 311. G. Schubert, D.L. Turcotte, P. Olson, *Mantle Convection in the Earth and Planets* (Cambridge University Press, Cambridge, 2008)
- 312. J.S. Turner, Buoyancy Effects in Fluid (Cambridge University Press, Cambridge, 1973)
- 313. E.N. Lorenz, J. Atmos. Sci 20, 130 (1963)
- 314. R.A. Meyers, Encyclopedia of Complexity and Systems Science (Springer, Berlin, 2009)
- 315. G. Nicolis Foundations of Complex Systems WS (2007)
- 316. M. Schroeder, Fractals, Chaos, Power Laws. Minutes from an Infinite Paradise (W.H. Freeman and Company, New York, 2001)
- 317. S.H. Strogatz, Nonlinear Dynamics and Chaos (Perseus, New York, 2000)
- 318. G.S. Golitsyn, J. Fluid Mech. 95, 567 (1979)
- 319. B.M. Koporov Tsvang L.R. Fizika atmosfery i okeana 6 643 (1965)
- 320. R.H. Kraichnan, Phys. Fluids 5, 1374 (1962)
- 321. L.N. Howard In Proc 11th Int. Congr., Appl. Mech Munchen FRG, 1109-1115 (1966)
- 322. R. Verzicco, K.R. Sreenivasan, J. Fluid Mech. 595, 203 (2008)
- 323. E.M. Sporrow, J. Fluid Mech. 41, 792 (1970)
- 324. B. Castaing et al., J. Fluid Mech. 204, 1-30 (1989)
- T. Zhao, Convective and Advective Heat Transfer in Geological Science (Springer, Berlin, 2008)
- 326. C. Normand, Y. Pomeau, M.G. Velarde, Per. Mod. Phys. 49, 581 (1977)
- 327. A. Boubnov, G.S. Golitsin, Convection in Rotating Fluids (Springer, Berlin, 1995)
- 328. A.M. Obuchov, Dokl. Akad. Nauk SSSR 125, 1246–1248 (1959)
- 329. R. Bolgiano, J. Geophys. Res. **46**(12), 2226–2229 (1959)
- 330. M.V. Osipenko, O.P. Pogutse, N.V. Chudin, Sov. J. Plasma Phys. 13, 550 (1987)
- 331. M.N. Rosenbluth, H.L. Berk, I. Doxoas, W. Horton, Phys. Fluids 30, 2636 (1987)
- 332. M.R. Maxey, S. Corrsin, J. Atmos. Sci. 43, 1112 (1986)
- 333. O. Cardoso, P. Tabeling, Euro. J. Mech. B/Fluids 8, 459 (1989)
- 334. O. Cardoso, P. Tabeling, Europhys. Lett. 7, 225 (1988)
- 335. M.B. Nezlin, Zg. Eksp. Teoret. Fiz. Lett. **34**, 83 (1981)

336. S.B. Antipov, M.B. Nezlin, E.H. Snegkin, A.S. Trubnikov, Zg. Eksp. Teoret. Fiz. **89**, 1905 (1985)

- 337. T.H. Solomon, E. Weeks, H.L. Swinney, Physica D 76, 70 (1994)
- 338. E.R. Weeks, J.S. Urbach, H.L. Swinney, Physica D 97, 291 (1996)
- 339. T. Solomon, J. Gollub, Phys. Rev. A 38, 6280 (1988)
- 340. T. Solomon, J. Gollub, Phys. Fluids A 31, 1372 (1988)
- 341. S. Childress, A.M. Soward, J. Fluid Mech. 205, 99 (1989)
- 342. M.B. Isichenko, YaL Kalda, E.V. Tatarinova, O.V. Telkovskaya, V.V. Yankov, Sov. Phys. J. Exp. Theor. Phys. 69, 517 (1989)
- 343. A.V. Gruzinov, M.B. Isichenko, YaL Kalda, Sov. Phys. J. Exp. Theor. Phys. 70, 263 (1990)
- 344. O.G. Bakunin, Turbulent and Diffusion, Scaling Versus Equations (Springer, Berlin, 2008)
- 345. V. Rom-Kedar et al., J. Fluid Mech. 214, 347 (1990)
- 346. J.-D. Reuss, F. Spineanu, J.H. Misguich, J. Plasma Phys. 59, 707 (1998)
- 347. P.N. Yushmanov, Comm. Plasma Phys. Control. Fusion 14, 313 (1992)
- 348. A.I. Smolyakov, P.N. Yushmanov, Nucl. Fusion 3, 383 (1993)
- 349. M.B. Isichenko, W. Horton, D.E. Kim, E.G. Heo, D.-I. Choi, Phys. Fluids 4(12), 3973 (1992)
- 350. G. Zimbardo, P. Veltri, P. Pommois, Phys. Rev. E 61, 1940 (2000)
- 351. M. Ottaviani, Europhys. Lett. 20, 111 (1992)
- 352. E. Knobloch, W.J. Werryfield, Astrophys. J. 401, 196 (1992)
- 353. Y.B. Zeldovich, Zg. Eksp. Teoret. Fiz. **7**(12), 1466 (1937)
- 354. A.E. Gledzer, Fizika atmosfery i okeana 35, 838 (1999)

A ABC-flow, 70–72 Advection, 21–34, 69, 75, 114, 116, 219, 225, 300, 309, 315, 328 Advection–diffusion equation, 21–23, 65, 158, 219, 300–302, 322, 323 Alexander–Orbach conjecture, 155	Boltzmann, 8, 9, 39, 42 Boltzmann law, 56–57 Bond percolation, 165–168 Boundary layer, 281, 283–287, 290, 300–303, 307, 309, 311 Boussinesq, 269–271, 291 Boussinesq approximation, 274
Anisotropy, 6, 61, 62, 119, 195	Braded magnetic field, 23
Anisotropy effect, 59, 199	Brownian motion, 37–40, 43, 46, 57, 103, 129,
Anomalous diffusion, 23, 59–62, 124, 131,	131, 134, 136, 139, 142
149–153, 165, 186, 192–195, 201,	Buoyancy, 267, 269–271, 274, 289–292
239, 315	Buoyancy force, 267–269, 284
Anomalous transport, 62, 65, 111, 124, 134,	Burgers' equation, 23–24
135, 145, 148, 149, 151–153, 156,	Burgers'model, 24
171, 173, 181–201, 216, 231–234,	
242, 297, 303–306, 308	
Arnold–Beltrami–Childress chaotic flow, 69–73	C Consider 80, 82, 200, 210, 212, 214, 210, 224
	Cascade, 80, 83, 209, 210, 213, 214, 219, 224, 228–229, 234, 250, 252, 254, 256, 257,
Astrophysics, 83, 205, 254 Atmospheric boundary layer, 281	259, 291, 324
Atmospheric cloud, 98	Cascade mechanism, 44
Atmospheric turbulence, 33, 211, 258–260	Cascade phenomenology, 83, 207–211, 224
Autocorrelation function, 42–44, 92, 97, 100,	Cauchy distribution, 183
101, 145–147	Chaos, 72–74, 78, 93, 239, 327
Averaging, 39, 47, 55, 60, 89–93, 107, 138,	Chaotic advection, 32, 72, 73, 80
147, 187, 227, 235, 240, 305, 323, 330	Chaotic flow,
	Characteristic frequency, 48, 77, 100, 140, 322, 331, 333
В	Chicago scaling, 287–290
Backbone, 170, 177, 194, 195	Cloud of marked particles, 31, 32
Ballistic mode, 49, 236–238	Coastal basin, 114–116
Ballistic motion, 23, 139, 157, 308	Coastline exponent, 173
Basset "history,", 99	Coherent structure, 6, 44, 84, 93, 192, 267, 293,
Batchelor dissipation scale, 80, 227	297–315, 319, 320
Batchelor mixing scale, 79	Cole–Hopf change of variables, 24
Beltrami condition, 70	Comb structures, 170–171, 176, 178, 194–199
Bolgiano spatial scale, 292, 293	Complex comb structure, 171

Complex correlation effect, 93, 96, 124	101, 102, 107, 116, 119, 120, 122, 123,
Complex structure, 23, 165–178, 287, 297	136, 150, 151, 170, 175, 177, 181, 182,
Concentration gradient, 3, 56, 107	184, 195, 227, 228, 232–235, 238–240,
Conduction cut-off, 225, 226	302, 303, 312, 320, 321, 324, 330
Conformally invariant, 8, 10	Diffusion equation, 4, 6–12, 14, 15, 18, 21, 24,
Conservation law, 10, 31, 207, 219	46–49, 59, 66, 89, 95, 108, 115, 116,
Continuity equation, 3, 47, 89, 90, 270, 271, 274	146, 182, 183, 193, 195–200, 227,
Continuous time random walk, 186, 193, 243,	239, 323
245, 246, 308	Diffusion mechanism, 6
Continuum percolation, 171, 172, 309	Diffusion phenomenon, 3–7
Contour loop, 143	Diffusion process, 40, 103, 303
Convection, 21, 22, 81, 110, 267–293, 300,	Diffusive front, 134, 305
302, 303, 306–308, 320, 326	Dirac function, 89, 102
Convection—diffusion equation, 21, 23, 26, 27	Dispersion, 5, 54, 65, 66, 80, 107–124,
Convective cells, 23, 276, 297, 300–303, 308,	231–233, 236, 237, 239–242, 254,
309, 311, 313, 319, 321, 325, 326	258–261, 272, 273, 300, 322 Discipation rate 118, 175, 208, 211, 214
Convective cloud, 99 Correlation concept, 53–56, 117	Dissipation rate, 118, 175, 208, 211, 214, 215, 219, 235, 242, 244, 253, 256, 257,
Correlation effect, 57, 63, 65, 75, 89–104, 113,	281, 292
124, 129, 135, 145, 150, 156, 161, 171,	Dissipation subrange, 237–239
173, 194, 199, 200, 309, 321	Dissipative spatial scale, 99, 238
Correlation exponent, 155, 170, 199, 312	Distribution function, 5, 11, 23, 28, 44–47,
Correlation length, 6, 43, 59, 124, 133, 166,	89, 90, 99, 101, 111–113, 159, 161,
167, 169, 171, 173–176, 320, 330	171, 188, 189, 191, 193, 240, 242,
Correlation mechanism, 23, 59	244, 303, 305
Correlation scale, 6, 44, 61, 75, 110, 123, 139,	Droplets, 99
178, 312, 315, 319, 320, 329–333	Dupree approximation, 100–102
Correlation spatial scale, 178, 314	
Correlation temporal scale, 44, 60, 61, 75	
Corrsin conjecture, 64, 65, 148, 152	E
Corrsin shear wind model, 124	Effective diffusive coefficient, 15, 16, 29, 33,
Critical exponent, 165–167	56, 57, 84, 107, 116, 122, 151, 153, 303,
Critical probability, 165	312, 321, 330
Critical Rayleigh number, 286, 325	Effective diffusivity, 18, 27–29, 33–34, 57,
	107, 116, 119, 151, 153, 154, 229, 313,
P.	320, 321, 323, 324, 326, 329
D Danasia a tima 40, 42	Effective transport, 6, 27, 63, 107, 139, 140,
Damping time, 40, 43	145, 156, 173, 177, 178, 191, 302,
Dead-end, 170, 177, 178, 195, 314 Decorrelation mechanisms, 77, 83, 93	308, 333 Finatain formula, 02
Density fluctuation, 27, 29, 91, 108, 269, 270	Einstein formula, 92 Electrostatic turbulence, 101–103
Density gradient, 13, 14, 28, 116, 216, 267	Elliptic point, 73, 74
Density gradient, 13, 14, 26, 116, 216, 267 Density perturbation, 33, 90–92, 109, 115,	Embedding dimension, 130
150, 229	Energy-containing eddies, 234
Diffusion, 3–5, 14–18, 23, 28–32, 37–40, 48,	Energy dissipation, 100, 175, 208, 211, 242,
53, 59, 62–66, 79, 81, 89, 94, 95, 99,	244, 245, 279–281, 292
100, 107, 110, 118, 120, 122, 129,	Energy spectrum, 209, 210, 219, 222, 227,
150–151, 153, 157–160, 170, 171, 181,	252–255, 292, 293
195, 219, 220, 225, 231–246, 269, 290,	Ensemble mean, 31
303, 304, 306, 309	Enstrophy, 250, 251, 253–257, 259
Diffusion characteristic time, 81	Enstrophy cascade, 254, 256, 259
Diffusion coefficient, 3-5, 12, 15, 16, 27, 33,	Environmental flow, 59, 62, 119, 121, 284, 319
37, 40, 43, 44, 48, 56–58, 61, 63, 84, 92,	Equation of vorticity, 249, 255, 275

Equipartition theorem, 39, 42 Euclidean dimension, 130, 245 Eulerian acceleration, 215 Eulerian characteristic spatial scale, 63–65 Eulerian characteristic time, 63–65 Eulerian correlation function, 63, 64, 151, 152, 199, 211	Fractional equation, 242–244 Fractional Fick law, 194–199 Freely evolving two-dimensional turbulence, 255–256 Frequency path, 320, 333 Frequency spectrum, 262 Fully developed turbulence, 214, 215, 231, 252
Eulerian description, 53, 63	1 uny de veloped turbulence, 214, 213, 231, 232
Eulerian (laboratory) coordinate frame, 53	
Eulerian velocity, 21, 63, 69, 205	G
Eulerian velocity, 21, 63, 67, 263 Eulerian velocity field, 53	Gauss distribution, 5, 138
Exponential instability, 32, 77, 224	Gaussian approximation, 239–242
Exponential regime, 84, 237–239	Gaussian distribution, 7, 64, 132, 148, 160,
Exponential stretching, 82, 224, 234, 237	171, 183, 184, 305
	Gaussian probability density, 132
	Gaussian statistics, 102, 103
F	Golitsyn formula, 280
Fastest mode rule, 321	Green function method, 91, 150, 196, 198
Fastest mode selection, 321	GreenKubo-Green formula, 92, 93
Fick relation, 95	
Fick's first law, 3	
Fick's second law, 4	Н
Finite size scaling, 169–170	Hamiltonian description, 92, 329
Fisher relation, 160–161	Hamiltonian dynamics, 74, 330
Flat scaling, 229, 333	Hamiltonian form, 70
Flory scaling, 138	Hamiltonian model, 75
Flow topology reconstruction, 80, 306, 315,	Hamiltonian system, 73–77, 326, 327
319–333	Hamiltonian theory, 49
Flow topology reorganization, 321, 324, 329 Fluctuation amplitude, 31, 34, 90, 211, 213,	Hausdorff dimension, 130, 134, 135 Heat conductivity, 24, 85, 269, 271
289, 291, 309, 333	Heat flux, 270, 279, 280, 282, 283, 285,
Fluctuation–dissipation relation, 27, 29, 32, 33,	289, 290
228–229	Heat wave front, 13
Fluctuations, 30–32	Heavy particle, 95–99
Fluid dynamics, 53, 260, 297	Hentschel, 246
Fokker-Plank equation, 45, 46, 242	Heteroclinic trajectories, 327
Folding, 78, 81, 82	High frequency regime, 319–321
Fourier component, 101, 219, 220	Hilly landscape, 139, 171–174
Fourier inversion, 5	Homoclinic point, 74
Fourier procedure, 7	Homogenous turbulence, 119
Fourier representation, 5, 182, 183, 194, 242	Howells expression, 151, 227
Fourier transform, 4, 5, 146, 151, 181, 182,	Hull, 143, 168, 176, 311, 312
187–189, 196–198, 200, 240	Hull fractal dimension, 168
Fractal dimension, 129–131, 133, 134,	Hurst exponent, 23, 61, 134, 138, 140, 142,
137–139, 142, 143, 167–168, 177, 178, 245, 277	145, 149, 152, 154, 155, 158–161, 171, 178, 184, 199, 315
Fractal line, 133	Hyperbolic point, 73, 74
Fractal model, 134	Tryperbone point, 73, 74
Fractal object, 129–143	
Fractal streamline, 139, 312, 315	I
Fractal time, 189–192	Incompressible flow, 21, 25, 75, 90, 139, 152,
Fractal topology, 134–137	201, 275, 297
Fractional derivative, 192–194, 243	Incompressible velocity field, 18, 97, 153

Independence hypothesis, 64, 102, 104	Lagrangian description, 53–66, 85, 119, 139
Industrial flow, 59	Lagrangian position, 54
Inertial particles, 96–98	Lagrangian representation, 56, 57, 69, 89, 119
Inertial subrange, 209, 219–222, 256	Lagrangian trajectory, 75, 328
Infinite percolating cluster, 165, 167, 172	Lagrangian turbulence, 70
Inhomogeneous media, 11-14	Lagrangian velocity, 54, 66, 145
Instantaneous release, 231	Laminar flow, 56, 73, 80, 81, 107–111,
Intermittency, 244, 245, 267	205, 223
Intersections, 134–137	Landau damping, 100, 101
Invariants, 8-10, 74, 129, 130, 132, 177, 214	Landau representation, 168
Inverse cascade, 252–254, 257, 258	Landscape roughness, 140
Irreversible statistical mechanics, 7	Langevin approach, 37, 96
Ising model, 168	Langevin equation, 37–49
Isotropic turbulence, 205–216, 221, 224, 226,	Langevin model, 45, 46, 96
237, 242, 244, 260	Laplace operator, 7
	Laplace transformation, 58, 193, 196, 200
	Larcheveque, 259
K	Large-scale behavior, 165
KAM theory, 73	Lattice structure, 165
Kinetic coefficient, 24, 25	Levy flight, 183, 243
Kinetic equation, 46-49, 215, 241, 242	Levy–Khintchine exponent, 184, 186, 243
Kinetic problem, 99	Levy-Smirnov distribution, 183, 186
Klein-Kramers equation, 46, 215	Lie theory of groups, 8
Kolmogorov, 32, 208, 209, 214, 219, 222,	Linear group, 8, 11
224, 227, 229, 234, 236, 237, 241,	Linear-response, 89–93
243, 245, 252, 253, 260, 279, 280,	Lobe transport, 324–329
292, 319, 320	Long range correlations, 135, 145, 173, 194,
Kolmogorov-Arnold-Moser theory, 71	199, 312, 321
Kolmogorov cascade, 213, 324	Loop (vortex) structure, 139
Kolmogorov constant, 210, 280	Lyapunov's exponent, 76, 77
Kolmogorov entropy, 76, 77	
Kolmogorov hypothesis, 213, 319	
Kolmogorov length, 208	M
Kolmogorov scaling, 213-214, 222, 223, 226,	Macroscopic equation, 14
228, 244, 291, 319, 324	Magnetic turbulence, 85
Kolmogorov similarity, 214	Magnetized plasma, 297
Kolmogorov spatial scale, 77, 211, 213,	Manhattan grid flow, 153-155, 161
238, 243	Manhattan random flow, 299
Kolmogorov theory, 83, 215, 244	Mapping parameter, 78
Kolmogorov time scale, 208	Marked particles, 30–32, 53, 54
Kramers equation, 46, 215	Markovian character, 215
Kubo-Green relation, 93	Markov's postulate, 182
Kubo number, 78, 175, 320, 326, 332	Mass conservation law, 31
	Maxwell distribution, 45
	Mean density, 90–92, 99, 108, 122, 323
L	Mean square distance, 5
Lagrangian approach, 53, 89, 98	Melnikov formula, 74
Lagrangian chaos, 69–85, 327	Melnikov function, 328
Lagrangian characteristic spatial scale, 61–63,	Memory effect, 49, 95, 103, 121–122, 182,
65, 77, 79, 80, 82–84	186, 194, 216, 234, 236, 237, 243
Lagrangian characteristic temporal scale, 97	Memory function, 93, 95–97, 122, 150, 151
Lagrangian correlation function, 55, 58, 63, 64,	Microchannel, 80–83
148, 227	Microscopic dynamics, 14

Mixing, 7, 11, 12, 28, 79–84, 93, 94, 100,	Percolation theory, 165, 167, 172,
107, 114, 116, 117, 119–120, 228, 239, 241, 254, 287, 306	173, 312 Percolation threshold, 165–168, 170–174,
Mixing length, 81, 83, 228, 287	176, 194, 311
Mixing time, 79, 80, 82, 83	Percolation transport, 149, 170–171
Mobility, 38, 40, 42, 57, 222	Perturbation technique, 33, 302
Molecular diffusivity, 29, 31, 32, 79, 81, 84,	Phase element, 78
118, 148, 153, 219, 300, 301, 309	Phase-space, 48, 49, 70, 71, 73, 79, 99–100,
Molecular motion, 30	215, 216, 241, 242, 277, 326
Multiscale method, 16	Plasma physics, 24, 83, 297
Multiscale technique, 14, 18	Point vortex, 186
	Point vortex distribution, 186
	Poiseuille flow, 80, 107, 111
N	Poisson equation, 275
Navier–Stokes equation, 23, 205, 214, 215,	Potts model, 168
249–252, 255, 270	Power-law shear flow, 157–160
Newtonian fluid, 23, 205	Prandtl number, 24, 25, 223, 225–226,
Newton second law, 267	276, 283
Non-diffusive character, 23 Non-integrable dynamics, 327	
Nonlinear equations, 8, 24, 99	Q
Non-local effect, 121, 216, 241, 242	Quasi-ballistic motion, 234
Nusselt number, 279–284, 287, 289, 290	Quasi-linear approach, 92, 93, 99-100, 104,
	150, 278
	Quasi-linear approximation, 99–101
0	Quasi-linear diffusion coefficient, 100, 101
Obukhov–Corrsin constant, 220	Quasi-linear equation, 91, 99, 150–151,
Onsager equation, 92	199, 200 Quenched randomness, 122
Order parameter, 166 Oscillatory instability, 326	Quenched fandomness, 122
Oscillatory roll, 324–329	
Oscillatory foli, 324–327	R
	Random percolation cluster, 168
P	Random processes, 93, 129, 242
Particle flux, 7, 14, 16, 23, 92, 94, 95	Random velocity field, 27, 90, 122,
Particle inertia, 95–98, 302	303, 311
Particle trapping, 308	Random walk, 124, 133-140, 142, 143, 157
Passive scalar equation, 89, 150	160, 161, 165, 181–184, 186, 189,
Passive scalar transport, 3, 14, 78	193, 197, 199, 243, 245, 246, 301,
Peclet number, 22, 29, 30, 33, 34, 79, 81, 83,	304, 308, 312
84, 109, 175, 224, 228, 282, 284, 301,	Rate of stretching, 79
302, 307, 309, 312, 313	Rayleigh-Benard convection, 270, 271, 274
Percolating cluster, 165, 167, 176	278, 284, 299, 324
Percolation, 129, 149, 165–178, 306, 308, 309,	Rayleigh–Benard instability, 270–274
311–315, 321, 328–330, 332, 333	Rayleigh number, 267–278, 282, 283,
Percolation hull, 143, 176, 311	285–287, 290, 325
Percolation method, 165, 311, 313	Reconnection of streamlines, 6
Percolation networks, 167, 177	Reconstruction of chaotic flow topology, 80
Percolation parameter, 167, 173–176, 311,	306, 330, 333
313, 331 Paraelation regime, 314, 315	Regular comb structure, 170, 195
Percolation regime, 314–315 Percolation streamline, 134, 173, 175, 311,	Regular structures, 297–300 Relative diffusion, 231–246, 258, 260, 262
312, 330, 331, 333	Relaxition, 30, 240, 243, 269
312, 330, 331, 333	Komamon, 30, 270, 273, 207

Renormalization, 56–57, 65, 92, 101–104, 138, 155, 173–175, 178, 199, 200, 228,	Spatial scale, 16, 31, 44, 60–63, 65, 75, 77, 79, 80, 82–84, 89, 98, 99, 110, 115, 116,
312, 313	139, 140, 171, 173, 177, 178, 205, 211,
Renormalized diffusion equation, 95	213, 222, 227–229, 233, 234, 238, 243,
Renormalized quasilinear equation, 150	256, 258–260, 291–293, 311, 313, 314,
Resonant particle, 104	320, 325, 329, 330
Return effect, 136, 147–149	Spectra, 205–216, 221, 224–226, 253–258,
Return of a walking particle, 135	262, 291–293
Return probability, 136, 171, 184–186	Spectral transfer rate, 219
Reynolds number, 64, 80, 81, 98, 118, 119,	Steady turbulent flow, 33
	•
205–208, 211, 215, 220, 227, 244,	Stochastic fractal, 131
250, 287, 319	Stochastic instability, 6, 76–80, 83, 85, 93,
Reynolds similarity law, 205–207	100, 320
Reynolds stress, 117, 120	Stochastic instability increment, 79, 83
Richardson constant, 232	Stochastic layer, 71, 72, 74, 75, 173, 175, 303,
Richardson law, 232, 233, 246, 263	311, 312, 315, 327, 330, 331, 333
Richardson's formula, 231	Stokes drag force model, 99
Richardson's scaling, 233, 234, 236–238,	Stokes' law, 38, 40
245, 258, 260–263	Strange attractor, 274–278
Roll system, 303	Stream function, 71, 73, 75, 82, 139, 141, 142,
Rough landscape, 140	147, 153, 172, 191, 192, 249, 252, 275, 297–299, 302, 303, 309, 311, 325–328
	Streamlines reconnection, 6, 63, 320
S	Streamlines reorganization, 330
Saddle point, 71, 73, 309	Streamline topology, 72, 139, 140, 299, 319
Scalar cascade, 83, 219, 224, 291	Stretching, 77–79, 81, 224, 274
Scalar spectrum, 220, 222–226, 256–258,	Strong convective turbulence, 283–285
292, 293	Strong turbulence, 205, 229, 285, 306, 308,
Scaling, 5, 23, 58–59, 77, 102, 109, 129–143,	320, 333
151–153, 169–170, 189–192, 213–214,	Subdiffusive regime, 152, 186, 200, 201, 315
220, 231–246, 260–263, 278–281,	Subdiffusive transport, 23, 303
287–290, 300–303, 329–333	Superdiffusion, 23, 147–149, 153, 201
Secondary flow, 82	Suprathermal electrons, 48
Seed diffusion, 6, 27, 62, 115, 122, 150, 157,	Supramermar electrons, 10
171, 181, 191, 200, 320, 327	
Self-affine surface, 143	Т
	_
Self-avoiding random walk, 137–139, 142, 160	Taylor convective dispersion, 121
Self-diffusion coefficient, 3, 227	Taylor definition, 54, 58, 63, 149, 154, 213, 238
Self-intersections, 137–139	Taylor diffusion, 53–56, 152
Self-similar behavior, 8	Taylor microscale, 211–213
Self-similar solution, 7–11	Taylor relationship, 58, 145
Self-similar variable, 8–12	Taylor shear dispersion, 107–124
Separatrix, 71–75, 77, 80, 308, 327–330	Taylor statistical approach, 54, 119
Separatrix splitting, 73–76, 309, 327, 328	Telegraph equation, 93–95
Serpinski gasket, 129–131	Temporal scale, 16, 97, 213, 238, 321
Settling velocity, 96	Time-periodic instability, 325
Shape exponent, 159–161	Total flux, 22
Shear flow, 25–27, 59–62, 122–124, 145–161,	Transport coefficient, 92, 93, 330
199–201, 321–324	Transport equation, 10, 15, 23, 49, 89–104,
Single puff of particles, 30, 31, 231	107, 121, 122, 181, 186, 193, 200, 281,
Single-scale approximation, 76–80, 83, 85,	282, 284
224, 255, 256	Transport model, 6, 65, 75, 148, 301, 328,
Solomon–Gollub model, 324	329, 333
*****************************	,

Transport scaling, 5, 58, 83, 123, 184, 302 Turbulence, 3, 32, 53, 70, 94, 117, 129,	311, 313, 315, 320, 321, 324, 326, 332, 333
205–216, 219–229, 233, 249–263, 267, 279–293, 308, 320	Turbulent velocity field, 33, 65, 233
Turbulent diffusion, 6, 28, 55, 60, 63, 65, 92,	
94, 95, 100, 119, 120, 145, 173, 227,	V
242, 246, 302, 308, 314, 315, 322,	Viscosity effect, 238, 282, 319
330, 331	Viscous layer, 119
Turbulent flow, 6, 24, 27, 28, 30, 33, 44, 56,	Viscous sublayer, 117, 118
57, 59, 63, 65, 89, 96, 116, 119–120,	Vortex structure, 6, 122, 139, 185, 191, 192,
129, 141, 191, 206, 210, 211, 213,	251, 297, 303, 306, 308, 327
214, 219, 223, 228, 233, 237, 252,	
254, 255, 258, 259, 267, 284, 291,	
297, 320, 324	$\mathbf{W}$
Turbulent fluctuations, 34, 211, 213	Week turbulence, 229
Turbulent mixing, 94, 116, 119	Well-developed turbulence, 32, 214, 256, 280,
Turbulent plasma, 48, 100	319, 320
Turbulent pulsation, 60, 61, 95, 97, 242, 321	
Turbulent spectrum, 252, 262, 333	
Turbulent thermal convection, 291–293	Z
Turbulent transport, 23, 55, 56, 58–59, 62–66,	Zeldovich fluctuation-dissipation relation, 29
93, 95, 129, 131, 142, 161, 215, 222,	Zeldovich prediction, 282, 308
227–229, 234, 239, 279, 283, 302,	Zonal flow, 23